

**Development of RNA-free particles of
Cowpea mosaic virus
for applications in Nanotechnology**

by

Pooja Saxena

This thesis is submitted in partial fulfilment of the requirements of the degree of
Doctor of Philosophy at the University of East Anglia.

John Innes Centre, Norwich

September 2012

© This copy of the thesis has been supplied on condition that anyone who consults it is understood to recognise that its copyright rests with the author and that use of any information derived there from must be in accordance with current UK Copyright Law. In addition, any quotation or extract must include full attribution.

Declaration

I hereby certify that the work contained within this thesis is my own original work, except where due reference is made to other contributing authors. This thesis is submitted for the degree of Doctor of Philosophy at the University of East Anglia and has not been submitted to this or any other university for any other qualification.

Pooja Saxena

Abstract

A method for the efficient production of RNA-free particles of Cowpea mosaic virus (CPMV) has been developed. These are generated by co-expression of the precursor of the coat proteins (VP60) and the viral proteinase (24K) using the highly-efficient plant expression system, CPMV-*HT*, in the model plant *Nicotiana benthamiana*. Particles thus produced were shown to be identical to CPMV on the outside and devoid of RNA on the inside and were hence named CPMV empty virus-like particles (eVLPs). The availability of large quantities of purified eVLPs represents a significant milestone in the development of CPMV-based particle technologies and their potential applications in nanotechnology have been investigated.

eVLPs were shown to be genuinely empty unlike other VLPs which package random cellular RNAs from the host. The high specificity of CPMV in packaging led to the investigation of the requirements for efficient packaging in CPMV where the functional coupling of replication and encapsidation was identified. Methods have been presented to extend this approach for packaging heterologous nucleic acids in eVLPs for their application as delivery vehicles.

To obtain a continuous supply of eVLPs, methods for its stable expression were developed for which the suppressor of silencing deployed in the CPMV-*HT* system, P19, was modified as the use of wt P19 inhibits regeneration of leaf tissue. A mutant form of P19, R43W, with reduced but still substantial suppressor activity was shown to permit the regeneration of transgenic plants. P19/R43W was used for the stable expression of a variety of heterologous proteins showing the broad applicability of this system. To reduce the possibility of homologous recombination, an alternative to the CPMV-*HT* system was developed by deploying the UTRs from CPMV RNA-1. Expression with RNA-1 UTRs was rapid as compared to CPMV-*HT* and hence, the expression system was named *Rapid-Trans*.

Acknowledgements

First and foremost, I would like to thank Prof. George Lomonosoff for being a great supervisor and philosopher. Right from day one, George's positivity, encouragement and enthusiasm broke all myths I had about Ph.D. supervisors. For all the fun I have had in the lab, at conferences and at parties at George's house, I just want to say, "George, thanks for being you!"

I would like to thank the other members of my supervisory committee, Prof. David Evans and Prof. Nick Brewin for providing sound advice and expertise throughout my degree.

I would also like to thank my past and present colleagues in the department of Biological Chemistry: Keith, Paolo, Yulia, Frank, Eva, Hadrien, Alberto, Alaa, Nick, Lesley and Elaine, for putting up with me and for being awesome company in the lab, in glasshouses and at coffee breaks.

My time at the John Innes Centre would not have been as productive as it has been without the support of staff in horticultural services, photography and the media kitchen and I am very grateful to them.

To my friends in Norwich and Brighton for always being there for me, for being my support system and for never letting me miss home.

Last but not the least; I extend my gratitude to my Mum and Dad and my darling sister for their unconditional love and support, and to the rest of my loving family for always believing in me.

I would like to dedicate this thesis to the memory of my grandmother who was an integral part of my childhood in India and contributed immensely in making me who I am today.

Table of contents

Title	1
Declaration	2
Abstract	3
Acknowledgements	4
Table of Contents	5
List of Figures	10
List of Tables	13
List of Abbreviations	14
Chapter 1: Introduction	16
1.1 Nanotechnology	16
1.2 Nanoparticles	17
1.3 Viruses in nanotechnology	18
1.4 Cowpea mosaic virus (CPMV)	21
1.4.1 CPMV infection	22
1.4.2 CPMV capsid	23
1.4.3 CPMV genome	24
1.4.4 Translation in CPMV	26
1.4.5 Replication in CPMV	27
1.4.6 Assembly of CPMV particles	28
1.5 Applications of CPMV in nanotechnology	29
1.5.1 Genetic modification of CPMV	29
1.5.2 Chemical modification of CPMV	30
1.6 Limitations with wild-type (wt) CPMV	31
1.7 Plant expression	32
1.7.1 Plant viral vectors	35
1.7.2 CPMV-based plant expression systems	36
1.8 CPMV empty virus-like particles or eVLPs	38
1.9 Aims of this thesis	39

Chapter 2: Materials and Methods	41
2.1 Media, Buffers and Solutions	41
2.2 Vectors	42
2.3 Recombinant DNA methodology	44
2.3.1 PCR	44
2.3.2 Digestion	45
2.3.3 Ligation	45
2.3.4 Transformation	45
2.3.5 Purification of plasmids	45
2.3.6 Sequencing	45
2.3.7 Site-directed mutagenesis (SDM)	46
2.3.8 Agarose gel electrophoresis of DNA fragments	46
2.4 Plant growth and transformation	46
2.4.1 Plant growth	46
2.4.2 Transient expression of proteins in plants	46
2.4.3 Stable expression of proteins in plants	47
2.5 Production of wt CPMV	48
2.5.1 Propagation	48
2.5.2 Purification	48
2.5.3 Fractionation into Top, Middle and Bottom components	49
2.6 Production of CPMV eVLPs	49
2.6.1 Expression	49
2.6.2 Purification	50
2.7 Extraction and analysis of viral RNA	50
2.7.1 Extraction of RNA from virus particles	50
2.7.2 Electrophoresis of viral RNA	50
2.8 Analysis of protein expression	51
2.8.1 Protein extraction and detection	51
2.8.2 Analysis of expression of GFP	52
2.8.3 Analysis of expression of VLPs	52
2.9 Photography	54

Chapter 3: Results I	55
Production and Characterisation of CPMV eVLPs	
3.1 Introduction	55
3.2 Optimisation of particle purification protocols	57
3.3 Optimisation of the plant expression system	61
3.3.1 Optimisation of expression constructs	61
3.3.2 Optimisation of plants used for infiltration	64
3.3.3 Optimisation of time of harvest	64
3.4 Scale-up of production	66
3.5 Current eVLP yields	68
3.6 Characterisation of eVLPs	69
3.6.1 SDS-PAGE	69
3.6.2 UV-Vis spectrophotometry	70
3.6.3 Native gel electrophoresis	71
3.6.3.1 Coomassie-staining of wt CPMV and eVLPs	72
3.6.3.2 Ethidium bromide-staining of wt CPMV and eVLPs	72
3.6.4 TEM	73
3.6.5 Cryo-electron microscopy (cryo-EM)	74
3.6.6 Neutron scattering studies	76
3.7 Discussion	77
Chapter 4: Results II	81
Study of replication and encapsidation of RNA in CPMV	
4.1 Introduction	81
4.2 Study of encapsidation of a replication-deficient mutant of RNA-1	83
4.3 Study of encapsidation of a non-replicatable mutant of RNA-2	90
4.4 Discussion	95

Chapter 5: Results III	100
Creation of transgenic plants producing eVLPs	
5.1 Introduction	100
5.2 Creation of lines transgenic for GFP	103
5.2.1 Generation of constructs	103
5.2.2 Transient expression of GFP in presence of P19/R43W	105
5.2.3 Stable integration of GFP and P19/R43 in <i>N. benthamiana</i>	106
5.2.4 Analysis of GFP expression levels in transgenic <i>N. benthamiana</i>	107
5.2.5 Identification and analysis of plants homozygous for P19/R43W	110
5.3 Creation of lines transgenic for pharmaceutically valuable proteins	112
5.3.1 Human HIV-1 antibody 2G12	112
5.3.1.1 Transient expression of 2G12 and P19/R43W	112
5.3.1.2 Transgenic expression of 2G12 and P19/R43W	115
5.3.2 Human gastric lipase	117
5.3.2.1 Transgenic expression of hGL and P19/R43W	117
5.4 Creation of lines transgenic for eVLPs	118
5.4.1 Generation of the construct	118
5.4.2 Transient expression of eVLPs and P19/R43W	120
5.4.3 Transgenic expression of eVLPs and P19/R43W	121
5.5 Discussion	123
 Chapter 6: Results IV	 128
Development of expression vectors based on CPMV RNA-1	
6.1 Introduction	128
6.2 Generation of expression vectors based on RNA-1	129
6.3 Analysis of expression from RT vectors	131
6.4 Comparison of RNA-1 and RNA-2 based expression systems	133
6.5 Expression using a combination of RNA-1 and RNA-2 sequences	136

6.5.1 Generation of constructs	136
6.5.2 Expression of GFP in the absence of the 3' UTR	137
6.5.3 Expression of GFP using the 5' UTR of RNA-1 and the 3' UTR of RNA-2	139
6.6 Discussion	140
Chapter 7: Conclusions and Outlook	144
References	149
Appendix I: List of Primers	165
Appendix II: List of Vectors	167
Appendix III: Publications	171

List of Figures

Figure 1.1	CPMV infections	22
Figure 1.2	CPMV capsid	23
Figure 1.3	CPMV genome	25
Figure 1.4	Three components of CPMV	26
Figure 1.5	<i>Agrobacterium</i> -mediated transformation of plant cells ...	34
Figure 1.6	Schematic diagram depicting development of iron oxide-eVLPs	39
Figure 3.1	Constructs used for expression of eVLPs in plants	56
Figure 3.2	Immunodetection of eVLPs	58
Figure 3.3	Effect of organic solvents on eVLP recovery	60
Figure 3.4	Schematic representation of the construct designed for eVLP expression	62
Figure 3.5	Analysis of eVLP expression	63
Figure 3.6	eVLP expression over time	65
Figure 3.7	Syringe vs. vacuum-infiltration of GFP	67
Figure 3.8	Vacuum infiltration of <i>N. benthamiana</i> biomass	68
Figure 3.9	SDS-PAGE of wt CPMV and eVLPs	70
Figure 3.10	UV-Vis spectrophotometry	71
Figure 3.11	Native gel electrophoresis of wt CPMV and eVLPs	72
Figure 3.12	TEM of wt CPMV and eVLPs	73
Figure 3.13	Three-dimensional reconstructions of wt CPMV and eVLPs	74
Figure 3.14	Three-dimensional reconstructions of CPMV-Bottom	75
Figure 3.15	Comparison of CPMV-Bottom and eVLPs around the 5-fold axis	76
Figure 4.1	Analysis of RNA within particles	83
Figure 4.2	Schematic diagrams of constructs expressing RNA-1 and 32E	84
Figure 4.3	SDS-PAGE analysis of particles	85
Figure 4.4	Particle analysis using agarose gel electrophoresis	86

Figure 4.5	Schematic diagrams of constructs expressing mutants of RNA-2	91
Figure 4.6	Symptoms in the upper leaves of plants upon expression of RNA-2 mutants in presence of wt RNA-1	93
Figure 4.7	Analysis of RNA within capsids generated by co-expression of mutant versions of RNA-2 and wt RNA-1	94
Figure 4.8	Summary	97
Figure 4.9	Proposed model for co-expression and encapsidation of modified RNA-2	99
Figure 5.1	Location of R43 in P19-siRNA duplex complex	102
Figure 5.2	Schematic diagrams of constructs used for expression of GFP	104
Figure 5.3	Transient expression of GFP in presence of wt P19 and P19/R43W	105
Figure 5.4	Phenotype of plants transgenic for GFP and P19/R43W	107
Figure 5.5	GFP expression levels in T1 populations of Line 3 and Line 5	108
Figure 5.6	Comparison of expression levels of GFP in Line 3 and Line 5	109
Figure 5.7	GFP expression in the T2 generation of Line 3 and Line 5	111
Figure 5.8	Design of constructs used for expression of 2G12	113
Figure 5.9	Analysis of 2G12 expression by SDS-PAGE	114
Figure 5.10	T0 transgenic plants expressing 2G12 and P19/R43W	116
Figure 5.11	Detection of 2G12 in T0 transgenic plants	116
Figure 5.12	Schematic diagram of the construct used for expression of eVLPs	119
Figure 5.13	Analysis of eVLP expression by SDS-PAGE	121
Figure 5.14	Immunodetection of CPMV coat protein	123
Figure 5.15	Phenotype of plants transgenic for P19/R43W	124
Figure 6.1	The <i>RT</i> expression cassette	130
Figure 6.2	Schematic diagram of pEAQexpress- <i>RT</i> -GFP	131

Figure 6.3	Expression of <i>RT</i> -GFP over time	132
Figure 6.4	Schematic diagrams of constructs	133
Figure 6.5	Expression of <i>RT</i> -GFP and <i>HT</i> -GFP	134
Figure 6.6	Expression of <i>RT</i> -GFP and <i>HT</i> -GFP over time	135
Figure 6.7	Schematic diagrams of constructs generated for expression of mutants of the 3' UTR of pEAQexpress- <i>RT</i> -GFP	137
Figure 6.8	Expression of <i>RT</i> -GFP and <i>HT</i> -GFP in the absence of their 3' UTRs	138
Figure 6.9	Expression of <i>RT</i> -GFP in presence of the 3' UTR from RNA-2	139
Figure 6.10	Predicted secondary structures of the 3' UTRs of RNA-1 and RNA-2 generated using the software RNAfold	143

List of Tables

Table 1.1	Examples of organic and inorganic materials being developed for applications in nanotechnology	17
Table 1.2	Viruses exploited in nanotechnology	21
Table 2.1	Recipes of media, buffers and solutions	41
Table 2.2	pEAQ plasmids and their properties	43
Table 2.3	Antibodies used for western blots	52
Table 2.4	Molar extinction coefficients of wt CPMV and eVLPs	53
Table 3.1	Fundamental differences between wt CPMV particles and eVLPs	57
Table 3.2	Modifications made to the original extraction protocol to enhance yield and purity	59
Table 4.1	Combinations of constructs infiltrated into <i>N. benthamiana</i> leaves for comparative analysis of RNA-1 and 32E	84
Table 4.2	Combinations of constructs infiltrated into <i>N. benthamiana</i> leaves for analysis of replication and encapsidation of different versions of RNA-2	92

List of Abbreviations

BMV	Brome mosaic virus
bp(s)	Base-pair(s)
CaMV	Cauliflower mosaic virus
CCMV	Cowpea chlorotic mottle virus
CFP	Cyan fluorescent protein
CHO	Chinese hamster ovary
CPMV	Cowpea mosaic virus
Cryo-EM	Cryo-electron microscopy
C-terminus/-terminal	Carboxy-terminus/-terminal
dpi	Days post infiltration
dsRNA/DNA	Double-stranded RNA/DNA
ER	Endoplasmic reticulum
eVLP(s)	Empty virus-like particle(s)
FGRB	Formaldehyde gel running buffer
FHV	Flock house virus
FMDV	Foot-and-mouth disease virus
FWT	Fresh weight tissue
GDD	glycine-aspartate-aspartate
GFP	Green fluorescent protein
HBV	Hepatitis B virus
hGL	Human gastric lipase
HIV-1	Human immunodeficiency virus-1
HRP	Horseradish peroxidase
<i>HT</i>	<i>Hyper-Trans</i>
IgG	Immunoglobulin G
kDa	Kilodalton
L	Large coat protein
LB	Left border
LB-media	Luria-Bertani media
MCS	Multiple cloning site

MS- agar	Murashige and Skoog agar
NEB	New England Biolabs
nos	Nopaline synthase
npt	Neomycin phosphotransferase
nt(s)	Nucleotide(s)
N-terminus/-terminal	Amino-terminus/-terminal
OD ₆₀₀	Optical density at 600 nm
PBS	Phosphate buffered saline
PEG	Poly(ethylene glycol)
PTGS	Post-transcriptional gene silencing
PVPP	Polyvinylpyrrolidone
RB	Right border
RGD	arginine-glycine-aspartate
<i>RT</i>	<i>Rapid-Trans</i>
S	Small coat protein
SDS-PAGE	Sodium dodecyl sulphate polyacrylamide gel electrophoresis
siRNA	Small interfering RNA
ssRNA/DNA	Single-stranded RNA/DNA
TBE	Tris-borate-EDTA
TBSV	Tomato bushy stunt virus
TCV	Turnip crinkle virus
T-DNA	Transferred DNA
TEM	Transmission electron microscopy
Ti plasmid	Tumour-inducing plasmid
TMV	Tobacco mosaic virus
UTR(s)	Untranslated region(s)
UV	Ultraviolet
VLP(s)	Virus-like particle(s)
wt	Wild-type
YFP	Yellow fluorescent protein

Chapter 1: Introduction

1.1 Nanotechnology

Nanotechnology is a relatively new, multi-disciplinary field that involves manipulation of matter on the nanometre (10^{-9} m) scale. It advocates the bottom-up approach to build and shape matter, i.e. one atom at a time. The underlying principle of this field is manipulation at the atomic/molecular level for precise control at the macromolecular level (Goodsell, 2004).

The first concepts of nanotechnology were introduced by physicist Richard Feynman in 1959 in his ground-breaking lecture, 'There's plenty of room at the bottom' where he presented his vision on miniaturization and controlling things on a small scale (Feynman, 1959). Later in 1986, K. Eric Drexler popularised the idea of nanotechnology in his book, 'Engines of Creation: the coming era of nanotechnology', which presents ideas on developing a nano-scale machine for forcibly pressing atoms together into desired molecular shapes (Drexler, 1986). Since then, the field of nanotechnology has grown by leaps and bounds and today, nanotechnology ranges from improvisation of conventional devices such as semiconductor wires and transistors to completely new approaches like molecular self-assembly.

Bio-nanotechnology or nano-biotechnology is a subset of nanotechnology that involves using concepts of nanotechnology to monitor and engineer biological systems (Gazit, 2007). Being able to manipulate biomolecules on the nanoscale has the potential to revolutionise medical sciences and for this reason, today, nanotechnology approaches are being developed for diagnostic as well as therapeutic applications in medicine. Nano-scale machines are being designed to perform specific biological tasks, such as monitoring the environment of living cells or to seek out and destroy cancerous cells. Nano-scale sensors for diagnosing diseased states and vehicles for controlled drug release are under development. Nanoparticles are also being developed as scaffolds for the presentation of epitopes to elicit immune responses in mammalian systems.

1.2 Nanoparticles

Generally, nanotechnology works with materials with at least one dimension in the range of 1-100 nm. Examples of such nanoparticles and their potential applications are given in Table 1.1.

Nanoparticle	Description	Applications
Fullerenes	Molecules composed entirely of carbon such as carbon nano-tubes (cylindrical) or buckyballs (spherical)	Semiconductors (Dekker, 1999); Drug delivery vehicles and imaging contrast agents (Bakry et al., 2007)
Liposomes	Lipid-based liquid crystals	Drug and vaccine delivery vehicles (Gregoriadis, 1995)
Nanorods	Elongated objects made of silicon, gold or inorganic phosphate	Semiconductors for solar cells, detectors for biomolecules (Sadeghi, 2012)
Dendrimers	Highly branched structures made of natural polymers	Drug delivery vehicles and imaging contrast agents (Dykes, 2001)
Magnetic Nanoparticles	Superparamagnetic iron oxide or iron platinum nanoparticles	High-density data storage (Lu et al., 2007); Tumour destruction via heating (hyperthermia) (Armijo et al., 2012)
Quantum Dots	Semiconductor nano-crystals	Imaging of live cells, <i>in situ</i> tissue profiling (Xing and Rao, 2008)
Viruses	Natural nanoparticles of various shapes and sizes that infect bacteria, plants and animals	Building blocks for multi-layered arrays, biomedical imaging, novel vaccines and delivery vehicles (Manchester and Steinmetz, 2009)

Table 1.1 Examples of organic and inorganic materials being developed for applications in nanotechnology.

Nanotechnology is still quite a new field and a number of unexplored avenues exist. New nanoparticles are constantly being developed expanding the breadth of

this field. The next section discusses the development of viruses for use in nanotechnology and the progress that has been made so far.

1.3 Viruses in nanotechnology

For over a hundred years, viruses have been looked at as ‘disease-causing entities’ and studies on viruses have mainly focused on understanding viral infection to develop strategies for prevention and treatment of viral diseases. However, the last 20 years have seen a shift in this paradigm and more and more studies on the use of viruses in nanotechnology have been published. Today, several animal viruses, plant viruses and bacteriophages are being developed for beneficial uses in a range of applications from material sciences to medicine.

Viruses are the most abundant biological entities on earth and exist in various shapes and sizes, ranging from 17 to 700 nm [smallest virus known: *Porcine circovirus* (Finsterbusch and Mankertz, 2009); largest virus known: *Megavirus chilensis* (Arslan et al., 2011)], thereby presenting a whole library of viral nanoparticles to choose from. Thanks to extensive studies on viral diseases, there is a wealth of information available about the biological, chemical and physical properties of viruses, including crystallographic structures of the particles of some, allowing precise genetic and chemical modifications to be made to the viral capsids.

In addition to their nano-scale size, there are a number of properties that make viruses ideal for use in nanotechnology. Firstly, viruses have the ability to self-assemble into highly regular particles. Viruses usually have very simple structures consisting of multiple copies of one or more type of subunit arranged in either icosahedral (for spherical viruses) or helical (for rod-shaped viruses) symmetry. The repetitive structure of the viral capsid serves as a platform for presentation of multiple copies of a peptide or for attachment to multiple sites in a macromolecular system. The fact that virus capsids are homogeneous makes it easy to modify them, both chemically and genetically, in a predictable manner.

A property that puts viral nanoparticles above other available nanoparticles is their plasticity. Viral capsids are designed for protection of encapsulated nucleic

acids and so, the capsids are very robust. But at the same time, capsids are designed to disassemble under certain physiological conditions to release their genome to initiate infection. This means that the capsid has the potential to both survive in harsh environments (for instance a range of temperatures, pH conditions and in a variety of solvents) and to break apart releasing its cargo when needed.

Viruses are naturally occurring, which makes them both bio-compatible and biodegradable. This is very important for applications in mammalian systems where it is essential that nanoparticles are cleared from the system after they have served their purpose. Toxicity and bioavailability studies of several viruses are being undertaken. From a human health perspective, bacteriophages and plant viruses are safer to use in medicine compared to animal viruses, due to their inability to replicate in mammalian systems. However, detailed risk assessments would still need to be carried out.

A significant advance in the field of viruses in nanotechnology has been the ability to produce virus-like particles (VLPs) by expression of viral coat proteins in heterologous systems. VLPs are devoid of genomic nucleic acid, rendering them non-infectious. This reduces bio-safety concerns associated with their use, extending the range of their applications. Also, since VLPs do not have to be functional in a virological sense, i.e. they don't have to be capable of causing an infection, a more extensive range of modifications can be made to the capsid. The only factor that would need to be considered is that the modifications do not interfere with the ability of coat proteins to assemble into particles.

Last but not the least, viruses are easy to produce and purify. When expressed in their natural host, viruses replicate and assemble *in vivo* often resulting in high titres of virions. In addition, viruses and VLPs can be produced in heterologous hosts to high levels. For example, cowpea chlorotic mottle virus (CCMV) VLPs can be produced using the yeast-based *Pichia pastoris* heterologous expression system to levels of 0.5 g/kg wet cell mass (Brumfield et al., 2004). Bacteriophage M13 yields 200 mg of particles from a 1 litre cell culture (Mao et al., 2004).

Virus-based nanoparticles can be modified at three levels to impart various applications: the exterior surface, the capsid interface and the interior (Douglas and Young, 2006; Young et al., 2008). The exterior surface of viral capsids provides for the multivalent display of ligands and peptides for use in 2D/3D arrays and as novel vaccines (Blum et al., 2011; Smith et al., 2009). The interface can be manipulated to control capsid architecture to generate particles for use as bio-templates (Bothner et al., 2005; Brumfield et al., 2004). The interior cavity of viral nanoparticles, especially in case of empty particles, provides a constrained environment where the interior surface can direct attachment or nucleation of nano-materials (Douglas and Young, 1998). The interior space can also be filled with contrast agents for use in imaging or desired cargos for delivery to specific locations in a biological system (Aljabali et al., 2010a).

Modifications to the viral capsid can be introduced chemically (by conjugation to surface residues or by incubation under different reaction conditions) or genetically (by making mutations in the nucleotide sequence encoding viral coat proteins). Often, both chemical and genetic approaches are used together. For instance, in an approach to develop adenovirus particles for targeted gene therapy, capsids were first genetically modified to incorporate cysteine residues at solvent-exposed positions and subsequently chemically modified by covalent coupling of incorporated cysteines to the ligand transferrin (Kreppel et al., 2005).

Table 1.2 shows examples of viruses that have been developed for potential uses in nanotechnology. The focus of this thesis will be the further development of cowpea mosaic virus (CPMV) VLPs for such applications.

Virus	Potential applications
Adenovirus	Gene delivery vehicles for treatment of cancer (Bachtarzi et al., 2008)
Brome mosaic virus	Scaffold for gold nanoparticles (Chen et al., 2005); Semi-conductor quantum dots (Dixit et al., 2006)
Canine parvovirus	Tumour targeted drug delivery (Singh et al., 2006)
Cowpea chlorotic mottle virus	Nano-reaction vessel; Delivery vehicle (Douglas and Young, 1998)
Cowpea mosaic virus	2D/3D arrays (Blum et al., 2011); Quantum dot decoration (Medintz et al., 2005); Imaging agents (Lewis et al., 2006)
Tobacco mosaic virus	Carrier for immunogenic epitopes (Smith et al., 2009); Nanowires (Niu et al., 2007)
Bacteriophage Q-beta	Delivery vehicle for DNA/RNA aptamers (Lau et al., 2011)
Bacteriophage M13	Nanotubes for batteries (Nam et al., 2008)
Bacteriophage MS2	Imaging contrast agents (Meldrum et al., 2010)

Table 1.2 Viruses exploited in nanotechnology. Examples of some spherical and rod-shaped viruses that are being developed for various applications in nanotechnology have been presented in the above table.

1.4 Cowpea mosaic virus (CPMV)

CPMV is a non-enveloped plant virus that belongs to the *Comoviridae* family and is the type member of the genus *Comovirus*. It was first identified and characterised by H. O. Agrawal (1964). Based on similarities in capsid structure, genome organisation and replication strategies, comoviruses are thought to be evolutionarily related to mammalian picornaviruses (family *Picornaviridae*), which include important pathogens such as the foot-and-mouth disease virus, poliovirus and rhinovirus (Lin and Johnson, 2003).

1.4.1 CPMV infection

CPMV naturally infects legumes such as the cowpea plant (*Vigna unguiculata*; family *Leguminosae*) and soybean (*Glycine max*; family *Fabaceae*). Upon infection in cowpea, CPMV causes yellowing of leaves resulting in a mosaic pattern (Figure 1.1a). Other symptoms include a decrease in leaf area, reduced flower production and yield losses of up to 75%. CPMV is mechanically transmissible and in nature, CPMV is transmitted by chrysomelid beetles (family *Coleoptera*).

For a number of years, many studies on CPMV were conducted using cowpea mesophyll protoplasts (Hibi et al., 1975). However, today, with the advent of *Agrobacterium*-mediated plant transformation techniques for the efficient establishment of infections (Liu and Lomonosoff, 2002), CPMV is most easily studied in its experimental host *Nicotiana benthamiana*. CPMV infection in *N. benthamiana* is typified by crinkling of leaves and vein clearing in young leaves (Figure 1.1b).

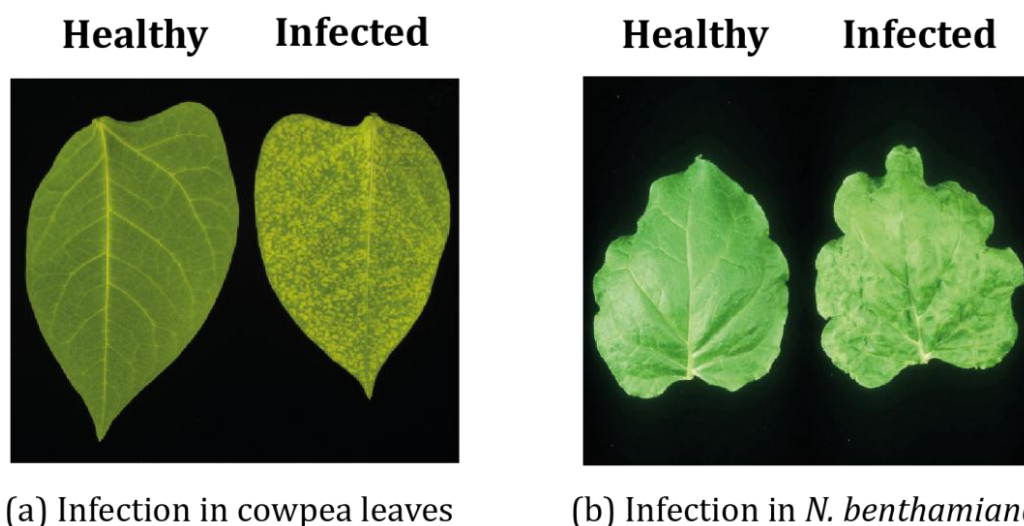


Figure 1.1 CPMV infections in its natural host cowpea (a) and experimental host *N. benthamiana* (b). In cowpea, chlorotic spots with diffuse borders (diameter of 1-3 mm) are produced in inoculated primary leaves. Trifoliolate leaves develop a bright yellow mosaic. Plants do not show necrosis. In *N. benthamiana*, leaves show crinkling and vein clearing.

1.4.2 CPMV capsid

CPMV exists as isometric particles with $T=1$ (pseudo $T=3$) symmetry and a diameter of 28-30 nm. Each virion comprises 60 copies of two coat proteins: the Large (L) coat protein (374 residues) with two β -barrel domains and the Small (S) coat protein (213 residues) with one β -barrel domain. The three domains form one asymmetric unit, sixty of which are arranged in icosahedral symmetry to form the CPMV capsid (Figure 1.2).

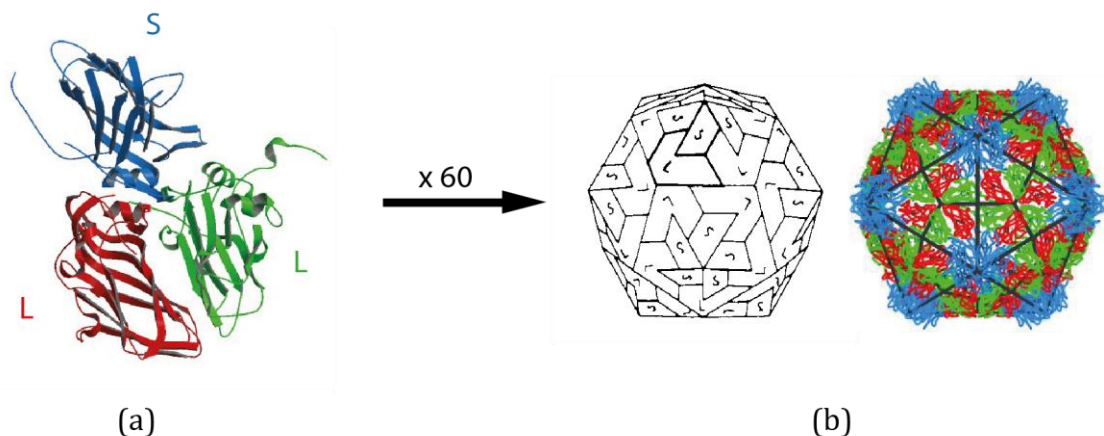


Figure 1.2 CPMV capsid. (a) Asymmetric unit comprising the Large coat protein with two domains (in green and red) and the Small coat protein with one domain (in blue). (b) 60 asymmetric units are arranged in icosahedral symmetry to form the CPMV capsid. Images from VIPER database, Scripps Research (Shepherd et al., 2006).

The structure of the CPMV capsid is known to atomic resolution (Lin et al., 1999; Stauffacher et al., 1987). The only portion of the capsid that is not visible in the crystal structure is a peptide of 24 amino acids at the carboxyl-terminus of the S coat protein (residues 190-213). This peptide is exposed on the surface of the virus and is frequently lost by proteolysis at Leucine 189 (Lomonossoff and Johnson, 1991; Taylor et al., 1999). Loss of the peptide occurs during late stages of a natural infection and, though not affecting the stability of the particles, is thought to increase the specific infectivity of virions (Niblett and Semancik, 1969, 1970).

Amongst the 24 residues in the C-terminal peptide are several positively charged amino acids (four arginines and two lysines) contributing to its pI of 11.9. Loss of this peptide results in loss of both mass and positive charge, resulting in faster migration of particles towards the anode upon electrophoresis. Hence, C-terminally processed particles are referred to as CPMV_{fast}. Conversion of CPMV from its slow to its fast form takes place through proteolysis, either naturally by ageing or synthetically using chymotrypsin (Niblett and Semancik, 1969).

Analysis of deletion mutants shows that the 24 amino acid peptide plays a role in packaging of RNA (Taylor et al., 1999) and in suppression of virus-induced silencing (Canizares et al., 2004), both of which are important during the early stages of infection; loss of the peptide during late stages of infection does not have any deleterious effects on particle viability. Recent studies have shown that the presence of the intact peptide inhibits internal mineralization of CPMV VLPs suggesting a possible role of the peptide in controlling permeability of the CPMV capsid (Sainsbury et al., 2011).

1.4.3 CPMV genome

The CPMV genome consists of two separately encapsidated positive-sense single stranded RNA molecules: RNA-1 and RNA-2 (Figure 1.3). RNA-1 is 5889 bases long and encodes the replication machinery of CPMV, including the RNA-dependent RNA polymerase and the helicase. RNA-2 is of 3481 bases in length and encodes proteins essential for cell-to-cell movement and systemic spread of the virus, namely the movement proteins (48K and 58K) and coat proteins (L and S). Both RNAs are polyadenylated and possess a small (28 amino acids) genome-linked viral protein (VPg) covalently attached to their 5' end (Hull, 2009).

Both RNA-1 and RNA-2 are required for an infection since RNA-2 depends on RNA-1 for its replication and RNA-1 depends on RNA-2 for production of coat proteins for its encapsidation.

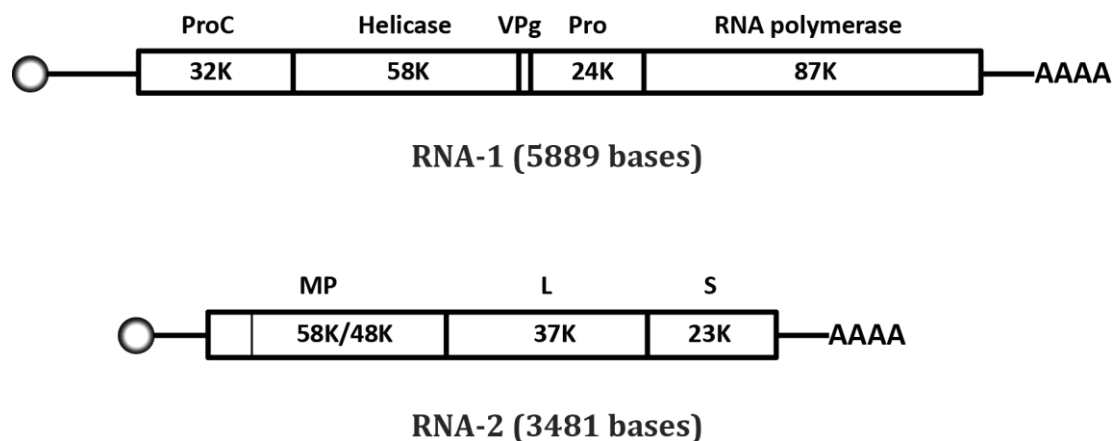


Figure 1.3 CPMV genome. The CPMV genome consists of two plus-sense ssRNA. RNA-1 encodes a 32 kDa proteinase co-factor (ProC); a 58 kDa helicase; a 2 kDa genome-linked viral protein (VPg); a 24 kDa viral proteinase (Pro) and a 87 kDa RNA-dependent RNA polymerase (polymerase). RNA-2 encodes the 58 kDa and 48 kDa viral movement proteins (MP) and the large and small coat proteins (L and S). The circle at the 5' end denotes covalently-attached VPg and 'AAAA' at the 3' end denotes the poly-A tail.

Purified preparations from a natural CPMV infection can be fractionated into three kinds of particles on the basis of their buoyant density (van Kammen, 1967) (Figure 1.4). These are: RNA-1 containing particles (Bottom component), RNA-2 containing particles (Middle component) and empty particles (Top component). The proportion of Top component in a natural infection is usually less than 10%, while Middle and Bottom are found in approximately equal amounts.

The natural occurrence of Top particles shows that the presence of RNA is not necessary for capsid formation. However, comparison of the pressure stability of the three kinds of particles shows that the presence of RNA stabilizes particles. Middle and Bottom particles were found to be 50% more stable than Top at a pressure of 2.5 kbar (Da Poian et al., 1994). It was also found that the capsid proteins continued to be bound to the RNA even after protein-protein contacts were broken by pressure, highlighting the strength of these RNA-protein interactions.

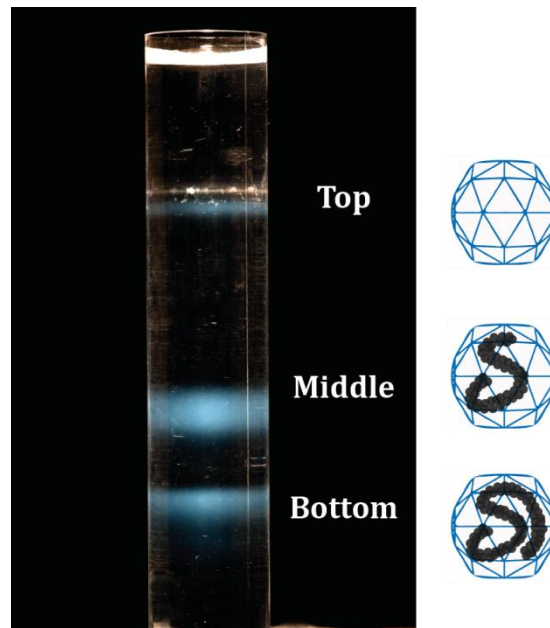


Figure 1.4 Three components of CPMV. CPMV can be separated into its three components using a density gradient. All three components have identical protein compositions but differ in their RNA contents. The Bottom component comprises RNA-1 containing particles, Middle comprises RNA-2 containing particles and Top comprises RNA-free/empty particles of CPMV. Bands visualised on the gradient are shown along with cartoons of the corresponding particles.

1.4.4 Translation in CPMV

Expression of CPMV RNA occurs via the production and subsequent processing of polyproteins, a strategy common amongst viruses. Using the host cell machinery, RNA-1 is translated from a start codon AUG at position 207 to produce a single 200 kDa polyprotein, which is processed *in cis* by the RNA-1 encoded proteinase, 24K to generate proteins for RNA replication. By contrast, initiation of translation of RNA-2 occurs at two positions, namely at AUG 161 and at AUG 512 (Holness et al., 1989), generating polyproteins of 105 kDa and 95 kDa respectively. As both these start codons are in-frame, the polyproteins generated as a result of each initiation are cleaved by 24K to yield: (i) the movement protein of 58 or 48 kDa depending on the site of initiation and (ii) the coat protein precursor VP60. VP60 is subsequently cleaved by 24K to generate coat proteins L and S (Franssen et al., 1982).

A 32 kDa proteinase co-factor (32K) encoded by RNA-1 appears to be needed for processing at the junction between the 58K/48K proteins and VP60 (Vos et al., 1988). The reason for the presence of two start codons is not fully understood, although it is speculated to be a mechanism for regulation of translation. 90% of the time, translation is initiated from AUG 512 and is thought to be a result of both reinitiation and leaky scanning by the ribosomes (Holness et al., 1989).

1.4.5 Replication in CPMV

CPMV replicates in the cytoplasm in small membranous vesicles produced from the endoplasmic reticulum (ER) (Carette et al., 2000). Replication occurs via a double-stranded RNA replicative intermediate (Lomonosoff et al., 1985). Viral RNA is first transcribed into a negative-sense RNA complement, which is used as a template for the formation of positive-sense progeny RNA. Newly synthesised progeny RNA are either used as mRNA for translation of viral proteins or are packaged within capsids to form mature virions. To the 5' untranslated regions (UTRs) of both RNA strands in the replicative intermediate is attached a VPg (28 amino acid protein encoded by RNA-1), which is thought to have a role in initiation of RNA synthesis (Lomonosoff et al., 1985).

RNA-1 replication occurs *in cis* whereas RNA-2 is replicated *in trans* (Van Bokhoven et al., 1993). Consequently, RNA-1 is capable of replicating independently (Goldbach et al., 1980). Work done in cowpea protoplasts suggests that replication and translation of CPMV RNAs are tightly linked (Wellink et al., 1994). Moreover, analysis of RNA-1 mutants shows that RNA-1 molecules function as a template only for its own proteins (Van Bokhoven et al., 1993).

Translation of the N-terminal of the 58K protein has been shown to be necessary for replication of RNA-2 as removal of AUG 161 or disruption of the reading frame downstream of this start codon effectively eliminates replication of RNA-2 (Holness et al., 1989; Van Bokhoven et al., 1993). In addition to the N-terminal region of 58K, it has been shown that both the 5' and 3' UTRs of RNA-2 are essential and sufficient for its replication (Canizares et al., 2006; Eggen et al., 1989; Rohll et al., 1993).

1.4.6 Assembly of CPMV particles

Although the structure of CPMV is known to atomic resolution, the mechanism by which sixty copies of the L and S coat proteins come together to form each capsid remains unknown. Reconstitution of CPMV particles *in vitro* has not been possible till date due to the lack of solubility of L and S in absence of strong denaturants (Wu and Bruening, 1971). *In vivo*, CPMV VLPs have been generated by co-expression of L and S from separate promoters in cowpea protoplasts (Wellink et al., 1996) and *Spodoptera frugiperda* insect cell expression systems (Shanks and Lomonosoff, 2000). However, in both cases, the yields of assembled particles obtained were low suggesting the requirement of other viral or host proteins for efficient assembly.

Given that during a natural CPMV infection, L and S coat proteins are generated upon processing of the RNA-2-encoded protein VP60 by the RNA-1-encoded proteinase 24K (Franssen et al., 1982), Saunders et al. (2009) attempted to express VLPs by mimicking this situation *in vivo* and indeed, co-expression of VP60 and 24K, first in insect cells and subsequently in plants, resulted in efficient generation of empty VLPs of CPMV, abbreviated as eVLPs. eVLPs thus generated appeared to be identical to wt CPMV from the outside and devoid of RNA on the inside, resembling natural Top component.

Furthermore, co-expression of VP60 and wt RNA-1 resulted in production of particles containing RNA-1 (Saunders et al., 2009), demonstrating the ability of 24K to cleave VP60 both when expressed independently and as a part of RNA-1. This work was the first demonstration of efficient production of CPMV VLPs without an infection. eVLPs have been discussed in detail in Section 1.8.

1.5 Applications of CPMV in nanotechnology

CPMV was the first plant virus to be successfully developed as a system for display of foreign peptides (Porta et al., 1994; Usha et al., 1993). Subsequently, CPMV has been used extensively as a template for both genetic and chemical modifications to develop CPMV as a nanoparticle for various applications in medicine and in electronics (Steinmetz et al., 2009), such as vehicles for drug delivery, carriers for imaging agents, templates for mineralization and templates for immobilization of active enzymes (Aljabali et al., 2012a; Aljabali et al., 2010b; Aljabali et al., 2012b; Steinmetz, 2010).

CPMV attracts attention as a candidate for use in nanotechnology for a number of reasons. CPMV particles can be readily obtained through infection of plants. Yields of 1 gram of CPMV per kilogram of infected leaves are obtained routinely in cowpea plants. The virus capsid is stable over a variety of reaction conditions, such as moderately high temperatures of around 60 °C, across the range of pH 4 – 9 and in a variety of organic-solvent mixtures. This level of stability increases the range of modifications that can be made to CPMV through chemical reactions. The availability of the crystal structure of CPMV (Lin et al., 1999) and infectious clones of its RNA (Liu and Lomonosoff, 2002) mean that precise changes to the CPMV capsid can be introduced both genetically by modification of cDNA sequences and chemically by modification of amino acids exposed on the surface of the capsid.

1.5.1 Genetic modification of CPMV

CPMV particles have been genetically modified successfully for presentation of foreign peptides including epitopes (Lomonosoff and Hamilton, 1999; Porta et al., 2003; Porta et al., 1996; Porta et al., 1994). Using the crystal structure of CPMV, sites for peptide insertion were determined such that the inserted peptides were surface exposed yet did not interfere with particle assembly. In most cases, the foreign peptide was inserted into the most exposed loop of the virus surface: the β B- β C loop of the S coat protein. The chimeric particles displayed 60 copies of the inserted peptide on its surface. An assessment of immunological properties of chimeric particles revealed CPMV's ability to stimulate protective immunity

demonstrating the potential utility of CPMV as a vaccine (Dalsgaard et al., 1997). However, there are some limitations on the sizes and charges of peptides that can be stably incorporated in CPMV capsids without affecting virus assembly, transmissibility and yield (Porta et al., 2003).

1.5.2 Chemical modification of CPMV

CPMV particles have been chemically modified extensively by addressing functional molecules on its exterior surface. For instance, surface lysines of CPMV have been conjugated to peptides that promote specific mineralization of metals such as FePt and CoPt, to generate mixed-metal nanoparticles for applications in nanoelectronics (Aljabali et al., 2010b). Similarly, carboxylates exposed on the surface of CPMV have been labelled with drugs such as doxorubicin to develop CPMV for drug delivery applications (Aljabali et al., 2012b).

Genetic and chemical modifications have been combined in certain cases to achieve a higher degree of flexibility. For instance, in an approach to develop CPMV as building blocks for use in material sciences, cysteine residues were genetically introduced on the outer surface of the CPMV capsid for subsequent chemical modification with thiol-selective moieties (Wang et al., 2002).

A particular attraction to use of plant viruses is that they are non-infectious to animals and humans and so can be developed for application in mammalian systems with reduced bio-safety concerns. However, toxicity and bio-availability need to be determined before deploying any nanoparticle for applications in medicine. *In vivo* studies on CPMV in mice have shown CPMV to be safe, non-toxic and naturally bio-available (Rae et al., 2005; Singh et al., 2007). When CPMV was administered to mice by oral or intravenous inoculation, CPMV was found to be stable in the gastrointestinal tract and was found to disseminate to a wide variety of tissues throughout the body, including the spleen, kidney, liver, lung, stomach, small intestine, lymph nodes, bone marrow and brain (Rae et al., 2005). CPMV particles were found to clear rapidly from blood plasma, falling to undetectable levels and accumulating in the liver and spleen by the end of 30 minutes (Singh et al., 2007). This process can be slowed down if desired, as in the case of specific

targeting to cells or tissues, by coating the particles with polyethylene glycol (PEG) or other immune masking agents (Raja et al., 2003). CPMV is internalized in endothelial cells through binding to vimentin, the intermediate filament protein present on the surface of endothelial cells (Koudelka et al., 2009)

Over the past twenty years, publications on the development of CPMV as a potential vaccine, extensive chemical modifications to the CPMV capsid and studies on the bio-availability of CPMV have highlighted the promise that CPMV holds for diverse applications in nano-technology and nano-medicine.

1.6 Limitations with wild-type (wt) CPMV

Despite several advantages of CPMV, there are some limitations with the use of naturally occurring CPMV particles. Firstly, the presence of RNA within CPMV capsids leaves little room for encapsulation of desired cargos, such as drugs and nucleic acids, limiting its application as a delivery vehicle or nano-container. Secondly, CPMV from a natural infection retains its ability to infect plants and spread in the environment. The use of such particles raises bio-safety concerns.

To address the problem of bio-containment, there have been some attempts to inactivate viral RNA in capsids by irradiation with ultraviolet (UV) light (Langeveld et al., 2001; Rae et al., 2008). Attempts have also been made to eliminate viral RNA by changing pH conditions (Ochoa et al., 2006) or by chemical treatment (Phelps et al., 2007). However, all these processes have to be carefully monitored as they risk altering the structural properties of the particles. Further, the processes that rely on inactivation of RNA do not actually remove RNA from the particles, posing limits on the space available within the capsid for loading.

There is also a regulatory concern about the introduction of nucleic acids into humans. Although CPMV cannot infect mammals, there is a possibility that its RNA could replicate if introduced into individual cells, given the similarities between CPMV and mammalian picornaviruses.

A related problem with the use of infection to produce CPMV particles is that only particles which are functional viruses, i.e. competent in terms of genome packaging

and cell-to-cell movement, can be produced in this way. Porta et al (2003) found that in order to maintain the ability to systemically infect the plant and produce high yields of chimeric particles, inserted sequences were strictly required to be shorter than 30 residues and have a pI below 8. This greatly restricts the range of modifications that can be introduced genetically, further limiting applications of these particles.

Given the limitations with the use of wt CPMV for applications in nanotechnology and promising data on production of eVLPs by processing of VP60, it was recognised that eVLPs have the potential to be a superior substitute for wt CPMV for applications in nanotechnology. The next section introduces the expression system used for production of eVLPs in plants.

1.7 Plant expression

Plants are being developed as a commercial platform for production of recombinant proteins since they offer several advantages over current established bacterial, yeast or animal cell production systems. These include high biomass, ease of scalability, cost effectiveness and a low risk of contamination with endotoxins or human pathogens (Fischer et al., 2004; Ma et al., 2003; Twyman et al., 2003). Unlike prokaryotic expression systems, plants are capable of introducing eukaryotic post-translational modifications such as glycosylation and hence, can be used for expression of complex eukaryotic-derived proteins. Another advantage with the use of plants for production of biopharmaceuticals is that products expressed in edible plant organs can be administered directly as unprocessed plant material (Sala et al., 2003).

Work described in this thesis uses plants for expression of numerous proteins including reporter proteins such as the green fluorescent protein (GFP), human antibodies and enzymes, viral proteins and virus-like particles. In all cases, expression was carried out in the model plant *Nicotiana benthamiana*. Two approaches have been used for expression of heterologous proteins in *N. benthamiana*: (i) stable transformation of the genome of the plant; (ii) transient

transformation of plant tissue. Both approaches involve vector-mediated gene transfer into plant cells using the soil bacterium *Agrobacterium tumefaciens*.

A. tumefaciens is a pathogenic bacterium that has the ability to transfer genetic material from its tumour-inducing plasmid (Ti plasmid) to its plant host. Once within the plant cell, this transferred DNA (T-DNA) targets the nucleus where it eventually integrates into the host genome (Figure 1.5). This allows the T-DNA to be transcribed by the plant cell as if it were a part of the normal complement of plant genes (Gelvin, 2005). The natural ability of *Agrobacterium* to transfer DNA into plants has been exploited in biotechnology for genetic engineering of plants. The Ti plasmid of the agrobacteria is disarmed by deletion of its T-DNA region and the T-DNA component is carried on another plasmid called the binary plasmid. The binary plasmid has the following features:

- (i) The ability to replicate in *A. tumefaciens*;
- (ii) Origin of replication for high copy number in *Escherichia coli* (*ColEI*);
- (iii) T-DNA region with the natural border sequences referred to as the left border (LB) and the right border (RB). Genes to be transferred are cloned in between the left and right borders along with their promoters, such as the 35S promoter from cauliflower mosaic virus (CaMV) and terminators, such as nopaline synthase (*nos*) terminator for expression in plants;
- (iv) A selectable marker gene for selection of transformed bacteria and in case of stable transformation, for selection of transformed plant cells. For instance, gene encoding the neomycin phosphotransferase (*npt*) II or III which confers resistance to kanamycin.

N. benthamiana was selected as the host as it is particularly amenable to agro-infiltration, with negligible damage being caused to the inoculated tissue during the process. This is particularly beneficial in case of GFP where wound-derived auto-fluorescence can interfere with quantification of expression (Sainsbury et al., 2008). For transient expression of proteins, *Agrobacterium* cultures are infiltrated into leaves of 3-4 week old plants. The gene of interest is only expressed in the infiltrated region from the time of infiltration until the leaf reaches senescence.

Transient expression enables quick testing of constructs before undertaking the time-consuming process of leaf disc regeneration for stable expression. For stable expression of proteins, leaf discs are dipped in *Agrobacterium* cultures and regenerated on agar to obtain transgenic plants. Since the gene of interest is incorporated in the genome, it is passed on to future generations.

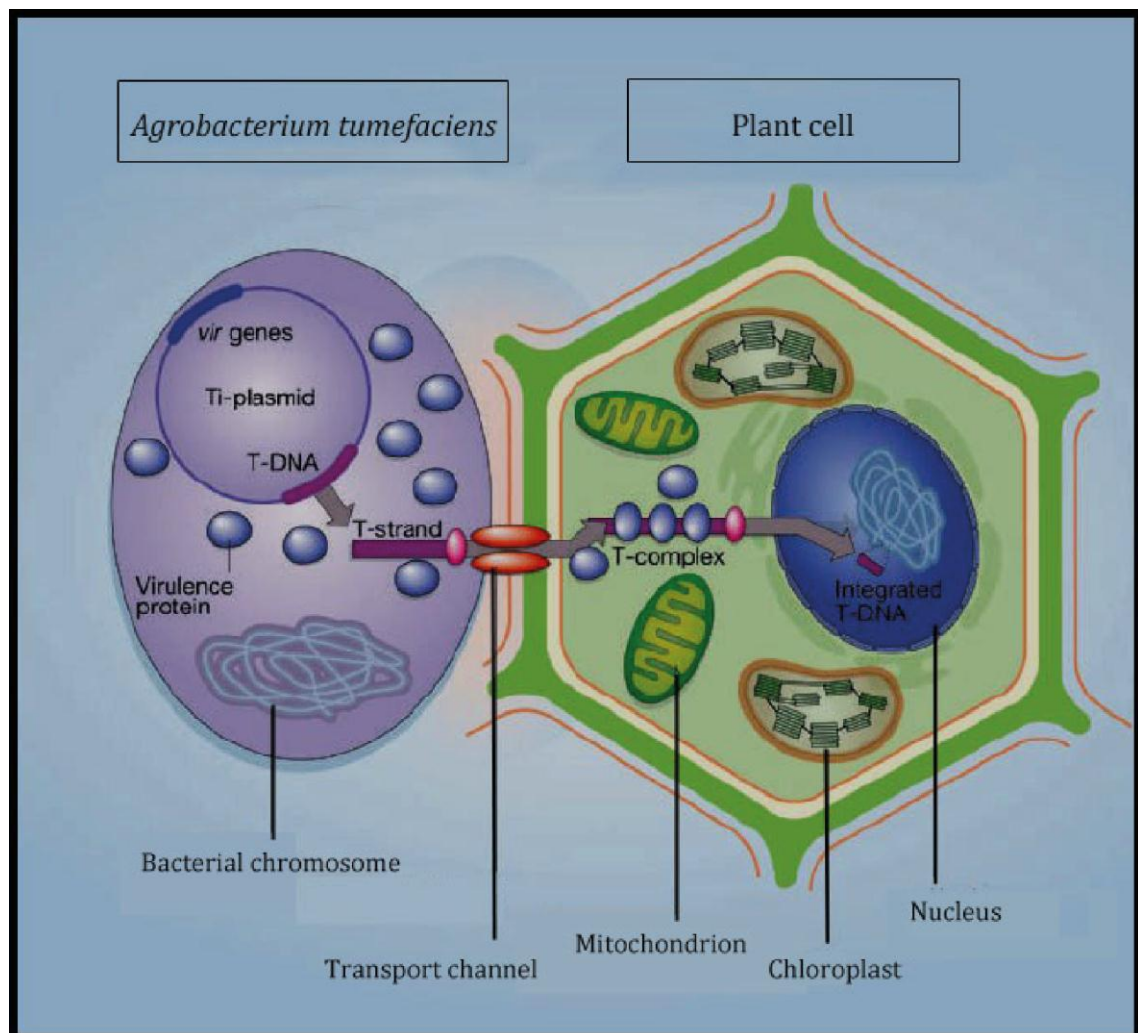


Figure 1.5 *Agrobacterium*-mediated transformation of plant cells (Gelvin, 2005). In nature, *A. tumefaciens* transfers its T-DNA to the plant cell with the help of virulence proteins. Virulence proteins target the T-complex to the nucleus of the plant cell and mediate its integration into the plant genome. For genetic engineering applications, the Ti plasmid of *Agrobacterium* is modified so that it lacks the T-DNA region but still carries the virulence genes. Genes of interest are presented on another plasmid, called the binary plasmid.

Over time, a number of strategies have been devised by researchers to improve expression of recombinant proteins in plants. A successful approach to enhance both the yield and purity is sub-cellular compartmentalization of expressed proteins. Proteins can be expressed in plants with signals that target proteins to specific compartments of the cell, such as the vacuole, chloroplast or apoplast or to the endoplasmic reticulum (ER)-secretory pathway. Trafficking proteins to a secretory pathway not only allows complex post translational modifications but also often increases protein stability and hence their levels of accumulation (Desai et al., 2010; Fischer et al., 2004).

Another approach to enhance protein expression in plants involves use of virus-encoded proteins for suppression of post-transcriptional gene silencing (PTGS). PTGS is a well-known phenomenon in plants for regulation of gene expression at the post-transcriptional level. PTGS is triggered by presence of replicating viruses, transgenes and transposons. It is mediated by small RNAs that bind to mRNAs in a sequence-specific manner leading to their degradation, thus hampering foreign gene expression (Baulcombe, 2002).

PTGS is thought to have evolved in plants as a mechanism for defence against viruses (Waterhouse et al., 2001). As counter-defence, viruses have evolved to express suppressors of silencing (Vance and Vaucheret, 2001; Voinnet et al., 1999). Viral suppressors of silencing are proteins that interfere with various steps of the silencing pathway leading to its suppression and hence, an up-regulation of gene expression. For this reason, suppressors of silencing are exploited in biotechnology for enhancement of expression. Suppressors of silencing that have been used to effectively prevent/reverse PTGS include HcPro from potyviruses (Anandalakshmi et al., 1998), P19 from tombusviruses (Voinnet et al., 2003) and 2b protein from cucumber mosaic virus (Brigneti et al., 1998). The work described in this thesis has been conducted using P19, where required, for enhancement of expression.

1.7.1 Plant viral vectors

Plant viral vectors exploit the natural ability of plant viruses to replicate and express proteins in plant cells. Such vectors deploy engineered viral genomes to

deliver genes to plants for transient expression of heterologous proteins, with or without causing an infection. The use of viruses has the advantage that any sequence inserted into a virus vector is highly amplified during replication. Also, because the gene does not get incorporated in the plant genome, it does not form a heritable trait and is thus contained.

First-generation viral vectors were based on replication-competent full-size genomes, with the gene of interest being expressed in addition to all other genes of the functional virus. This 'full-virus' strategy had several limitations: (i) there were size limits on the sequences that could be inserted while retaining viability; (ii) the inserted sequences were susceptible to mutations during virus replication; and (iii) there were bio-containment concerns since the vectors encoded fully functional viruses. These limitations led to the design of second-generation viral vectors based on deconstructed viral genomes. These vectors only encoded viral elements essential for efficient expression of foreign sequences. Genes essential for virus replication, assembly and movement, if required, were supplied *in trans* (Gleba et al., 2007).

Over the last two decades, CPMV has served as the basis for the development of a variety of replicating (based on the full-virus as well as the deconstructed virus strategy) and non-replicating virus vectors suitable for the production of heterologous proteins in plants (Sainsbury et al., 2010a). Significant milestones in its development as an expression vector have been summarized in the section below.

1.7.2 CPMV-based plant expression systems

CPMV-based expression systems initially focused on modifying the sequence of RNA-2 to express foreign genes along with full-length or deleted versions of RNA-2 (Canizares et al., 2006; Sainsbury et al., 2008). To achieve amplification of expression, modified RNA-2 vectors were co-inoculated with wt RNA-1 (to provide the machinery for replication and polyprotein processing) and in case of vectors based on deleted RNA-2, also with a suppressor of silencing. The replicating viral-vector approach led to high levels of expression but had several disadvantages.

Firstly, vectors based on full-length RNA-2 were capable of causing an infection thereby raising bio-containment issues. Secondly, inserted sequences were often lost upon systemic spread of the virus. In case of heteromeric proteins encoded on two separate RNA-2 vectors, segregation of vectors occurred upon systemic spread and hence, co-expression was restricted to the inoculated tissue (Sainsbury et al., 2008).

To overcome the above problems, vectors based on deleted RNA-2 were modified to abolish their replication by introducing two mutations in the 5' UTR of RNA-2. Mutations of the start codon at position 161 (AUG161) and another out-of-frame start codon at position 115 (AUG115) destroyed the ability of the vector to replicate and unexpectedly, led to a massive increase in protein expression levels in transient expression studies (Sainsbury and Lomonosoff, 2008). Since high level expression was achieved due to enhanced translation, this system was named CPMV- '*Hypertrans*' or CPMV-*HT*. The CPMV-*HT* system was subsequently refined through the creation of the 'pEAQ' series of expression plasmids (Sainsbury et al., 2009). Using these plasmids, the gene of interest can be positioned between the modified 5' UTR and the 3' UTR of RNA-2 in a single step using either restriction enzyme-based cloning or GATEWAY® recombination.

Today, the CPMV-*HT* system has been successfully used for high-level expression of a number of proteins, including single proteins (such as GFP), heteromeric proteins (such as IgG antibodies), active enzymes (such as the human gastric lipase) and complex virus-like particles (such as bluetongue virus VLPs). While existing CPMV-*HT* vectors provide a quick, easy and inexpensive eukaryotic transient expression system, there is still a need to engineer this system for controlled simultaneous expression of multiple proteins in transient systems and stable expression of proteins in transgenic systems.

Although CPMV eVLPs were first expressed in insect cell expression systems, higher expression levels were achieved in plants (Saunders et al., 2009). Therefore, subsequent production of eVLPs was carried out in plants by deploying the CPMV-*HT* expression system to achieve high-level expression of VP60 and 24K.

1.8 CPMV empty virus-like particles or eVLPs

The availability of eVLPs has added a whole new dimension to applications of CPMV in nanotechnology since it is now possible to internally modify CPMV particles as well as modifying their external surface. eVLPs produced by co-expression of VP60 and 24K (Section 1.4.6) have a number of advantages over wt CPMV:

- (i) There are no bio-safety concerns involved with the use of eVLPs since they are RNA-free.
- (ii) The space inside eVLPs is available for encapsulation of desired cargos, such as drug molecules, metal ions, nucleic acids, etc.
- (iii) eVLPs do not need to be functional viruses since they are not produced via an infection and are not required to spread, encapsidate nucleic acid or disassemble. So, the range of modifications that can be introduced genetically to both its inner and outer surfaces is potentially greater, being limited only by the need to maintain particle assembly.

The ability to both encapsulate material within eVLPs and to chemically or genetically modify the external surface of the capsid opens up the possibility for use of eVLPs in targeted delivery of therapeutic/diagnostic agents. Encapsulation of agents such as drugs would have the additional advantage of protection from breakdown in plasma.

Since eVLPs have only recently been available, not much is known about the optimum methods for loading of eVLPs. From studies on wt CPMV, it is known that CPMV particles become permeable to caesium ions at pHs above 7.5 (Lin and Johnson, 2003). Penetration of Cs⁺ is thought to occur via funnel-shaped pores at each 5-fold axis of CPMV. The diameter of the pore at the narrow-end, which is at the outer surface of the particle, is about 7.5 Å (Lin et al., 1999). Current loading strategies rely on simple diffusion of molecules through this pore. However, studies on controlling permeability of eVLPs are on-going.

The potential application of eVLPs in magnetic hyperthermia for treatment of cancer has been demonstrated by generation of iron oxide-eVLPs (Aljabali et al.,

2010a). Incubation of eVLPs with ferrous and ferric ions, under reaction conditions that favour formation of iron oxide, generates eVLPs loaded with iron oxide, which can then be modified chemically by attachment of targeting peptides to the surface of the eVLP capsid (Figure 1.6). Thermal and magnetic properties of iron oxide-eVLPs generated in this way, are being characterised with the objective of developing them for heat-induced destruction of cancerous cells. Using a similar approach, eVLPs are also being developed for drug targeting by loading eVLPs with the cancer drug gemcitabine and chemically or genetically attaching targeting peptides to surface of the eVLP capsid (A. Aljabali, pers. comm.).

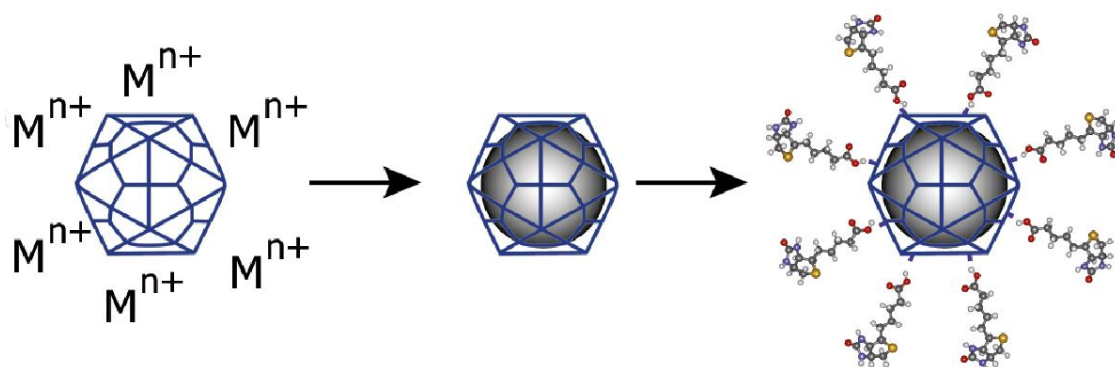


Figure 1.6 Schematic diagram depicting development of iron oxide-eVLPs (Aljabali et al., 2010a). Ferrous and ferric ions (M^{n+}) are loaded into eVLPs by diffusion through the pore at the 5-fold axis. Reaction conditions are changed to favour formation of iron oxide (shown in grey), which remains trapped within eVLPs. Iron oxide-loaded eVLPs are subsequently chemically modified for targeting to specific cells.

1.9 Aims of this thesis

Work presented in this thesis was undertaken with the general objective of developing CPMV eVLPs for various applications in nanotechnology. During the course of this work, two fundamental processes in the CPMV lifecycle – viral replication and encapsidation, were also studied. This was followed by work on developing CPMV-based expression systems for stable expression of proteins, including CPMV eVLPs themselves. The aims of my thesis are as follows:

(1) Production and characterisation of CPMV eVLPs

Methods for large-scale expression and purification of eVLPs will be described along with quantitative and qualitative characterisation of eVLPs. This will aid genetic and chemical modifications of eVLPs for various applications in bio-nanotechnology.

(2) Study of replication and encapsidation of RNA in CPMV

The requirements for RNA packaging in CPMV will be presented based on work done with various mutants. In addition to providing an insight into replication and encapsidation of RNA in wt CPMV, this will help develop methods to package nucleic acids of choice within eVLPs, thereby increasing the range of its applications.

(3) Creation of transgenic plants producing eVLPs

Attempts to create stable transgenic lines of *N. benthamiana* for large-scale production of eVLPs will be described. Initial work done with GFP will be presented followed by work on other pharmaceutically valuable proteins and eVLPs.

(4) Development of plant expression vectors based on CPMV RNA-1

For use in transient and transgenic expression systems, generation of plant expression vectors based on CPMV RNA-1 will be described, along with their comparison with previously existing CPMV-*HT* vectors.

Chapter 2: Materials and Methods

2.1 Media, Buffers and Solutions

Recipes of growth media, buffers and solutions used for the work described in this thesis are summarised in Table 2.1. All chemicals and reagents were purchased from Sigma Aldrich (Suffolk, U.K.).

Name	Recipe
Luria-Bertani (LB) media	10 g/L Bacto-tryptone, 10 g/L NaCl, and 5 g/L Yeast extract, pH adjusted to 7
LB-agar	As LB with 10 g/L agar added
SOC	20 g/L tryptone, 5 g/L yeast extract, 0.58 g/L NaCl, 0.19 g/L KCl, 2.03 g/L MgCl ₂ , 2.46 g/L magnesium sulphate 7-hydrate, 3.6 g glucose
Murashige and Skoog (MS)-agar	0.8% w/v agar, MS salts, 3% sucrose in 3 mM MES buffer, pH adjusted to 5.7
Pre-callusing media	MS-agar as above with the following additional ingredients: 1 µg/ml BAP (benzyl aminopurine); 0.1 µg/ml NAA (naphthalene acetic acid) and organic supplements (0.5 µg/ml nicotinic acid, 0.5 µg/ml pyridoxine, 0.5 µg/ml thiamine, 0.5 µg/ml glycine)
Rooting media	Pre-callusing media with appropriate antibiotic selection and without the hormones BAP and NAA
Antibiotics	100 µg/ml Kanamycin (in water) 50 µg/ml Rifampicin (in methanol) 500 µg/ml Carbenicillin (in water)
MMA	10 mM MES pH = 5.6, 10 mM MgCl ₂ , 100 µM Acetosyringone
1 x Tris-borate EDTA (TBE)	89 mM Tris-HCl pH=7.6, 89 mM boric acid, 2 mM EDTA
TEN/NET buffer	100 mM NaCl, 10 mM Tris-HCl pH = 7.5, 1 mM EDTA

Table 2.1 Recipes of media, buffers and solutions

5 x Formaldehyde gel running buffer (FGRB)	100 mM MOPS, 40 mM sodium acetate, 5mM EDTA, pH adjusted to 7 with 2N NaOH
Protein extraction buffer	50 mM tris-HCl pH = 7.25, 150 mM NaCl, 2 mM EDTA, protease inhibitor cocktail tablet
0.1 M sodium phosphate buffer pH=7	305 ml of 0.2 M Na ₂ HPO ₄ , 195 ml of 0.2 M NaH ₂ PO ₄ , 500 ml of Milli-Q water
1 x phosphate buffered saline (PBS)	140 mM NaCl, 80 mM Na ₂ HPO ₄ and 15 mM KH ₂ PO ₄ , 27 mM KCl, pH adjusted to 7.4 with HCl
Western blot transfer buffer	120 mM Tris-HCl, 40 mM glycine, 0.1% (w/v) sodium dodecyl sulphate (SDS), 20% (v/v) methanol
Western blot blocking solution	5% (w/v) skimmed milk powder in 1x PBS; 0.05% (v/v) Tween-20
6 x sample buffer for agarose gels	0.025 g xylene cyanol, 0.025 g bromophenol blue, 0.025 g orange-G dissolved in 60% (v/v) glycerol in 1x TBE
4 x sample buffer for protein gels	NuPAGE® LDS sample buffer (Novex®)
Coomassie staining solution	0.25% (w/v) Coomassie Brilliant Blue R, 40% (v/v) methanol, 7% (v/v) acetic acid
Destaining solution	15% (v/v) methanol; 7.5% (v/v) acetic acid

Table 2.1 Recipes of media, buffers and solutions

2.2 Vectors

cDNA copies of full-length CPMV RNA-1 and RNA-2 were provided by constructs pBinPS-1-NT and pBinPS-2-NT respectively (Liu and Lomonosoff, 2002). For enhancing expression from vectors that did not encode a suppressor of silencing, P19 was co-expressed from pBIN61-P19 (Voinnet et al., 2003).

For sub-cloning ‘genes of interest’, pM81-FSC-POW (Sainsbury et al., 2009) was used, which allows for expression of genes with the modified 5’ UTR and 3’UTR of RNA-2. For plant expression, the gene of interest was transferred to the appropriate ‘pEAQ’ vector (Sainsbury et al., 2009). pEAQ vectors are a series of

small binary vectors tailored for expression of proteins in plants. The various pEAQ vectors and their features are listed in Table 2.2.

Plasmid Name	Accession No.	Features
pEAQ- <i>HT</i>	GQ497234	Designed for high-level expression of a 'gene of interest' in plants. Its T-DNA comprises: <ul style="list-style-type: none"> • the CPMV-<i>HT</i> expression cassette with a polylinker to insert the gene of interest; • the suppressor of gene silencing P19; • nptII to confer resistance to kanamycin.
pEAQexpress	GQ497230	Designed for cloning multiple CPMV- <i>HT</i> expression cassettes in the same vector for transient expression in plants. Its T-DNA comprises: <ul style="list-style-type: none"> • a multiple cloning site for insertion of multiple expression cassettes digested using enzymes <i>PacI</i> and <i>AscI</i>; • the suppressor of gene silencing P19.
pEAQselectK	GQ497231	Designed for expression from a CPMV- <i>HT</i> expression cassette in the absence of a suppressor of silencing. Its T-DNA comprises: <ul style="list-style-type: none"> • a multiple cloning site for insertion of the expression cassette; • nptII to confer resistance to kanamycin.
pEAQspecialK	GQ497232	Designed for expression from a CPMV- <i>HT</i> expression cassette in the presence of a suppressor of silencing. Its T-DNA comprises: <ul style="list-style-type: none"> • a multiple cloning site for insertion of the expression cassette; • the suppressor of gene silencing P19; • nptII to confer resistance to kanamycin.
pEAQspecialKm	GQ497233	Best suited for stable expression of proteins in whole plants. Same as pEAQspecialK apart from a mutation in suppressor of gene silencing: P19/R43W (Saxena et al., 2011).

Table 2.2 pEAQ plasmids and their properties

2.3 Recombinant DNA methodology

Standard molecular biology procedures, as described by Sambrook et al. (1989), were followed for cloning and the manufacturer's instructions were followed wherever possible.

2.3.1 Polymerase Chain Reaction (PCR)

Primers for amplification of DNA (listed in Appendix I) were ordered from Sigma Aldrich. Reactions were set up using high-fidelity polymerase Phusion (New England Biolabs or NEB) as follows:

Phusion HF buffer (5x)	4.0 μ l
dNTPs (10 mM)	0.5 μ l
Forward primer (10 μ M)	1.0 μ l
Reverse primer (10 μ M)	1.0 μ l
Template DNA (20-25 ng)	1.0 μ l
Phusion polymerase	0.2 μ l
Water	12.3 μ l
	20 μl

The following program was run to amplify DNA:

Step	Setting	Duration
1	98 °C	2:00 mins
2	98 °C	0:15 mins
3	65 °C	0:30 mins
4	72 °C	1:00 mins
5	Go to step 2	24 times
6	72 °C	5:00 mins
7	10 °C	Forever

PCR products were analysed by agarose gel electrophoresis and purified using PCR clean up kits (Qiagen). Reactions for colony/plasmid screening were set up using the GoTaq® Green Master Mix (Promega).

2.3.2 Digestion

For digestion of DNA fragments and plasmids, restriction enzymes supplied by NEB were used and digests were performed as per the manufacturer's recommendations. In case of double digests with incompatible enzymes, the following universal digestion buffer was used:

5x cuts all buffer: 100 mM Tris pH 7.5, 500 mM KCl, 35 mM MgCl₂, 14.6 mM β-mercaptoethanol, 0.5 mg/ml BSA in 10 ml H₂O

2.3.3 Ligation

DNA ligations were carried out using the Quick ligation™ kit (NEB) and reactions were set up as recommended by the manufacturer.

2.3.4 Transformation

- One Shot® TOP10 chemically competent *E. coli* (Invitrogen) was used for propagation of recombinant plasmids. *E. coli* was grown in LB media with appropriate antibiotic selection and transformed using heat shock.
- *A. tumefaciens* strain LBA4404 (Hoekema et al., 1983) was used for plant transformation. *A. tumefaciens* was grown in LB with appropriate antibiotic selection and transformed by electroporation.

2.3.5 Purification of plasmids

For purification of plasmids from bacterial cultures, QIAprep spin Miniprep kits (Qiagen) were used. Plasmids were analysed by agarose gel electrophoresis.

2.3.6 Sequencing

Routine sequencing of plasmid DNA for verification of clones was done using the BigDye® Terminator v3.1 Cycle Sequencing Kit (Applied Biosystems). Reactions were set up according to the manufacturer's instructions using the appropriate DNA template and primers and run in a thermal cycler. These 'ready reactions' were then sent for sequencing reads at the Genome Analysis Centre (TGAC), Norwich. Reads were analysed using Vector NTI version 11 (Invitrogen).

2.3.7 Site-directed mutagenesis (SDM)

Point mutations in plasmids were introduced using Geneart® Site-directed mutagenesis system (Invitrogen) and the manufacturer's instructions were followed closely.

2.3.8 Agarose gel electrophoresis of DNA fragments

For analysis of PCR products, digested DNA fragments and plasmids, DNA was separated on 0.8% (w/v) agarose gels in 1x TBE buffer. Routinely, samples were mixed with 6x loading buffer and migrated on gels at 70 V for 1 hour. HyperLadder™ I (Bioline) was used as the standard DNA marker in the range of 0.2 – 10 kb. DNA bands on gels were stained by placing the gel in a 0.5 µg/ml solution of ethidium bromide for 10 mins. Bands were visualised in UV light (wavelength = 302 nm) and imaged using Gene Snap (Syngene).

2.4 Plant growth and transformation

2.4.1 Plant growth

N. benthamiana and *V. unguiculata* (cowpea) plants were grown in glasshouses maintained at 25°C with supplemental lighting to provide 16 hours of daylight. Plants were watered daily.

2.4.2 Transient expression of proteins in plants (Agro-infiltration)

A. tumefaciens suspensions were prepared by pelleting cells from an overnight culture and resuspending them in MMA buffer to make a solution of final optical density at 600 nm (OD_{600}) = 0.4. For co-expression of two constructs, solutions of OD_{600} = 0.8 were prepared and mixed in 1:1 ratio to result in a final OD_{600} = 0.4 for each construct. The suspensions were left at room temperature for 0.5–3 hours prior to infiltration to allow acetosyringone in the buffer to induce virulence of agrobacteria.

The agro-suspension was pressure-infiltrated into young fully expanded leaves of 3-4 week old *N. benthamiana* plants with the help of a syringe (for small scale

expression; 1-10 plants) or a vacuum pump (for large scale expression; 10-100 plants). For syringe infiltration, a sterile needle was used to wound the leaf surface followed by infiltration of the *Agrobacterium*-suspension into the leaf through the wound using a 1 ml sterile syringe. For vacuum infiltration, the plant was inverted into a beaker containing the agro-suspension and placed under negative pressure of 170 mbar (25 inches of Hg relative to atmospheric pressure) for 60 secs to suck air out of intracellular spaces. The vacuum was gently released allowing the solution to infiltrate leaves by occupying intracellular spaces. Infiltrated leaves were harvested from 1-12 days post infiltration (dpi), depending on the nature of the study.

2.4.3 Stable expression of proteins in plants

For integration of T-DNA from pEAQ vectors into the *N. benthamiana* genome for transgenic expression, leaf discs were transformed with *A. tumefaciens* cultures harbouring the desired pEAQ construct using the 'leaf disc method', first described by Horsch and Klee (1986).

Briefly, young fully expanded leaves of *N. benthamiana* were rinsed in 5% (v/v) bleach and 70% (v/v) ethanol before punching out discs of about 1 cm diameter using a sterile cork borer. Leaf discs were placed on pre-callusing media in sterile plates sealed with micropore tape and transferred to a growth chamber. After 24 hours, discs were dipped in appropriate *A. tumefaciens* cultures (freshly grown overnight without antibiotics) and placed back on pre-callusing plates in the growth chamber. After 48 hours, leaf discs were transferred to fresh plates with pre-callusing media, this time with 500 µg/ml carbenicillin and 100 µg/ml kanamycin for selection of transformed tissue. Shoots that appeared on calluses after 3-5 weeks were transferred to rooting media to allow roots to form. Once the roots developed, plantlets were moved to soil and placed in the glasshouse. Young leaves were harvested from regenerated plants for analysis of expressed proteins from time to time.

To obtain subsequent generations of transgenic plants by self-fertilisation, flowers were taped just as they started developing and seeds were collected from the seed

Pods that developed from the taped flowers. Transgenic seeds were plated on MS-agar and placed in the growth chamber for 4-6 weeks to allow development of seedlings. Seedlings were subsequently transferred to soil for generation of plants. In some cases, antibiotic selection (100 µg/ml kanamycin) was used on MS-agar plates to select for the presence of the transgene (untransformed seedlings 'bleach' due to their sensitivity to kanamycin). In other cases, seedlings were grown in absence of antibiotic selection and screened subsequently for presence of the transgene using other methods, such as visualisation under UV light for detection of GFP or immunodetection of proteins.

2.5 Production of wt CPMV

2.5.1 Propagation

To grow CPMV, 12 day old *V. unguiculata* plants were infected by mechanical inoculation of primary leaves with 5 µg of purified CPMV virions per leaf. Infected primary and trifoliolate leaves were harvested on 12-15 dpi and frozen at -20 °C.

2.5.2 Purification

To purify virus from frozen leaf tissue, a method adapted from van Kammen (1967) was used. Briefly, frozen plant tissue was homogenised in 3 volumes of 0.1 M sodium phosphate buffer pH 7.0. The homogenate was filtered through two layers of muslin and clarified by centrifugation at 13,000 g for 20 min at 4 °C. To the supernatant, 0.7 volumes of a 1:1 mixture of chloroform and butanol was added, mixed and centrifuged at 6000 g for 20 min at 4 °C. After centrifugation, the clear aqueous phase (containing CPMV) was carefully transferred to a glass beaker and particles were precipitated at 4 °C overnight by adding a solution of PEG 6000 (final concentration of 4% (w/v)) and NaCl (final concentration of 0.2 M). The PEG precipitate was obtained by centrifugation for 20 min at 13,000 g and resuspended thoroughly in 10 mM sodium phosphate buffer pH=7 (0.5 ml buffer per g of leaf tissue). CPMV was purified further by centrifugation at 27,000 g for 20 min to obtain the supernatant and then at 118,700 g for 2 hours and 15 mins to obtain a pellet of purified virions.

On most occasions, this was followed by an additional clearing spin at 16,000 g for 15 mins using the bench-top centrifuge. For further purification of virions, Float-a-lyzer® dialysis devices (Spectra/Por®) and/or PD-10 desalting columns (Amersham Biosciences) were used.

2.5.3 Fractionation into Top, Middle and Bottom components

Density gradient centrifugation was used to separate the different nucleoprotein components of CPMV on the basis of their buoyant density. The density gradient was prepared using 30%, 40%, 50% and 60% (w/v) solutions of Nycodenz® (Axis Shield) in 10 mM sodium phosphate buffer pH=7.0. 2.5 ml of each Nycodenz® solution was layered in a thin-walled ultracentrifuge tube using the technique of under-layering (low density end first). 1 ml of the viral suspension (at 10 mg/ml CPMV) was layered on top of the gradient. The gradient was centrifuged at 163,500 g for 23 hours to allow viral components to move down the gradient until the point was reached where density of the medium equalled density of the virus. The separated viral components were visualised by shining a beam of white light directly through the length of the tube (Figure 1.4) and Top, Middle and Bottom fractions were removed through the side of the tube using a syringe.

Nycodenz® was removed from particle suspensions by ultracentrifugation of each fraction at 130,000 g for 3 hours followed by re-suspension of the pellet in 100 µl buffer (10 mM sodium phosphate buffer pH = 7). This was repeated three times to remove all traces of Nycodenz®.

2.6 Production of CPMV eVLPs

2.6.1 Expression

eVLPs were produced by co-expression of the CPMV coat protein precursor VP60 and the viral proteinase 24K, either from constructs pEAQ-*HT*-VP60 and pEAQ-*HT*-24K (Saunders et al., 2009) or from pEAQexpress-eVLP (described in Section 3.3.1), using agro-infiltration (as per Section 2.4.2) in *N. benthamiana*. Leaves were harvested on 5-7 dpi and processed to obtain eVLPs.

2.6.2 Purification

For purification of eVLPs from infiltrated *N. benthamiana* leaves, the method described in Section 2.5.2 for purification of wt CPMV was used with the following modifications: (i) Leaf tissue was processed fresh and not frozen; (ii) 2% (w/v) polyvinyl-polypyrrolidone (PVPP) was added to the 0.1 M sodium phosphate buffer used for homogenisation of leaves; (iii) the chloroform/butanol step was omitted; (iv) the ultra-centrifugation spin was done for 2.5 hours. The reasons behind each modification are explained in Section 3.2.

2.7 Extraction and analysis of viral RNA

2.7.1 Extraction of RNA from virus particles

50-100 µg CPMV was purified in TEN/NET buffer and incubated at 60 °C for 5 mins in presence of 2% (w/v) SDS to denature the viral coat proteins. To the denatured sample, two volumes of a 1:1 mixture of phenol and chloroform was added and mixed by vortex. The mixture was centrifuged at 16,000 g in a bench-top centrifuge for 10 mins. After centrifugation, the aqueous layer was transferred carefully to a fresh tube and re-extracted using two volumes of phenol/chloroform. To precipitate RNA from the aqueous fraction, 0.2 volumes of 3 M sodium acetate at pH 5.5 and 2.5 volumes of ice-cold 100% ethanol were added and the sample was kept at -20 °C overnight. The sample was centrifuged at 16,000 g for 15 mins at 4 °C to recover the RNA pellet. The pellet was washed with 70% (v/v) ethanol, air-dried and resuspended in a small volume (5-10 µl) of sterile water.

2.7.2 Electrophoresis of viral RNA

Extracted RNA was analysed by agarose gel electrophoresis under denaturing conditions. A 1.2% agarose gel was prepared in 1x FGRB and 2.2 M formaldehyde. RNA samples were prepared as follows:

Extracted RNA (upto 30 µg)	4.5 µl
5x FGRB	2.0 µl
Deionised formamide	10.0 µl
12.3 M Formaldehyde	3.5 µl
	<hr/>
	20 µl
	<hr/>

Samples were heated at 65 °C for 10 mins to denature RNA and placed on ice immediately. 0.5 µl of ethidium bromide (10 mg/ml) and 2 µl of Orange-G loading dye were added to the sample to enable detection of RNA and the sample was loaded on the gel. In parallel, 5 µl of Transcript RNA marker from Sigma was prepared as above and run as a standard. Samples were electrophoresed at 60 V for 1.5–2 hours. RNA bands were visualised under UV light (wavelength = 302 nm) and imaged using Gene Snap (Syngene).

2.8 Analysis of protein expression

2.8.1 Protein extraction and detection

Infiltrated leaf tissue was homogenised in three volumes of protein extraction buffer. The lysate was clarified by centrifugation and proteins were separated by sodium dodecyl sulphate polyacrylamide gel electrophoresis (SDS-PAGE) under reducing or non-reducing conditions using 12% (w/v) Bis-Tris NuPAGE® gels (Invitrogen). Post electrophoresis, proteins were detected by one or both of these methods:

- **Coomassie staining**

To visualise separated proteins, Instant blue Coomassie stain (Expedeon) was applied to gels for 15 minutes followed by de-staining in sterile water for 1-2 hours.

- **Western blotting**

To detect specific proteins, gels were electro-blotted onto nitrocellulose membranes in transfer buffer. Target proteins were detected using antibodies raised against that specific protein (primary antibody) and a horseradish peroxidase (HRP)-conjugated antibody raised against the

primary antibody (secondary antibody). Non-specific sites on the membrane were blocked using blocking solution and binding of antibodies was detected using chemiluminescence. Table 2.3 lists primary and secondary antibodies used for work described in this thesis.

Antigen	Antibody
CPMV coat protein	Rabbit anti-CPMV polyclonal serum G49
Human IgG Fc region	Goat anti-human IgG (Fc specific)-HRP conjugate (Sigma)
Rabbit IgG	Goat anti-rabbit IgG-HRP conjugate (Amersham Biosciences)

Table 2.3 Antibodies used for western blots

2.8.2 Analysis of expression of GFP

- **Visualisation under UV light**

GFP expression in infiltrated and transformed *N. benthamiana* plants was monitored with a 100 AP handheld UV lamp (Blak Ray ®).

- **Fluorescence assay**

GFP fluorescence measurements were made using a protocol described by Richards et al. (2003). Soluble protein extracts were diluted 100-fold in 0.1 M Na₂CO₃ and loaded onto a fluorescently neutral black 96-well plate (Greiner bio-one). Recombinant GFP from Clontech was used to generate standard curves. Excitation (395 nm) and emission (509 nm) maxima were matched to Clontech's GFP and read using a SPECTRAmax spectrofluorometer (Molecular Devices). Measurements were done in triplicate to account for experimental variation and averaged to give a final value for each sample.

2.8.3 Analysis of expression of VLPs

- **Transmission electron microscopy (TEM)**

TEM was routinely used to assess the integrity of VLPs. Samples were diluted to a conc. of approximately 0.1 mg/ml in sterile water (to dilute

phosphate in the sample buffer). Droplets of the sample were placed on carbon-coated copper grids (400 mesh; obtained from Agar Scientific). Grids were negatively stained by application of a droplet of 2% (w/v) uranyl acetate and dried after 20 secs using filter paper. Grids were visualized using a Technai F20 transmission electron microscope (FEI UK Ltd.) at 200 kV and imaged using a bottom-mounted AMT XR60 CCD camera (Deben UK Ltd.).

- **UV/Vis spectroscopy**

Photometric measurements of VLPs were made using either a Lambda 25 UV-Vis spectrophotometer with UV WinLab software (Perkin Elmer) or a NanoVue spectrophotometer (GE Healthcare). The Beer-Lambert law was used to calculate VLP concentration from absorbance measurements, using molar extinction coefficients (ϵ) determined by van Kammen (1967) and shown in Table 2.4.

	Absorbance maxima at wavelength (λ)	Molar extinction coefficients (ϵ)
wt CPMV	260 nm	8.1 ml mg ⁻¹ cm ⁻¹
CPMV Bottom	260 nm	10.0 ml mg ⁻¹ cm ⁻¹
CPMV Middle	260 nm	6.2 ml mg ⁻¹ cm ⁻¹
CPMV Top or eVLPs	280 nm	1.28 ml mg ⁻¹ cm ⁻¹

Table 2.4 Molar extinction coefficients of wt CPMV and eVLPs

- **Bradford assays**

VLP concentrations were determined by a colorimetric protein assay using Bradford reagent (Sigma Aldrich). Bradford assays enable quantification of proteins in presence of nucleic acids and hence can be used to quantify both wt CPMV and eVLPs on the basis of coat proteins present in each sample. Serial dilutions of standards (wt CPMV in the range of 0.1-1.5 mg/ml) and the unknown samples were pipetted in a 96-well clear plate. To each well, 250 μ l of Bradford reagent was added, mixed and incubated at room temperature for 15 mins. Absorbance of the protein-dye complex was

measured at 595 nm using SPECTRAmax spectrophotometer (Molecular Devices). An absorbance versus concentration curve was plotted for wt CPMV standards and used for calculations of concentrations of unknown VLP samples.

- **Agarose gel electrophoresis of particles**

Intact VLPs were analysed on 1% (w/v) agarose gels in 1x TBE (pH=7.6) due to the fact that the CPMV capsid has a net negative charge at pH 7.6 which causes particles to migrate towards the anode in an electric field (Steinmetz et al., 2007). Routinely, 5-10 µg VLPs were mixed with 6x loading buffer and electrophoresed at 60 V for 2.5 hours. To visualise particles, their coat proteins were fixed by placing the gel in Coomassie Blue staining solution for 20 mins followed by destaining overnight. Alternatively, to check for presence of nucleic acids within particles, the gel was placed in a 0.5 µg/ml solution of ethidium bromide for 10 mins and visualised in UV light (wavelength = 302 nm).

- **SDS-PAGE**

VLPs were prepared in LDS sample buffer and denatured by incubation at 98 °C for 5 mins. Denatured samples were separated on 12% (w/v) Bis-Tris NuPAGE® gels (Invitrogen) according to the manufacturer's instructions. Post electrophoresis, coat proteins from the VLPs were detected by staining with Coomassie blue or by western blotting, as described in Section 2.8.1. Known amounts of wt CPMV (usually 1 µg, 2 µg and 4 µg) were run in parallel and used as standards to quantify VLPs by eye or by densitometry.

2.9 Photography

A Nikon D700 digital camera with a 60 mm macro lens was used for image acquisition under visible light or, for the detection of GFP, under UV illumination. Images were edited using Photoshop CS4 (Adobe).

Chapter 3: Results I

Production and Characterisation of CPMV eVLPs

3.1 Introduction

Production of apparently RNA-free particles of CPMV without an infection, as reported by Saunders et al. (2009), was a big leap for CPMV technology. Even though all evidence suggested that eVLPs thus produced were RNA-free versions of wt CPMV (which in a natural infection is the Top component of CPMV), conclusive experiments needed to be performed. It was important to establish that on the outside, the capsid of eVLPs was similar to wt CPMV and that inside, eVLPs were genuinely empty i.e. no heterologous RNA from the host cell got packaged within the capsid. The lack of any RNA within capsids is unusual as most VLPs are known to encapsidate random host nucleic acids if their own viral RNA is not available. The availability of potentially genuinely empty VLPs of CPMV was recognised as being very valuable for applications in nanotechnology and therefore, detailed studies on their production and characterisation were undertaken.

Initial work showing that eVLPs can be produced in insect cells and plants (Saunders et al., 2009) looked promising in terms of the quality of eVLPs but their yield and purity was relatively low. eVLPs were produced in *N. benthamiana* by co-expression of the coat protein precursor VP60 and the viral proteinase 24K by deploying the two constructs: pEAQ-*HT*-VP60 and pEAQ-*HT*-24K (Figure 3.1) and the yields obtained were estimated to be around 0.1-0.2 g/kg fresh weight tissue (FWT) (Saunders et al., 2009). This was found to be true when small-scale infiltrations were done (3-4 plants) but when production was scaled-up, yields dropped to as low as 0.01 g/kg FWT. In addition to the scale of the experiment, expression levels were seen to vary with the age of the plants, size of leaves and the time of the year. It was known that environmental factors affected expression levels of heterologous proteins in plants (K. Saunders and E. Thuenemann, pers. comm.) but parameters for optimal expression had not been established.

This chapter describes work aimed at defining the conditions for optimal expression and purification of eVLPs by working at three levels: particle purification, plant expression and scale of production. In addition, this chapter examines eVLPs on the basis of their structure and composition and compares and contrasts eVLPs to wt CPMV. Table 3.1 summarizes fundamental differences between wt CPMV and eVLPs, which have been exploited in characterisation of eVLPs described later in this chapter.

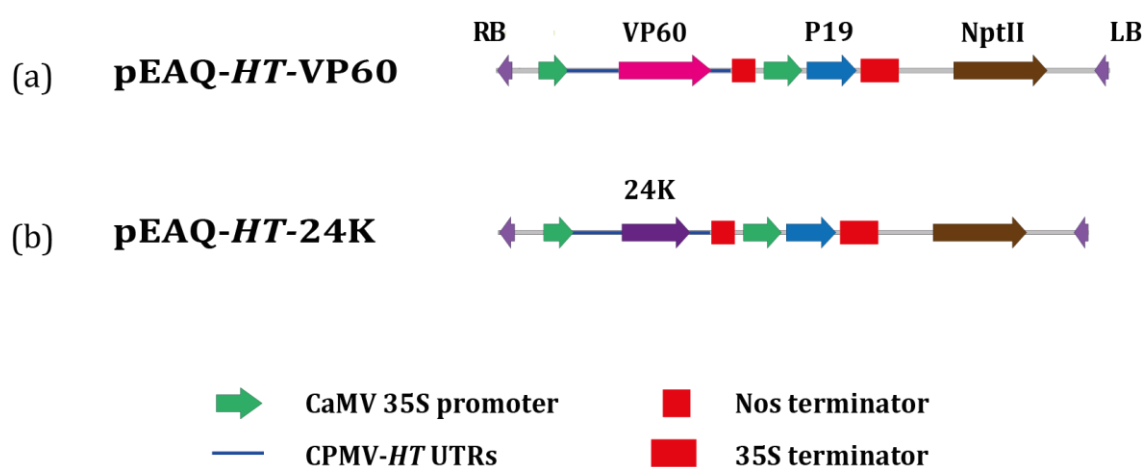


Figure 3.1 Constructs used for expression of eVLPs in plants (Saunders et al., 2009). Schematic diagrams of the T-DNA regions of constructs used for the expression of VP60 (a) and 24K (b) in *N. benthamiana*. RB and LB represent right and left borders respectively. Both constructs were harboured in agrobacteria and the two bacterial suspensions were mixed in 1:1 ratio prior to infiltration. Particles were extracted from infiltrated leaves on 6 dpi.

	wt CPMV	eVLPs
Host system	Produced in cowpea	Produced in <i>N. benthamiana</i>
Method of expression	Expressed by viral infection of plant	Expressed by agro-infiltration of leaves
Composition	More than 90% of the particles contain RNA	Particles don't contain any nucleic acids
Density	Highly dense particles due to presence of RNA; high sedimentation coefficients	Less dense due to absence of RNA; lower sedimentation coefficients
Stability	Very stable and compact as RNA makes stabilizing bonds with positively charged pockets in the capsid	Less stable due to absence of negatively charged RNA

Table 3.1 Fundamental differences between wt CPMV particles and eVLPs

3.2 Optimisation of particle purification protocols

The method for extraction of eVLPs from infiltrated *N. benthamiana* leaves was based on the protocol for extraction of wt CPMV from infected cowpea leaves (van Kammen, 1967; van Kammen and de Jager, 1978) as described in Section 2.5. However, since eVLPs differ from wt CPMV in a number of ways (as listed in Table 3.1), including their stability, modifications to the extraction protocol were investigated. Samples at every stage of the extraction process were analysed by immunodetection to identify where particles were being lost (Figure 3.2) and changes were made to the protocol accordingly. Modifications made to the extraction protocol and specific reasons for each modification have been explained in Table 3.2. In summary, steps that led to degradation of eVLPs were omitted and steps that removed impurities from the extract were added to the protocol.

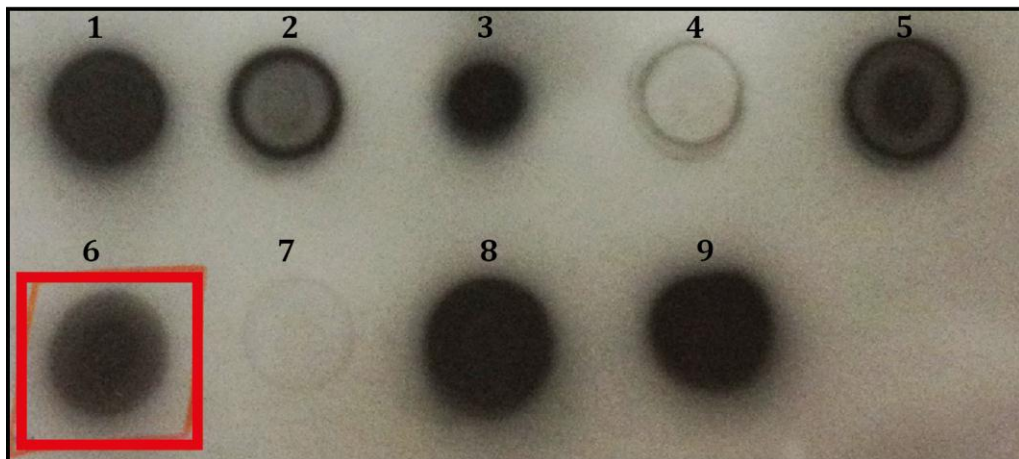
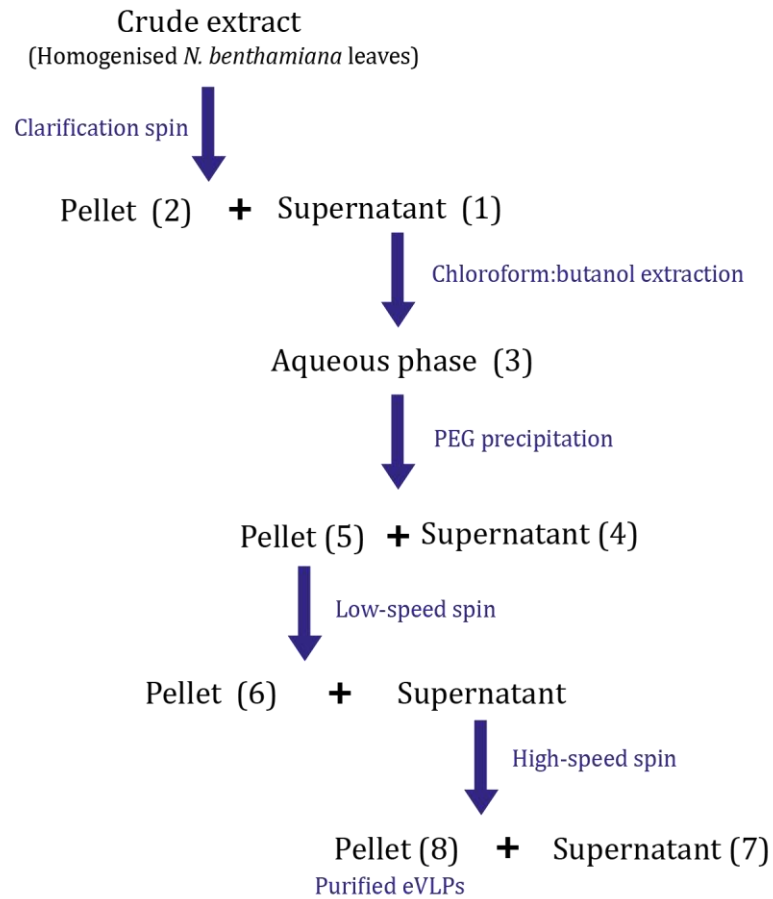


Figure 3.2 Immunodetection of eVLPs. 10 μ l samples from each step of the extraction process were blotted on nitrocellulose and incubated with anti-CPMV antibody for immunodetection of CPMV coat proteins. Dots 1-8 correspond to fractions, as numbered in the flow-diagram. Dot 9 corresponds to 200 ng of purified eVLPs, used as the positive control. In particular, eVLPs were being lost in the pellet after the low-speed spin (Fraction 6).

Original protocol	Modification	Reason
Leaf tissue was harvested and frozen.	Leaf tissue was processed fresh.	eVLPs degrade upon freezing and thawing.
Leaves were homogenised in 0.1 M sodium phosphate buffer.	Leaves were homogenised in 0.1M sodium phosphate buffer with 2% PVPP (polyvinyl-pyrrolidone).	PVPP binds to phenolics and polysaccharides from <i>N. benthamiana</i> , thereby reducing impurities in the prep. Since PVPP is insoluble in phosphate buffer, it pellets during the first spin and doesn't affect subsequent steps.
A 1:1 chloroform-butanol mixture was used to remove chlorophyll and other plant proteins from the extract.	This step was omitted.	Chloroform and butanol denature proteins including coat proteins from the eVLP capsid. wt CPMV survives this step due to the presence of RNA that stabilises the capsid.
PEG precipitation was either done for 2 hours at room temperature or overnight in the cold room.	PEG precipitation was always done in the cold room overnight (12-16 hours).	2 hours at room temperature was not enough to precipitate all eVLPs.
After PEG precipitation, the pellet was quickly resuspended and spun at 27,000 g to remove impurities from the sample.	After PEG precipitation, the pellet was resuspended thoroughly by vortexing, shaking and vigorous pipetting before the 27,000 g spin.	eVLPs were being lost in the pellet after the spin at 27,000 g. This indicates that the PEG precipitate was not being resuspended completely prior to the spin.
The ultra-centrifugation was done for 2 hrs and 15 mins.	The centrifugation time was increased to 2 hrs and 30 mins.	The sedimentation coefficient of eVLPs (58 S) is lesser than that of the wt CPMV particles (115 S for CPMV-Bottom and 95 S for CPMV-Middle).

Table 3.2 Modifications made to the original extraction protocol to enhance yield and purity.

By making all the changes listed in Table 3.2, loss of particles during extraction was minimised. In particular, omission of the protein denaturation step involving the chloroform/butanol treatment increased recovery of eVLPs by 50% (Figure 3.3). This is consistent with work published on other viruses where the use of chloroform and butanol in virus purification caused loss of yield and affected relative amounts of virus components (Markham, 1962). Moreover, it is already known that in purification of wt CPMV, the chloroform and butanol step considerably decreases the proportion of empty particles (van Kammen, 1967).

Some other modifications were made to the original protocol but these either did not improve the yield or even reduced it. These modifications included: changes to PEG/NaCl concentration, centrifugation through a 40% (w/v) sucrose cushion and changes to the durations of incubations or several centrifuge spins.

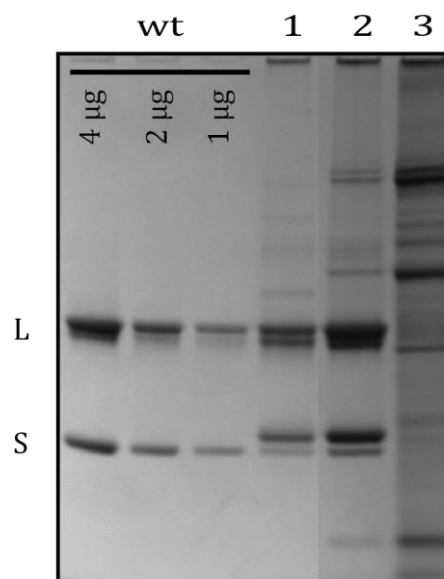


Figure 3.3 Effect of organic solvents on eVLP recovery. eVLPs extracted from the same amount of leaf tissue, with (Lane 1) and without (Lane 2) the organic clarification step, were denatured by heat-incubation and analysed by separation of coat proteins using SDS-PAGE and subsequent staining with Coomassie blue. Indicated amounts of wt CPMV were run as standards and the crude extract was run in Lane 3. Bands for L and S coat proteins have been indicated. Differences in the sizes of bands for S are due to differences in the processing of the C-terminus of the S coat protein which will be discussed in more detail in Section 3.6.1.

3.3 Optimisation of the plant expression system

3.3.1 Optimisation of expression constructs

Originally, expression of eVLPs was achieved by co-infiltration of leaves with a 1:1 mixture of two *Agrobacterium* strains, one harbouring the plasmid pEAQ-*HT*-VP60 and the other pEAQ-*HT*-24K (Figure 3.1) (Saunders et al., 2009). To ensure efficient co-expression, each strain had to be infiltrated at an OD₆₀₀ of at least 0.8 so that the final OD₆₀₀ of each construct in the mixture was 0.4. This made the inoculum dense and difficult to infiltrate. This also increased the amount of bacterial proteins being delivered to the plant, therefore putting the plant under greater stress and increasing contaminants in the host cell. Previous studies on co-expression of proteins, conducted using the yellow fluorescent protein (YFP) and cyan fluorescent protein (CFP) (Montague et al., 2011), have shown that even by mixing equal amounts of two cultures, it cannot be guaranteed that every plant cell would receive both strains in sufficient amounts. Hence, there would always be a proportion of cells receiving only one strain resulting in production of only one of the two proteins (VP60 or 24K) but no eVLPs.

To improve eVLP yields by solving the issues mentioned above, genes for VP60 and 24K were cloned within the T-DNA of a single expression vector. pEAQexpress (Sainsbury et al., 2009) was modified to create pEAQexpress-eVLP (Figure 3.4) using a two-step cloning procedure. First, the expression cassette for 24K, consisting of the 35S promoter, the 5' UTR, gene encoding VP60, the 3' UTR and the nos terminator, was amplified from pEAQ-*HT*-24K and inserted in the restriction sites *Asi*SI and *Mlu*I of pEAQexpress. The plasmid thus generated was then modified further by insertion of the expression cassette for VP60 (amplified from pEAQ-*HT*-VP60) using the restriction sites *Pac*I and *Asc*I. The resultant plasmid, pEAQexpress-eVLP, was verified by sequencing and transformed into *A. tumefaciens* for subsequent expression in plants.

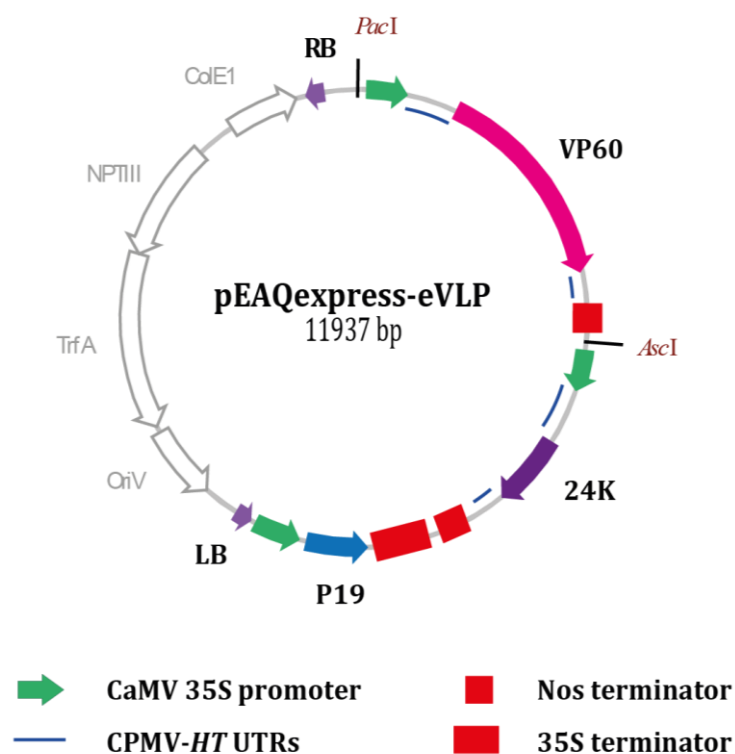


Figure 3.4 Schematic representation of the construct designed for eVLP expression. pEAQexpress-eVLP was constructed for expression of VP60 and 24K from a single T-DNA. RB and LB represent right and left borders respectively.

To assess the eVLP yields obtained from expression with pEAQexpress-eVLP, agrobacteria cultures harbouring this construct were infiltrated at $OD_{600} = 0.4$ into *N. benthamiana*. In parallel, the original constructs, pEAQ-HT-VP60 and pEAQ-HT-24K were co-expressed by syringe infiltration of plants from the same batch with a 1:1 solution of agrobacteria harbouring each construct (at final $OD_{600} = 0.4$ each). Leaves from both sets of infiltrations were harvested on 6 dpi and the same amount of leaf tissue (in terms of FWT) was processed to obtain eVLPs in both cases. Analysis of purified particles using SDS-PAGE showed that infiltration of leaves with pEAQexpress-eVLP resulted in a remarkable increase in eVLP yield and a noticeable reduction of contaminants in the final prep. in comparison to co-infiltrations conducted using two separate constructs (Figure 3.5). Therefore, pEAQexpress-eVLP was used for all subsequent expression of eVLPs.

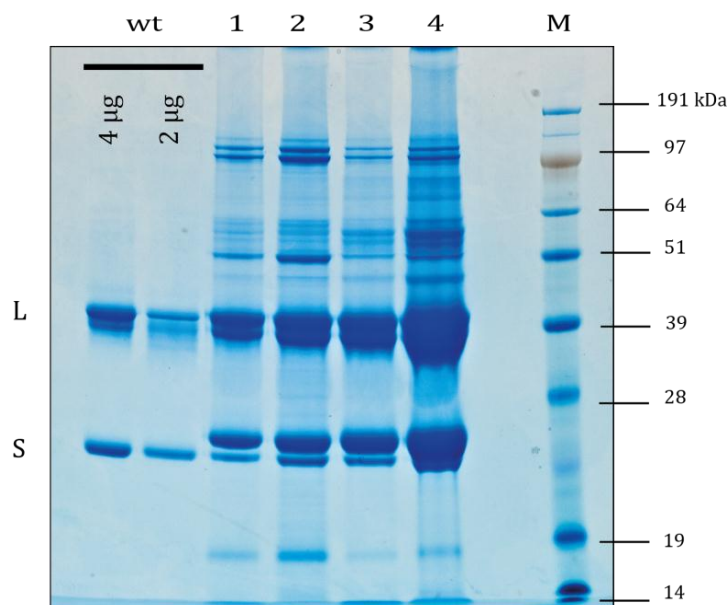


Figure 3.5 Analysis of eVLP expression. Particles purified from same amounts of leaf tissue infiltrated with agrobacteria harbouring different constructs were analysed using SDS-PAGE. Samples were run as follows:

- wt:** Indicated amounts of wt CPMV particles run as a standard
- 1:** eVLPs produced by co-expression of pEAQ-*HT*-VP60 and pEAQ-*HT*-24K; plants in **small pots**
- 2:** eVLPs produced by co-expression of pEAQ-*HT*-VP60 and pEAQ-*HT*-24K ; plants in **big pots**
- 3:** eVLPs produced by expression of **pEAQexpress-eVLP**; plants in **small pots**
- 4:** eVLPs produced by expression of **pEAQexpress-eVLP**; plants in **big pots**
- M:** Protein Marker

Bands for L and S are indicated. Differences in the sizes of bands for S in wt CPMV and eVLPs are due to differences in its processing and will be discussed later (Section 3.6.1). Expression levels were estimated from the intensity of bands. From this gel, comparisons can be made between constructs used (lane 1 compared with lane 3; lane 2 compared with lane 4) and sizes of pots used (lane 1 compared with lane 2; lane 3 compared with lane 4).

3.3.2 Optimisation of plants used for infiltration

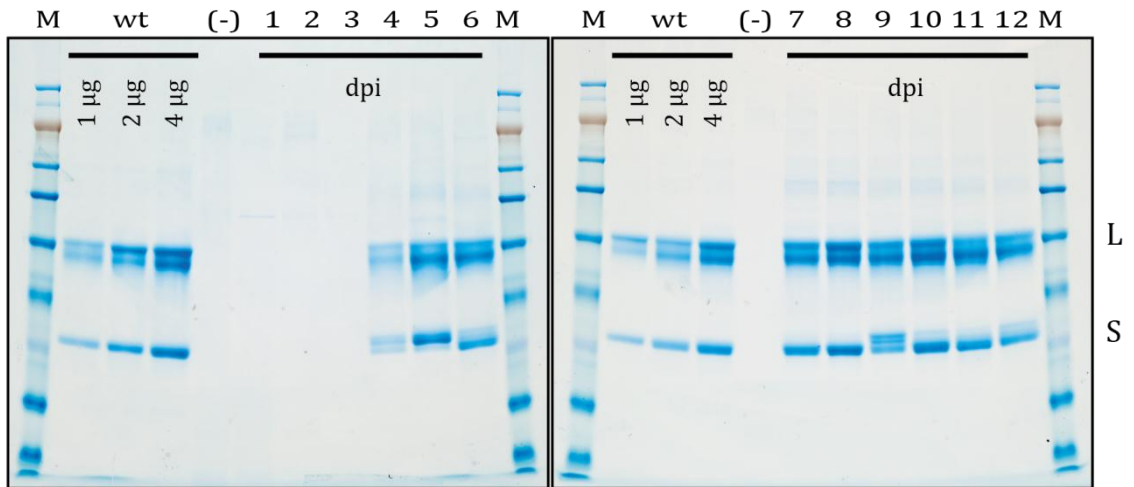
Expression of eVLPs in different *N. benthamiana* plants was monitored and it was found that the youngest fully expanded leaves of 4-week old plants express best. *Agrobacterium* suspensions diluted to an OD₆₀₀ of 0.4 for infiltration gave the best yields with the least agrobacterial contaminants in the prep. Plants that were grown in bigger pots showed better expression levels (Figure 3.5). In general, healthier plants yielded more eVLPs since their leaves were bigger and thicker. Expression levels decreased as plants went into flowering and dropped dramatically at plant senescence.

Expression of eVLPs in cowpea was investigated since wt CPMV naturally infects cowpea and grows to high titres (usually 1 g/kg FWT) in cowpea. It was found that eVLP expression in cowpea by agro-infiltration was almost a tenth of the expression achieved in *N. benthamiana*. This is likely to be due to the reduced ability of agrobacteria to transform cowpea (Bakshi et al., 2011). In addition, syringe infiltration of cowpea leaves was harder as they are thicker and waxier.

3.3.3 Optimisation of time of harvest

To determine the time after infiltration required for optimal expression of eVLPs, a time-course was conducted over 12 days. To this end, three leaves each of twelve *N. benthamiana* plants were infiltrated with pEAQexpress-eVLP. As controls, two plants were infiltrated with the empty vector pEAQexpress. From 1-12 dpi, three independent leaves (approximately 3 g FWT), each from different infiltrated plants selected randomly, were harvested daily and processed using the standard protocol for particle purification. Purified samples were stored at 4°C and subsequently analysed using SDS-PAGE (Figure 3.6). Detectable levels of eVLPs were found from 4 dpi onwards and levels were observed to increase steadily until day 7. Optimal expression was achieved from 6-10 dpi and the same level of expression was maintained until plant senescence.

(a)



(b)

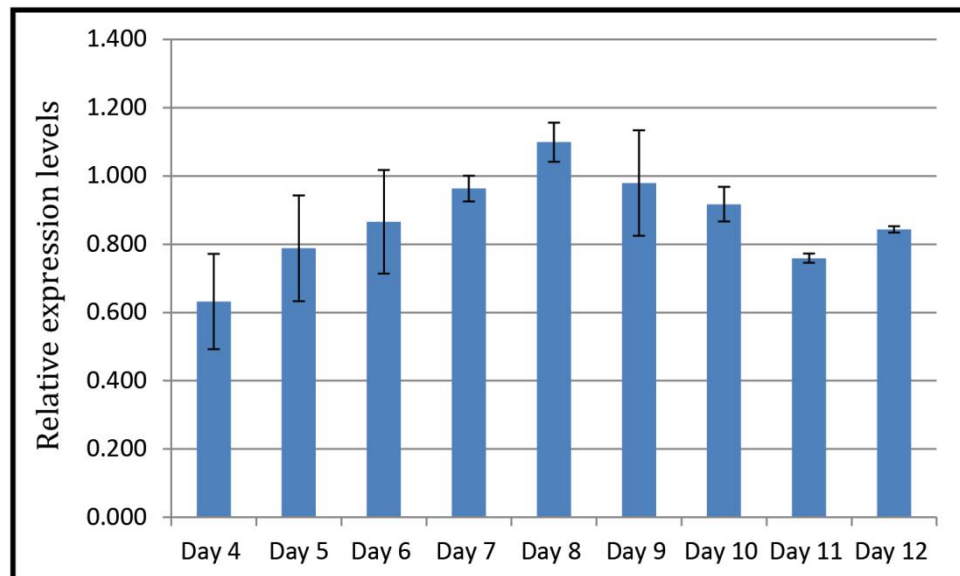


Figure 3.6 eVLP expression over time. (a) eVLPs purified from leaf tissue harvested daily from 1-12 dpi (Lanes 1-12) were denatured by heat-incubation and separated using SDS-PAGE. Amounts of wt CPMV run as standards and bands obtained for L and S have been indicated. **(b)** Relative expression levels, estimated from intensity of bands on the gel using GS-800 calibrated densitometer (Bio-Rad), are shown. Results shown are combined results from measurements of all the bands for L and S and show expression relative to 4 µg wt CPMV loaded on the same gel.

3.4 Scale-up of production

Large-scale production of proteins involves infiltration of hundreds of grams of leaf tissue. Although syringe infiltration is an effective method for infiltration of *N. benthamiana*, it is too labour-intensive. Hence, the alternative approach of vacuum-mediated infiltration was adopted for large-scale production of eVLPs. The idea behind this approach was to use negative pressure to draw air out of intra-cellular spaces in leaves, making agro-infiltration easy and quick. By using this system, whole plants could be infiltrated in under two minutes.

To ensure plant health and expression levels were not compromised by vacuum infiltration as compared to syringe infiltration, the two methods were initially compared for using GFP expression. *Agrobacterium* cultures harbouring the plasmid pEAQ-HT-GFP (Sainsbury et al., 2009) were infiltrated both using a syringe and using the vacuum system and plants were compared. It was found that neither plant health nor expression levels were affected by the use of vacuum. In fact, the area of leaves infiltrated with culture was greater when the vacuum system was used (Figure 3.7). In addition, vacuum infiltration was quicker and less tedious enabling infiltration of more tissue in less time. Vacuum infiltration was then extended to eVLPs enabling production of milligram quantities of eVLPs from infiltration of 10-100 plants with ease.

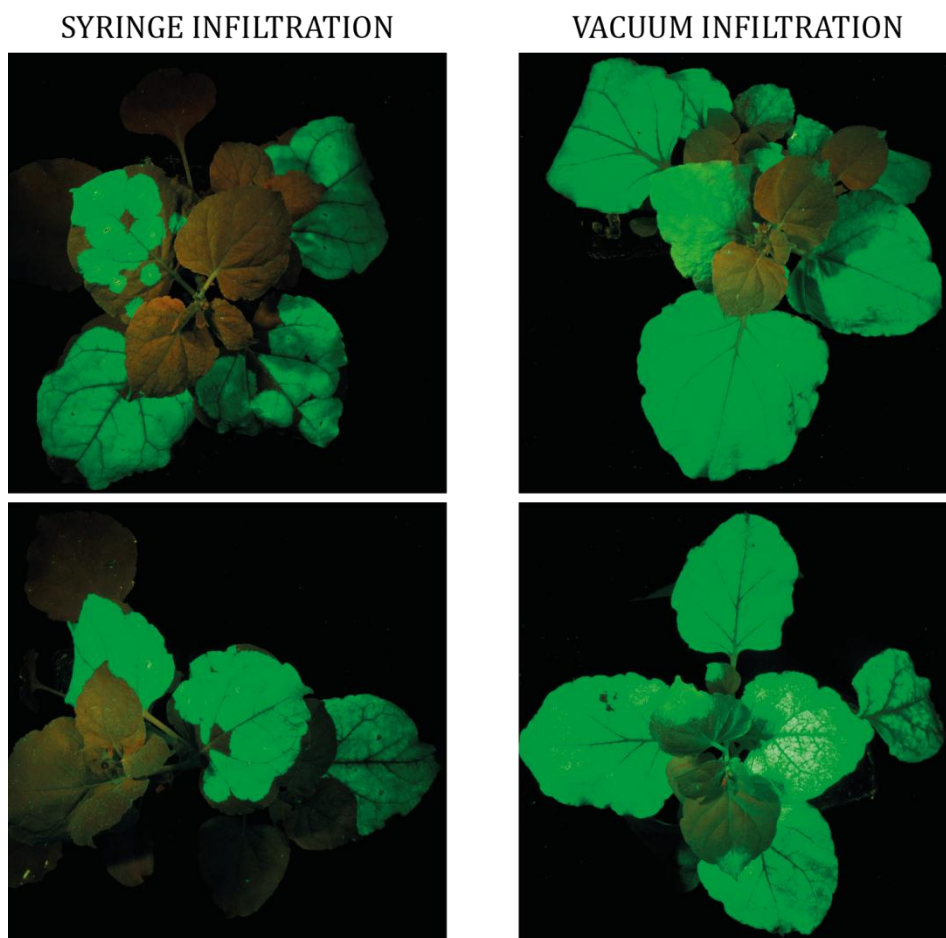


Figure 3.7 Syringe vs. vacuum-infiltration of GFP. Expression of GFP in 4-week old *N. benthamiana* plants infiltrated with the vector pEAQ-HT-GFP (Sainsbury et al., 2009) using a syringe (left column) and vacuum (right column).

In another approach to scale-up eVLP production, *N. benthamiana* callus was grown in specialized immersion bio-reactors (Michoux et al., 2011) and vacuum-infiltrated with *Agrobacterium* cultures harbouring construct pEAQexpress-eVLP for eVLP expression (Figure 3.8). Preliminary results on expression of eVLPs looked promising. Plant growth conditions and precise eVLP expression levels are currently being characterized by Mr. Sherwin Barretto and Dr. Franck Michoux at the Imperial College, London. This method has the potential to be used for infiltration of hundreds of grams of *N. benthamiana* tissue in one go.



Figure 3.8 Vacuum infiltration of *N. benthamiana* biomass. Around 100 g of *N. benthamiana* tissue was grown in specialized bio-reactors (shown above) under sterile conditions and infiltrated with *Agrobacterium* cultures harbouring pEAQexpress-eVLP using vacuum infiltration techniques. Analysis of levels of eVLP expression and feasibility of this approach is being conducted at the Imperial College, London.

3.5 Current eVLP yields

Upon expression using the new construct pEAQexpress-eVLP (Section 3.3) and vacuum infiltration methods (Section 3.4) and subsequent purification using the modified protocol (Section 3.2), eVLP yields in excess of 0.3 g/kg FWT were achieved. This is at least 2-fold more than what was previously reported (Saunders et al., 2009). On some occasions, eVLP yields of up to 0.5 g/kg FWT have also been obtained owing to healthier plants. This is nearly half of the average titre obtained from a natural virus infection in cowpea and therefore very impressive for expression from a non-replicative vector.

Currently, eVLP expression is carried out on a scale of 30-40 plants (approximately 100-150 g FWT) resulting in generation of 20-40 mgs of eVLPs per batch.

3.6 Characterisation of eVLPs

3.6.1 SDS-PAGE

As a routine technique to examine particles, wt CPMV and eVLP particles were denatured by incubation at 98°C for 5 mins and separated on polyacrylamide gels. Bands of approximately 39 and 22-25 kDa were seen corresponding to the L and S coat proteins respectively (Figure 3.9). The intensity of both bands was similar showing that both L and S were present in equal amounts.

The L coat protein generated two bands of similar size upon SDS-PAGE (Figure 3.9). This was surprising as differently processed forms of L had never been previously observed. To investigate this further, both bands were analysed by mass spectrometry which identified both bands to be the L coat protein and 100% identical to each other. Subsequently, SDS-PAGE was done in presence of reducing agents, such as beta-mercaptoethanol in the samples and now only one band was detected for L. So, it was concluded that, unlike the two forms of S generated by differential processing of the protein, the two bands for L are seen on the gel due to the presence/absence of disulphide bonds between cysteine residues of the L coat protein.

Slow (S_s) and fast (S_f) electrophoretic forms of S coat protein (described in Section 1.4.2) produced distinct bands upon separation by SDS-PAGE due to differences in their molecular weights. In wt CPMV, the S coat protein was seen to be present in its fast-migrating form producing a band of approximately 22 kDa whereas in eVLPs, the S coat protein was predominantly in the slow-migrating form producing a band of approximately 25 kDa (Figure 3.9). The reason for this difference is attributed to the age of the sample. It is known that S coat protein gets converted from S_s to S_f during the course of a natural infection (Niblett and Semancik, 1969). Since wt CPMV was harvested from infected leaf tissue during the late stages of infection, the S coat protein was only present in its fast-migrating form in wt particles.

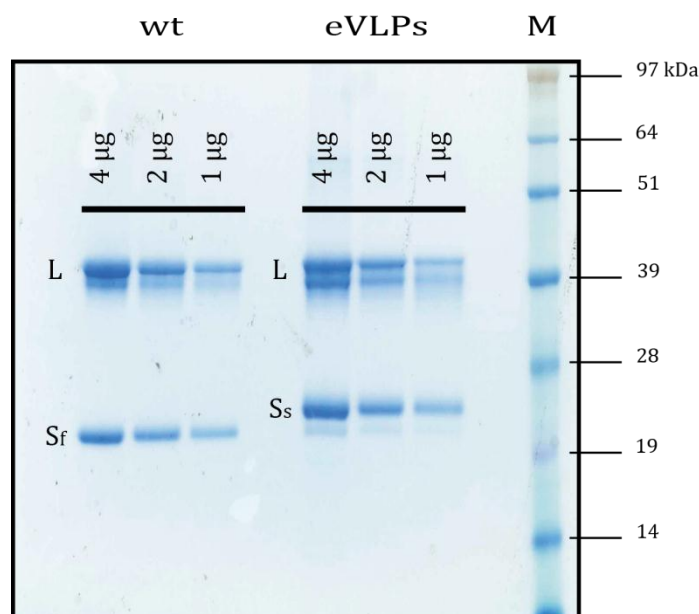


Figure 3.9 SDS-PAGE of wt CPMV and eVLPs. Indicated amounts of wt CPMV and eVLPs were denatured by heat-incubation and separated on polyacrylamide gels using SDS-PAGE. Two bands of approx. 39 kDa were seen for the L coat protein. The S coat protein was predominantly seen in its fast-migrating form S_f (approx. 22kDa) in wt CPMV and in its slow-migrating form S_s (approx. 25 kDa) in eVLPs.

3.6.2 UV-Vis spectrophotometry

Analysis of the UV/Vis spectrum of wt CPMV shows absorption at 260 nm due to the presence of RNA. In absence of RNA, as in the case of eVLPs, a peak is produced at 280 nm due to the absorbance of aromatic amino acids such as tyrosine, tryptophan and phenylalanine present in the coat proteins of CPMV. An additional shoulder at 292 nm is seen in eVLPs due to the absorption profile of tryptophan residues (Figure 3.10).

Absorbance measurements at 280 nm were routinely used for calculations of eVLP concentrations using the molar extinction coefficient for CPMV-Top ($1.28 \text{ ml mg}^{-1} \text{ cm}^{-1}$). However, this method had the limitation that measurements could not be taken for very dilute eVLP samples. Also, the presence of other protein impurities in the sample influenced absorption and concentration calculations.

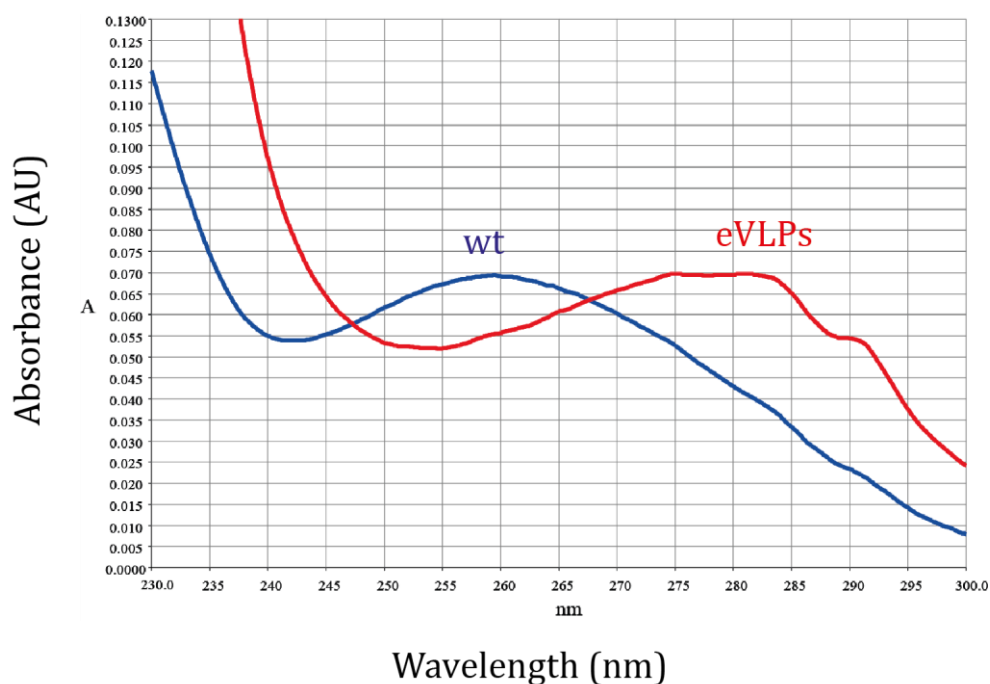


Figure 3.10 UV/Vis spectrophotometry. UV-Vis spectra of wt CPMV and eVLPs are shown in blue and red respectively.

3.6.3 Native gel electrophoresis

Native gel electrophoresis of virus particles in an agarose matrix is a technique routinely used for characterization of chemically-modified virus particles (Steinmetz et al., 2007) as this compares intact virus particles on the basis of their size and charge. Particles are electrophoresed on agarose under native conditions and analysed by either coomassie-staining (to detect the viral coat proteins) or ethidium bromide-staining (to intercalate any encapsulated RNA) as described in Section 2.8.3. Here, native gel electrophoresis was used to compare and contrast wt CPMV and eVLPs.

For consistency, the results shown in this section were obtained using preparations of wt CPMV and eVLPs that only contained the fast form of CPMV, i.e. C-terminally processed form of the S coat protein. In all the preparations used, the C-terminal peptide was cleaved off, either naturally by ageing or by proteolysis using chymotrypsin (Niblett and Semancik, 1969).

3.6.3.1 Coomassie-staining of wt CPMV and eVLPs

When separated on agarose gels and stained with Coomassie blue, wt CPMV generated three bands for Bottom, Middle and Top components due to differences in each component's mass and charge. On the other hand, eVLPs generated a single band showing homogeneity between eVLPs (Figure 3.11a). The migration of Top component of wt CPMV appeared slightly retarded as compared to eVLPs even though CPMV-Top and eVLPs have the same mass and charge. This difference in migration is believed to be due to the presence of Bottom and Middle components in the wt CPMV mixture. When purified Top component is run in parallel, it migrates exactly like eVLPs.

3.6.3.2 Ethidium bromide-staining of wt CPMV and eVLPs

When particles were separated on agarose and stained with ethidium bromide for identification of nucleic acids, two bands were seen in the wt CPMV sample, for RNA-1 and RNA-2 in Bottom and Middle fractions respectively. No band was seen in case of eVLPs reiterating the absence of RNA from eVLP capsids (Figure 3.11b).

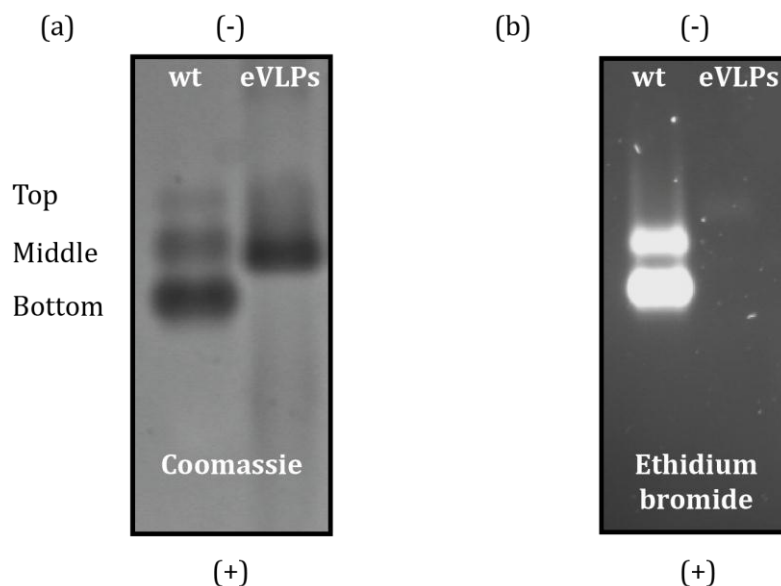


Figure 3.11 Native gel electrophoresis of wt CPMV and eVLPs. Approximately 10 μ gs each of wt CPMV and eVLPs were separated on 1% agarose gels and stained with Coomassie blue (a) or ethidium bromide (b). Both gels were imaged under UV light.

3.6.4 TEM

eVLPs were visualised under the TEM to assess their integrity, appearance and approximate size. TEM imaging of eVLPs showed intact monodisperse particles of 28-30 nm in diameter. At a magnification of 50000x, the appearance of eVLPs was very similar to wt CPMV apart from one obvious difference: there were dark spots in the middle of some eVLPs (Figure 3.12). This is because the negative stain penetrates and accumulates in empty eVLPs whereas in wt CPMV, dense RNA occupies the capsid preventing accumulation of negative stain.

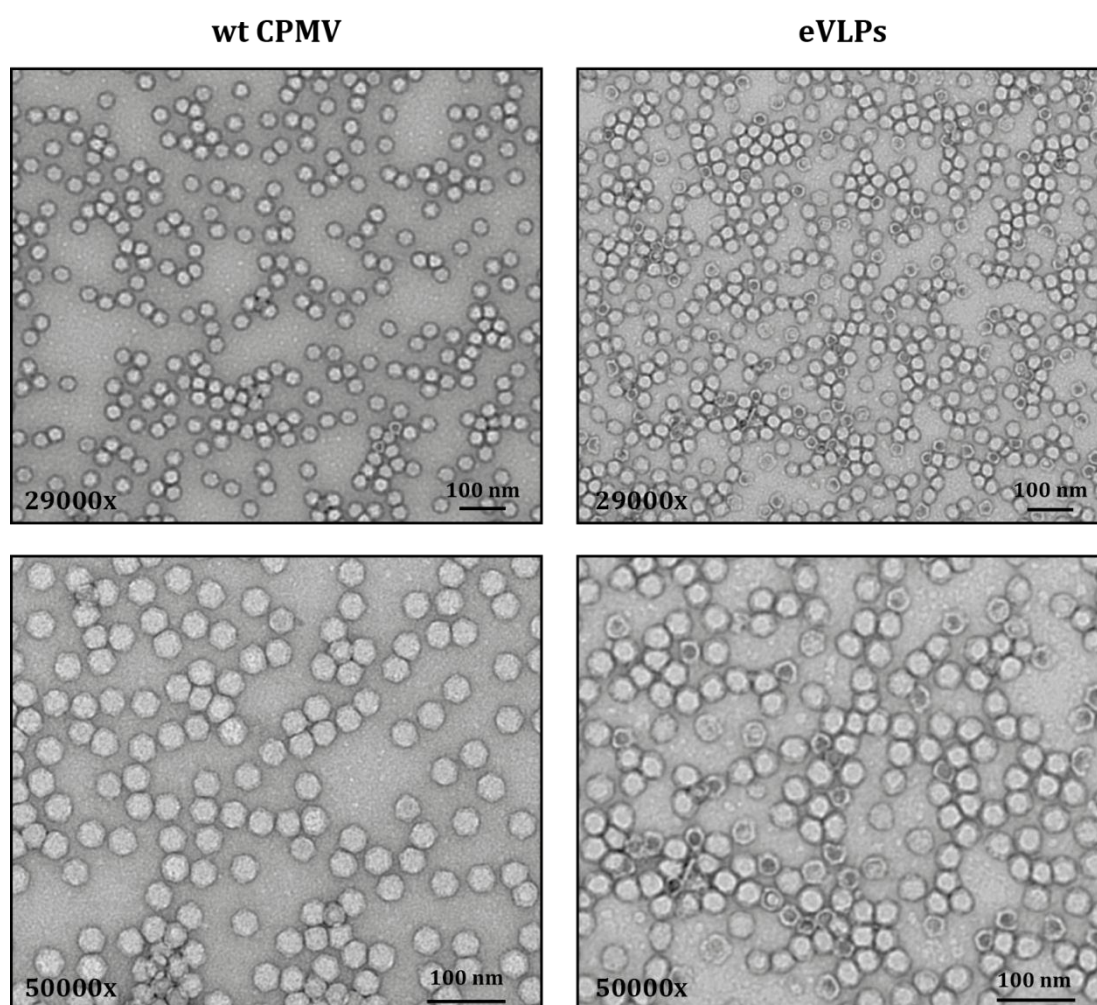


Figure 3.12 TEM of wt CPMV and eVLPs. wt CPMV (left) and eVLPs (right) were negatively-stained and visualised by TEM at a magnification of 29000x (top row) and 50000x (bottom row).

Recent studies on eVLPs possessing the processed and unprocessed forms of S have shown that the presence of the C-terminal peptide influences particle permeability by blocking access to the pore at the 5-fold axis (Sainsbury et al., 2011). This may explain why penetration of the negative stain is only seen in a few eVLPs, given that a majority of the eVLPs possess the unprocessed form of S.

3.6.5 Cryo-electron microscopy (cryo-EM)

Cryo-EM on wt CPMV and eVLP particles was performed by Mr. Kyle Dent and Dr. Neil Ranson at the University of Leeds, UK using material prepared at the John Innes Centre. 3D reconstructions of wt CPMV and eVLPs showed that both species possessed identical capsids. Computational analysis of the interior of capsids showed eVLPs to be RNA-free, as density attributable to RNA could not be observed in any of the recorded eVLP images (Figure 3.13).

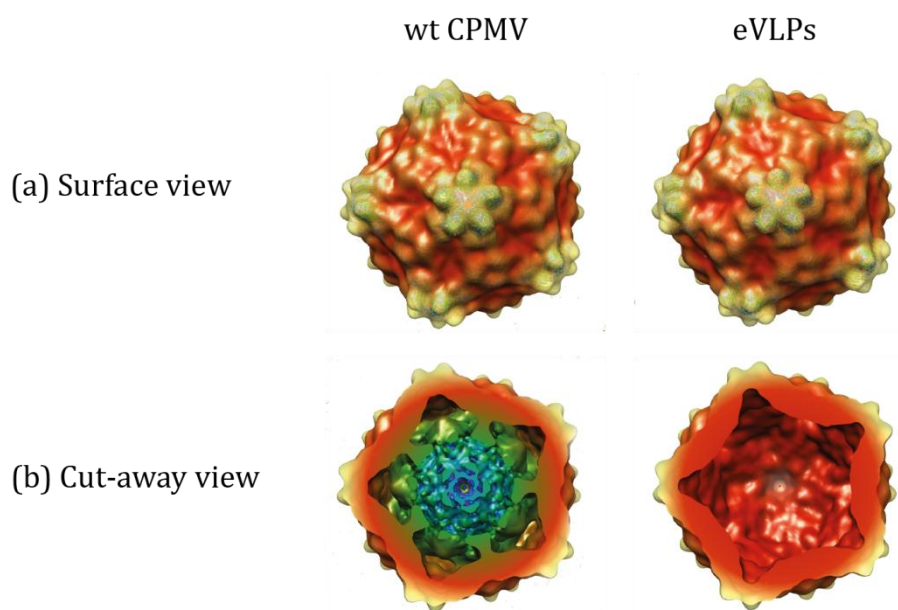


Figure 3.13 Three-dimensional reconstructions of wt CPMV and eVLPs. wt CPMV (left) and eVLPs (right) were loaded on copper grids, frozen rapidly by plunging into liquid ethane and imaged at a magnification of 84900x. 3D reconstructions of recorded images were done by iterative-projection-matching using a spherical starting model and the published crystal structure of CPMV (Lin et al., 1999). Surface view (a) and cut-away view (b) of particles is shown.

The above cryo-EM studies represent the first time RNA has been visualised within a CPMV particle and therefore present an opportunity for analysing the structure of RNA within the particles. However, the wt CPMV preparation used for this work was from a natural infection and hence, contained a mixture of Bottom, Middle and Top particles. Though Top component can be easily distinguished on frozen grids, Middle and Bottom components cannot. Thus, any data obtained on the RNA structure would be an average of the structures adopted by RNA-1 and RNA-2. To obtain high-resolution data on the structures adopted by either RNA within the particles, it was necessary to fractionate a CPMV preparation so that Middle and Bottom components could be analysed separately. To this end, a 30 mg sample of wt CPMV was applied to a Nycodenz® gradient (as described in Section 2.5.3) and fractionated on the basis of particle density. Upon fractionation, 3, 4.5 and 0.2 mgs of Bottom, Middle and Top components, respectively, were recovered and these were sent for further cryo-EM.

Cryo-EM on the Bottom component of wt CPMV generated preliminary data on the secondary structure of encapsidated RNA, which suggested that RNA-1 adopts the structure of a dodecahedral cage (Figure 3.14). The structures of the Middle and Bottom components, as well as the eVLPs, continue to be refined and should provide insights on interactions between RNA and coat proteins in wt CPMV.

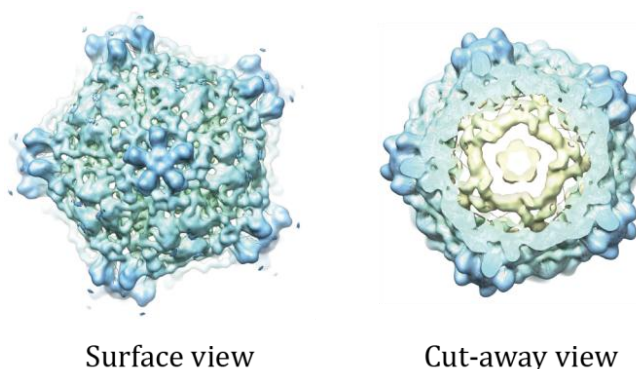


Figure 3.14 Three-dimensional reconstructions of CPMV-Bottom. Exclusively RNA-1 containing particles (CPMV-Bottom) were analysed by cryo-EM. 3D reconstructions at 7.5 Å show presence of highly dense RNA within the capsid. The coat proteins are depicted in blue and encapsulated RNA is shown in yellow.

Close comparison of surfaces of CPMV-Bottom and eVLPs using data generated by cryo-EM revealed one difference between the two species: some extra density was seen around the five-fold axis in eVLPs (Figure 3.15). This mapped to the C-terminus of the S coat protein and is thought to result from the presence of the slow rather than the fast form of the S coat protein in eVLPs, as seen previously on SDS-PAGE gels (Section 3.6.1). The fact that at least some of the C-terminal 24 amino acids from the S protein can be seen in the cryo-EM reconstructions suggested that it may be possible to obtain some structural information on this previously unresolved aspect in the structure of CPMV. To investigate this, fresh preparations of eVLPs with and without the C-terminal peptide were recently sent to the University of Leeds for cryo-EM.

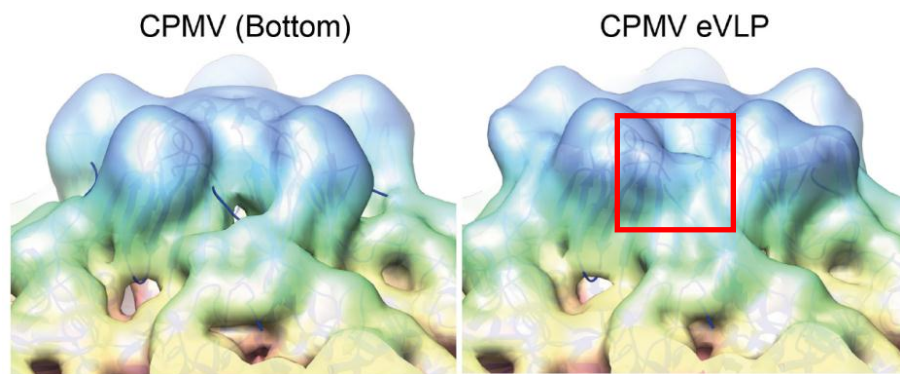


Figure 3.15 Comparison of CPMV-Bottom and eVLPs around the 5-fold axis. The red box highlights the differences between the Bottom component (left) and eVLPs (right) around the 5-fold axis.

3.6.6 Neutron scattering studies

The internal dynamics of eVLP capsids were compared to wt CPMV using neutron spin echo experiments conducted by Dr. Simon Titmuss at the University of Edinburgh. Clear differences were observed in the effective diffusion coefficients for the empty and filled capsids, at a length-scale corresponding to the overall diameter of the capsid. The analysis of this data is on-going, but suggests that there are differences in the elastic properties of wt CPMV and eVLPs, that could be due to the presence and absence of favourable interactions between the capsids and the RNA, respectively.

3.7 Discussion

One of the main criteria for a reagent to be chosen for development as a nanoparticle is its ease of production. Therefore, for development of eVLPs as potential reagents for application in nanotechnology, it was important that methods for its large-scale production and purification were established. This chapter presented ways to produce milligram quantities of eVLPs from transiently-infiltrated leaves. Every step in the production pipeline was analysed and optimised resulting in an overall increase in eVLP yield.

Despite various levels of purification, some contaminants, albeit in small amounts, were seen to be present in standard eVLP preps. (Figure 3.5). Using mass spectrometry, the contaminants were mainly identified to be the large and small subunits of the plant protein RuBisCo. The level of purity attained was sufficient for all the work described in this thesis and other preliminary experiments in the lab. However if desired, eVLPs can be purified further using downstream purification techniques such as desalting columns, centrifugal devices and incubation in a selection of buffers at different pH.

Starting from average eVLP yields of 0.05 g/kg FWT, the expression and purification system was optimised to deliver yields in excess of 0.3 g/kg FWT. This not only helped conduct experiments that involved the use of eVLPs by providing abundant starting material, but also threw light on various steps of the production pathway making it easier to design purification protocols for genetically and chemically modified versions of eVLPs. The average yields currently achieved for eVLPs are comparable to yields for other VLPs expressed transiently in *N. benthamiana*. For instance, Norwalk virus VLPs are expressed at 0.4 g/kg FWT (Lai and Chen, 2012) and for Hepatitis B VLPs, average expression levels of 0.25-0.3 g/kg FWT are attained (pers. comm., Alberto Berardi).

Using a selection of techniques, namely, gel electrophoresis, TEM, cryo-EM and neutron scattering studies, it was concluded that eVLPs possessed capsids identical to wt CPMV and that eVLPs were genuinely empty. This also confirmed similarities between eVLPs and natural Top component.

eVLPs were generally found to possess the slow form of the S coat protein since eVLPs were routinely harvested after 5-6 dpi. Analysis of particles over time using SDS-PAGE (Figure 3.6a) showed that the S coat protein pre-dominantly remains in its slow form until 5 dpi, after which it undergoes natural proteolysis to generate S_{fast} . Analysis of native particles on agarose is a quick and easy method for detection of C-terminal processing of CPMV. Particles possessing S_{slow} show retarded mobility on agarose in comparison to CPMV possessing the processed form of S. This is due to two reasons:

- (i) Presence of two lysine and four arginine residues in the C-terminal peptide confers an overall positive charge to the peptide, thereby retarding its mobility towards the anode;
- (ii) Presence of sixty copies of the 24 amino acid peptide adds approximately 160 kDa to the mass of each CPMV capsid.

Repeated analysis of $CPMV_{slow}$ particles showed that their pattern of migration in agarose is not always the same. This raises questions about the efficiency of proteolytic processing of the S coat protein. It is not known if the 24 amino acid peptide simultaneously cleaves from all sixty S coat proteins in a particle. Kridl and Bruening (1983) suggest that even after proteolysis, the peptide may remain attached to the capsid via non-covalent bonds until all sixty S coat proteins are processed to generate S_f . Processing of the C-terminal peptide is still not completely understood.

The fact that eVLPs can be readily generated by co-expression of VP60 and 24K proves that presence of RNA is not a pre-requisite for capsid formation. However, it is still not understood why empty particles, albeit in small amounts, are naturally produced in an infection (as Top component). It is not known whether empty particles of CPMV provide any benefit to the virus or if they are just produced as a bi-product of RNA-containing virions. Production of empty particles could be a strategy of the virus to regulate expression levels by depleting unassembled coat proteins in the host cell.

Following production and characterisation of eVLPs, the focus of the work shifted to development of eVLPs for various applications. In parallel to chemical modification of eVLPs, attempts were made to genetically fuse peptides to (i) the exterior surface of eVLPs for cell-specific targeting and (ii) the interior surface of eVLPs for promoting mineralization.

A 20 amino acid peptide from the foot-and-mouth disease virus (FMDV) was selected for expression on the exterior surface of the eVLP capsid since this peptide contains an arginine-glycine-aspartate (RGD) motif that mediates specific binding to integrin $\alpha\beta6$ (DiCara et al., 2008). Integrin $\alpha\beta6$ is an epithelial-specific integrin expressed at undetectable levels in healthy cells but is up-regulated during tissue remodelling, as in the case of wound healing, inflammation and cancer (Caswell and Norman, 2008). So, eVLPs displaying the FMDV peptide on their surface would specifically bind to cells expressing integrin $\alpha\beta6$, i.e. cancerous cells.

To generate chimeric eVLPs, the FMDV peptide was fused to the C-terminus of the S coat protein by genetic modification of the plasmid encoding the coat proteins. The C-terminus of the S coat protein was chosen because it was expected that upon assembly, sixty copies of the peptide would be exposed on the surface of the eVLP capsid. However, it was found that modifications to the peptide at the C-terminus increased its tendency to cleave and resulted in particles with the processed form of the S coat protein. Even though particles were extracted at 5 dpi and analysed straightaway, the C-terminus peptide was found to be absent from all particles.

Attempts were also made to introduce peptides on the interior surface of eVLPs by genetic modification of the sequence encoding the N-terminus of the L coat protein. The peptides chosen for this purpose were peptides that promote mineralization of materials such as metals, metal oxides and alloys (Seker and Demir, 2011). In particular, a 13 amino acid peptide that specifically promotes mineralization of iron and platinum was chosen (Reiss et al., 2004). Upon genetic modification of plasmids and their expression in plants, it was seen that particles could not be generated in presence of the N-terminally modified form of the L coat

protein, suggesting that modifications to the N-terminus of the large coat protein affected particle assembly.

Other potential sites for modification of eVLPs, identified using literature on modified wt CPMV (Porta et al., 2003) and the crystal structure of wt CPMV (Lin and Johnson, 2003), continue to be investigated. Internal labelling of eVLPs with dyes, such as Oregon Green 488 and Rhodamine Red, has been successfully achieved by conjugation of dyes to available lysines on the interior surface of eVLPs (Wen et al., 2012). Labelled eVLPs are being developed for studies on the uptake of CPMV in mammalian cells.

The availability of eVLPs has opened opportunities for novel applications of CPMV due to reduced bio-safety issues and their ability to encapsulate. One such application is the use of eVLPs as a delivery vehicle for nucleic acids and this idea has been explored in the following chapter.

Chapter 4: Results II

Study of replication and encapsidation of RNA in CPMV

4.1 Introduction

The fact that empty particles of CPMV can be generated, both during an infection as the Top component and without an infection by co-expression of VP60 and 24K, demonstrates two things: first, that presence of RNA is not a pre-requisite for particle assembly in CPMV and second, that cellular RNAs of the host are excluded from the capsid during assembly. This makes CPMV different from other viruses, such as turnip crinkle virus (TCV) or Hepatitis B virus (HBV), which package random host nucleic acids if their own genomic DNA/RNA is not available. This ability of CPMV to specifically package RNA makes it a good candidate for use as a delivery vehicle for specific nucleic acids, such as antisense oligonucleotides and small interfering RNA (siRNA), for research and therapeutic applications.

siRNAs are being developed to target therapeutically important genes involved in cancer, viral infections, autoimmune and neurodegenerative diseases (Tokatlian and Segura, 2010). Although siRNA therapy has the potential to be a powerful therapeutic drug, its delivery remains a major limitation (Kesharwani et al., 2012). There is a requirement for vehicles that can offer protection to siRNA while circulating in the body of the host, target siRNA to the desired tissue in the body and subsequently upon internalization, release encapsulated siRNA in the cytoplasm. Since viruses are designed to protect their genomic nucleic acids in harsh environments and release encapsulated material upon internalisation, they make ideal candidates for this application.

This chapter explores the idea of developing CPMV eVLPs for delivery of nucleic acids of choice. Preliminary experiments on loading eVLPs with small nucleic acids through the five-fold axis pore suggested that loading via simple diffusion into particles was not a viable approach. The size and secondary structure of nucleic acids made it very difficult to direct short nucleic acids towards the pore and thread them into the particle (M. Nelson and P. Saxena, unpublished results). So, it

was concluded that methods for packaging DNA or RNA within eVLPs would have to involve assembly of the coat proteins around the desired cargo. To develop such methods, an understanding of the process of encapsidation in CPMV was needed. The work described in this chapter is aimed at defining the elements required for packaging of RNA in CPMV with the intention of exploiting the findings to develop CPMV eVLPs as carriers of DNA or RNA of choice. Once the requirements for packaging nucleic acids within eVLPs are established, methods for the incorporation of desired nucleic acids within eVLPs could be developed. Combined with previously established methods for the modification of the outer particle surface, this could lead to the development of methods for the targeting of specific nucleic acids to particular cells.

Saunders et al. (2009) showed that CPMV eVLPs are formed in absence of wt RNA-1 and wt RNA-2 by co-expression of VP60 and 24K. A point to note here is that the mRNAs which direct the synthesis of VP60 and 24K contain viral sequences yet do not get packaged within eVLPs. By contrast, when wt RNA-1 is expressed in presence of VP60, particles are generated with RNA-1 packaged within them (Figure 4.1). This shows that in CPMV, presence of partial sequences from wt RNA-1 or RNA-2 is not sufficient for packaging. The reason could simply be that they are too small to be efficiently packaged (mRNAs for VP60 and 24K are 2.5 kb and 1.3 kb long respectively) or that they lack specific recognition sequences needed for encapsidation. An alternative hypothesis could be that RNA replication and packaging are coupled and only replicating RNAs can be packaged as found with picornaviruses (Nugent et al., 1999).

To investigate the requirements for packaging further, several mutants of RNA-1 and RNA-2 were generated and their translation, replication and encapsidation were studied. The results were consistent with replication being required for the packaging of RNAs.

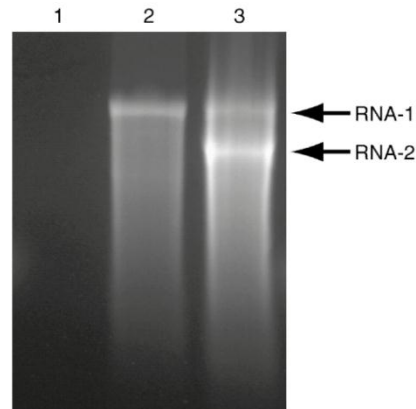


Figure 4.1 Analysis of RNA within particles (Saunders et al., 2009). RNA was extracted from VLPs (generated as below) using phenol/chloroform and analysed on a 1.2% formaldehyde gel. Bands obtained for RNA-1 and RNA-2 have been indicated. Samples were run as follows:

- Lane 1: RNA from particles generated by co-expression of 24K and VP60
- Lane 2: RNA from particles generated by co-expression of RNA-1 and VP60
- Lane 3: RNA from particles generated by co-expression of RNA-1 and RNA-2

4.2 Study of encapsidation of a replication-deficient mutant of RNA-1

A previously generated mutant of RNA-1 called 32E (Liu et al., 2004) was deployed to investigate the dependency of RNA encapsidation on RNA replication in CPMV. The plasmid for expression of 32E, named pBinPS-32E-NT, was originally designed to study the replication of RNA-1 where it was shown that 32E can neither self-replicate nor support the replication of RNA-2 (Liu et al., 2005; Liu et al., 2004). This is because 32E was engineered to lack the 5' UTR of RNA-1 (Figure 4.2).

The accuracy of pBinPS-32E-NT was verified by sequencing and the plasmid was used in the study described below to compare the abilities of 32E and wt RNA-1 to be encapsidated and to support the encapsidation of RNA-2.

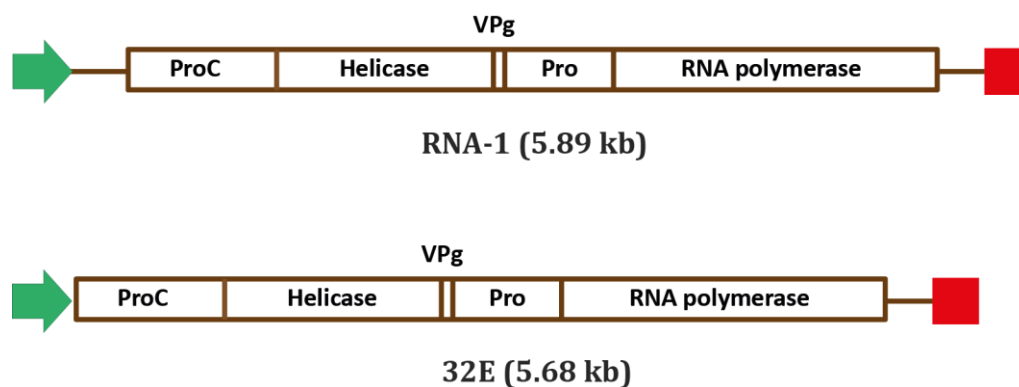


Figure 4.2 Schematic diagrams of constructs expressing RNA-1 and 32E. Relevant sections of pBinPS-1-NT and pBinP-32E-NT (Liu et al., 2004), deployed for expression of wt RNA-1 and 32E respectively, are shown. The green arrow and red box represent the CaMV 35S promoter and nos terminator respectively. The indicated sizes correspond to the length of the transcribed RNA and do not include the size of the promoter and terminator.

The constructs pBinPS-1-NT and pBinP-32E-NT were each co-infiltrated into plants with either pBinPS-2-NT (Liu and Lomonosoff, 2002) for expression of wt RNA-2 (samples 1 and 3) or pEAQ-*HT*-VP60 for expression for VP60 (samples 2 and 4). While pEAQ-*HT*-VP60 encoded P19 for enhancement of expression, in case of pBinPlus-based constructs, P19 was supplied by co-infiltration with pBIN61-P19 (Voinnet et al., 2003). In parallel, pEAQ-*HT*-VP60 was infiltrated as a control (sample 5). Details of all sets of infiltrations are presented in Table 4.1.

Sample	Infiltrated constructs
1	pBinPS-1-NT + pBinPS-2-NT + pBIN61-P19
2	pBinPS-1-NT + pEAQ- <i>HT</i> -VP60
3	pBinPS-32E-NT + pBinPS-2-NT + pBIN61-P19
4	pBinPS-32E-NT + pEAQ- <i>HT</i> -VP60
5	pEAQ- <i>HT</i> -VP60

Table 4.1 Combinations of constructs infiltrated into *N. benthamiana* leaves for comparative analysis of RNA-1 and 32E.

For all combinations of constructs, 10-12 g of infiltrated leaf tissue was harvested after 6 dpi and subjected to the standard protocol for particle purification. The purified samples were analysed by TEM, which confirmed the presence of particles, similar to CPMV in morphology, in samples 1-4. In line with expectation, sample 5 did not yield viral particles due to absence of 24K for processing of VP60.

To further characterise the particles obtained in samples 1-4, 4 μ l of each purified sample was separated using SDS-PAGE. Bands corresponding to L and S coat proteins were observed in samples 1-4 demonstrating that the constructs were being translated to generate VP60 and 24K, and that VP60 was being processed to yield L and S (Figure 4.3). Particle yield was estimated to be in the range of 0.4-0.5 g/kg FWT based on the intensities of bands on the gel. The fact that similar yields of L and S were obtained in all four samples provided some evidence that even in the absence of replication, coat proteins were being translated at levels similar to those in presence of replication.

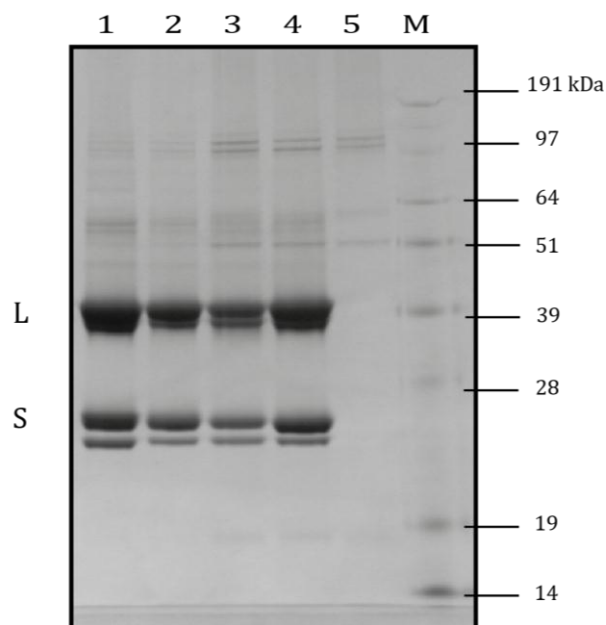


Figure 4.3 SDS-PAGE analysis of particles. 4 μ l of samples 1-5 were denatured by heat-incubation and separated using SDS-PAGE. The number of the lane corresponds to the number of the sample, as per Table 4.1. The standard protein marker was run in lane M. Bands observed for L and S upon staining of the gel with Coomassie blue are indicated.

Particles purified from samples 1-4 were then subjected to native agarose gel electrophoresis to verify the presence of intact particles by staining with Coomassie blue and to assess the presence of encapsulated RNA within particles by staining with ethidium bromide. Approximately 10 μg of particles per sample were electrophoresed on agarose. It was observed that in all four samples, particles were a mixture of CPMV_{fast} and CPMV_{slow}, i.e. particles possessing the processed and unprocessed forms of the C-terminus of the S coat protein, resulting in separate bands on agarose (Figure 4.4). Staining with Coomassie blue showed presence of particles in all four lanes, while staining of the agarose gel with ethidium bromide revealed presence of RNA within particles generated using wt RNA-1 (samples 1 and 2) but not within particles generated using 32E constructs (samples 3 and 4) (Figure 4.4).

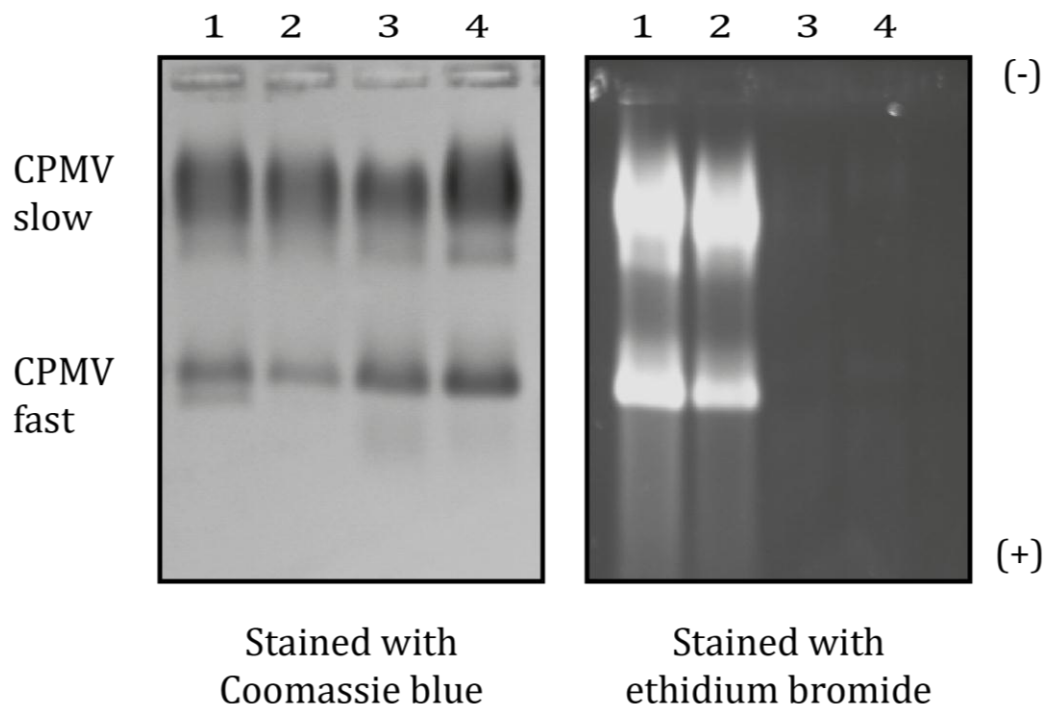


Figure 4.4 Particle analysis using agarose gel electrophoresis. Particles generated by co-expression of various combinations of constructs (as per Table 4.1) were analysed on agarose by staining with Coomassie blue (left) or ethidium bromide (right). The number of the lane corresponds to sample number. The two bands seen are due to differentially processed forms of the S coat protein in particles, thereby generating CPMV_{slow} and CPMV_{fast}.

RNA within particles in samples 1-4 was subsequently extracted and analysed by denaturing gel electrophoresis. It was found that either RNA-1 or RNA-2 was present within particles from sample 1 while only RNA-1 was detected in particles from sample 2, consistent with results shown in Figure 4.1. No RNA was detected within particles in samples 3 and 4 showing lack of encapsidation in presence of 32E.

The finding that co-infiltration with wt RNA-1 but not 32E results in RNA encapsidation points to replication and packaging being coupled. Infiltration with 32E clearly resulted in the production of RNA since this was subsequently translated to produce the 24K proteinase essential for the generation of particles. Yet, no RNA transcripts were packaged within capsids in the presence of the non-replication competent 32E transcripts. While the lack of packaging of 32E transcripts could be explained if the deletion of the 5' UTR resulted in the elimination of a packaging signal, the lack of packaging of wt RNA-2 constructs co-infiltrated with 32E (Sample 3) cannot be explained this way. The wt RNA-2 expressed was not genetically manipulated in any way and was therefore expected to contain any packaging signals; furthermore the RNA-2 produced from the same construct pBinPS-2-NT was packaged in the presence of wt RNA-1 (sample 1) showing that it is potentially fully competent for packaging. The only difference between the RNA-2 molecules produced in the presence of wt RNA-1 and 32E is that they will be replicated in the former but not the latter situation. Overall, the results suggest that the requirement for packaging in CPMV is more than just the presence of a sequence or secondary structure within the RNA with the simplest explanation being that only replicating RNAs can be packaged.

To obtain further evidence that replication was necessary for encapsidation, it was decided to create other replication-incompetent versions of RNA-1, this time with minimal changes to the wt sequence. It was decided to create point mutations in the active site of the 87K replicase encoded by RNA-1 such that the mutations abolished the ability of the replicase to function. CPMV shares sequence homology with other RNA polymerases around a motif in the 87K replicase that contains the amino acids: glycine-aspartate-aspartate (GDD). The GDD motif is known to be

important for RNA polymerase activity since the first aspartate co-ordinates magnesium divalent (Mg^{2+}) cations during RNA synthesis thereby stabilizing the leaving pyrophosphate group (Delarue et al., 1990). Mutations within the GDD motif, especially of the first aspartate residue, result in loss of enzyme function (Jablonski and Morrow, 1995; Kim et al., 2007; Shwed et al., 2002; Vazquez et al., 2000; Wang and Gillam, 2001; Wang et al., 2007). Hence, a point mutation in the GDD motif of CPMV RNA-1 would knock-out replicase activity without any substantial changes to the sequence of RNA-1.

Primers (listed in Appendix I) were designed to separately introduce the following mutations in the replicase:

- (1) G389A – to change glycine to alanine, i.e. GDD to ADD
- (2) D390A – to change aspartate to alanine, i.e. GDD to GAD
- (3) D390E – to change aspartate to glutamine, i.e. GDD to GED

G389A and D390E were chosen since substitution of glycine with alanine or aspartate with glutamate was expected to cause minimal changes to the structure of the replicase due to similarities in the properties of these amino acids. On the other hand, D390A was expected to completely disrupt the structure of the replicase. Either way, all three mutations were expected to knock-out replicase activity without affecting the expression and activity of the other proteins encoded by RNA-1.

In order to introduce the above mutations, plasmid pBinPS-1-NT (Liu and Lomonosoff, 2002) was subjected to SDM and potential mutant colonies were transferred to liquid media to obtain plasmid for analysis by sequencing. It was found that a majority of colonies obtained on plates did not grow in liquid media suggesting that the bacteria had lost viability. Amongst the few that grew, substantial rearrangements were found in the sequences of their plasmids. The desired mutations in the GDD motif were detected in some of these plasmids but the presence of other sequence rearrangements meant that the plasmids no longer encoded wt RNA-1 from CPMV with just one amino acid substitution.

Either loss of viability or sequence rearrangements upon propagation of wt RNA-1 in *E. coli* has previously been observed during manipulation of RNA-1 sequences (G. P. Lomonosoff, pers. comm.). In addition, the vast amount of literature available on RNA-2 as compared to RNA-1 also shows that in the past, most work has concentrated on manipulation of RNA-2 sequences, suggesting difficulties in manipulation of RNA-1. This is likely to be due to leaky promotion of RNA-1 leading to accumulation of viral proteins with catalytic activities, such as the helicase, the proteinase and the replicase, in the bacterial cell. Such proteins are capable of acting on bacterial nucleic acids and therefore, possibly interfere with housekeeping processes in *E. coli*.

One of the ways to combat problems with bacterial expression of toxic proteins is to slow down the rate of growth of the bacteria to suppress basal expression of toxic genes. This approach was tried by incubating *E. coli* colonies transformed with RNA-1 constructs at 28°C instead of the optimum growth temperature of 37°C. In addition, 2% glucose was added to the media since it mediates catabolic repression thereby reducing basal expression levels in bacteria leading to reduced growth rates (Saida, 2007). However, RNA-1 mutants could still not be obtained.

4.3 Study of encapsidation of a non-replicable mutant of RNA-2

After several failed attempts at creation of GDD mutants of RNA-1 to study the possible coupling of replication and packaging, an alternative approach was adopted. This involved the creation of a non-replicable form of RNA-2 that could still be translated to generate all RNA-2-encoded proteins. The question was asked whether this mutant RNA-2, that did not replicate, would be encapsidated in presence of RNA-1.

To this end, a version of RNA-2 with *HT* mutations in its 5' UTR was created using the vector pEAQ-*HT* (Sainsbury et al., 2009). The sequence of RNA-2 starting from AUG 512 was amplified from the plasmid bearing wt RNA-2, namely pBinPS-2-NT (Liu and Lomonosoff, 2002), and cloned in pEAQ-*HT* using the restriction sites *AgeI* and *StuI* in its polylinker. As mentioned previously, the *HT* mutations eliminate the start codon at position 161 (AUG161) and another out-of-frame start codon at position 115 (AUG115) in the 5' UTR (Sainsbury and Lomonosoff, 2008). Based on previous studies (Holness et al., 1989; Rohll et al., 1993; Wellink et al., 1993), these mutations, as well as enhancing translation, would be expected to abolish replication of any RNA-2-based construct bearing them. So pEAQ-*HT*-RNA-2 (Figure 4.5), thus generated was not expected to replicate and hence, was ideal for investigation of the link between replication and encapsidation.

At the same time, another version of RNA-2 was created by amplifying the entire coding region of RNA-2 (starting from AUG 161) from the plasmid pBinPS-2-NT and inserting it downstream of the *HT* 5' UTR in the vector pEAQ-*HT* using sites *AgeI* and *StuI*. The construct thus generated, named pEAQ-*HT*-full length RNA-2 (Figure 4.5), contained a repeat of the region between AUG161 and AUG512. This construct was produced to determine whether the presence of both AUGs and the maintenance of their frame relationship positioned downstream of the *HT* leader would restore the ability of *HT*-full length RNA-2 to be replicated.

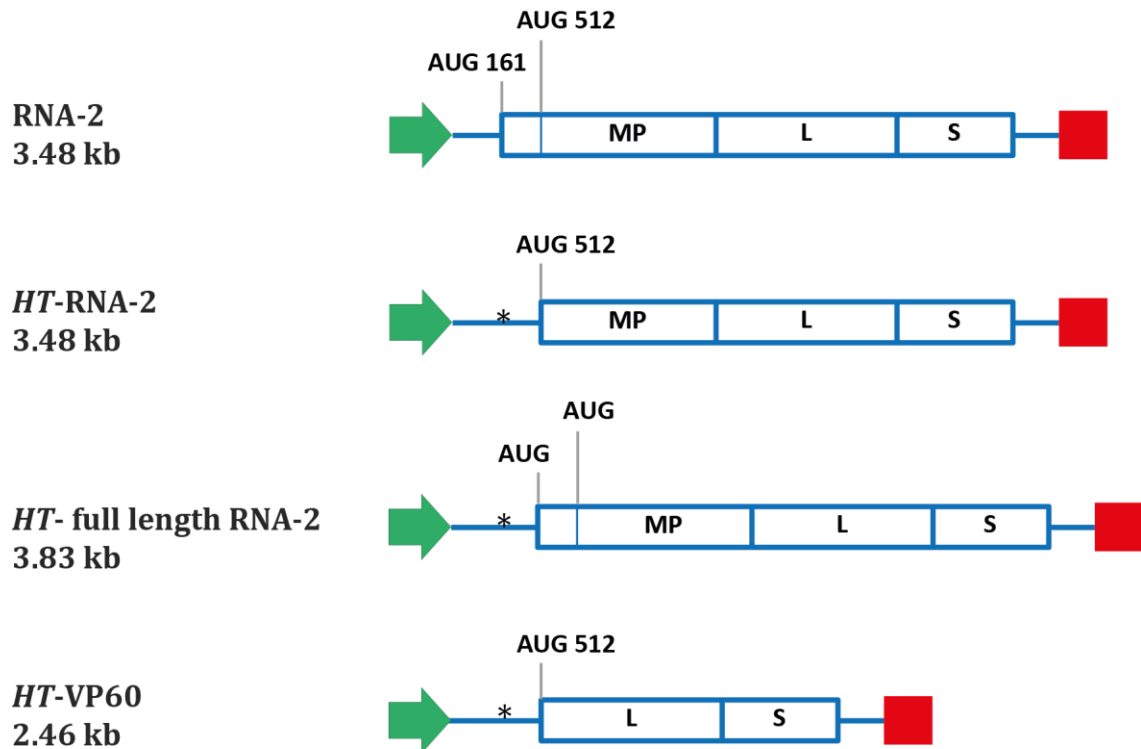


Figure 4.5 Schematic diagrams of constructs expressing mutants of RNA-2. wt RNA-2 was expressed from pBinPS-2-NT (Liu and Lomonosoff, 2002) while the RNA-2 mutants were encoded in pEAQ-*HT*-based vectors (Sainsbury et al., 2009). *HT*-RNA-2 is a mutant of RNA-2 with two point mutations in its 5' UTR (*HT* mutations; represented by an asterisk). *HT*-full length RNA-2 is a mutant of RNA-2 containing both the *HT* mutations as well as the full-length coding sequence of RNA-2. *HT*-VP60 also contains the *HT* mutations and encodes the L and S coat proteins. The green arrow and red box represent the CaMV 35S promoter and nos terminator respectively. The indicated sizes correspond to the length of the transcribed RNA and do not include the size of the promoter and terminator.

The mutants of RNA-2, defined in Figure 4.5, were each infiltrated into *N. benthamiana* leaves in presence of wt RNA-1 (from pBinPS-1-NT). Since pEAQ-*HT*-based vectors encoded P19 for enhancement of expression, in case of non-pEAQ vectors, P19 was supplied by co-infiltration of pBIN61-P19 (Voinnet et al., 2003). Details of the different sets of infiltrations are presented in Table 4.2.

Sample	Infiltrated constructs
1	pBinPS-1-NT + pBinPS-2-NT + pBIN61-P19
2	pBinPS-1-NT + pEAQ- <i>HT</i> -full length RNA-2
3	pBinPS-1-NT + pEAQ- <i>HT</i> -RNA-2
4	pBinPS-1NT + pEAQ- <i>HT</i> -VP60

Table 4.2 Combinations of constructs infiltrated into *N. benthamiana* leaves for analysis of replication and encapsidation of different versions of RNA-2.

At 12-15 dpi, plants infiltrated with construct combinations 1 and 2 showed symptoms characteristic of a CPMV infection, such as crinkling of leaves and vein clearing in upper leaves. By contrast, no such symptoms were observed in plants infiltrated with construct combinations 3 and 4 (Figure 4.6). The same results were observed in four independent plants infiltrated with each of the above combinations of constructs. This provided evidence that wt RNA-2 (sample 1) and *HT*-full length RNA-2 (sample 2) were being replicated, encapsidated and systemically moved through the plant. On the other hand, *HT*-RNA-2 (sample 3) and *HT*-VP60 (sample 4) were neither being replicated nor packaged, limiting their expression to the infiltrated tissue.

The appearance of symptoms in plants infiltrated with wt RNA-1 and *HT*-full length RNA-2 (sample 2) was indistinguishable from symptoms in plants infiltrated with wt RNA-1 and wt RNA-2 (sample 1).

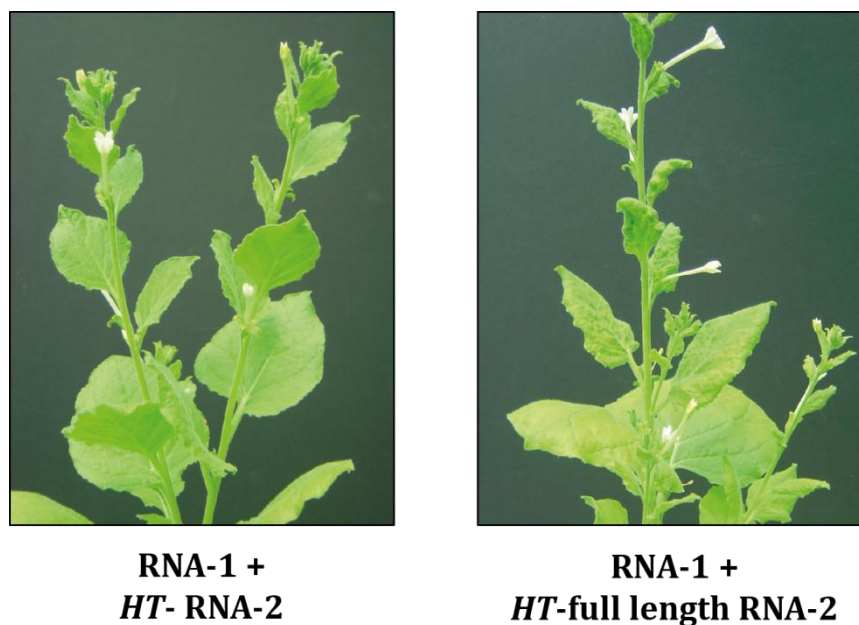


Figure 4.6 Symptoms in the upper leaves of plants upon expression of RNA-2 mutants in presence of wt RNA-1. wt RNA-1 co-expressed with *HT*-RNA-2 (left) did not result in symptoms characteristic of a viral infection in the upper leaves of *N. benthamiana*. Co-expression of *HT*-full length RNA-2 and wt RNA-1 (right) resulted in systemic movement of particles resulting in viral symptoms. Plants were photographed on 18 dpi.

Infiltrations listed in Table 4.2 were repeated for further analysis of the expression of the constructs and the particles thereby produced. The infiltrated leaves were harvested at 6 dpi and subject to the standard protocol for particle purification. Separation of purified extract using SDS-PAGE confirmed presence of particles in all four samples. This showed that all constructs were functional and coat proteins were being produced from all versions of RNA-2, regardless of their ability to be replicated.

Approximately 100 µg of particles from each sample were used for extraction of RNA encapsidated within them. RNA-1 was expected to be replicated and packaged in each case but encapsidation of the RNA-2 mutants was questionable. Analysis of extracted RNA on denaturing agarose gels showed that versions of RNA-2 that could be replicated were packaged and others that could not be replicated were

not packaged (Figure 4.5). In other words, wt RNA-2 and *HT*-full length RNA-2 were packaged in presence of RNA-1, whereas *HT*-RNA-2 and *HT*-VP60 were not.

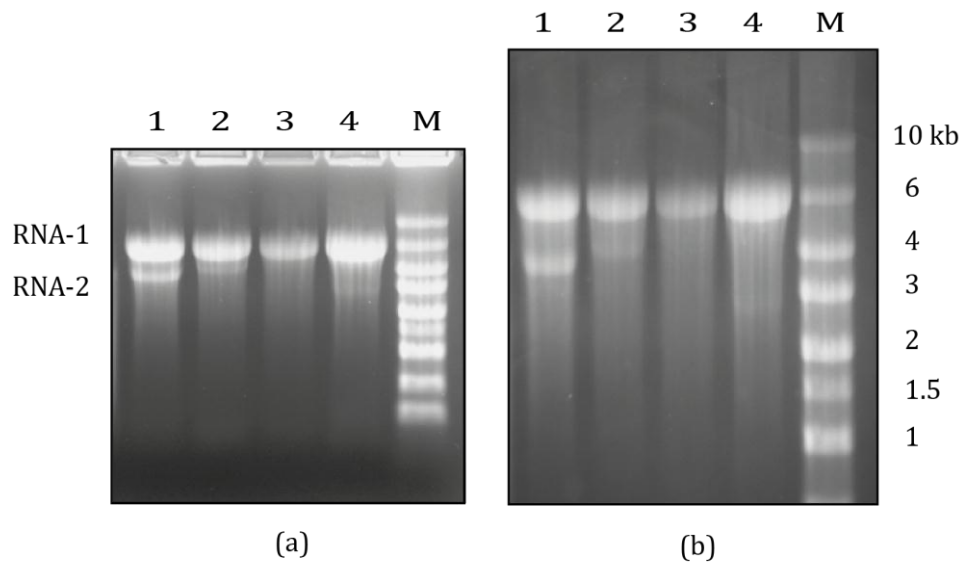


Figure 4.7 Analysis of RNA within capsids generated by co-expression of mutant versions of RNA-2 and wt RNA-1. RNA extracted from particles (as below) electrophoresed on denaturing agarose gels to resolve RNA on the basis of its size and imaged after 1 hour (a) and after 2 hours (b). Bands for wt RNA-1 and RNA-2 have been indicated.

- Lane 1: RNA from particles generated by co-expression of RNA-1 and RNA-2
 Lane 2: RNA from particles generated by co-expression of RNA-1 and ***HT*-full length RNA-2**
 Lane 3: RNA from particles generated by co-expression of RNA-1 and ***HT*- RNA-2**
 Lane 4: RNA from particles generated by co-expression of RNA-1 and *HT*- VP60
 Lane M: RNA marker

The 2.5-3 kb band observed in Lane 4 of Figure 4.7 is likely to be due to degradation of RNA-1. The band was not seen in previous and subsequent RNA extractions from particles generated using the same combinations of constructs, i.e. pBinPS-1NT + pEAQ-*HT*-VP60.

Further experiments on RNA-2 mutants were hampered due to the fact that during design of primers for generation of construct pEAQ-*HT*-RNA-2, two extra bases were inadvertently incorporated upstream of the start codon (AUG 512). Although this did not affect results that have been reported, it made it cumbersome to generate a construct encoding wt RNA-2 in the vector pEAQ-*HT*. This aspect continues to be worked upon.

4.4 Discussion

The specific recognition of viral genomic RNA for encapsidation is a critical event in the infection cycle of plant viruses from the *Comoviridae* family since encapsidation of RNA is essential for systemic spread of the infection and cell-to-cell movement of the virus. In natural infections of most viruses, viral RNA encapsidation is seen to be highly specific and cellular RNAs are only rarely packaged into virions (Rochon and Siegel, 1984). In CPMV, even in the absence of the viral RNAs, cellular RNAs are not encapsidated suggesting particularly high specificity in its packaging.

Different viruses adopt different mechanisms to achieve specificity in recognition of RNA by their coat proteins. The presence of a specific packaging signal or origin of assembly within the RNA has been well characterised for viruses such as TMV (Turner et al., 1988; Zimmern, 1977) and TCV (Qu and Morris, 1997). Similar packaging signals have been observed to be present on the genomes of HBV (Junker-Niepmann et al., 1990), Sindbis virus (Weiss et al., 1994) and cucumber necrosis virus (Reade et al., 2010). However, no such packaging signal has been identified on the RNAs of CPMV. The only homology that exists between RNA-1 and RNA-2 of CPMV lies in their 5' and 3' UTRs and there has been speculation that these might contain packaging signals (Verver et al., 1998; Wellink et al., 1994). However, experiments described in this chapter involving expression of wt RNA-2 in a non-replicating system (Section 4.2) showed that the presence of the 5' and 3' UTRs was not sufficient for encapsidation.

Studies using replication-deficient mutants of CPMV RNA-1 and RNA-2, presented in this chapter and summarized in Figure 4.8, show that encapsidation of an RNA molecule only occurs when it is replicating, suggesting coupling of RNA replication and encapsidation. However, the underlying mechanism whereby a replicating but not a non-replicating version of the same RNA molecule is packaged (for instance the RNA-2 molecules in Fig. 4.4) is not clear.

One of the factors that might play a role in determining RNA that gets encapsidated in CPMV is the presence of the genome-linked viral protein VPg. All newly synthesised RNAs emerging from a replication complex possess a VPg covalently-bound to their 5' end, which is thought to act as a primer for RNA synthesis (Lomonossoff et al., 1985; Wimmer, 1982). On the other hand, non-replicating RNAs, expressed using *Agrobacterium*-mediated expression vectors, are transcribed from their DNA complement in the nucleus of the plant cell and therefore, possibly possess a 5' 7-methylguanosine cap structure, as commonly observed in eukaryotic mRNAs originating from the nucleus (Kapp and Lorsch, 2004). This may influence recognition of the RNA by coat proteins for encapsidation. In addition, the proximity of RNA and coat proteins may affect RNA encapsidation; in a replicating system, translation of coat proteins and replication of RNA occurs close to one another in the cytoplasm.

Another possibility that cannot be ruled out is that the lack of packaging of RNA in the non-replicating system was due to the lack of availability of RNA transcripts. Although an unlikely possibility, it is required to demonstrate that, for instance in case of experiments with 32E, wt RNA-1 and 32E were both present in sufficient amounts in the host cell despite differences in their method and location of production (RNA-1 transcripts were synthesised by replication in the cytoplasm; 32E transcripts were produced by transcription of its DNA complement in the nucleus). Studies for quantification of RNA could not be undertaken due to time constraints but are recognised as being essential for culmination of this work.

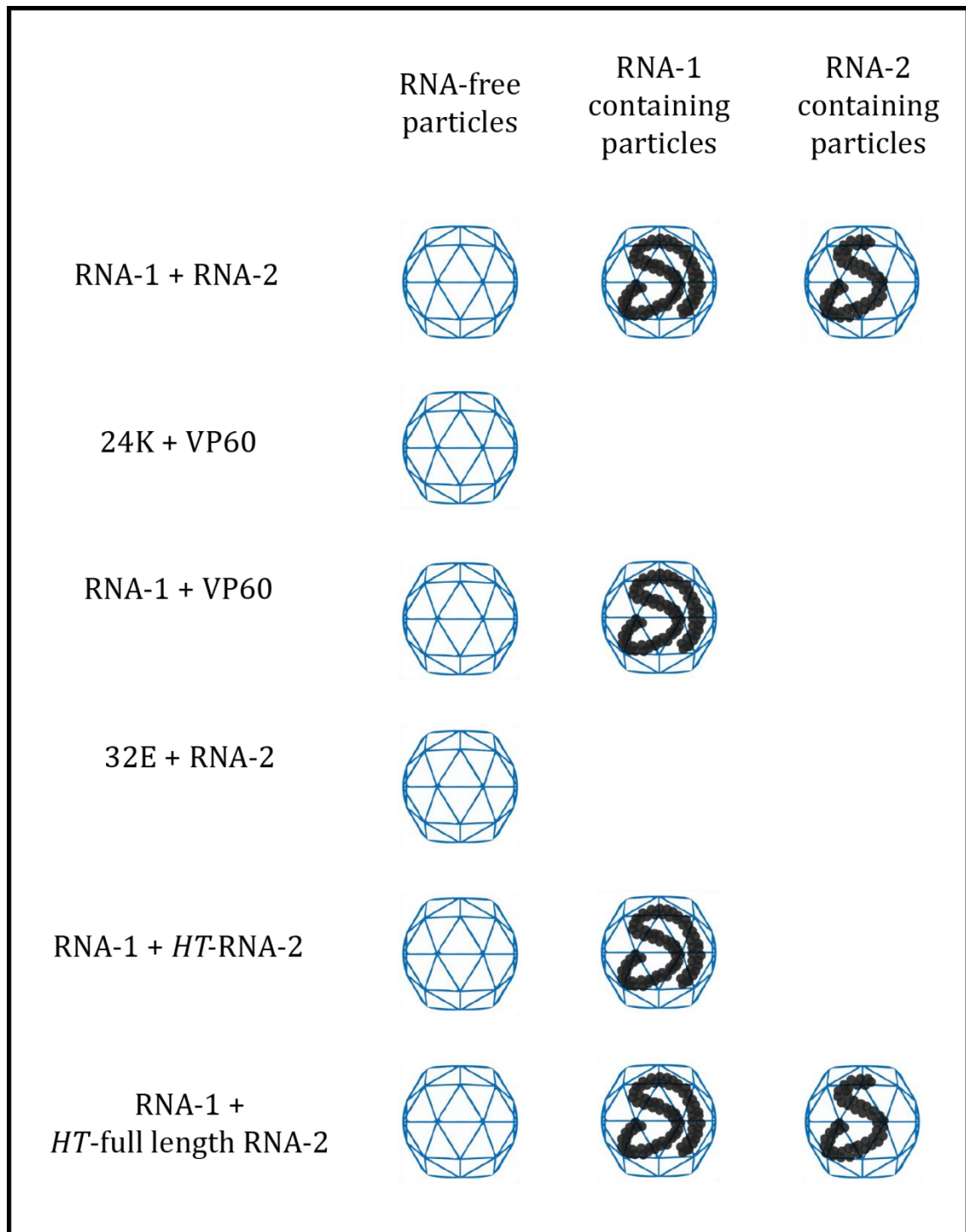


Figure 4.8 Summary. Species of virus-like particles obtained upon co-expression of various constructs (as listed in the first column).

Functional coupling between replication and packaging of RNA has been previously demonstrated in positive-strand viruses of diverse origins. In poliovirus, a member of *Picornaviridae* family, coupling of RNA packaging to replication and of replication to translation has been shown (Novak and Kirkegaard, 1994). The observed coupling is thought to be a result of direct interactions between the RNA replication machinery and the capsid proteins, so that only newly synthesised RNAs emerging from the replication complex get packaged (Nugent et al., 1999). Coupling between replication and packaging in the *Flaviviridae* family has also been shown using Kunjin virus (Khromykh et al., 2001).

Coupling of translation and packaging in viruses makes evolutionary sense as this ensures that only those genomes capable of translating a full complement of functional proteins get packaged. Consequently, other genomes with mutations, which abolish their ability to produce functional proteins, do not get packaged. Also, since a majority of the RNA viruses are assembled in the cytoplasm, it is economical for the virus to replicate and encapsidate RNA simultaneously.

A similar coupling between replication-dependent translation and encapsidation has been observed in brome mosaic virus (BMV) from the *Bromoviridae* family (Annamalai and Rao, 2006) and flock house virus (FHV) from the *Nodaviridae* family (Venter et al., 2005). In FHV, the requirement of a physical interaction between the viral replicase and capsid proteins for specificity in packaging has also been demonstrated (Seo et al., 2012). An interesting observation in FHV was that uncoupling of viral protein synthesis from RNA replication affected packaging of RNA. It was seen that neither RNA-1 nor RNA-2 of FHV, which were both being replicated, were packaged when the capsid protein was supplied *in trans* from non-replicating RNA (Venter et al., 2005). The situation in CPMV, however, is different since it has been shown that CPMV RNA-1 is packaged by capsid proteins supplied *in trans* from a non-replicating vector (pEAQ-*HT*-VP60) (Saunders et al., 2009). The ability of capsid proteins to package RNA-1 *in trans* suggest that efficient packaging of any replicating RNA is likely to be achieved by the coat proteins supplied using pEAQ-*HT*-VP60.

Based on the above hypothesis and the observation that RNA replication is needed for encapsidation, I wish to propose a tripartite system for packaging 'RNA of choice' in CPMV capsids (Figure 4.9). To package any desired RNA within CPMV, using this system, three species of RNA will need to be co-expressed:

- (i) wt RNA-1 to provide the replication machinery;
- (ii) RNA encoding VP60 to supply the coat proteins;
- (iii) modified RNA-2 which could contain any RNA sequence along with the minimum sequence recognised as being essential for replication in CPMV (Canizares et al., 2006).

This would be expected to result in replication of (i) and (iii) followed by their encapsidation in separate particles using coat proteins supplied *in trans* by (ii). Capsids containing the modified RNA-2 could be purified using a density gradient and used for the delivery of the RNA, probably after modification of the outer capsid surface.

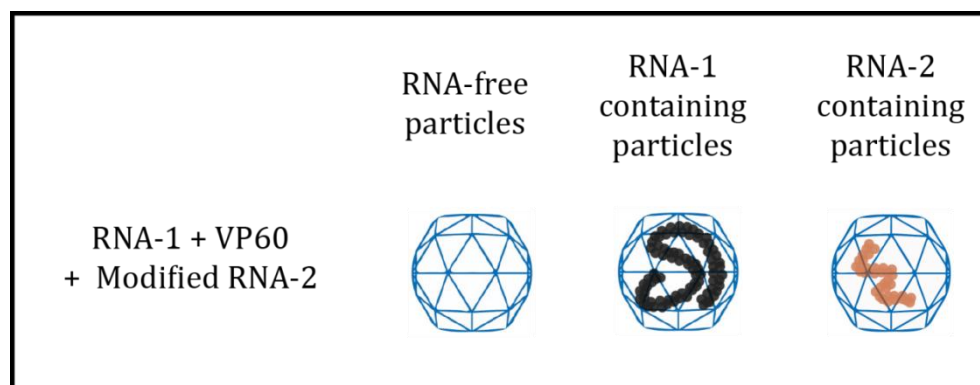


Figure 4.9 Proposed model for co-expression and encapsidation of modified RNA-2. Expression of a replication competent mutant of RNA-2 encoding the 'RNA of choice', in presence of wt RNA-1 and VP60 will result in formation of the three kinds of particles shown above.

Chapter 5: Results III

Creation of transgenic plants producing eVLPs

5.1 Introduction

Stable transgenic plants are an attractive alternative to transient protein expression systems in situations where continuous production of a defined product is required. Though creation of a transgenic line requires considerable initial effort, once a stable line has been generated by transformation of leaf tissue and self-fertilised to obtain transgenic seeds, large-scale protein expression can be achieved with little further effort. Transgenic seeds can be stored for years and are easy to transport. They can be sown on any desired scale and plants can be harvested as per convenience since transgenes are constitutively expressed throughout the lifetime of the plant. This is a complete contrast to transiently-infiltrated leaf tissue where optimal expression is achieved on a certain day post-infiltration and only in the infiltrated region of the leaf. In addition, transient infiltration requires a higher degree of containment since live *Agrobacterium* cultures are infiltrated into plants. Moreover, delivery of concentrated solutions of agrobacteria puts host plant cells under unnatural stress, often leading to degradation of expressed proteins. The great advantage of transient expression is its speed and flexibility which enables a wide variety of different constructs to be expressed and the properties of the resultant proteins analysed. However, once a construct expressing a product with the required properties has been identified using this approach, it may be advantageous to express it continuously using stable transformation. Indeed, the optimum approach may be to use transient expression for initial studies followed by the generation of stable transformants for long-term production, ideally using exactly the same construct.

For all the above reasons, it was decided to investigate the possibility of creating transgenic lines of *N. benthamiana* for continuous production of eVLPs since there appears to be a considerable, on-going demand for this material. However, it is

generally the case that the levels of expression achieved from transient expression are much higher than those from plants transformed with conventional binary vectors. So, prior to creation of eVLP transgenic lines, I wished to create an expression system for transgenic plants which incorporates the features of the CPMV-*HT* system with the aim of achieving high levels of expression from stably integrated transgenes. Such a system would be extremely valuable not only for the production of eVLPs but also for many other proteins where continuous production is required.

One of the factors that contributes to high levels of expression obtainable with the CPMV-*HT* system is the use of the suppressor of silencing P19 from the tomato bushy stunt virus (TBSV) (Voinnet et al., 2003). P19 is a 19 kDa protein which self-interacts to form homodimers that specifically sequester 21 nucleotide siRNAs regardless of their sequence (Omarov et al., 2006; Ye et al., 2003). Binding of P19 to siRNAs blocks post-transcriptional gene silencing and leads to up-regulation of protein expression. When co-expressed with GFP, P19 leads to as much as 50-fold increase in GFP expression (Voinnet et al., 2003). However, when used in transgenic systems, P19 was found to inhibit plant regeneration, though it can be used in transgenic cell cultures (Sun et al., 2011). Published studies report that leaf discs transformed with P19 do not regenerate and the only transformants that survive are ones with negligible levels of P19 (Scholthof et al., 1995). This is not surprising as it has now been demonstrated that P19 interferes with miRNA pathways involved in growth and development by binding to miRNA duplexes thereby making it impossible to regenerate plants from transformed leaf discs (Chapman et al., 2004; Dunoyer et al., 2004). Hence, P19 cannot be deployed in stably transformed plants for enhancement of expression. Inability of leaf discs to regenerate and other severe developmental defects have also been found with transgenic expression of other silencing suppressors such as HcPro of tobacco etch virus, HcPro of potato virus Y and AC2 of African cassava mosaic virus (Mallory et al., 2002; Siddiqui et al., 2008; Soitamo et al., 2011).

This chapter investigates the use of a previously characterized mutant of P19, P19/R43W, to suppress virus-induced RNA silencing without the concomitant

developmental effects. P19/R43W was first identified in an attenuated strain of TBSV where it was found to prevent the onset of systemic lethal necrosis in *N. benthamiana* (Chu et al., 2000) while maintaining some ability to bind siRNAs (Omarov et al., 2006). Sequestration of siRNAs by P19 is modulated by a central region of P19 that is positioned at the inner core of the dimer whereas R43 is located on the periphery of each monomer (Scholthof, 2006). So, the single amino acid substitution of arginine at position 43 with tryptophan still allows P19 to bind siRNA duplexes but the binding is weaker. The crystal structure of P19 bound to a 21 nt siRNA duplex suggests that the R43W mutation destabilizes the interaction of a tryptophan residue (W39) in each P19 monomer with the 3' end of siRNA (Figure 5.1) (Xia et al., 2009; Ye et al., 2003). This makes the binding of P19/R43W with siRNA duplexes unstable, resulting in reduced suppression of RNA silencing.

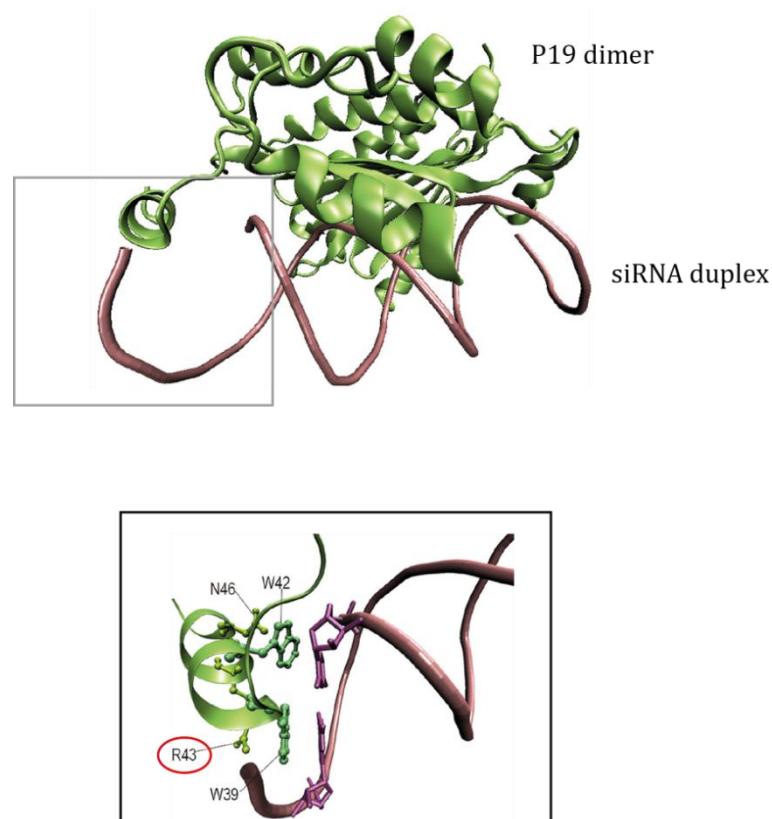


Figure 5.1 Location of R43 in P19-siRNA duplex complex. (Xia et al., 2009). Structural diagram of a P19 dimer (green) bound to a helical 21 bp siRNA duplex (purple). R43 is located on the periphery of the P19 dimer and makes indirect contacts with the siRNA duplex.

Even though it had been demonstrated that P19/R43W had reduced but sufficient ability to sequester virus-derived siRNAs and suppress virus-induced RNA silencing in the context of a viral infection (Omarov et al., 2007; Qiu et al., 2002), no evidence was available that P19/R43W would effectively suppress RNA silencing of heterologous genes outside the context of a viral infection. The results in this chapter demonstrate the effectiveness of P19/R43W in enhancement of expression of foreign genes in transiently-infiltrated as well as permitting the regeneration of homozygous transgenic plants. GFP was used for proof-of-principle studies followed by expression of pharmaceutically valuable proteins, such as human anti-HIV antibody 2G12 and the human gastric lipase (hGL). Finally, these results were used to design constructs for creation of transgenic *N. bethamiana* lines expressing high levels of eVLPs.

Generation of constructs and regeneration of leaf discs for the hGL transgenics (described in Section 5.3.2) and for the eVLP transgenics (Section 5.4) was done with the help of two rotation students in the lab, Mr. Hadrien Peyret and Miss Tilly Eldridge.

5.2 Creation of lines transgenic for GFP

5.2.1 Generation of constructs

To test expression of GFP in presence of P19/R43W, pEAQspecialKm-GFP-*HT* (Figure 5.2a) was generated by SDM of pEAQspecialK-GFP-*HT* (Sainsbury et al., 2009). Primers P19-R43W-SDM-F and P19-R43W-SDM-R (Appendix I) were used to change nts. 'CGG' (encoding arginine) to 'TGG' (encoding tryptophan) in order to introduce the point mutation R43W in wt P19 encoded by pEAQspecialK-GFP-*HT*. After verification of the mutation by sequencing, pEAQspecialKm-GFP-*HT* was transformed into agrobacteria for expression in plants.

In parallel, the expression cassette for GFP in the above vectors was replaced with a multiple cloning site to generate plasmids pEAQspecialK and pEAQspecialKm, which were used for expression of 2G12 described in Section 5.3.1.

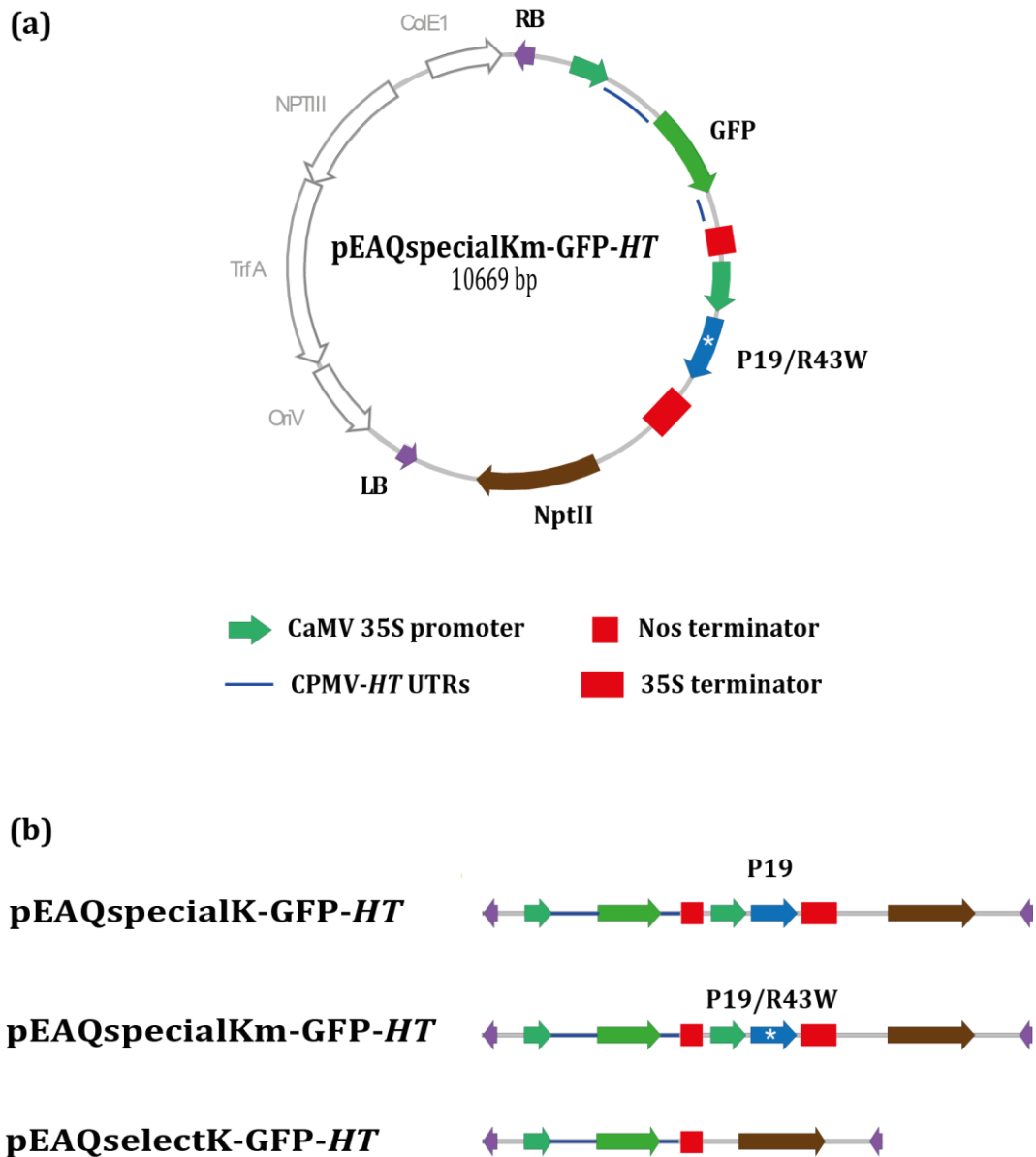


Figure 5.2 Schematic diagrams of constructs used for expression of GFP. **(a)** pEAQspecialKm-GFP-*HT* was created by SDM of pEAQspecialK-GFP-*HT* (Sainsbury et al., 2009) to introduce the R43W mutation in P19. The mutation is represented by an asterisk. LB and RB represent left and right borders respectively. **(b)** T-DNA regions of the plasmids used in this study for comparison. The main difference is the presence/absence of the P19 expression cassette.

5.2.2 Transient expression of GFP in presence of P19/R43W

Before proceeding with leaf disc transformation experiments to create transgenic plants, constructs pEAQspecialK-GFP-*HT* and pEAQspecialKm-GFP-*HT* were tested by transient expression in plants. pEAQselectK-GFP-*HT* (Sainsbury et al., 2009) was used as a control since the T-DNA of this vector does not encode any suppressor of silencing. Agrobacteria cultures, separately harbouring the three vectors (Figure 5.2b), were infiltrated into *N. benthamiana* leaves for comparison of GFP expression. At 6 dpi, the expression levels of GFP were assessed visually by the illumination of the infiltrated leaves in UV light and by spectrofluorometry (Figure 5.3).

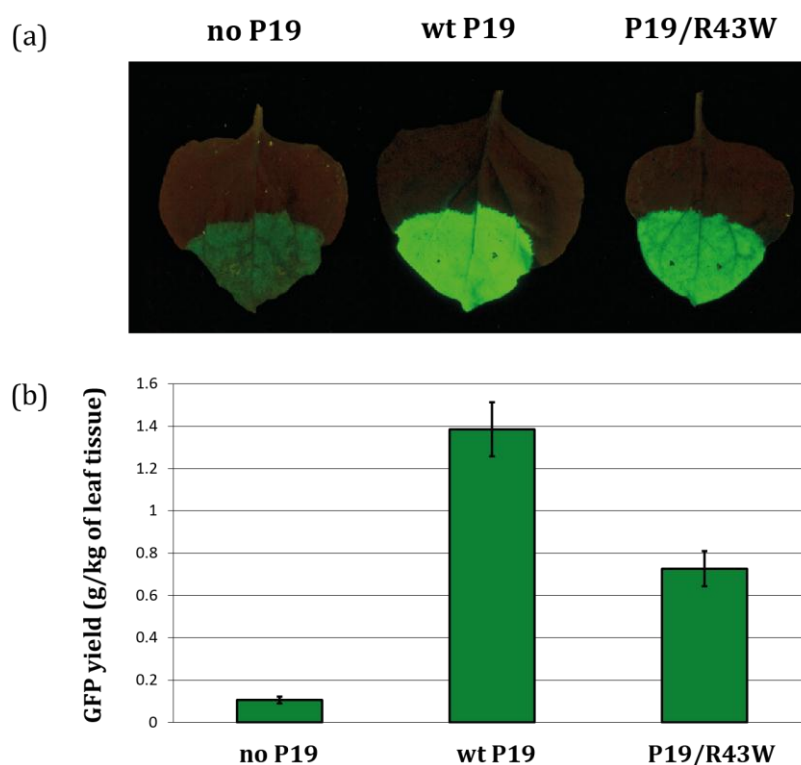


Figure 5.3 Transient expression of GFP in presence of wt P19 and P19/R43W.

(a) Leaves expressing GFP from plasmids pEAQselectK-GFP-*HT* (no P19), pEAQspecialK-GFP-*HT* (wt P19) and pEAQspecialKm-GFP-*HT* (P19/R43W) were photographed on 6 dpi under UV light. **(b)** Infiltrated leaves were harvested and processed for quantification of fluorescence. Yield calculations based on spectrofluorometry readings are shown above. Values are averages of expression levels of three biological replicates.

As seen in Figure 5.3, in the absence of any suppressor of silencing (pEAQselectK-GFP-*HT*), GFP expression levels of 0.1 g/kg FWT were obtained while pEAQspecialK-GFP-*HT* (encoding wt P19) gave GFP levels of 1.4 g/kg of FWT, a result similar to that reported previously (Sainsbury et al., 2009). In the case of pEAQspecialKm-GFP-*HT*, harbouring P19/R43W, GFP levels of 0.7 g/kg of FWT were achieved, approximately half that observed when the wt P19 was used and about 7-fold greater than those obtained in the absence of any suppressor. This demonstrates the reduced, though still substantial, ability of P19/R43W to enhance expression of a transiently expressed gene.

5.2.3 Stable integration of GFP and P19/R43 in *N. benthamiana*

Once transient studies confirmed that P19/R43W retained a substantial ability to enhance the expression of a heterologous gene, the next step was to determine its ability to allow the regeneration of stably transformed *N. benthamiana* and, if this proved possible, to determine its ability to enhance gene expression. To this end, leaf discs were separately transformed with the three vectors described in Figure 5.2b using the method described in Section 2.4.3. In 3-4 weeks, formation of callus was observed in transformed leaf discs and *calli* were moved to fresh media for development of shoots. While a number of primary transformants (T0) could be isolated when pEAQspecialKm-GFP-*HT* or pEAQselectK-GFP-*HT* were used for transformation, no plants could be regenerated when pEAQspecialK-GFP-*HT*, expressing wt P19, was used. This is consistent with previously reported toxigenic properties of wt P19 (Scholthof, 2006). By contrast, primary transformants suggested that P19/R43W was being tolerated within the plant.

One plant each from the T0 population generated upon transformation with pEAQselectK-GFP-*HT* (expressing no suppressor of silencing; referred to as Line 3) and with pEAQspecialKm-GFP-*HT* (expressing P19/R43W; referred to as Line 5) was selected for analysis of GFP expression. Both T0 plants grew normally and fluoresced under UV light showing successful integration of the GFP gene (Figure 5.4). Upon visualization under UV light, Line 5 appeared to give higher fluorescence than Line 3. However, assays for quantification of GFP needed to be

undertaken before any conclusions could be drawn. The plants were self-fertilized and the resultant seeds were sown on MS agar (without any antibiotic selection) to generate a T1 population of around 50 plants from each line. None of the T1 plants from Line 3 or Line 5 showed any obvious developmental defects.



Figure 5.4 Phenotype of plants transgenic for GFP and P19/R43W. T0 plants of Line 3 and Line 5 were brought to flower to illustrate their normal development independent of the presence of P19/R43W. Under UV light, GFP fluorescence is evident in transgenic plants in comparison to a non-transformed plant which appears red due to the fluorescence of leaf chlorophyll in UV light.

5.2.4 Analysis of GFP expression levels in transgenic *N. benthamiana*

Initial characterization of GFP expression was performed by visually scoring each T1 plant for green fluorescence under UV light followed by verification using spectrofluorometry. T1 plants from both Line 3 and Line 5 appeared to give three distinct levels of GFP fluorescence, with the ratio of plants showing high, medium and no fluorescence being approximately 1:2:1 (Figure 5.5). Even though a strict correlation between zygosity and level of expression cannot be assumed, these

results fit with the occurrence of a single integration event in both cases, where the ratio 1:2:1 corresponds to homozygotes : heterozygotes : null segregants.

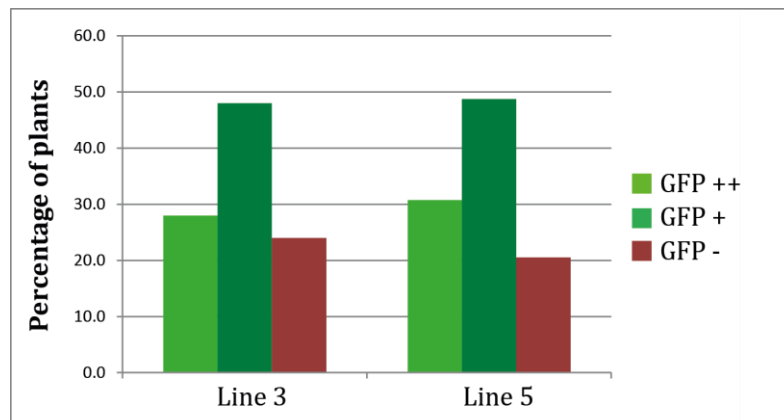


Figure 5.5 GFP expression levels in T1 populations of Line 3 and Line 5. Bars show the percentage of plants expressing high levels of GFP (bright green bars), medium levels of GFP (dark green bars) and no GFP (red bars) amongst the T1 population of Line 3 and Line 5, as judged by visualisation of leaves under UV light. The ratio is roughly 1:2:1.

For detailed quantitative analysis of GFP expression, the fifteen highest expressing plants were chosen from Line 3 and Line 5 each based on the initial spectrofluorometry results. This selection was done to reduce the number of plants to be analysed over generations. Moreover, I was interested in finding plants homozygous for P19/R43W and the fifteen highest expressing plants (top-third of the T1 population) had the highest probability of being homozygous for the transgene.

Leaf tissue was harvested from all fifteen plants of Line 3 and Line 5 and GFP fluorescence was quantified by spectrofluorometry. Although there was considerable variation in the levels of GFP in T1 plants from the same line, overall, GFP expression levels were higher in plants of Line 5 in comparison with those of Line 3 (Figure 5.6). For Line 3, the average level of GFP expression was 48 mg/kg FWT whereas that the average level of GFP expression in Line 5 was 66 mg/kg FWT, which is an increase of almost 40%. This shows that the chances of getting a

high-expressing transgenic line for GFP are much higher if P19/R43W is co-expressed with GFP.

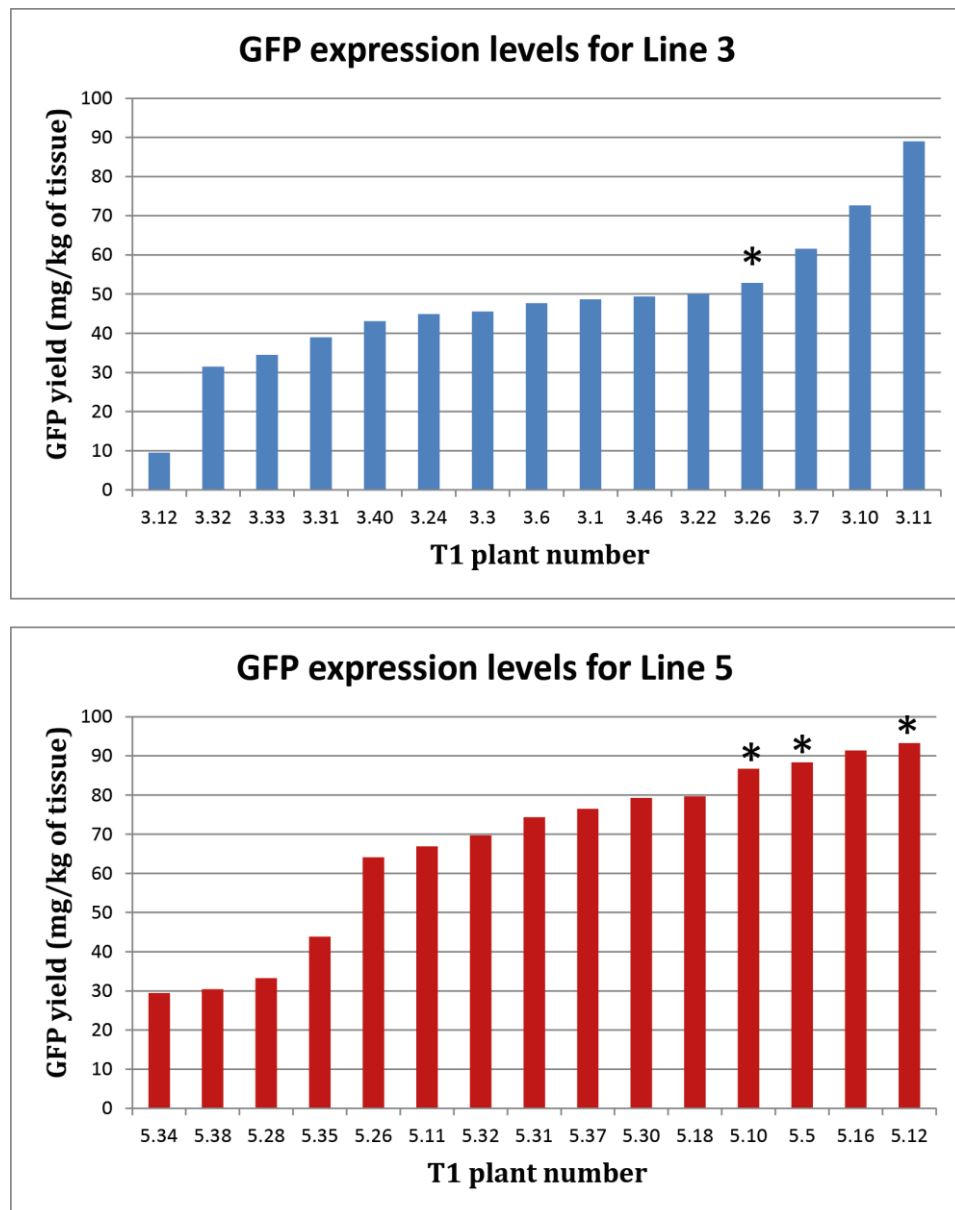


Figure 5.6 Comparison of expression levels of GFP in Line 3 and Line 5. Fifteen plants (numbers along the X-axis) from the T1 population of Line 3 (blue bars) and Line 5 (red bars) have been arranged in increasing order of GFP expression. Although the difference between the highest expressor of both lines is only 4.3 mg/kg FWT, the average level of expression is higher in Line 5, i.e. in presence of P19/R43W. Plants subsequently identified as homozygotes (details in Section 5.2.5) have been marked with an asterisk (*).

5.2.5 Identification and analysis of plants homozygous for P19/R43W

If transformation with P19/R43W was to be used as a practical method of enhancing transgene expression, it was essential to determine if plants homozygous for P19/R43W could be made since the ability to produce homozygous plants is a pre-requisite for the creation of a true-breeding line. Previous attempts to produce transgenic plants homozygous for other suppressors of silencing have been unsuccessful (Mallory et al., 2002).

To identify homozygotes among the fifteen T1 plants of Line 3 and Line 5, each plant was self-fertilised and seeds were collected. These were then germinated on agar in the absence of any antibiotic selection in the media to enable growth of the null segregants in addition to the transgenic seedlings. After 3-4 weeks, the seedlings were scored for GFP expression by visualisation under UV light. In the majority of cases, only 50-75% of the T2 seedlings expressed GFP showing that there was a proportion of null segregants in the T2 generation, indicating that selfed T1 parent was heterozygous. However, for plant 3.26 of Line 3 and plants 5.5, 5.10, and 5.12 of Line 5, 100% of the T2 seedlings expressed GFP demonstrating that their parent plant was homozygous for GFP (Figure 5.7). Since P19/R43W was encoded on the same T-DNA as GFP, it was very likely that plants homozygous for GFP were also homozygous for P19/R43W.

Plants identified to be homozygous for GFP and P19/R43W in this way have been marked with an asterisk in Figure 5.6. As expected, these homozygotes were found to be amongst the highest expressors for each line. On comparing the average yield of homozygous plants of Line 3 and Line 5, the presence of P19/R43W appears to enhance expression of GFP approximately 1.7 fold. All homozygous individuals of Line 3 and Line 5 were phenotypically normal which demonstrated that even when expressed from two alleles, P19/R43W did not interfere with growth and development in *N. benthamiana*.

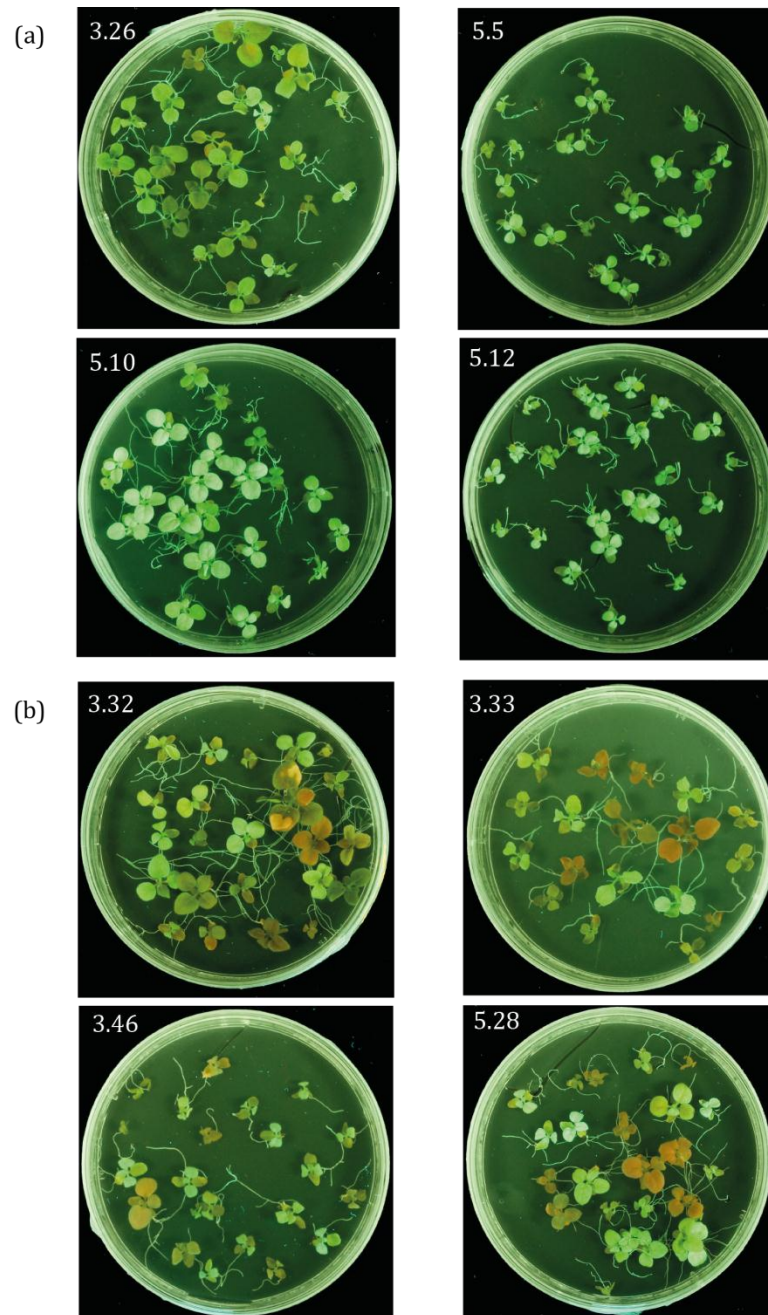


Figure 5.7 GFP expression in the T2 generation of Line 3 and Line 5. Seeds of T1 plants (numbered on the top-left corner of each picture) from Line 3 and Line 5 were germinated on agar to assess GFP expression and four-week old seedlings were photographed under UV light. Section **(a)** shows plates where 100% of the seedlings expressed GFP showing that their parent plant was homozygous for GFP. Section **(b)** shows plates where around 75% of the seedlings expressed GFP indicating that their parent plant was heterozygous for GFP.

5.3 Creation of lines transgenic for pharmaceutically valuable proteins

Following promising results achieved with GFP, the P19/R43W-based expression system was extended to two pharmaceutically valuable proteins: a human IgG antibody named 2G12 and the human gastric lipase.

5.3.1 Human HIV-1 antibody 2G12

2G12 is a human monoclonal antibody to a surface glycoprotein (gp120) of human immunodeficiency virus type 1 (HIV-1) (Buchacher et al., 1994). 2G12 is a good candidate for treatment of HIV-1 infections by passive immunization since it possesses potent and broad neutralizing activity against primary strains of HIV-1 (Trkola et al., 1996). In addition, recent studies in primates have demonstrated the ability of 2G12 to prevent HIV-1 transmission when supplied through mucosal tissue (Mascola et al., 1999; Mascola et al., 2000). However in all these cases, multiple high doses of 2G12 are needed for effective treatment. Currently produced using Chinese Hamster Ovary (CHO) cell lines, there is a clear demand for a low-cost high-level production method for 2G12 and a transgenic plant expression system would be a good option.

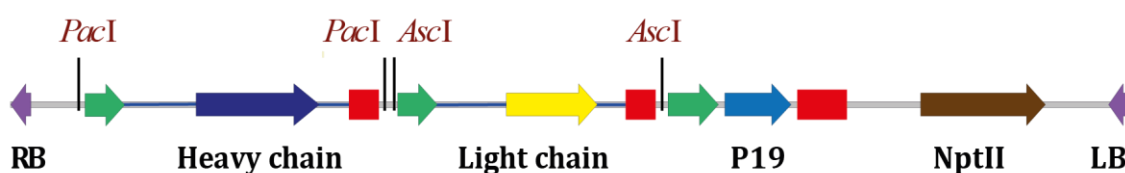
Plant production of 2G12 involves co-expression of heavy and light chains of 2G12 and purification under non-reducing conditions. 2G12 was chosen for this work since it had previously been produced in *N. benthamiana* leaves by transient infiltration and preliminary studies suggested that the binding and neutralization properties of plant-produced 2G12 were generally similar to that of CHO cell-produced 2G12 (Sainsbury et al., 2010b). In addition, the approval for Phase I clinical trials of 2G12 produced in transgenic tobacco (Fox, 2011) encouraged further research on methods for its large-scale production in plants.

5.3.1.1 Transient expression of 2G12 and P19/R43W

The cassettes for expression of the heavy and light chains of 2G12, consisting of the 35S promoter, the *HT* 5' UTR, the gene encoding the heavy/light chain, the 3' UTR and the nos terminator, were amplified from plasmids pBD2G12HE-*HT* and pBD2G12L-*HT* (Sainsbury et al., 2010b) respectively. In addition, pBD2G12HE-*HT*

encoded an ER-retention signal at the 5' end of the gene encoding the heavy chain to target the protein to the ER for higher expression levels (Sainsbury and Lomonosoff, 2008). Post amplification, the expression cassette for the light chain was cloned within the *AscI* sites of the vectors pEAQspecialK and pEAQspecialKm (Section 5.2.1), followed by cloning of the heavy chain within the *PacI* sites of both the above vectors. The resultant vectors were named pEAQspecialK-HEL and pEAQspecialKm-HEL (Figure 5.8).

T-DNA of pEAQspecialK-HEL



T-DNA of pEAQspecialKm-HEL

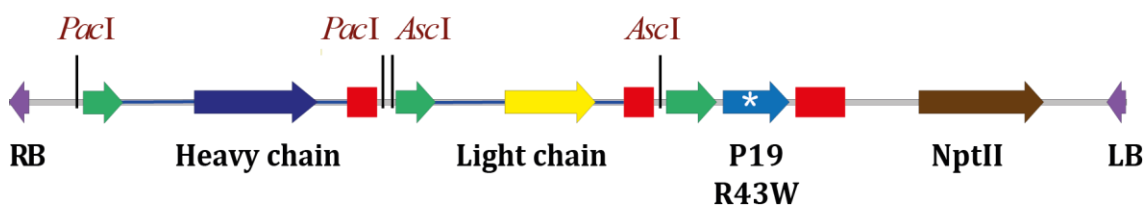


Figure 5.8 Design of constructs used for expression of 2G12. Schematic representation of the T-DNA regions of vectors pEAQspecialK-HEL and pEAQspecialKm-HEL. LB and RB represent left and right borders respectively. The asterisk denotes the R43W mutation in P19.

pEAQspecialK-HEL and pEAQspecialKm-HEL were tested by transient infiltration of agrobacteria harbouring each construct into *N. benthamiana* plants followed by separation of crude extracts of infiltrated leaves on SDS-PAGE gels. Under reducing conditions, bands of about 50 kDa and 25 kDa were obtained in both samples, corresponding to heavy and light chains of 2G12 respectively; thereby confirming expression of constructs. Under non-reducing conditions, a band of about 220 kDa was obtained confirming assembly of the heavy and light chains into an IgG protein (Figure 5.9). The unexpectedly high molecular weight of the fully assembled antibody (220 kDa instead of 150 kDa) is commonly observed for antibodies when analysed by electrophoresis using Tris-glycine running buffers (Sainsbury et al., 2008).

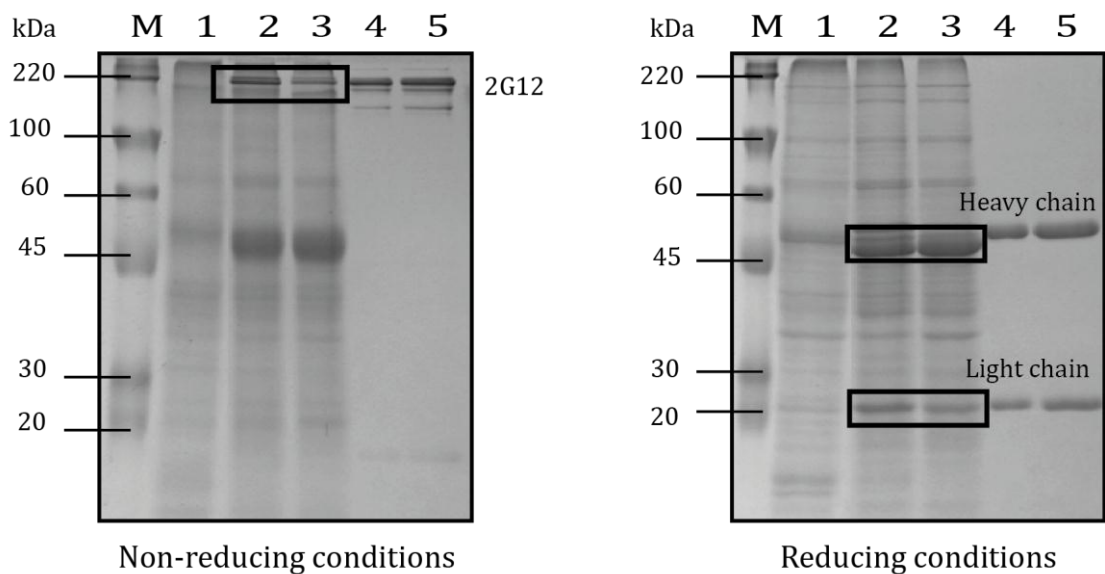


Figure 5.9 Analysis of 2G12 expression by SDS-PAGE. Total protein extracts of infiltrated leaves were separated on polyacrylamide gels under reducing and non-reducing conditions and visualized by staining with Coomassie blue. Samples were run as follows: Lane (1) Extract from plant infiltrated with empty vector pEAQ-HT, (2) extract from plant infiltrated with pEAQspecialK-HEL, (3) extract from plant infiltrated with pEAQspecialKm-HEL, (4) 1 µg of CHO-produced 2G12, (5) 2 µg of CHO-produced 2G12 and (M) standard protein marker.

Known amounts of CHO-produced 2G12 were run in parallel as standards and used to estimate expression levels. In presence of wt P19 (pEAQspecialK-HEL), 2G12 expression levels approaching 400 mg/kg FWT were attained, while in presence of P19/R43W (pEAQspecialKm-HEL), 2G12 expression levels appeared to be approximately half as much. This is consistent with the results obtained with GFP expression and reiterates that P19/R43W retains a reduced but significant ability to enhance expression.

Presence of the heavy and light chains of 2G12 within the same T-DNA, as in the case of pEAQspecialK-HEL and pEAQspecialKm-HEL, was essential since the constructs were ultimately designed for transgenic expression of 2G12 and simultaneous integration of the genes encoding the heavy chain and the light chain into the genome of the plant was a pre-requisite for transgenic expression of 2G12.

5.3.1.2 Transgenic expression of 2G12 and P19/R43W

After confirming that pEAQspecialKm-HEL was a functional clone from transient studies, *A. tumefaciens* harbouring pEAQspecialKm-HEL was used to transform 20-25 *N. benthamiana* leaf discs. Plantlets regenerated from discs were transferred to soil and five T0 transgenic plants were subsequently obtained. However, all five plants came from different sections of the same disc, so it was possible that all of these were generated from the same transformation event. A number of transformed leaf discs were lost due to contamination and other technical problems with the growth chamber. Nonetheless, the five plants obtained were analysed independently for 2G12 expression. At this stage, plants grew normally and showed no obvious morphological defects (Figure 5.10).

Crude leaf extracts from the five T0 plants were separated using SDS-PAGE and analysed for presence of 2G12 using the technique of western blotting. Bands for IgG heavy chains were detected in extracts from all five plants confirming successful integration of the T-DNA and expression of 2G12 (Figure 5.11). On comparison of the intensities of bands with known standards, the five T0 plants were estimated to express levels of 2G12 in the range of 40-60 mg/kg FWT.



Figure 5.10 T0 transgenic plants expressing 2G12 and P19/R43W. 8-week old plants regenerated from leaf discs transformed with pEAQspecialKm-HEL, showed no morphological defects.

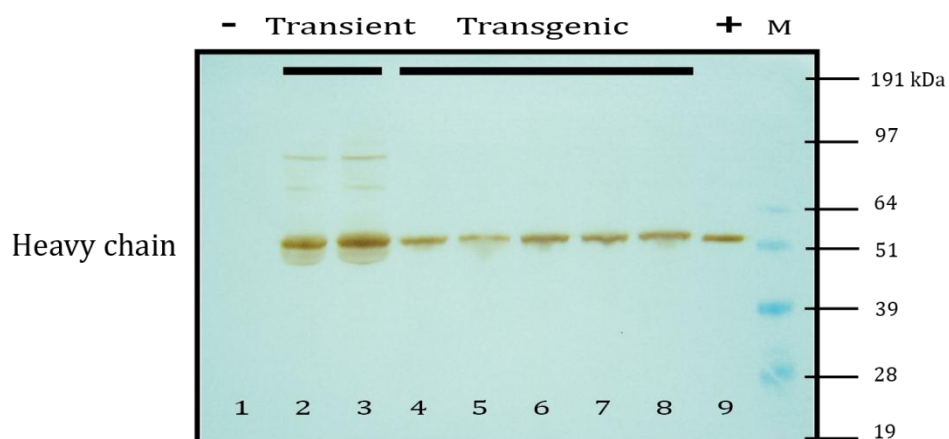


Figure 5.11 Detection of 2G12 in T0 transgenic plants. Using anti-human IgG (Fc specific) antibody, bands for the 2G12 heavy chain were detected in all five transgenic plants (Lanes 4-8). Extracts from plants transiently infiltrated with 2G12 constructs were analysed in parallel (Lanes 2-3). Extract from a healthy plant was run in Lane 1 and 200 ng of CHO cell-produced 2G12 was run in Lane 9.

T0 plants expressing 2G12 were allowed to flower and self-fertilized to obtain the T1 generation. However, despite several normal-looking flowers developing on each plant, none set seed. Flowers were taped at different stages of their development to avoid putting the plant under any kind of stress but seed pods did not develop in any of the flowers under any of the conditions examined. This suggests that during genome integration of T-DNA, functional genes of the plant were disrupted and as a consequence, the plants could not produce seeds. However, the precise reason for this is unclear. Since all transformed discs were likely to be a result of the same transformation event, it was not surprising that all plants displayed the same phenotype. Due to lack of seed, this work could not be taken any further as time did not permit the production of additional primary transformants. Nevertheless, T0 plants of 2G12 provided further evidence that P19/R43W was tolerated in plants and could enhance transgene expression.

5.3.2 Human gastric lipase

Human gastric lipase (hGL) is a member of the family of preduodenal lipases, primarily responsible for initiation of lipolysis of dietary fats, such as triglycerides in the gastrointestinal tract (Carriere et al., 1993). It is a candidate for treatment of pancreatic enzyme insufficiency, as a superior substitute for the current treatment that uses enzyme obtained from porcine pancreatic extract (DiMagno et al., 1977). Recently, it was demonstrated that active recombinant hGL can be produced in *N. benthamiana* by transient expression using the CPMV-*HT* system (Vardakou et al., 2012). Given the demand for a reliable hGL production system and promising results obtained from transient expression studies, it was decided to attempt creation of transgenic plants producing hGL.

5.3.2.1 Transgenic expression of hGL and P19/R43W

Transgenic plants expressing hGL in presence of P19/R43W were created by Mr. Hadrien Peyret by transformation of *N. benthamiana* leaf discs with the vector pEAQspecialKm-hGL, generated by replacement of the gene for GFP in pEAQspecialKm-GFP-*HT* with the gene encoding hGL. Phenotypically normal T0 plants expressing active hGL were obtained. These were selfed to produce the T1

generation of plants transgenic for hGL. While active hGL was obtained from a majority of the T1 plants, it was observed that seed production was significantly reduced amongst the T1 population. For every 10 developing flowers that were taped, 2-3 produced seeds. Nonetheless, resultant seeds were analysed to identify homozygotes amongst the T1 population. Homozygotes grew normally and expressed high levels of active hGL, averaging around 0.3 mg/kg FWT. Although further work needs to be done on purification of plant produced- hGL, this promises to be a cheap and reliable production system and continues to be worked upon in the lab.

5.4 Creation of lines transgenic for eVLPs

Following the success of P19/R43W in enhancement of transgenic expression of GFP, 2G12 and hGL, the prospect of creating a transgenic line of *N. benthamiana* that constitutively produced high levels of eVLPs was considered. A transgenic eVLP-producing line would be an efficient way of obtaining a regular supply of eVLPs for their further characterization and their use in nanotechnology.

Creation of a line transgenic for eVLPs would involve stable transformation of leaf discs with a plasmid encoding VP60 (coat protein precursor), 24K (viral proteinase) and P19/R43W (suppressor of silencing) within its T-DNA region. This section describes the creation of this plasmid and attempts to transform leaf discs with it.

5.4.1 Generation of the construct

To generate a construct for transgenic expression of eVLPs in presence of P19/R43W, three fragments of DNA, namely, the VP60 expression cassette, the 24K expression cassette and the pEAQspecialKm vector backbone, were combined using a three-part ligation reaction. First, the VP60 expression cassette was amplified from pEAQ-*HT*-VP60 (Saunders et al., 2009) using primers FSC2-F and FSC5-R (Appendix I) which resulted in introduction of the restriction sites *PacI* and *SbfI* on either side of the expression cassette. In parallel, the 24K expression cassette was amplified from pEAQ-*HT*-24K (Saunders et al., 2009) using primers

FSC6-F and FSC2-R (Appendix I) which introduced the restriction sites *SbfI* and *AscI* on either side of the expression cassette. The amplified fragments and the vector pEAQspecialKm were then digested as follows:

- (i) Amplified VP60 expression cassette was digested with *PacI* and *SbfI*;
- (ii) Amplified 24K expression cassette was digested with *SbfI* and *AscI*;
- (iii) Vector backbone pEAQspecialKm was digested with *PacI* and *AscI*.

The digested fragments were ligated together using standard ligation protocols (Section 2.3.3) to generate pEAQspecialKm-eVLP (Figure 5.12).

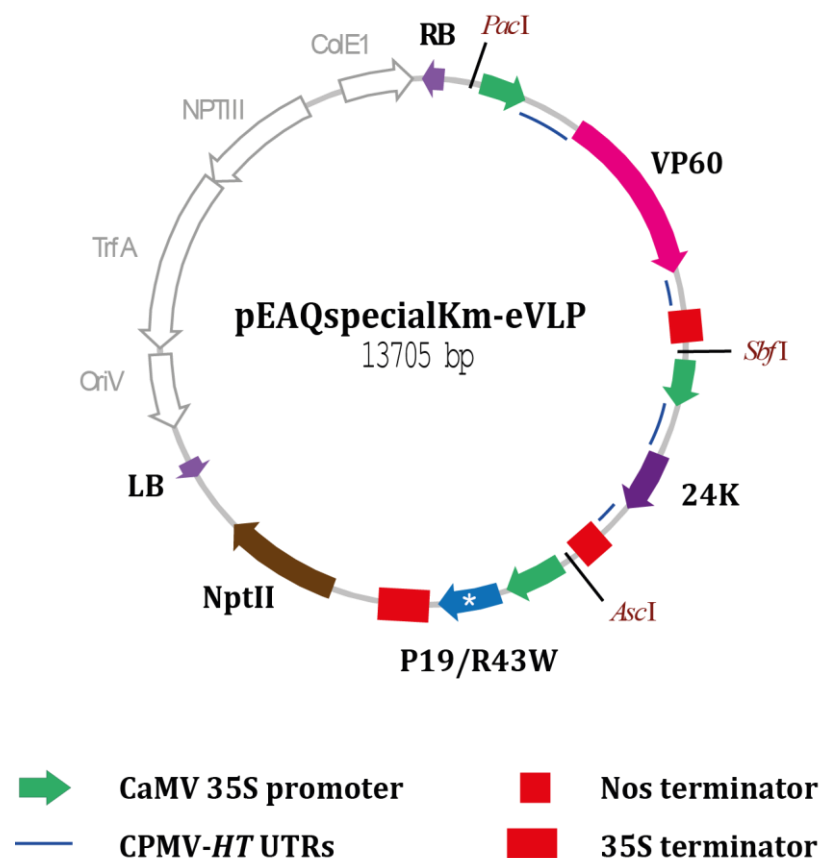


Figure 5.12 Schematic diagram of the construct used for expression of eVLPs. The plasmid map of pEAQspecialKm-eVLP is shown. LB and RB represent left and right borders respectively. The asterisk denotes the R43W mutation in P19.

5.4.2 Transient expression of eVLPs and P19/R43W

pEAQspecialKm-eVLP was initially tested for its ability to direct the synthesis of eVLPs by transient expression in *N. benthamiana* leaves. pEAQexpress-eVLP, described previously in Section 3.3.1, was used for comparison since it expresses eVLPs in presence of wt P19. An empty pEAQ vector was used as the negative control for transient expression of eVLPs. Leaves infiltrated with either of the eVLP constructs or with the empty pEAQ vector were harvested on 6 dpi and the crude leaf extracts were subjected to the standard eVLP purification protocol (Section 2.6.2). The resulting proteins were analysed by SDS-PAGE.

Prominent bands were seen for L and S coat proteins from denatured eVLPs in the extracts from plants inoculated with either pEAQexpress-eVLP or pEAQspecialKm-eVLP, while no proteins of the size of L and S were seen in the extract from leaves infiltrated with the empty pEAQ vector (Figure 5.13). On the basis of the intensity of the bands on the gel, it was estimated that expression of eVLPs from pEAQspecialKm-eVLP was higher than that from pEAQexpress-eVLP. This was unexpected as the latter encoded wt P19 which, from previous results, is known to enhance expression 2-fold more than the P19/R43W encoded by the former. This observation could not really be explained and was attributed to differences in infiltration technique, health of plants, health of agrobacteria, etc. Nonetheless, these transient infiltration studies confirmed that pEAQspecialKm-eVLP was a functional clone and could be taken forward for stable transformation of leaf discs.

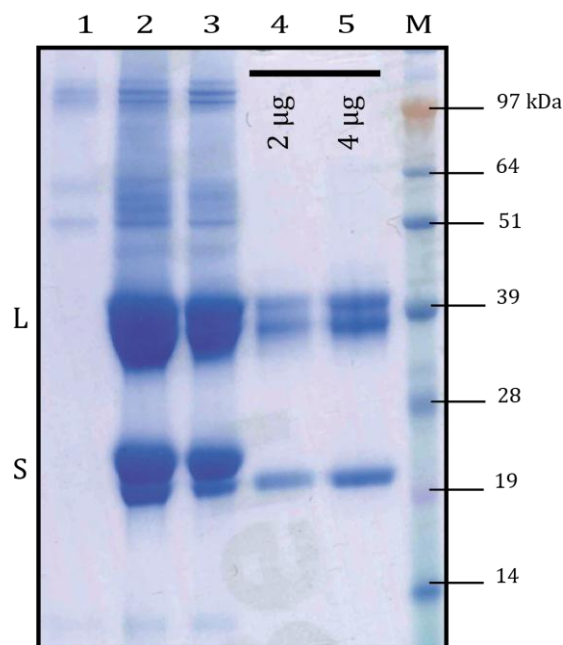


Figure 5.13 Analysis of eVLP expression by SDS-PAGE. Proteins purified from crude extracts of infiltrated leaves were denatured by heat-incubation and separated on polyacrylamide gels. The gel was stained with Coomassie blue for detection of proteins. Samples were run as follows: Lane (1) extract from leaves infiltrated with an empty pEAQ vector (2) extract from leaves infiltrated with pEAQspecialKm-eVLP, (3) extract from leaves infiltrated with pEAQexpress-eVLP, (4) 2 μ g of purified eVLPs, (5) 4 μ g of purified eVLPs and (M) standard protein marker. Bands for L and S are indicated.

5.4.3 Transgenic expression of eVLPs and P19/R43W

Leaf discs were transformed with pEAQspecialKm-eVLP using the standard protocol for stable transformation of tissue (Section 2.4.3). This resulted in the regeneration of six primary transformants out of which four were from independent leaf discs. All six plants developed normally and showed no morphological defects. About eight weeks after regenerated primary transformants were transferred to soil, leaf tissue from each T0 plant was analysed for eVLP expression. 4-5 leaves (5 g FWT) were harvested from each of the T0 plants and subjected to the standard particle purification protocol. Analysis of purified extracts from infiltrated leaves using TEM and SDS-PAGE showed the absence of particles in all T0 plants.

Integration of the T-DNA into the plant genome was confirmed by PCR, using primers C1 and C3 (Appendix I) that bind to the *HT* UTRs, on genomic DNA extracted from the leaves of T0 plants (H. Peyret, pers. comm). Moreover, since the entire T0 population was germinated on agar plates containing kanamycin, the expression of the gene for kanamycin resistance was confirmed. This implied that it was likely that VP60 and 24K, encoded on the same T-DNA, were being expressed but were either aggregating due to their insolubility or getting degraded by the host cell machinery.

To investigate this further, a western blot was conducted on the crude leaf extracts of the T0 plants using the anti-CPMV antibody G49 (Table 2.3) which specifically recognizes the coat proteins of CPMV. To prepare each sample for blotting, 4-5 leaf discs (150 mg FWT) from each T0 plant were homogenized in three volumes of 0.1 M sodium phosphate buffer (pH=7). As a control, leaf extracts from plants transiently infiltrated with the constructs pEAQ-*HT*-VP60 and pEAQ-specialKm-eVLP were used. The homogenized extracts were heat-denatured and subjected to SDS-PAGE, followed by their transfer to a nitrocellulose membrane. The levels of expression in the transgenic plants were expected to be lower than those achieved from transiently-infiltrated plants and therefore, higher amounts of the crude extracts from the transgenic plants were loaded on the gel. The membrane was probed with anti-CPMV antibody G49 and its binding was subsequently detected using a secondary antibody and chemiluminescence. Results showed that neither VP60 nor L and S coat proteins were present in the transgenic tissue (Figure 5.14). A band for VP60 was detected in the leaf extract of the plant transiently-infiltrated with pEAQ-*HT*-VP60 and bands for L and S were detected in the leaf extract of the plant infiltrated with pEAQspecialKm-eVLP.

The western blot confirmed the absence of VP60 in all transgenic lines and it was recognized that the method for expression of VP60 would need to be refined further to achieve transgenic expression of eVLPs. Expression of 24K could not be verified since no antibodies against it were available.

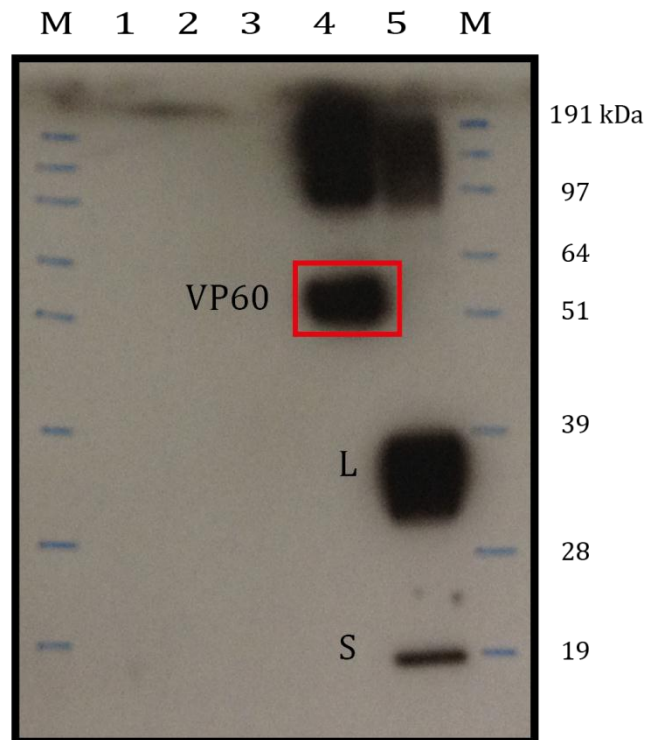


Figure 5.14 Immunodetection of CPMV coat protein. Leaf extracts of selected T0 transgenic plants (Lanes 1-3) and of plants transiently infiltrated with pEAQ-*HT*-VP60 (Lane 4) and pEAQspecialKm-eVLP (Lane 5) were analysed by western blotting using the anti-CPMV antibody G49. Bands for VP60, L and S have been indicated. The high molecular weight bands (over 100 kDa) are aggregates of VP60 or L and S coat proteins.

5.5 Discussion

A novel system for stable expression of foreign genes in plants has been presented in this chapter. In this system, the modified suppressor of silencing P19/R43W was deployed to enhance expression of heterologous genes in transient and transgenic systems. Initial studies were undertaken with GFP, followed by their validation by expression of two pharmaceutically valuable proteins and finally, the system was used in an attempt to produce lines of plants for the stable expression of eVLPs.

In parallel to our studies with GFP and P19/R43W, *N. benthamiana* plants transgenic solely for P19/R43W were created by our collaborators, Dr. Yi-Cheng

Hsieh and Prof. Herman Scholthof at Texas A&M University. Out of fourteen regenerated transformants, three were confirmed to be transgenic for P19/R43W by western blot analysis of leaf tissue (Saxena et al., 2011). All fourteen T₀ plants developed normally, flowered and set fertile seed. The phenotype of the three plants accumulating detectable levels of P19/R43W was not very different from the rest apart from some evidence of cup shaped leaves and mild blistering (Figure 5.15). These results provided evidence that P19/R43W can accumulate at detectable levels in transgenic *N. benthamiana* with minimal effects on plant morphology, growth and development. This encouraged further work on the assessment of the effect of P19/R43W on expression levels of other heterologous proteins in the plant.

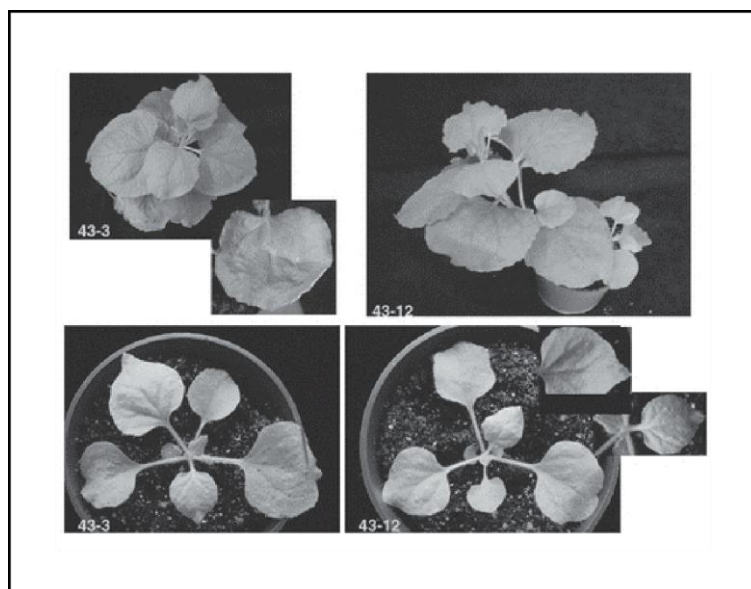


Figure 5.15 Phenotype of plants transgenic for P19/R43W. Plants transgenic for P19/R43W developed normally and only upon close inspection, displayed mild morphological features such as cupping of leaves and blistering (Data from Dr. Yi-Cheng Hsieh and Prof. Herman Scholthof, Texas A&M University).

Proof-of-principle studies undertaken with GFP showed that P19/R43W can be used to boost expression of GFP in plants, without deleterious effects on plant growth and development. Transient expression of GFP in presence of P19/R43W was seen to be half of that in presence of wt P19, but this was still significantly more than the expression in the absence of any suppressor. Plants transgenic for

GFP and P19/R43W also showed elevated levels of GFP expression (an average enhancement of 40% over expression seen in the absence of a suppressor). Since the emphasis of this study was to assess if P19/R43W could be tolerated within stably transformed plants and not the absolute expression levels achieved, no attempts were made to boost GFP expression levels further. However, if desired, the system can be optimized to achieve maximal expression of transgenes. One of the ways to maximize expression would be to boost the expression of P19/R43W itself by expressing it with CPMV-*HT* UTRs. This is expected to lead to increased RNA suppression activity and in turn, enhanced transgene expression. The use of different promoters and terminators for every expression cassette may also enhance expression levels. However, increasing the levels of P19/R43W could also adversely affect plant regeneration.

Studies on GFP were limited to one line each for expression in absence of any suppressor (Line 3) and for expression in presence of P19/R43W (Line 5). While this was enough to establish that P19/R43W does not affect growth and development of plants and contributes to elevated expression levels, more lines should be generated and analysed to obtain homozygotes with maximally enhanced expression. This would be critical if a line was to be used commercially as a source for a particular heterologous protein. In that case, detailed analysis of the site of integration and the copy number of the transgene would also be needed.

After success with GFP expression, the P19/R43W system was modified to enhance expression of an antibody (2G12), an enzyme (hGL) and virus-like particles (eVLPs). Work done with GFP, 2G12 and hGL demonstrated that the highly efficient transient expression system, CPMV-*HT*, can be adapted for stable transformation. However, plants transgenic for eVLPs could not be generated. Expression of neither VP60 nor 24K could be confirmed in any of the regenerated plants and due to time constraints, regeneration of further lines could not be undertaken. This continues to be worked upon in the lab. In addition, attempts to solubilize VP60 *in vivo* are being made. Once the issue of solubility of VP60 is resolved, other factors like accessibility of VP60 to 24K, stoichiometry of both proteins and the stability of both proteins will also need to be considered. Overall,

on-going work on generation of plants transgenic for eVLPs promises to deliver an easy and reliable method for high-level production of eVLPs.

The work presented in this chapter is the first study to report the accumulation of readily detectable levels of a constitutively expressed suppressor of silencing in transgenic plants without severe morphological defects. However, although the plant grows and develops normally, P19/R43W may have an effect on plant fitness, for instance on the defense response of the plant or its resistance to pathogens. Also, since the main problem observed in plants transgenic for 2G12 and hGL was a reduction in their ability to develop seeds, it may be possible that P19/R43W interferes with the development of the ovum or pollen or with the process of fertilization in *N. benthamiana*. This is because the underlying principle of enhancement of expression by P19/R43W is inhibition of RNA silencing in a non-specific manner and hence, in addition to the gene of interest, expression of other housekeeping genes in the host cell is also affected. From a biotechnological perspective, a reduction in plant fitness is a small price to pay to gain high yields. Use of suppressors of silencing such as wt P19 in transient expression is common practice and reduction in plant fitness has never been a problem in transient systems.

Since the CPMV-*HT* vectors are designed for easy and quick expression of proteins, a number of constructs can be generated and screened by transient-expression in plants in a matter of days and then, selected constructs can be taken forward for stable transformation, if required. However, a point to bear in mind while using CPMV-*HT* vectors in transgenic expression is that for every expression cassette in the vector, there will be present a 35S promoter, a nos terminator and CPMV-*HT* UTRs. Repetitive use of the same sequences encoding the promoters, terminators or UTRs increase the chances of homologous recombination within the T-DNA which can result in loss of the transgene(s). Although this was not found to be the case with GFP transgenic plants (selfed to two generations) and with hGL transgenic plants (selfed to three generations), it is a potential source of concern. A solution to this potential problem could be the use of different promoters and terminators for different expression cassettes. However, since the CPMV-*HT*

system is optimized for best expression levels, a change in its components may negatively affect transgene expression.

Published studies report expression of transgenes in stable transgenic plants to be around a tenth of the expression achieved using a transient expression system (Rybicki, 2010). As demonstrated by results shown in this chapter, the use of P19/R43W has the potential to enhance expression to almost half the levels obtained with transient expression. Thus, P19/R43W is a useful addition to the toolbox for high-level expression of heterologous proteins in plants.

Chapter 6: Results IV

Development of expression vectors based on CPMV RNA-1

6.1 Introduction

Work towards development of a system for transgenic expression of eVLPs highlighted two limitations of the current CPMV-*HT* expression system. First, that the high levels of expression obtained using CPMV-*HT* can lead to deleterious effects on the plant due to accumulation of proteins, as seen with the plants transgenic for 2G12 (Section 5.3.1.2). Also, in situations such as expression of metabolites in an enzymatic pathway, low levels of a certain substrate may be needed; or in expression of virus-like particles such as eVLPs, different components may be required in different amounts. Secondly, multiple copies of the same expression cassette, i.e. the promoter, terminator and the UTRs are used for co-expression of multiple proteins using the CPMV-*HT* system. While the repetitive use of the same sequences does not matter in transient expression, in transgenic expression systems, it increases the chances of homologous recombination, thereby risking loss of transgenes in subsequent generations.

To overcome the above limitations and to increase the range of CPMV-based expression vectors available, the possibility of creating expression vectors based on sequences derived from CPMV RNA-1 was explored. All CPMV-based expression systems developed to date have been based on modified versions of RNA-2 (Sainsbury et al., 2010a). This is because RNA-2 encodes the viral coat proteins (L and S) which are present in 60 copies each per virus particle and so RNA-2 is believed to be translated at high levels. By contrast, RNA-1 encodes proteins with catalytic activities (such as the 24K proteinase and RNA polymerase) which need to be present in much lower amounts and it has therefore been assumed that the translational efficiency of RNA-1 is likely to be lower than RNA-2. In addition, manipulation of RNA-1 sequences in bacterial systems has proved to be difficult leading to sequence rearrangements and loss of viability of the host (Section 4.2).

Work presented in this chapter demonstrates the use of the 5' and 3' UTRs of RNA-1 for transient expression of proteins. 5' and 3' UTRs have been shown to be important for efficient translation of mRNA in a number of viruses (Karetnikov and Lehto, 2008; Kneller et al., 2006; Sarawaneeyaruk et al., 2009; van Lipzig et al., 2002) and the ability of the UTRs to form secondary and higher-order structures has been recognised as one of the main reasons for their function (Liu et al., 2009). Although precise mechanisms remain unknown, one can speculate the reasons for elevation of expression in the presence of UTRs to be (i) increased stability of mRNA in presence of the UTRs; and (ii) improved translational efficiency by easier access and improved binding of ribosomes to the mRNA for translation.

The use of only the UTRs circumvents the problem with toxicity of wt RNA-1 since the UTRs do not code for any proteins. Also, since CPMV is a bipartite virus requiring co-expression of RNA-1 and RNA-2 for an infection, both RNAs are inherently non-competitive with each other. This implies that vectors based on UTRs from RNA-1 can be used in parallel with vectors based on UTRs from RNA-2, such as the CPMV-*HT* vectors.

Vectors based on the UTRs of RNA-1 were examined using GFP and it was found that GFP expression using these vectors was more rapid than the expression achieved using other available expression systems, including the *HT* system based on the UTRs of RNA-2 (Sainsbury and Lomonosoff, 2008). For this reason, the RNA-1 based expression system was named '*Rapid-Trans*' or *RT*.

6.2 Generation of expression vectors based on RNA-1

A basic RNA-1-based expression vector similar to pEAQ-*HT* (Sainsbury et al., 2009) was designed for expression of genes of interest flanked by the 5' and 3' UTRs of RNA-1. The RNA-1-based expression cassette of 924 bp in length, consisting of the CaMV 35S promoter, the 5' UTR of RNA-1, a multiple cloning site, the 3' UTR of RNA-1 and the nos terminator in that order (Figure 6.1), was ordered from Geneart ® and cloned in the T-DNA region of binary plasmid pEAQexpress (Sainsbury et al., 2009) using the restriction sites *PacI* and *AscI*. The vector thus generated was named pEAQexpress-*RT*.

Subsequently, the gene for reporter protein GFP was amplified using primers GFP-start-*XhoI*-F and GFP-stop-*XmaI*-R (Appendix I) and cloned within the multiple cloning site of pEAQexpress-*RT* using the restriction sites *XhoI* and *XmaI* to generate pEAQexpress-*RT*-GFP (Figure 6.2) for expression of GFP with RNA-1 UTRs, referred to as *RT*-GFP.

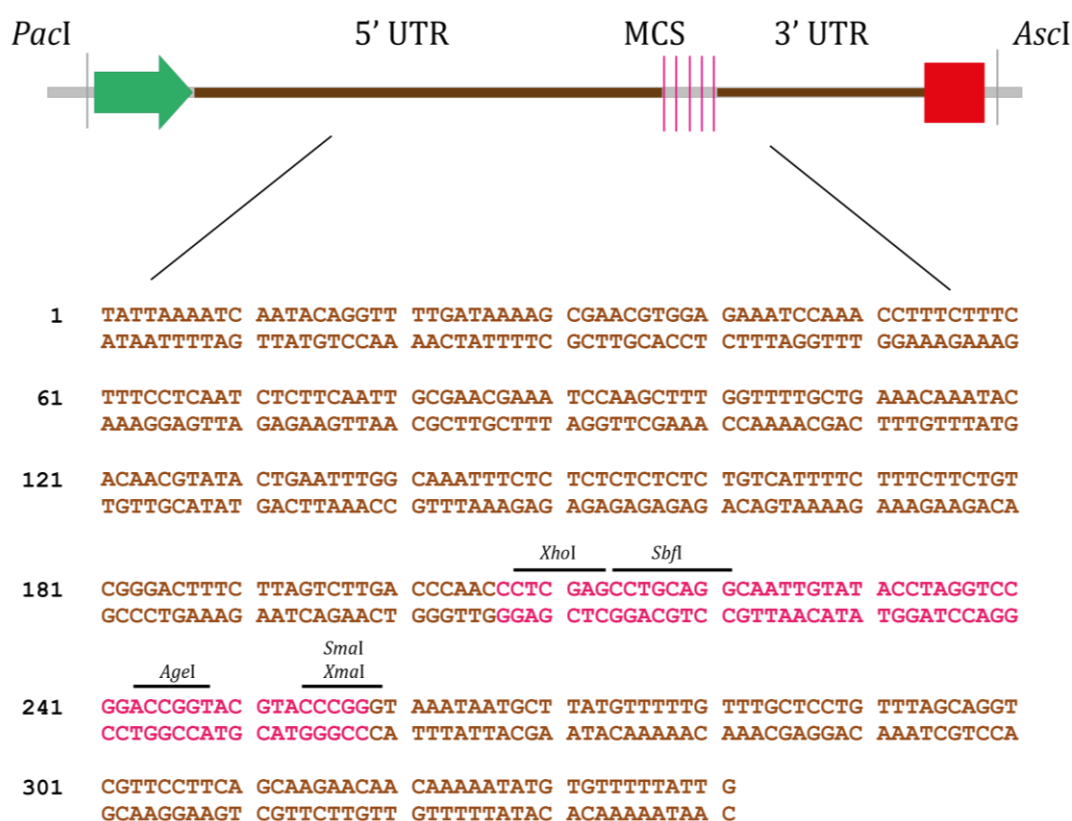


Figure 6.1 The *RT* expression cassette. A schematic diagram of the DNA synthesised by Geneart® for creation of pEAQexpress-*RT* is shown. The green arrow and the red box represent the CaMV 35S promoter and the nos terminator respectively. Sequences encoding the 5' UTR of 206 bp and the 3' UTR of 82 bp of RNA-1 are coloured in brown. Some restriction sites in the multiple cloning site (MCS) have also been shown.

6.3 Analysis of expression from RT vectors

To assess the performance of the *RT* cassette in promoting translation, *N. benthamiana* leaves were infiltrated with pEAQexpress-*RT*-GFP and the expression of GFP was monitored from 1-11 dpi by visualisation of the leaves under UV light. Expression of GFP was observed in leaves from 2 dpi onwards and expression seemed to increase remarkably by 3 dpi. Leaf samples were collected each day and frozen for quantification of expression. Separation of crude leaf extract using SDS-PAGE and measurement of fluorescence using spectrofluorometry (Figure 6.3) confirmed that GFP from pEAQ-*RT*-GFP was being expressed from 2 dpi, after which levels rapidly increased until 4 dpi. At 4 dpi, GFP expression levels of up to 0.5-0.6 g/kg FWT were attained. A similar level of expression was maintained until 7 dpi after which it declined.

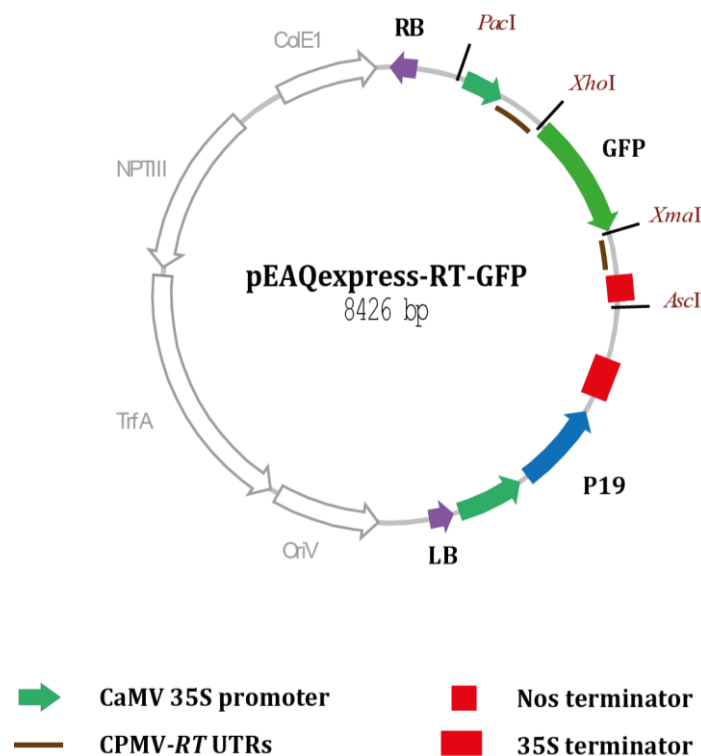


Figure 6.2 Schematic diagram of pEAQexpress-*RT*-GFP. The plasmid generated for expression of GFP with the 5' and 3' UTRs of RNA-1 has been shown.

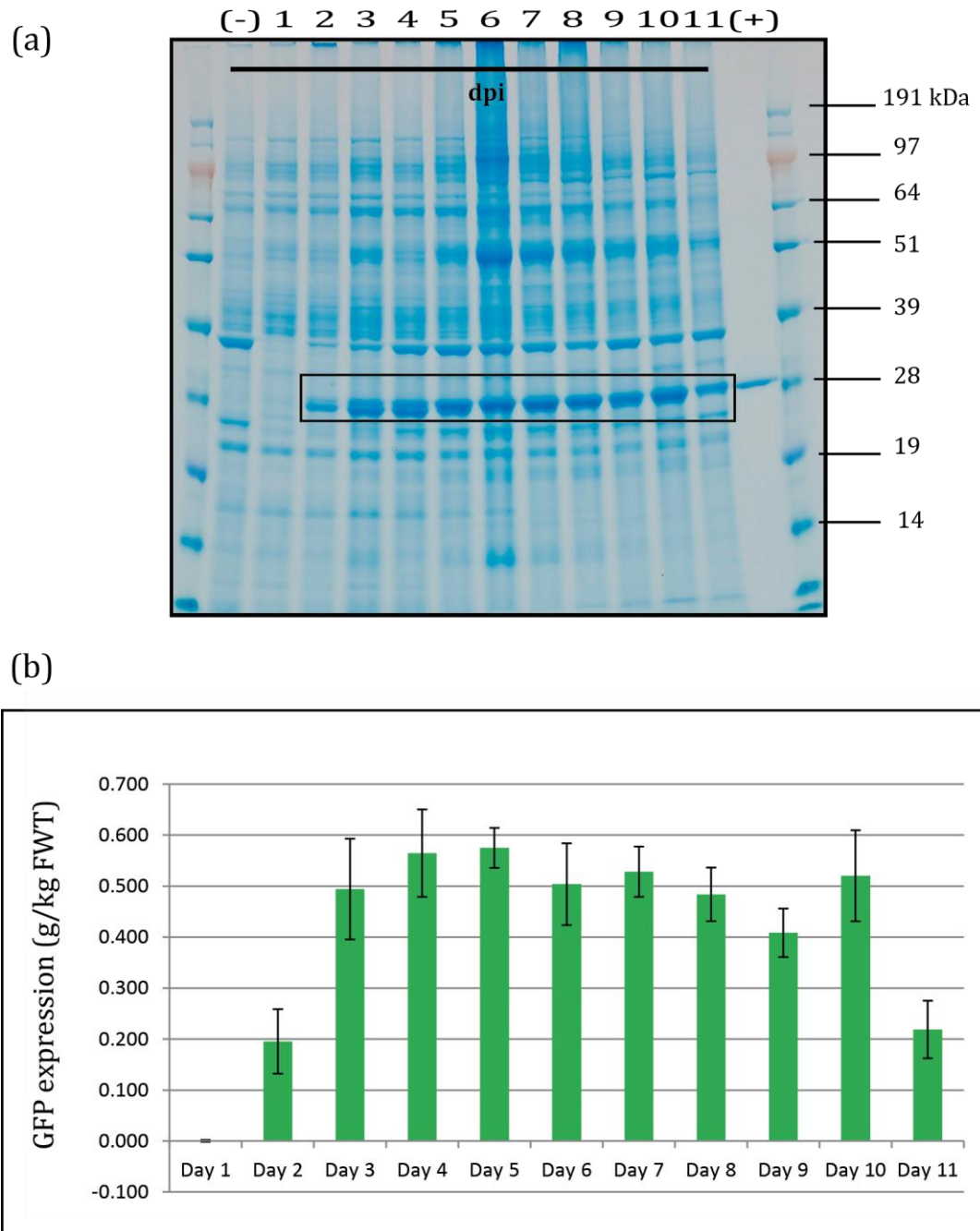


Figure 6.3 Expression of *RT-GFP* over time. (a) SDS-PAGE separation of proteins from leaf tissue infiltrated with pEAQ-*RT-GFP* and harvested on 1-11 dpi. Extract from a plant infiltrated with the empty vector (pEAQexpress-*RT*) was used as a negative control (-). 500 ng of commercially available recombinant GFP was used as the positive control (+). A 27 kDa band for GFP has been highlighted. **(b)** Expression levels of *RT-GFP* based on spectrofluorometry on leaf extracts from 1-11 dpi. Values are averages of expression levels of three biological replicates.

6.4 Comparison of RNA-1 and RNA-2 based expression systems

To assess the *RT* expression system in relation with the previously existing RNA-2-based *HT* system, expression from the construct pEAQexpress-*RT*-GFP was compared to expression from pEAQexpress-*HT*-GFP (Sainsbury et al., 2009) over a period of 12 days. The only difference in the T-DNA of the above vectors was in the sequences of the 5' UTR and 3' UTR flanking the gene for expression of GFP, as shown in Figure 6.4. *N. benthamiana* leaves were infiltrated with both constructs and GFP expression was monitored by visualisation of leaves under UV light (Figure 6.5) and analysis of crude leaf extracts using SDS-PAGE and spectrophotometry (Figure 6.6). On 3 dpi, expression of *RT*-GFP was observed to be very similar to that of *HT*-GFP. From 4 dpi onwards, expression of *RT*-GFP declined while the expression of *HT*-GFP was sustained over the period of 12 days. This shows the ability of the *HT* UTRs to enhance expression of GFP over a longer period, possibly by enhancing mRNA stability.

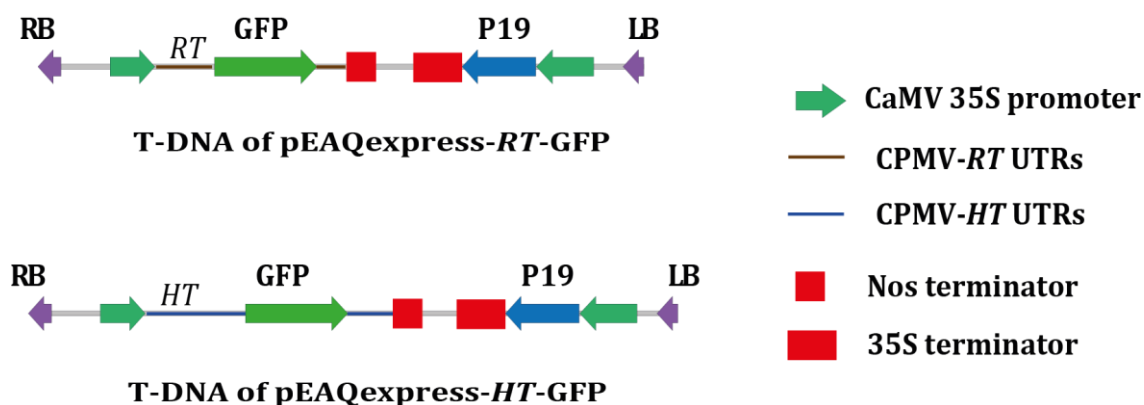


Figure 6.4 Schematic diagrams of constructs. T-DNA regions of constructs used for expression of GFP using the *RT* system (pEAQexpress-*RT*-GFP) and the *HT* system (pEAQexpress-*HT*-GFP) are shown. *RT*-GFP is expressed with the RNA-1 5' UTR of 206 nts and 3' UTR of 82 nts. *HT*-GFP is expressed with the RNA-2 5' UTR of 511 nts and 3' UTR of 184 nts.

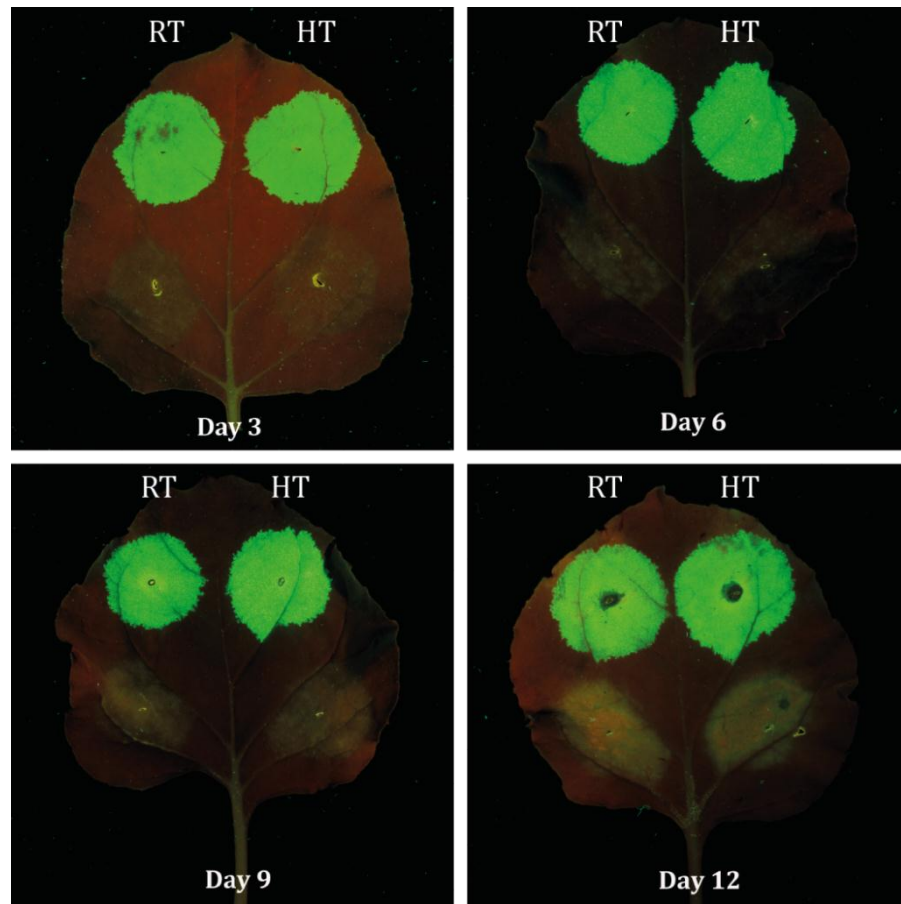


Figure 6.5 Expression of *RT*-GFP and *HT*-GFP. Leaves were photographed under UV light on 3, 6, 9 and 12 dpi. Each leaf has been infiltrated with four constructs for comparison: pEAQexpress-*RT*-GFP (top left); pEAQexpress-*HT*-GFP (top right) and empty vectors pEAQexpress-*RT* (bottom left) and pEAQexpress-*HT* (bottom right).

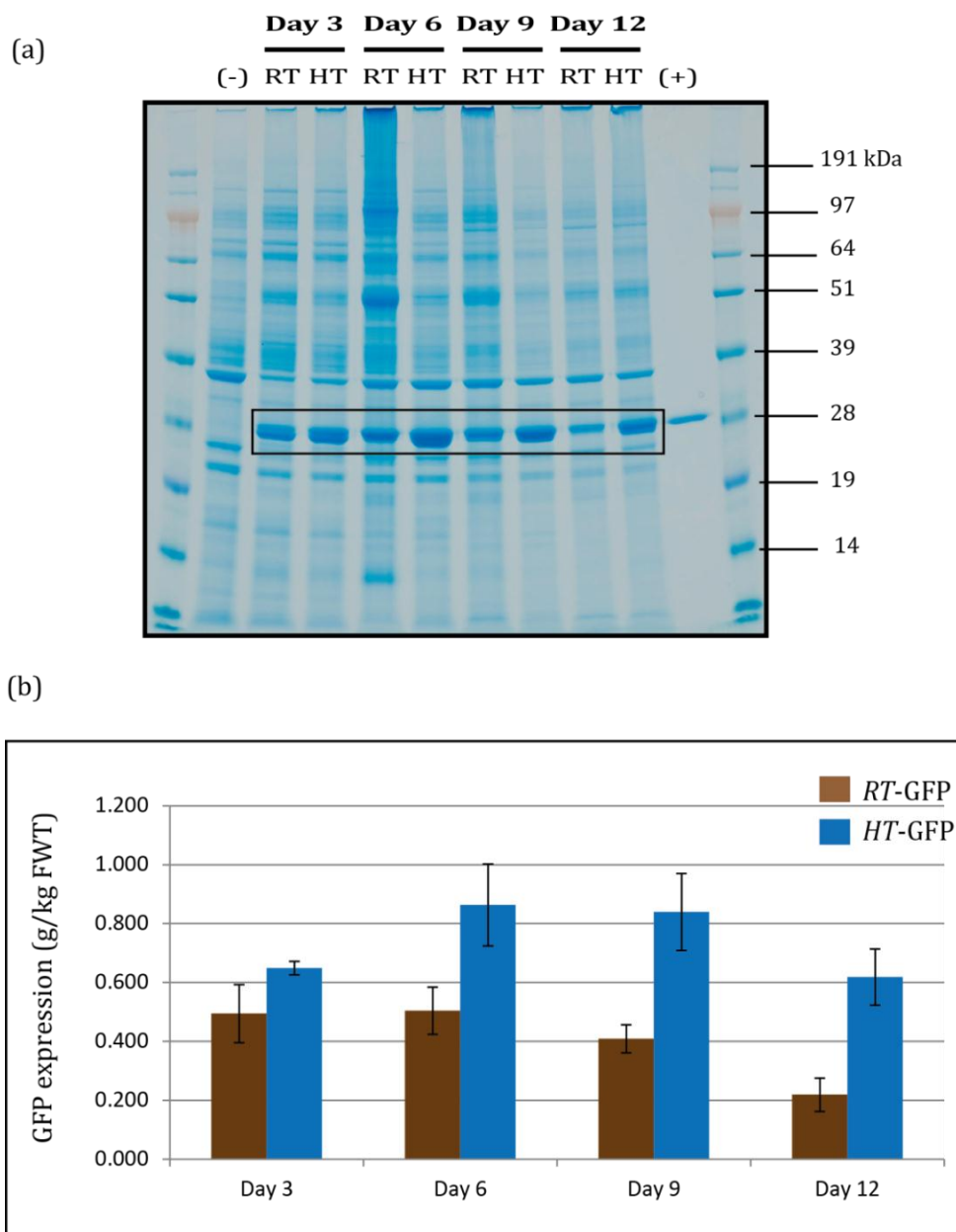


Figure 6.6 Expression of *RT*-GFP and *HT*-GFP over time. (a) The gel shows SDS-PAGE separation of proteins from leaf tissue expressing *RT*-GFP and *HT*-GFP harvested on 3, 6, 9 and 12 dpi. Extract from a plant infiltrated with the empty vector (pEAQexpress-*RT*) was used as a negative control (-) and 500 ng of commercially available recombinant GFP was used as the positive control (+). The band for GFP has been highlighted. **(b)** Expression levels of GFP in the *RT* system (brown bars) and the *HT* system (blue bars) based on spectrofluorometric analysis of extracts from leaves harvested on 3, 6, 9 and 12 dpi are shown. Values are averages of expression levels of three biological replicates.

6.5 Expression using a combination of RNA-1 and RNA-2 sequences

After establishing that the expression profile achieved using UTRs from RNA-1 was different to that achieved using RNA-2 UTRs, expression in presence of various combinations of sequences from RNA-1 and RNA-2 was investigated. It was recognised that the use of different combinations of 5' and 3' UTRs of RNA-1 and RNA-2 would enable the creation of expression vectors with varying translational strengths. This work was done in collaboration with Dr. Yulia Meshcheriakova who was undertaking detailed studies on the role of the 3' UTR of RNA-2 in enhancing expression in the CPMV-*HT* system. These studies indicated that the 3' UTR of RNA-2 plays a significant role in stabilising the mRNA produced during transient expression.

6.5.1 Generation of constructs

To assess the role of the 3' UTR, if any, in enhancement of translation in the *RT* expression system, deletion mutants were generated for expression of GFP in the absence of the 3' UTR. pEAQexpress-*RT*-GFP was modified to delete the entire 82 bp sequence encoding the 3' UTR of RNA-1. This was done by amplifying the segment immediately downstream of the 3' UTR in this vector using primers RT-del3'UTR-F and RT-del3'UTR-R (Appendix I) and inserting the amplified DNA fragment back in the same vector using the *Xma*I and *Bam*HI sites as shown in Figure 6.7a. The vector thus generated lacked the 3' UTR and was named pEAQexpress-*RT*-GFP-del3'UTR. In a similar fashion, construct pEAQexpress-*HT*-GFP-del3'UTR was created by deletion of the 184 bp-long 3' UTR in pEAQexpress-*HT*-GFP (Y. Meshcheriakova, unpublished results).

Another construct was generated by replacing the 3' UTR of RNA-1 with the 3' UTR of RNA-2. To this end, a segment containing the 3' UTR of RNA-2 was amplified from pEAQexpress-*HT*-GFP using primers RT-*HT*3'UTR-F and RT-del3'UTR-R (Appendix I) and cloned into the *Xma*I and *Bam*HI sites of pEAQexpress-*RT*-GFP as shown in Figure 6.7b. The vector thus generated was named pEAQexpress-*RT*-GFP-*HT*3'UTR.

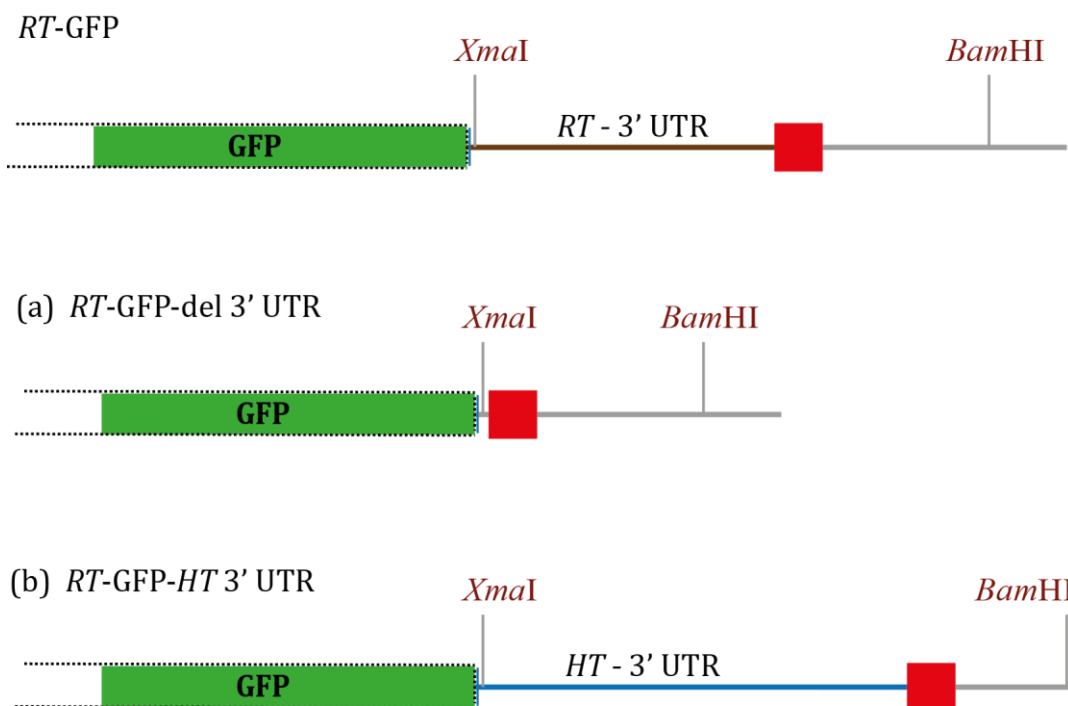


Figure 6.7 Schematic diagrams of constructs generated for expression of mutants of the 3' UTR of pEAQexpress-RT-GFP. Relevant sections of the plasmids generated by (a) deletion of the 3' UTR of pEAQexpress-RT-GFP (*RT-GFP-del3'UTR*) and (b) replacement of the 3' UTR of pEAQexpress-RT-GFP with the *HT*-3' UTR (*RT-GFP-HT3'UTR*) are shown.

6.5.2 Expression of GFP in the absence of the 3' UTR

Agrobacteria harbouring the two deletion constructs: pEAQexpress-*RT-GFP-del3'UTR* and pEAQexpress-*HT-GFP-del3'UTR* were infiltrated into plants to assess the impact of the deletion of the 3' UTR on the transient expression of GFP. It was found that in both the *RT* and *HT* systems, expression of GFP dropped significantly in the absence of the 3' UTR. At 6 dpi, expression of GFP in absence of the 3' UTR of RNA-1 was only 0.13 g/kg FWT, approximately one third of the level achieved in presence of the 3' UTR (Figure 6.8). A similar decline in expression was observed in the *HT* system where expression levels dropped from 0.5 g/kg FWT to 0.15 g/kg FWT in absence of the 3' UTR. These results show that the 3' UTRs play a significant role in enhancement of translation of RNA-1 and RNA-2.

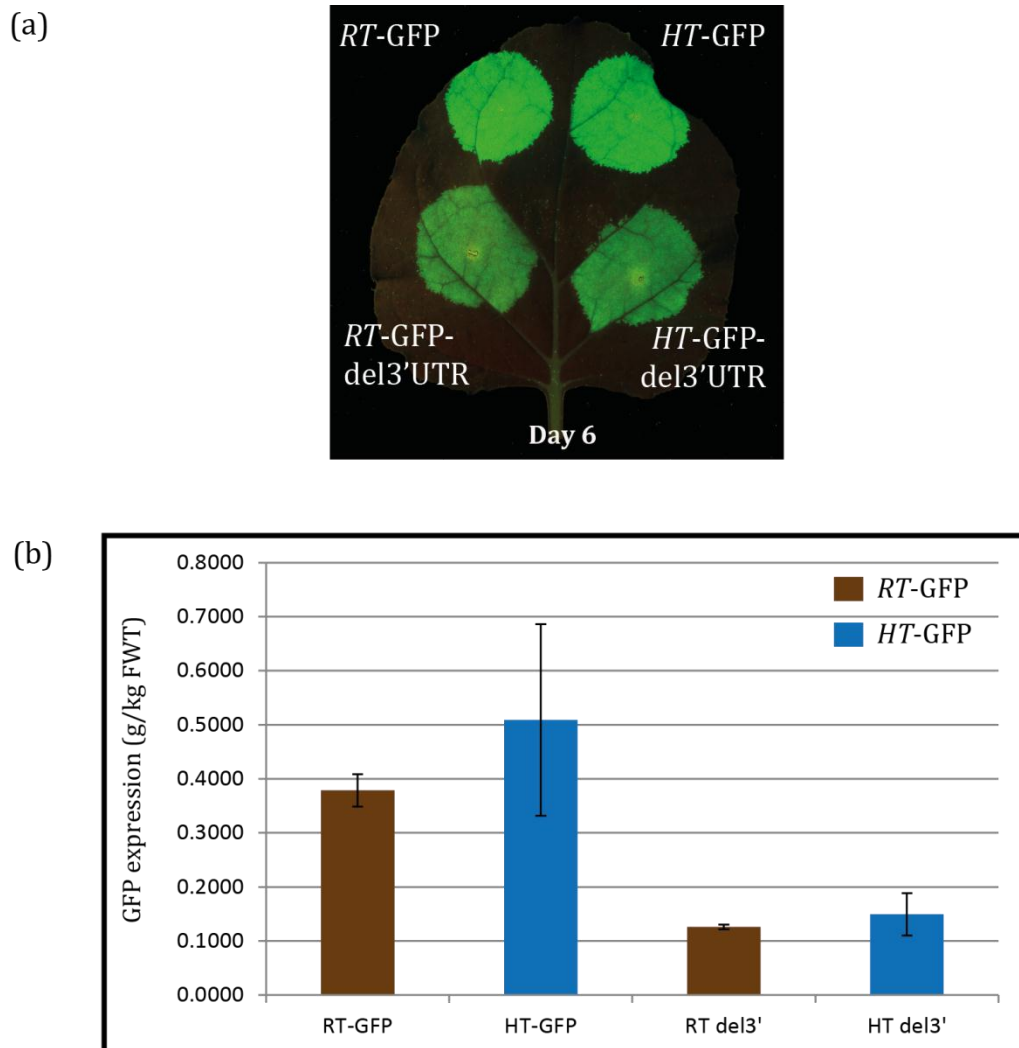


Figure 6.8 Expression of *RT-GFP* and *HT-GFP* in the absence of their 3' UTRs.

(a) Different sections of the leaf were infiltrated with four different constructs (as indicated) for comparison. The leaf was photographed on 6 dpi under UV light.

(b) Expression of GFP as quantified by spectrofluorometry. 'RT del3' and 'HT del 3' correspond to expression of GFP using pEAQexpress-*RT-GFP-del3'UTR* and pEAQexpress-*HT-GFP-del3'UTR* respectively. Values are averages of expression levels of three biological replicates. The error bars denote standard error of mean. The error bar for *HT-GFP* suggests significant variations between the individual readings recorded for its three biological replicates in this experiment.

6.5.3 Expression of GFP using the 5' UTR of RNA-1 and the 3' UTR of RNA-2

Following experiments involving the deletion of the entire 3' UTR of RNA-1, the level of translation achievable from a construct using a combination of the 5' UTR of RNA-1 and the 3' UTR of RNA-2 was investigated. A new construct named pEAQexpress-*RT*-GFP-*HT*3'UTR was generated by replacing the 3' UTR of RNA-1 in pEAQexpress-*RT*-GFP with the 3' UTR of RNA-2, as described in Section 6.5.1.

Leaves were infiltrated with this new construct and GFP expression was monitored over a period of 10 days. In parallel, pEAQexpress-*RT*-GFP and pEAQexpress-*HT*-GFP were also infiltrated into leaves for comparison. At 6 dpi, GFP expression achieved with pEAQexpress-*RT*-GFP-*HT*3'UTR was 0.67 g/kg FWT, which was more than the levels achieved separately using the *RT* and *HT* systems (Figure 6.9). This unexpected observation suggested that the 3' UTR of RNA-2 could not only fully complement the deletion of the 3' UTR of RNA-1, but also enhance translation of GFP mRNA even further.

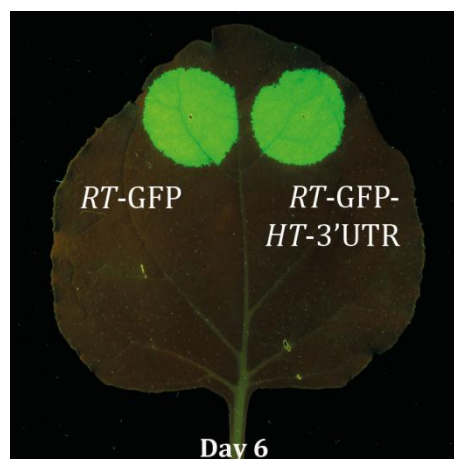


Figure 6.9 (a) Expression of *RT*-GFP in presence of the 3' UTR from RNA-2. Leaf infiltrated with pEAQexpress-*RT*-GFP (left) and pEAQexpress-*RT*-GFP-*HT*3'UTR (right) is shown above for comparison of GFP expression in presence of the 3' UTR from RNA-1 with that in presence of the 3' UTR from RNA-2. The leaf was photographed on 6 dpi under UV light.

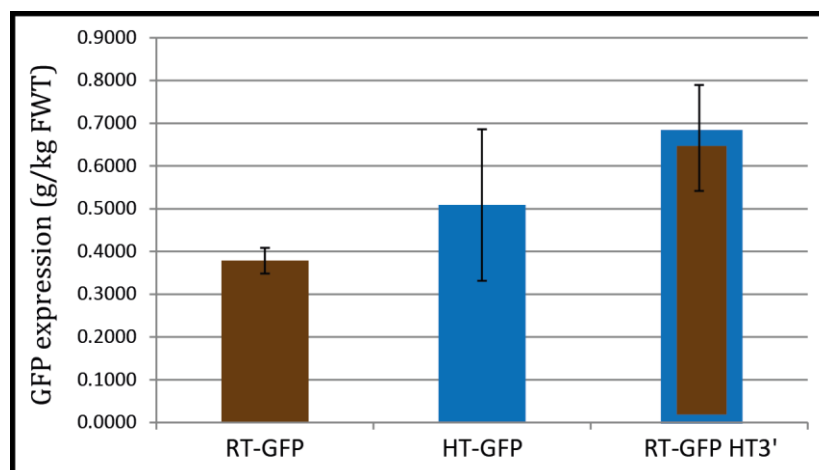


Figure 6.9 (b) Expression of RT-GFP in presence of the 3' UTR from RNA-2.

Expression of GFP as quantified by spectrofluorometry. 'RT-GFP HT3'' refers to expression of GFP from pEAQexpress-RT-GFP-HT3'UTR. Values are averages of expression levels of three biological replicates. The error bars denote standard error of mean. The error bar for HT-GFP suggests significant variations between the individual readings recorded for its three biological replicates in this experiment.

6.6 Discussion

The work described in this chapter exploits differences in the expression profiles of CPMV RNA-1 and RNA-2 for development of expression vectors based on RNA-1, to complement the existing CPMV-HT vectors based on RNA-2. It was observed that inserting a sequence between the 5' and 3' UTRs of RNA-1 can lead to rapid synthesis of proteins in transient systems. In view of the kinetics of protein synthesis, which differ from that seen with the CPMV-HT system, the RNA-1-based expression system was named *Rapid-Trans (RT)*. The rapid rise and decline in expression seen with the RT system could be particularly beneficial in achieving expression of a protein that is unstable or has toxic effects on the plant. The availability of two compatible expression systems with different strengths may be beneficial in circumstances where differing levels of expression are desired, for instance in metabolic pathways or to create complexes in which protein sub-units are required in different amounts.

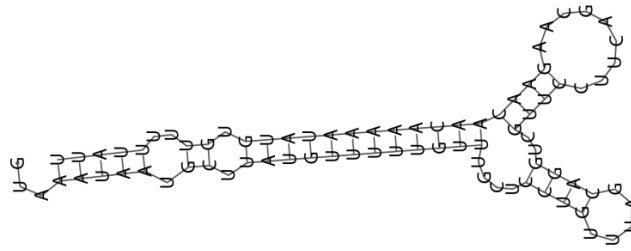
In contrast to the *HT* system which deploys the 5' UTR from RNA-2 with two point mutations engineered within its sequence, the *RT* system deploys wt sequences of the UTRs of RNA-1. The presence of multiple sites for initiation of translation in RNA-2 (AUG 115, AUG 161 and AUG 512) and a 10-fold increase in translation upon deletion of the sites upstream of AUG 512 (Sainsbury and Lomonosoff, 2008) suggests a somewhat-complicated mechanism for translational regulation of RNA-2. No such mechanism seems to exist for translation of RNA-1 where protein synthesis initiates at the first AUG encountered (Wellink et al., 1986).

The differences observed in expression using the *RT* and *HT* expression systems throw light on potential differences in the timings and levels of translation of RNA-1 and RNA-2 during the course of a natural viral infection. RNA-1 is expected to be translated first to provide proteins for replication and hence, expression with the RNA-1 UTRs is expected to be rapid; levels of proteins produced are expected to be lower as compared to RNA-2; and the levels of translation are expected to drop once the replication machinery has been generated. By contrast, RNA-2 is expected to be translated at high levels once replication of RNA-1 has commenced and the expression is expected to be sustained over a longer period to ensure availability of adequate coat proteins for packaging of replicating RNA and spread of infection. This fits with the expression profiles achieved with the *RT* and *HT* systems demonstrating the critical role played by the 5' and 3' UTRs in controlling expression levels.

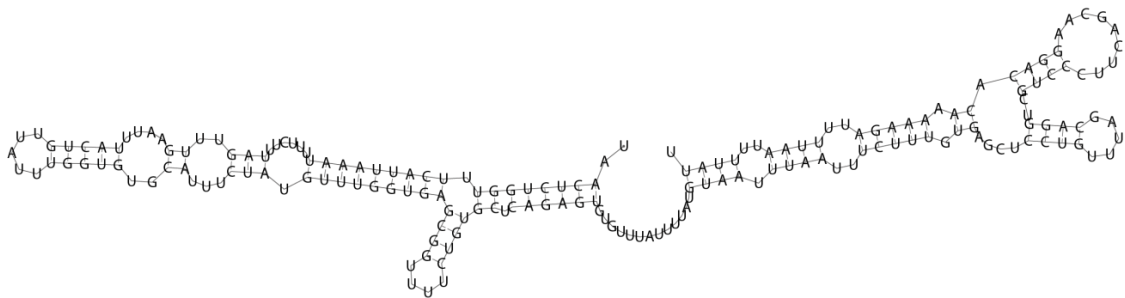
In CPMV, studies on various mutants of the 3' UTR of RNA-2 have shown that the 3' UTR of RNA-2 enhances expression by improving mRNA stability and that direct contacts between the 5' UTR and the 3' UTR are unlikely (Y. Meshcheriakova, unpublished results). This was confirmed when the combinations of UTRs from RNA-1 and RNA-2 were used. Based on the results with the combinatorial constructs, it can be speculated that the 5' and 3' UTRs work independent of each other. The 5' UTR is likely to work by enhancing the efficiency of translation while the 3' UTR has been shown to work by enhancing mRNA stability.

Demonstration of the requirement of 3' UTRs for the maximum enhancement of expression in both CPMV-*RT* and -*HT* systems prompted an investigation into the specificity of the sequence, specifically whether 5' and 3' UTRs from the same RNA had to be used to achieve maximum expression. To this end, the 3' UTRs of RNA-1 and RNA-2 were interchanged and its effect on GFP expression was monitored. GFP expression using the combination of the 5' UTR of RNA-1 with the 3' UTR of RNA-2, unexpectedly, led to higher expression levels than achieved with the individual *RT* or *HT* systems. On the other hand, the reverse combination, i.e. 5' UTR of RNA-2 and the 3' UTR of RNA-1 led to a 50% decline in expression levels compared to levels achieved with the *HT* system which deploys the cognate 5' and 3' UTRs of RNA-2 (Y. Meshcheriakova, unpublished results). These results suggest the possibility of the creation of different expression systems, using combinations of RNA-1 and RNA-2 sequences, to achieve a wide-range of controlled expression levels. They also indicate that the RNA-2 3' UTR is superior to that from RNA-1 in enhancing expression, most probably through a superior ability to stabilise mRNAs, regardless of the origin of the 5' UTR.

The superior performance of the 3' UTR of RNA-2 to enhance expression can be partially explained on the basis of predicted secondary structures of both 3' UTRs. Predictions of the secondary structures (Gruber et al., 2008) of the 3' UTRs of RNA-1 and RNA-2 reveal the presence of a 'Y-shaped' structure in both cases (Figure 6.10). This 'Y-shaped' structure has previously been shown to be important for enhancement of expression in the *HT* system, since mutations that disrupted the formation of this structure led to a decline in GFP expression (Y. Meshcheriakova, unpublished results). The exact function of this 'Y-shaped' structure is not known although it can be thought to be involved in enhancement of mRNA stability. Complementation of the 'Y-shaped' structure of the 3' UTR of RNA-1 by the 3' UTR of RNA-2 restores expression, while in the reverse situation, the 82 nt long 3' UTR of RNA-1 is not sufficient for complementation of the much longer, 3' UTR of RNA-2 of 184 bases. Overall, the results suggest that the Y-shaped structure of the 3' UTRs of RNA-1 and RNA-2 is important for mRNA stability but that its context also has an influence on its ability to enhance expression.



3'UTR of RNA-1 (82 nts)



3'UTR of RNA-2 (184 nts)

Figure 6.10 Predicted secondary structures of the 3' UTRs of RNA-1 and RNA-2 generated using the software 'RNAfold' (Gruber et al., 2008).

While further research into the role of the UTRs in translation is on-going, recent work on CPMV UTRs provides approaches to exploit sequences in the UTRs of RNA-1 and RNA-2 for control of gene expression for applications in biotechnology.

Chapter 7: Conclusions and Outlook

Today, CPMV is one of the best-studied plant viruses due to its diverse applications in biotechnology and nanotechnology. In the last twenty years, the CPMV particle has been exploited for applications such as epitope presentation or as a building block for supramolecular assemblies, while the CPMV genome has been exploited for expression of heterologous proteins in plants. The two aspects were brought together when an expression system based on the CPMV genome (CPMV-*HT*) was deployed for expression of its own coat proteins resulting in the generation of CPMV eVLPs (Saunders et al., 2009).

The availability of eVLPs took CPMV particle technology to another level since it was now possible both to use eVLPs for all the applications for which wt CPMV particles, containing RNA, had previously been used, with reduced bio-safety concerns, and for additional applications which make use of the space now available inside the capsid. The overall objective of this thesis was to advance this new eVLP technology through the complete characterisation of eVLPs and development of methods for applications in nanotechnology. In addition, the expression system based on CPMV RNA-2, CPMV-*HT* was further developed for stable expression of heterologous proteins in plants and a new transient expression system based on the UTRs of RNA-1 was created.

eVLPs were initially expected to be less stable as compared to wt CPMV since it was believed that generally, RNA makes a contribution to particle stability (Fisher and Johnson, 1993). This was found to be true in case of CPMV and hence the protocols for production and purification of eVLPs had to be optimised to account for their reduced stability and absence of RNA. Analysis of the structure of eVLPs using TEM and cryo-EM revealed that all protein-protein contacts were conserved in eVLPs and that the capsids were identical to wt CPMV. This was very valuable as it meant that published literature on the structure and modifications of wt CPMV could be applied to eVLPs. During the course of cryo-EM studies to gain further information about the structure of eVLPs in comparison to wt CPMV, insights were gained on two previously unexplored aspects of the CPMV structure.

Firstly, at least some of the 24 amino acid peptide at the C-terminus of the S coat protein was observed in cryo-EM images. No structural information has previously been available on this peptide due to its absence from the crystallographic structure of CPMV owing to a combination of its high mobility and susceptibility to proteolysis (Lin et al., 1999). The C-terminal peptide has been shown to be important for packaging of RNA (Taylor et al., 1999) and for suppression of virus-induced silencing (Canizares et al., 2004), both of which are important during the early stages of viral infection. Recent studies have shown that this peptide has a role in controlling the permeability of CPMV as particles possessing the intact peptide cannot be internally mineralised (Sainsbury et al., 2011). The reason for this is thought to lie in the location and structure of this peptide which enables it to block access to the pore at the 5-fold axis. So, any understanding of the structure or the precise location of the C-terminal peptide will provide methods to control the permeability of CPMV particles, a valuable trait for applications of eVLPs as nanocontainers, and provide information about the role of this peptide in the virus replication cycle.

Secondly, preliminary data on the secondary structure adopted by RNA-1 and RNA-2 within capsids in CPMV has been obtained from cryo-EM of purified Bottom and Middle components respectively. Further results will help identify RNA-binding sites in the interior of the CPMV capsid. This information can then be used to genetically modify of the interior of eVLPs for its application as a carrier for nucleic acids. Data generated by cryo-EM on residues that bind to RNA will also help in understanding the processes of RNA encapsidation and coat protein assembly in CPMV.

The three-dimensional structure of the protein component of the capsids of many non-enveloped spherical RNA viruses has been determined in great detail, mainly using X-ray crystallography. However, much less is known about the secondary and tertiary structure of the RNA within the capsid, due to a number of methodological problems (Bink and Pleij, 2002). Therefore, any structural data obtained from cryo-EM of CPMV will be useful to all spherical viruses to some

extent and certainly to picornaviruses, given the high degree of similarity in the genomes of CPMV and picornaviruses (Franssen et al., 1984).

Methods for high-level production of eVLPs using transient expression techniques have been described, resulting in average eVLP expression levels in excess of 0.3 g/kg FWT. However, approaches for transgenic expression of eVLPs continue to be developed. It is not clear why the expression of eVLPs was not achieved in plants generated from leaf tissue transformed with pEAQspecialKm-eVLP, given that the construct was functional in transient expression systems. This aspect will have to be investigated further. In particular, the stoichiometry and the solubility of VP60 and 24K will need to be taken into consideration. VP60 is likely to be required in higher amounts since one CPMV particle comprises sixty copies of VP60. On the other hand, the same molecule of the 24K proteinase could potentially be used for proteolytic processing of more than one VP60 molecule. Thus, the solution for transgenic expression of eVLPs may lie in expression of low levels of 24K, possibly by deploying the RNA-1-based *RT* system, along with expression of VP60 using the *HT* system. This would mimic the situation in a natural infection where 24K is translated from RNA-1 and expressed as a part of a polyprotein with the UTRs of RNA-1. The insolubility of VP60, as observed by Saunders et al (2009), will also need to be addressed for transgenic expression of VP60. This would involve optimisation of buffers for extraction of VP60 and possibly genetic modification of VP60.

The prospect of an *in vitro* assembly system for CPMV can be considered once the issue of insolubility of VP60 is resolved. Such *in vitro* assembly systems have been successfully used for other icosahedral viruses such as CCMV (Bancroft and Hiebert, 1967) and BMV (Chaturvedi et al., 2012). Moreover, the fact that eVLPs have been successfully generated in two very different expression systems, namely in insect cells and in plants (Saunders et al., 2009), suggests that the requirement of host proteins for assembly in CPMV is unlikely and that *in vitro* assembly can be achieved simply by making VP60 and 24K available. The specificity in packaging exhibited by CPMV combined with its potential to assemble *in vitro* makes it an attractive candidate for applications as delivery vehicles for nucleic acids.

Although the objective of the creation of transgenic plants producing eVLPs was not achieved during this thesis, demonstration that P19/R43W can be successfully deployed in a transgenic expression system to express diverse proteins, from enzymes to antibodies, is a valuable achievement in biotechnology. Studies with P19/R43W so far have only been undertaken in *N. benthamiana* but its use can easily be extended to other plant hosts since P19 is a protein from TBSV which has a broad host range of over a hundred plants in 20 families of mono- and dicotyledonous plants (Russo et al., 1994). Furthermore, the development of the pEAQspecialKm series of vectors encoding the CPMV-*HT* cassette provides a system for quick and efficient cloning for transient and transgenic expression. pEAQspecialKm has been tailored in such a way that once the gene of interest is cloned in this vector, it can be tested by transient expression in *N. benthamiana* and then the same vector can be used for leaf disc transformation.

A number of published studies report the high levels of expression achieved by deploying the pEAQ-*HT* system to express a variety of proteins and multi-protein complexes. These include the human gastric lipase (Vardakou et al., 2012), sesquiterpene synthases (Kanagarajan et al., 2012a), a rice chitinase (Miyamoto et al., 2012), human papillomavirus (Matic et al., 2011), human IgG 2G12 (Sainsbury et al., 2010b) and the hemagglutinin antigen H7N7 (Kanagarajan et al., 2012b). However, limited success has been achieved with the expression of membrane-bound proteins using this system since high levels of these proteins result in necrosis of the infiltrated tissue (P. Lenzi and L. Schellenberg, unpublished results). One solution to this problem has been to harvest tissue before necrosis has had time to develop. The development of expression vectors that deploy sequences from RNA-1 may prove to be useful in the expression of such proteins since the expression achieved in the *RT* system is rapid and lower than the levels achieved in the *HT* system. In fact, for the expression of a heterologous protein, the best approach would be to clone the gene of interest simultaneously with the *RT* and the *HT* UTRs in different pEAQ vectors and test expression by transient-infiltration of the constructs. Eventually, the expression cassette can be moved to

pEAQspecialKm in one-step using restriction enzyme-based cloning for stable expression of the gene of interest.

Overall, the work presented in this thesis has enabled sufficient quantities of purified eVLPs to be obtained for their detailed characterisation by a number of techniques and for investigations into their potential uses as a nanoparticle. CPMV eVLPs are currently being developed for applications in magnetic hyperthermia, as contrast agents for imaging, as vehicles for targeted drug delivery, as reaction vessels and as carriers for nucleic acids of choice. For the last application, the results reported in this thesis regarding the link between replication and encapsidation are of critical importance. A recent review by Mark Young et al. (2008) lists three main hurdles in the use of plant viruses in nanotechnology: (i) stability; (ii) efficacy and safety and (iii) production and costs. CPMV eVLPs have the potential to overcome all of these hurdles and the work described in this thesis is certainly a step in that direction.

References

- Agrawal, H.O. (1964). Identification of cowpea mosaic virus isolates Mededel Landbouwhogeschool Wageningen 64, 1-53.
- Aljabali, A.A., Barclay, J.E., Steinmetz, N.F., Lomonosoff, G.P., and Evans, D.J. (2012a). Controlled immobilisation of active enzymes on the cowpea mosaic virus capsid. *Nanoscale* 4, 5640-5645.
- Aljabali, A.A., Sainsbury, F., Lomonosoff, G.P., and Evans, D.J. (2010a). Cowpea mosaic virus unmodified empty viruslike particles loaded with metal and metal oxide. *Small* 6, 818-821.
- Aljabali, A.A., Shah, S.N., Evans-Gowing, R., Lomonosoff, G.P., and Evans, D.J. (2010b). Chemically-coupled-peptide-promoted virus nanoparticle templated mineralization. *Integr Biol (Camb)* 3(2), 119-125.
- Aljabali, A.A., Shukla, S., Lomonosoff, G.P., Steinmetz, N.F., and Evans, D.J. (2012b). CPMV-DOX Delivers. *Molecular pharmaceutics*. Epub DOI: 10.1021/mp3002057.
- Anandalakshmi, R., Pruss, G.J., Ge, X., Marathe, R., Mallory, A.C., Smith, T.H., and Vance, V.B. (1998). A viral suppressor of gene silencing in plants. *Proc Natl Acad Sci U S A* 95, 13079-13084.
- Annamalai, P., and Rao, A.L. (2006). Packaging of brome mosaic virus subgenomic RNA is functionally coupled to replication-dependent transcription and translation of coat protein. *J Virol* 80, 10096-10108.
- Armijo, L.M., Brandt, Y.I., Mathew, D., Yadav, S., Maestas, S., Rivera, A.C., Cook, N.C., Withers, N.J., Smolyakov, G.A., Adolphi, N.L., *et al.* (2012). Iron Oxide Nanocrystals for Magnetic Hyperthermia Applications. *Nanomaterials* 2, 134-146.
- Arslan, D., Legendre, M., Seltzer, V., Abergel, C., and Claverie, J.M. (2011). Distant Mimivirus relative with a larger genome highlights the fundamental features of Megaviridae. *Proc Natl Acad Sci U S A* 108, 17486-17491.
- Bachtarzi, H., Stevenson, M., and Fisher, K. (2008). Cancer gene therapy with targeted adenoviruses. *Expert opinion on drug delivery* 5, 1231-1240.
- Bakry, R., Vallant, R.M., Najam-ul-Haq, M., Rainer, M., Szabo, Z., Huck, C.W., and Bonn, G.K. (2007). Medicinal applications of fullerenes. *International journal of nanomedicine* 2, 639-649.
- Bakshi, S., Sadhukhan, A., Mishra, S., and Sahoo, L. (2011). Improved Agrobacterium-mediated transformation of cowpea via sonication and vacuum infiltration. *Plant Cell Rep* 30, 2281-2292.

- Bancroft, J.B., and Hiebert, E. (1967). Formation of an infectious nucleoprotein from protein and nucleic acid isolated from a small spherical virus. *Virology* *32*, 354-356.
- Baulcombe, D. (2002). RNA silencing. *Current biology* : CB *12*, R82-84.
- Bink, H.H., and Pleij, C.W. (2002). RNA-protein interactions in spherical viruses. *Archives of virology* *147*, 2261-2279.
- Blum, A.S., Soto, C.M., Sapsford, K.E., Wilson, C.D., Moore, M.H., and Ratna, B.R. (2011). Molecular electronics based nanosensors on a viral scaffold. *Biosensors & bioelectronics* *26*, 2852-2857.
- Bothner, B., Taylor, D., Jun, B., Lee, K.K., Siuzdak, G., Schultz, C.P., and Johnson, J.E. (2005). Maturation of a tetravirus capsid alters the dynamic properties and creates a metastable complex. *Virology* *334*, 17-27.
- Brigneti, G., Voinnet, O., Li, W.X., Ji, L.H., Ding, S.W., and Baulcombe, D.C. (1998). Viral pathogenicity determinants are suppressors of transgene silencing in *Nicotiana benthamiana*. *EMBO J* *17*, 6739-6746.
- Brumfield, S., Willits, D., Tang, L., Johnson, J.E., Douglas, T., and Young, M. (2004). Heterologous expression of the modified coat protein of Cowpea chlorotic mottle bromovirus results in the assembly of protein cages with altered architectures and function. *J Gen Virol* *85*, 1049-1053.
- Buchacher, A., Predl, R., Strutzenberger, K., Steinfellner, W., Trkola, A., Purtscher, M., Gruber, G., Tauer, C., Steindl, F., Jungbauer, A., *et al.* (1994). Generation of human monoclonal antibodies against HIV-1 proteins; electrofusion and Epstein-Barr virus transformation for peripheral blood lymphocyte immortalization. *AIDS Res Hum Retroviruses* *10*, 359-369.
- Canizares, M.C., Liu, L., Perrin, Y., Tsakiris, E., and Lomonossoff, G.P. (2006). A bipartite system for the constitutive and inducible expression of high levels of foreign proteins in plants. *Plant Biotechnol J* *4*, 183-193.
- Canizares, M.C., Taylor, K.M., and Lomonossoff, G.P. (2004). Surface-exposed C-terminal amino acids of the small coat protein of Cowpea mosaic virus are required for suppression of silencing. *J Gen Virol* *85*, 3431-3435.
- Carette, J.E., Stuiver, M., Van Lent, J., Wellink, J., and Van Kammen, A. (2000). Cowpea mosaic virus infection induces a massive proliferation of endoplasmic reticulum but not Golgi membranes and is dependent on de novo membrane synthesis. *J Virol* *74*, 6556-6563.

- Carriere, F., Laugier, R., Barrowman, J.A., Douchet, I., Priymenko, N., and Verger, R. (1993). Gastric and pancreatic lipase levels during a test meal in dogs. *Scandinavian journal of gastroenterology* 28, 443-454.
- Caswell, P., and Norman, J. (2008). Endocytic transport of integrins during cell migration and invasion. *Trends in cell biology* 18, 257-263.
- Chapman, E.J., Prokhnevsky, A.I., Gopinath, K., Dolja, V.V., and Carrington, J.C. (2004). Viral RNA silencing suppressors inhibit the microRNA pathway at an intermediate step. *Genes Dev* 18, 1179-1186.
- Chaturvedi, S., Jung, B., Gupta, S., Anvari, B., and Rao, A.L. (2012). Simple and robust in vivo and in vitro approach for studying virus assembly. *Journal of visualized experiments : JoVE* 61. e3645.
- Chen, C., Kwak, E.S., Stein, B., Kao, C.C., and Dragnea, B. (2005). Packaging of gold particles in viral capsids. *Journal of nanoscience and nanotechnology* 5, 2029-2033.
- Chu, M., Desvoyes, B., Turina, M., Noad, R., and Scholthof, H.B. (2000). Genetic dissection of tomato bushy stunt virus p19-protein-mediated host-dependent symptom induction and systemic invasion. *Virology* 266, 79-87.
- Da Poian, A.T., Johnson, J.E., and Silva, J.L. (1994). Differences in pressure stability of the three components of cowpea mosaic virus: implications for virus assembly and disassembly. *Biochemistry* 33, 8339-8346.
- Dalsgaard, K., Uttenthal, A., Jones, T.D., Xu, F., Merryweather, A., Hamilton, W.D., Langeveld, J.P., Boshuizen, R.S., Kamstrup, S., Lomonosoff, G.P., *et al.* (1997). Plant-derived vaccine protects target animals against a viral disease. *Nat Biotechnol* 15, 248-252.
- Dekker, C. (1999). Carbon Nanotubes as Molecular Quantum Wires. *Physics today* 52, 22-28.
- Delarue, M., Poch, O., Tordo, N., Moras, D., and Argos, P. (1990). An attempt to unify the structure of polymerases. *Protein engineering* 3, 461-467.
- Desai, P.N., Shrivastava, N., and Padh, H. (2010). Production of heterologous proteins in plants: strategies for optimal expression. *Biotechnol Adv* 28, 427-435.
- DiCara, D., Burman, A., Clark, S., Berryman, S., Howard, M.J., Hart, I.R., Marshall, J.F., and Jackson, T. (2008). Foot-and-mouth disease virus forms a highly stable, EDTA-resistant complex with its principal receptor, integrin alphavbeta6: implications for infectiousness. *J Virol* 82, 1537-1546.

-
- DiMagno, E.P., Malagelada, J.R., Go, V.L., and Moertel, C.G. (1977). Fate of orally ingested enzymes in pancreatic insufficiency. Comparison of two dosage schedules. *N Engl J Med* 296, 1318-1322.
- Dixit, S.K., Goicochea, N.L., Daniel, M.C., Murali, A., Bronstein, L., De, M., Stein, B., Rotello, V.M., Kao, C.C., and Dragnea, B. (2006). Quantum dot encapsulation in viral capsids. *Nano letters* 6, 1993-1999.
- Douglas, T., and Young, M. (1998). Host-guest encapsulation of materials by assembled virus protein cages. *Nature* 393, 152-155.
- Douglas, T., and Young, M. (2006). Viruses: making friends with old foes. *Science* 312, 873-875.
- Drexler, E.K. (1986). *Engines of Creation: The Coming Era of Nanotechnology* (New York: Anchor Books).
- Dunoyer, P., Lecellier, C.H., Parizotto, E.A., Himber, C., and Voinnet, O. (2004). Probing the microRNA and small interfering RNA pathways with virus-encoded suppressors of RNA silencing. *Plant Cell* 16, 1235-1250.
- Dykes, G.M. (2001). Dendrimers: a review of their appeal and applications. *Journal of Chemical Technology and Biotechnology* 76, 903-918.
- Eggen, R., Verver, J., Wellink, J., Pleij, K., van Kammen, A., and Goldbach, R. (1989). Analysis of sequences involved in cowpea mosaic virus RNA replication using site-specific mutants. *Virology* 173, 456-464.
- Feynman, R.P. (1959). There's Plenty of Room at the Bottom: An Invitation to Enter a New Field of Physics. In *Caltech's Engineering and Science*.
- Finsterbusch, T., and Mankertz, A. (2009). Porcine circoviruses--small but powerful. *Virus research* 143, 177-183.
- Fischer, R., Stoger, E., Schillberg, S., Christou, P., and Twyman, R.M. (2004). Plant-based production of biopharmaceuticals. *Current opinion in plant biology* 7, 152-158.
- Fisher, A.J., and Johnson, J.E. (1993). Ordered duplex RNA controls capsid architecture in an icosahedral animal virus. *Nature* 361, 176-179.
- Fox, J.L. (2011). HIV drugs made in tobacco. *Nat Biotechnol* 29.
- Franssen, H., Goldbach, R., Broekhuijsen, M., Moerman, M., and van Kammen, A. (1982). Expression of Middle-Component RNA of Cowpea Mosaic Virus: In Vitro Generation of a Precursor to Both Capsid Proteins by a Bottom-Component RNA-Encoded Protease from Infected Cells. *J Virol* 41, 8-17.

- Franssen, H., Leunissen, J., Goldbach, R., Lomonosoff, G., and Zimmern, D. (1984). Homologous sequences in non-structural proteins from cowpea mosaic virus and picornaviruses. *EMBO J* 3, 855-861.
- Gazit, E. (2007). *Plenty of Room for Biology at the Bottom: An Introduction to Bionanotechnology* I.C. Press, ed. (London: Imperial College Press), pp. 180.
- Gelvin, S.B. (2005). Agricultural biotechnology: gene exchange by design. *Nature* 433, 583-584.
- Gleba, Y., Klimyuk, V., and Marillonnet, S. (2007). Viral vectors for the expression of proteins in plants. *Current opinion in biotechnology* 18, 134-141.
- Goldbach, R., Rezelman, G., and Van Kammen, A. (1980). Independent replication and expression of B-component RNA of cowpea mosaic virus. *Nature* 286, 297-300.
- Goodsell, D.S. (2004). *Bionanotechnology: lessons from nature* (New Jersey, USA: Wiley).
- Gregoriadis, G. (1995). Engineering liposomes for drug delivery: progress and problems. *Trends in biotechnology* 13, 527-537.
- Gruber, A.R., Lorenz, R., Bernhart, S.H., Neuböck, R., and Hofacker, I.L. (2008). The Vienna RNA Websuite. *Nucleic Acids Res* 36, W70-74.
- Hibi, T., Rezelman, G., and Van Kammen, A. (1975). Infection of cowpea mesophyll protoplasts with cowpea mosaic virus. *Virology* 64, 308-318.
- Hoekema, A., Hirsch, P.R., Hooykaas, P.J.J., and Schilperoort, R.A. (1983). Binary vector strategy based on separation of vir- and T-region of the *Agrobacterium tumefaciens* Ti-plasmid. *Nature* 303, 179-180.
- Holness, C.L., Lomonosoff, G.P., Evans, D., and Maule, A.J. (1989). Identification of the initiation codons for translation of cowpea mosaic virus middle component RNA using site-directed mutagenesis of an infectious cDNA clone. *Virology* 172, 311-320.
- Horsch, R.B., and Klee, H.J. (1986). Rapid assay of foreign gene expression in leaf discs transformed by *Agrobacterium tumefaciens*: Role of T-DNA borders in the transfer process. *Proc Natl Acad Sci U S A* 83, 4428-4432.
- Hull, R. (2009). *Comparative Plant Virology* 2nd edn (China: Elsevier academic press).
- Jablonski, S.A., and Morrow, C.D. (1995). Mutation of the aspartic acid residues of the GDD sequence motif of poliovirus RNA-dependent RNA polymerase results in enzymes with altered metal ion requirements for activity. *J Virol* 69, 1532-1539.

Junker-Niepmann, M., Bartenschlager, R., and Schaller, H. (1990). A short cis-acting sequence is required for hepatitis B virus pregenome encapsidation and sufficient for packaging of foreign RNA. *EMBO J* 9, 3389-3396.

Kanagarajan, S., Muthusamy, S., Gliszczynska, A., Lundgren, A., and Brodelius, P.E. (2012a). Functional expression and characterization of sesquiterpene synthases from *Artemisia annua* L. using transient expression system in *Nicotiana benthamiana*. *Plant Cell Rep* 31, 1309-1319.

Kanagarajan, S., Tolf, C., Lundgren, A., Waldenstrom, J., and Brodelius, P.E. (2012b). Transient expression of hemagglutinin antigen from low pathogenic avian influenza A (H7N7) in *Nicotiana benthamiana*. *PLoS One* 7, e33010.

Kapp, L.D., and Lorsch, J.R. (2004). The molecular mechanics of eukaryotic translation. *Annual review of biochemistry* 73, 657-704.

Karetnikov, A., and Lehto, K. (2008). Translation mechanisms involving long-distance base pairing interactions between the 5' and 3' non-translated regions and internal ribosomal entry are conserved for both genomic RNAs of Blackcurrant reversion nepovirus. *Virology* 371, 292-308.

Kesharwani, P., Gajbhiye, V., and Jain, N.K. (2012). A review of nanocarriers for the delivery of small interfering RNA. *Biomaterials* 33, 7138-7150.

Khromykh, A.A., Varnavski, A.N., Sedlak, P.L., and Westaway, E.G. (2001). Coupling between replication and packaging of flavivirus RNA: evidence derived from the use of DNA-based full-length cDNA clones of Kunjin virus. *J Virol* 75, 4633-4640.

Kim, Y.G., Yoo, J.S., Kim, J.H., Kim, C.M., and Oh, J.W. (2007). Biochemical characterization of a recombinant Japanese encephalitis virus RNA-dependent RNA polymerase. *BMC molecular biology* 8, 59.

Kneller, E.L., Rakotondrafara, A.M., and Miller, W.A. (2006). Cap-independent translation of plant viral RNAs. *Virus research* 119, 63-75.

Koudelka, K.J., Destito, G., Plummer, E.M., Trauger, S.A., Siuzdak, G., and Manchester, M. (2009). Endothelial targeting of cowpea mosaic virus (CPMV) via surface vimentin. *PLoS pathogens* 5, e1000417.

Kreppel, F., Gackowski, J., Schmidt, E., and Kochanek, S. (2005). Combined genetic and chemical capsid modifications enable flexible and efficient de- and retargeting of adenovirus vectors. *Molecular therapy : the journal of the American Society of Gene Therapy* 12, 107-117.

Kridl, J.C., and Bruening, G. (1983). Comparison of capsids and nucleocapsids from cowpea mosaic virus-infected cowpea protoplasts and seedlings. *Virology* 129, 369-380.

- Lai, H., and Chen, Q. (2012). Bioprocessing of plant-derived virus-like particles of Norwalk virus capsid protein under current Good Manufacture Practice regulations. *Plant Cell Rep* 31, 573-584.
- Langeveld, J.P., Brennan, F.R., Martinez-Torrecuadrada, J.L., Jones, T.D., Boshuizen, R.S., Vela, C., Casal, J.I., Kamstrup, S., Dalsgaard, K., Meloen, R.H., *et al.* (2001). Inactivated recombinant plant virus protects dogs from a lethal challenge with canine parvovirus. *Vaccine* 19, 3661-3670.
- Lau, J.L., Baksh, M.M., Fiedler, J.D., Brown, S.D., Kussrow, A., Bornhop, D.J., Ordoukhanian, P., and Finn, M.G. (2011). Evolution and protein packaging of small-molecule RNA aptamers. *ACS nano* 5, 7722-7729.
- Lewis, J.D., Destito, G., Zijlstra, A., Gonzalez, M.J., Quigley, J.P., Manchester, M., and Stuhlmann, H. (2006). Viral nanoparticles as tools for intravital vascular imaging. *Nat Med* 12, 354-360.
- Lin, T., Chen, Z., Usha, R., Stauffacher, C.V., Dai, J.B., Schmidt, T., and Johnson, J.E. (1999). The refined crystal structure of cowpea mosaic virus at 2.8 Å resolution. *Virology* 265, 20-34.
- Lin, T., and Johnson, J.E. (2003). Structures of picorna-like plant viruses: implications and applications. *Adv Virus Res* 62, 167-239.
- Liu, L., Canizares, M.C., Monger, W., Perrin, Y., Tsakiris, E., Porta, C., Shariat, N., Nicholson, L., and Lomonosoff, G.P. (2005). Cowpea mosaic virus-based systems for the production of antigens and antibodies in plants. *Vaccine* 23, 1788-1792.
- Liu, L., Grainger, J., Canizares, M.C., Angell, S.M., and Lomonosoff, G.P. (2004). Cowpea mosaic virus RNA-1 acts as an amplicon whose effects can be counteracted by a RNA-2-encoded suppressor of silencing. *Virology* 323, 37-48.
- Liu, L., and Lomonosoff, G. (2002). Agroinfection as a rapid method for propagating Cowpea mosaic virus-based constructs. *J Virol Methods* 105, 343-348.
- Liu, Y., Wimmer, E., and Paul, A.V. (2009). Cis-acting RNA elements in human and animal plus-strand RNA viruses. *Biochimica et biophysica acta* 1789, 495-517.
- Lomonosoff, G.P., and Hamilton, W.D. (1999). Cowpea mosaic virus-based vaccines. *Curr Top Microbiol Immunol* 240, 177-189.
- Lomonosoff, G.P., and Johnson, J.E. (1991). The synthesis and structure of comovirus capsids. *Prog Biophys Mol Biol* 55, 107-137.
- Lomonosoff, G.P., Shanks, M., and Evans, D. (1985). The structure of cowpea mosaic virus replicative form RNA. *Virology* 144, 351-362.

- Lu, A.H., Salabas, E.L., and Schuth, F. (2007). Magnetic nanoparticles: synthesis, protection, functionalization, and application. *Angew Chem Int Ed Engl* 46, 1222-1244.
- Ma, J.K., Drake, P.M., and Christou, P. (2003). The production of recombinant pharmaceutical proteins in plants. *Nature reviews Genetics* 4, 794-805.
- Mallory, A.C., Parks, G., Endres, M.W., Baulcombe, D., Bowman, L.H., Pruss, G.J., and Vance, V.B. (2002). The amplicon-plus system for high-level expression of transgenes in plants. *Nat Biotechnol* 20, 622-625.
- Manchester, M., and Steinmetz, N.F. (2009). *Viruses and nanotechnology*. Preface. *Curr Top Microbiol Immunol* 327, v-vi.
- Mao, C., Solis, D.J., Reiss, B.D., Kottmann, S.T., Sweeney, R.Y., Hayhurst, A., Georgiou, G., Iverson, B., and Belcher, A.M. (2004). Virus-based toolkit for the directed synthesis of magnetic and semiconducting nanowires. *Science* 303, 213-217.
- Markham, R. (1962). The analytical ultracentrifuge as a tool for the investigation of plant viruses. *Adv Virus Res* 9, 241-270.
- Mascola, J.R., Lewis, M.G., Stiegler, G., Harris, D., VanCott, T.C., Hayes, D., Louder, M.K., Brown, C.R., Sapan, C.V., Frankel, S.S., *et al.* (1999). Protection of Macaques against pathogenic simian/human immunodeficiency virus 89.6PD by passive transfer of neutralizing antibodies. *J Virol* 73, 4009-4018.
- Mascola, J.R., Stiegler, G., VanCott, T.C., Katinger, H., Carpenter, C.B., Hanson, C.E., Beary, H., Hayes, D., Frankel, S.S., Birx, D.L., *et al.* (2000). Protection of macaques against vaginal transmission of a pathogenic HIV-1/SIV chimeric virus by passive infusion of neutralizing antibodies. *Nat Med* 6, 207-210.
- Matic, S., Rinaldi, R., Masenga, V., and Noris, E. (2011). Efficient production of chimeric human papillomavirus 16 L1 protein bearing the M2e influenza epitope in *Nicotiana benthamiana* plants. *BMC biotechnology* 11, 106.
- Medintz, I.L., Sapsford, K.E., Konnert, J.H., Chatterji, A., Lin, T., Johnson, J.E., and Mattoussi, H. (2005). Decoration of discretely immobilized cowpea mosaic virus with luminescent quantum dots. *Langmuir* 21, 5501-5510.
- Meldrum, T., Seim, K.L., Bajaj, V.S., Palaniappan, K.K., Wu, W., Francis, M.B., Wemmer, D.E., and Pines, A. (2010). A xenon-based molecular sensor assembled on an MS2 viral capsid scaffold. *Journal of the American Chemical Society* 132, 5936-5937.
- Michoux, F., Ahmad, N., McCarthy, J., and Nixon, P.J. (2011). Contained and high-level production of recombinant protein in plant chloroplasts using a temporary immersion bioreactor. *Plant Biotechnol J* 9, 575-584.

- Miyamoto, K., Shimizu, T., Lin, F., Sainsbury, F., Thuenemann, E., Lomonosoff, G., Nojiri, H., Yamane, H., and Okada, K. (2012). Identification of an E-box motif responsible for the expression of jasmonic acid-induced chitinase gene *OsChia4a* in rice. *Journal of plant physiology* *169*, 621-627.
- Montague, N.P., Thuenemann, E.C., Saxena, P., Saunders, K., Lenzi, P., and Lomonosoff, G.P. (2011). Recent advances of cowpea mosaic virus-based particle technology. *Hum Vaccin* *7*, 383-390.
- Nam, K.T., Wartena, R., Yoo, P.J., Liau, F.W., Lee, Y.J., Chiang, Y.M., Hammond, P.T., and Belcher, A.M. (2008). Stamped microbattery electrodes based on self-assembled M13 viruses. *Proc Natl Acad Sci U S A* *105*, 17227-17231.
- Niblett, C.L., and Semancik, J.S. (1969). Conversion of the electrophoretic forms of cowpea mosaic virus in vivo and in vitro. *Virology* *38*, 685-693.
- Niblett, C.L., and Semancik, J.S. (1970). The significance of the coat protein in infection by the electrophoretic forms of cowpea mosaic virus. *Virology* *41*, 201-207.
- Niu, Z., Liu, J., Lee, L.A., Bruckman, M.A., Zhao, D., Koley, G., and Wang, Q. (2007). Biological templated synthesis of water-soluble conductive polymeric nanowires. *Nano letters* *7*, 3729-3733.
- Novak, J.E., and Kirkegaard, K. (1994). Coupling between genome translation and replication in an RNA virus. *Genes Dev* *8*, 1726-1737.
- Nugent, C.I., Johnson, K.L., Sarnow, P., and Kirkegaard, K. (1999). Functional coupling between replication and packaging of poliovirus replicon RNA. *J Virol* *73*, 427-435.
- Ochoa, W.F., Chatterji, A., Lin, T., and Johnson, J.E. (2006). Generation and structural analysis of reactive empty particles derived from an icosahedral virus. *Chem Biol* *13*, 771-778.
- Omarov, R., Sparks, K., Smith, L., Zindovic, J., and Scholthof, H.B. (2006). Biological relevance of a stable biochemical interaction between the tombusvirus-encoded P19 and short interfering RNAs. *J Virol* *80*, 3000-3008.
- Omarov, R.T., Ciomperlik, J.J., and Scholthof, H.B. (2007). RNAi-associated ssRNA-specific ribonucleases in Tombusvirus P19 mutant-infected plants and evidence for a discrete siRNA-containing effector complex. *Proc Natl Acad Sci U S A* *104*, 1714-1719.
- Phelps, J.P., Dang, N., and Rasochova, L. (2007). Inactivation and purification of cowpea mosaic virus-like particles displaying peptide antigens from *Bacillus anthracis*. *J Virol Methods* *141*, 146-153.

- Porta, C., Spall, V.E., Findlay, K.C., Gergerich, R.C., Farrance, C.E., and Lomonosoff, G.P. (2003). Cowpea mosaic virus-based chimaeras. Effects of inserted peptides on the phenotype, host range, and transmissibility of the modified viruses. *Virology* 310, 50-63.
- Porta, C., Spall, V.E., Lin, T., Johnson, J.E., and Lomonosoff, G.P. (1996). The development of cowpea mosaic virus as a potential source of novel vaccines. *Intervirology* 39, 79-84.
- Porta, C., Spall, V.E., Loveland, J., Johnson, J.E., Barker, P.J., and Lomonosoff, G.P. (1994). Development of cowpea mosaic virus as a high-yielding system for the presentation of foreign peptides. *Virology* 202, 949-955.
- Qiu, W., Park, J.W., and Scholthof, H.B. (2002). Tombusvirus P19-mediated suppression of virus-induced gene silencing is controlled by genetic and dosage features that influence pathogenicity. *Mol Plant Microbe Interact* 15, 269-280.
- Qu, F., and Morris, T.J. (1997). Encapsidation of turnip crinkle virus is defined by a specific packaging signal and RNA size. *J Virol* 71, 1428-1435.
- Rae, C., Koudelka, K.J., Destito, G., Estrada, M.N., Gonzalez, M.J., and Manchester, M. (2008). Chemical addressability of ultraviolet-inactivated viral nanoparticles (VNPs). *PLoS One* 3, e3315.
- Rae, C.S., Khor, I.W., Wang, Q., Destito, G., Gonzalez, M.J., Singh, P., Thomas, D.M., Estrada, M.N., Powell, E., Finn, M.G., *et al.* (2005). Systemic trafficking of plant virus nanoparticles in mice via the oral route. *Virology* 343, 224-235.
- Raja, K.S., Wang, Q., Gonzalez, M.J., Manchester, M., Johnson, J.E., and Finn, M.G. (2003). Hybrid virus-polymer materials. 1. Synthesis and properties of PEG-decorated cowpea mosaic virus. *Biomacromolecules* 4, 472-476.
- Reade, R., Kakani, K., and Rochon, D. (2010). A highly basic KGKKGK sequence in the RNA-binding domain of the Cucumber necrosis virus coat protein is associated with encapsidation of full-length CNV RNA during infection. *Virology* 403, 181-188.
- Reiss, B.D., Mao, C.B., Solis, D.J., Ryan, K.S., Thomson, T., and Belcher, A.M. (2004). Biological routes to metal alloy ferromagnetic nanostructures *Nano letters* 4, 1127-1132.
- Richards, H.A., Halfhill, M.D., Millwood, R.J., and Stewart, C.N., Jr. (2003). Quantitative GFP fluorescence as an indicator of recombinant protein synthesis in transgenic plants. *Plant Cell Rep* 22, 117-121.
- Rochon, D., and Siegel, A. (1984). Chloroplast DNA transcripts are encapsidated by tobacco mosaic virus coat protein. *Proc Natl Acad Sci U S A* 81, 1719-1723.

- Rohll, J.B., Holness, C.L., Lomonosoff, G.P., and Maule, A.J. (1993). 3'-terminal nucleotide sequences important for the accumulation of cowpea mosaic virus M-RNA. *Virology* *193*, 672-679.
- Russo, M., Burgyan, J., and Martelli, G.P. (1994). Molecular biology of tombusviridae. *Adv Virus Res* *44*, 381-428.
- Rybicki, E.P. (2010). Plant-made vaccines for humans and animals. *Plant Biotechnol J* *8*, 620-637.
- Sadeghi, B. (2012). Synthesis and application of nanorods. *Nanorods*. Orhan Yalçın edn. ISBN: 978-953-51-0209-0.
- Saida, F. (2007). Overview on the expression of toxic gene products in *Escherichia coli*. *Current protocols in protein science / editorial board, John E Coligan [et al] Chapter 5, Unit 5.19*.
- Sainsbury, F., Canizares, M.C., and Lomonosoff, G.P. (2010a). Cowpea Mosaic Virus: The Plant Virus-Based Biotechnology Workhorse. *Annu Rev Phytopathol* *48*, 437-455.
- Sainsbury, F., Lavoie, P.O., D'Aoust, M.A., Vezina, L.P., and Lomonosoff, G.P. (2008). Expression of multiple proteins using full-length and deleted versions of cowpea mosaic virus RNA-2. *Plant Biotechnol J* *6*, 82-92.
- Sainsbury, F., and Lomonosoff, G.P. (2008). Extremely high-level and rapid transient protein production in plants without the use of viral replication. *Plant Physiol* *148*, 1212-1218.
- Sainsbury, F., Sack, M., Stadlmann, J., Quendler, H., Fischer, R., and Lomonosoff, G.P. (2010b). Rapid transient production in plants by replicating and non-replicating vectors yields high quality functional anti-HIV antibody. *PLoS One* *5*, e13976.
- Sainsbury, F., Saunders, K., Aljabali, A.A., Evans, D.J., and Lomonosoff, G.P. (2011). Peptide-Controlled Access to the Interior Surface of Empty Virus Nanoparticles. *ChemBiochem* *12(16)*, 2435-2440.
- Sainsbury, F., Thuenemann, E.C., and Lomonosoff, G.P. (2009). pEAQ: versatile expression vectors for easy and quick transient expression of heterologous proteins in plants. *Plant Biotechnol J* *7(7)*, 682-693.
- Sala, F., Manuela Rigano, M., Barbante, A., Basso, B., Walmsley, A.M., and Castiglione, S. (2003). Vaccine antigen production in transgenic plants: strategies, gene constructs and perspectives. *Vaccine* *21*, 803-808.

Sambrook, J., Fritsch, E.F., and Maniatis, T. (1989). *Molecular Cloning: A Laboratory Manual*. Cold Spring Harbour Press, Cold Spring Harbour, NY 2.

Sarawaneeyaruk, S., Iwakawa, H.O., Mizumoto, H., Murakami, H., Kaido, M., Mise, K., and Okuno, T. (2009). Host-dependent roles of the viral 5' untranslated region (UTR) in RNA stabilization and cap-independent translational enhancement mediated by the 3' UTR of Red clover necrotic mosaic virus RNA1. *Virology* 391, 107-118.

Saunders, K., Sainsbury, F., and Lomonosoff, G.P. (2009). Efficient generation of cowpea mosaicvirus empty virus-like particles by the proteolytic processing of precursors in insect cells and plants. *Virology* 393(2), 329-337.

Saxena, P., Hsieh, Y.C., Alvarado, V.Y., Sainsbury, F., Saunders, K., Lomonosoff, G.P., and Scholthof, H.B. (2011). Improved foreign gene expression in plants using a virus-encoded suppressor of RNA silencing modified to be developmentally harmless. *Plant Biotechnol J* 9, 703-712.

Scholthof, H.B. (2006). The Tombusvirus-encoded P19: from irrelevance to elegance. *Nat Rev Microbiol* 4, 405-411.

Scholthof, H.B., Scholthof, K.B., and Jackson, A.O. (1995). Identification of tomato bushy stunt virus host-specific symptom determinants by expression of individual genes from a potato virus X vector. *Plant Cell* 7, 1157-1172.

Seker, U.O., and Demir, H.V. (2011). Material binding peptides for nanotechnology. *Molecules* 16, 1426-1451.

Seo, J.K., Kwon, S.J., and Rao, A.L. (2012). A physical interaction between viral replicase and capsid protein is required for genome-packaging specificity in an RNA virus. *J Virol* 86, 6210-6221.

Shanks, M., and Lomonosoff, G.P. (2000). Co-expression of the capsid proteins of Cowpea mosaic virus in insect cells leads to the formation of virus-like particles. *J Gen Virol* 81, 3093-3097.

Shepherd, C.M., Borelli, I.A., Lander, G., Natarajan, P., Siddavanahalli, V., Bajaj, C., Johnson, J.E., Brooks, C.L., 3rd, and Reddy, V.S. (2006). VIPERdb: a relational database for structural virology. *Nucleic Acids Res* 34, D386-389.

Shwed, P.S., Dobos, P., Cameron, L.A., Vakharia, V.N., and Duncan, R. (2002). Birnavirus VP1 proteins form a distinct subgroup of RNA-dependent RNA polymerases lacking a GDD motif. *Virology* 296, 241-250.

- Siddiqui, S.A., Sarmiento, C., Truve, E., Lehto, H., and Lehto, K. (2008). Phenotypes and functional effects caused by various viral RNA silencing suppressors in transgenic *Nicotiana benthamiana* and *N. tabacum*. *Mol Plant Microbe Interact* *21*, 178-187.
- Singh, P., Destito, G., Schneemann, A., and Manchester, M. (2006). Canine parvovirus-like particles, a novel nanomaterial for tumor targeting. *Journal of nanobiotechnology* *4*, 2.
- Singh, P., Prasuhn, D., Yeh, R.M., Destito, G., Rae, C.S., Osborn, K., Finn, M.G., and Manchester, M. (2007). Bio-distribution, toxicity and pathology of cowpea mosaic virus nanoparticles in vivo. *Journal of controlled release : official journal of the Controlled Release Society* *120*, 41-50.
- Smith, M.L., Fitzmaurice, W.P., Turpen, T.H., and Palmer, K.E. (2009). Display of peptides on the surface of tobacco mosaic virus particles. *Curr Top Microbiol Immunol* *332*, 13-31.
- Soitamo, A.J., Jada, B., and Lehto, K. (2011). HC-Pro silencing suppressor significantly alters the gene expression profile in tobacco leaves and flowers. *BMC plant biology* *11*, 68.
- Stauffer, C.V., Usha, R., Harrington, M., Schmidt, T., Hosur, M., and Johnson, J.E. (1987). *The structure of cowpea mosaic virus at 3.5 Å resolution* (New York: Plenum Publishing Corporation).
- Steinmetz, N.F. (2010). Viral nanoparticles as platforms for next-generation therapeutics and imaging devices. *Nanomedicine*.
- Steinmetz, N.F., Evans, D.J., and Lomonosoff, G.P. (2007). Chemical introduction of reactive thiols into a viral nanoscaffold: a method that avoids virus aggregation. *Chembiochem* *8*, 1131-1136.
- Steinmetz, N.F., Lin, T., Lomonosoff, G.P., and Johnson, J.E. (2009). Structure-based engineering of an icosahedral virus for nanomedicine and nanotechnology. *Curr Top Microbiol Immunol* *327*, 23-58.
- Sun, Q.Y., Ding, L.W., Lomonosoff, G.P., Sun, Y.B., Luo, M., Li, C.Q., Jiang, L., and Xu, Z.F. (2011). Improved expression and purification of recombinant human serum albumin from transgenic tobacco suspension culture. *J Biotechnol* *155*, 164-172.
- Taylor, K.M., Spall, V.E., Butler, P.J., and Lomonosoff, G.P. (1999). The cleavable carboxyl-terminus of the small coat protein of cowpea mosaic virus is involved in RNA encapsidation. *Virology* *255*, 129-137.
- Tokatlian, T., and Segura, T. (2010). siRNA applications in nanomedicine. *Wiley interdisciplinary reviews Nanomedicine and nanobiotechnology* *2*, 305-315.

- Trkola, A., Purtscher, M., Muster, T., Ballaun, C., Buchacher, A., Sullivan, N., Srinivasan, K., Sodroski, J., Moore, J.P., and Katinger, H. (1996). Human monoclonal antibody 2G12 defines a distinctive neutralization epitope on the gp120 glycoprotein of human immunodeficiency virus type 1. *J Virol* *70*, 1100-1108.
- Turner, D.R., Joyce, L.E., and Butler, P.J. (1988). The tobacco mosaic virus assembly origin RNA. Functional characteristics defined by directed mutagenesis. *J Mol Biol* *203*, 531-547.
- Twyman, R.M., Stoger, E., Schillberg, S., Christou, P., and Fischer, R. (2003). Molecular farming in plants: host systems and expression technology. *Trends in biotechnology* *21*, 570-578.
- Usha, R., Rohll, J.B., Spall, V.E., Shanks, M., Maule, A.J., Johnson, J.E., and Lomonosoff, G.P. (1993). Expression of an animal virus antigenic site on the surface of a plant virus particle. *Virology* *197*, 366-374.
- Van Bokhoven, H., Le Gall, O., Kasteel, D., Verver, J., Wellink, J., and Van Kammen, A.B. (1993). Cis- and trans-acting elements in cowpea mosaic virus RNA replication. *Virology* *195*, 377-386.
- van Kammen, A. (1967). Purification and properties of the components of cowpea mosaic virus. *Virology* *31*, 633-642.
- van Kammen, A., and de Jager, C.P. (1978). Cowpea mosaic virus. *Description of Plant Viruses* *197*.
- van Lipzig, R., Gulyaev, A.P., Pleij, C.W., van Montagu, M., Cornelissen, M., and Meulewaeter, F. (2002). The 5' and 3' extremities of the satellite tobacco necrosis virus translational enhancer domain contribute differentially to stimulation of translation. *RNA* *8*, 229-236.
- Vance, V., and Vaucheret, H. (2001). RNA silencing in plants--defense and counterdefense. *Science* *292*, 2277-2280.
- Vardakou, M., Sainsbury, F., Rigby, N., Mulholland, F., and Lomonosoff, G.P. (2012). Expression of active recombinant human gastric lipase in *Nicotiana benthamiana* using the CPMV-HT transient expression system. *Protein Expr Purif* *81*, 69-74.
- Vazquez, A.L., Alonso, J.M., and Parra, F. (2000). Mutation analysis of the GDD sequence motif of a calicivirus RNA-dependent RNA polymerase. *J Virol* *74*, 3888-3891.
- Venter, P.A., Krishna, N.K., and Schneemann, A. (2005). Capsid protein synthesis from replicating RNA directs specific packaging of the genome of a multipartite, positive-strand RNA virus. *J Virol* *79*, 6239-6248.

- Verver, J., Wellink, J., Van Lent, J., Gopinath, K., and Van Kammen, A. (1998). Studies on the movement of cowpea mosaic virus using the jellyfish green fluorescent protein. *Virology* 242, 22-27.
- Voinnet, O., Pinto, Y.M., and Baulcombe, D.C. (1999). Suppression of gene silencing: a general strategy used by diverse DNA and RNA viruses of plants. *Proc Natl Acad Sci U S A* 96, 14147-14152.
- Voinnet, O., Rivas, S., Mestre, P., and Baulcombe, D. (2003). An enhanced transient expression system in plants based on suppression of gene silencing by the p19 protein of tomato bushy stunt virus. *Plant J* 33, 949-956.
- Vos, P., Verver, J., Jaegle, M., Wellink, J., van Kammen, A., and Goldbach, R. (1988). Two viral proteins involved in the proteolytic processing of the cowpea mosaic virus polyproteins. *Nucleic Acids Res* 16, 1967-1985.
- Wang, Q., Lin, T., Johnson, J.E., and Finn, M.G. (2002). Natural supramolecular building blocks. Cysteine-added mutants of cowpea mosaic virus. *Chem Biol* 9, 813-819.
- Wang, X., and Gillam, S. (2001). Mutations in the GDD motif of rubella virus putative RNA-dependent RNA polymerase affect virus replication. *Virology* 285, 322-331.
- Wang, Y., Xiao, M., Chen, J., Zhang, W., Luo, J., Bao, K., Nie, M., and Li, B. (2007). Mutational analysis of the GDD sequence motif of classical swine fever virus RNA-dependent RNA polymerases. *Virus Genes* 34, 63-65.
- Waterhouse, P.M., Wang, M.B., and Lough, T. (2001). Gene silencing as an adaptive defence against viruses. *Nature* 411, 834-842.
- Weiss, B., Geigenmuller-Gnirke, U., and Schlesinger, S. (1994). Interactions between Sindbis virus RNAs and a 68 amino acid derivative of the viral capsid protein further defines the capsid binding site. *Nucleic Acids Res* 22, 780-786.
- Wellink, J., Rezelman, G., Goldbach, R., and Beyreuther, K. (1986). Determination of the proteolytic processing sites in the polyprotein encoded by the bottom-component RNA of cowpea mosaic virus. *J Virol* 59, 50-58.
- Wellink, J., van Bokhoven, H., Le Gall, O., Verver, J., and van Kammen, A. (1994). Replication and translation of cowpea mosaic virus RNAs are tightly linked. *Archives of virology Supplementum* 9, 381-392.
- Wellink, J., Verver, J., and van Kammen, A. (1993). Mutational analysis of AUG codons of cowpea mosaic virus M RNA. *Biochimie* 75, 741-747.

- Wellink, J., Verver, J., Van Lent, J., and Van Kammen, A. (1996). Capsid proteins of cowpea mosaic virus transiently expressed in protoplasts form virus-like particles. *Virology* 224, 352-355.
- Wen, A.M., Shukla, S., Saxena, P., Aljabali, A.A., Yildiz, I., Dey, S., Mealy, J.E., Yang, A.C., Evans, D.J., Lomonossoff, G.P., *et al.* (2012). Interior engineering of a viral nanoparticle and its tumor homing properties. *Biomacromolecules* 13, 3990-4001.
- Wimmer, E. (1982). Genome-linked proteins of viruses. *Cell* 28, 199-201.
- Wu, G.J., and Bruening, G. (1971). Two proteins from cowpea mosaic virus. *Virology* 46, 596-612.
- Xia, Z., Zhu, Z., Zhu, J., and Zhou, R. (2009). Recognition mechanism of siRNA by viral p19 suppressor of RNA silencing: a molecular dynamics study. *Biophys J* 96, 1761-1769.
- Xing, Y., and Rao, J. (2008). Quantum dot bioconjugates for in vitro diagnostics & in vivo imaging. *Cancer biomarkers : section A of Disease markers* 4, 307-319.
- Ye, K., Malinina, L., and Patel, D.J. (2003). Recognition of small interfering RNA by a viral suppressor of RNA silencing. *Nature* 426, 874-878.
- Young, M., Willits, D., Uchida, M., and Douglas, T. (2008). Plant viruses as biotemplates for materials and their use in nanotechnology. *Annu Rev Phytopathol* 46, 361-384.
- Zimmern, D. (1977). The nucleotide sequence at the origin for assembly on tobacco mosaic virus RNA. *Cell* 11, 463-482.

Appendix I: List of Primers

Details of the primers used for amplification of inserts, verification of clones and introduction of mutations in the work described in this thesis are presented below. For convenience, restriction sites have been coloured in blue and start and stop codons are in green and red respectively.

For amplification of the VP60 expression cassette from pEAQ-*HT*-VP60

VP60-PacI-F	GCCAGTGAATTGTTAATTAAGAATTTCGAGC
VP60-SbfI-R	TATACCTGCAGGCTTGAGACTCTAGAGATCTAG
FSC2-F	CCGCTTAATTAAGAATTTCGAGCTCCACCGCGGAAACC
FSC5-R	AGTCTACGCGTTGGCCCTGCAGGCTTGAGACTCTAGAGATCTAG

For amplification of the 24K expression cassette from pEAQ-*HT*-24K

24K-XmaI-F	TATTCCTGGGTTTCGAGCTCCACCGCGGAAACC
24K-AscI-R	TTAAGCTGGCGCGCCAAGCTTGAGACTCTAGAG
FSC6-F	AAACGCGATCGCTCCTGCAGGTATTCGAGCTCCACCGCGGAAACC
FSC2-R	AAGCTGGCGCGCCAAGCTTGAAACTCTA

For SDM of the GDD motif of CPMV RNA-1

GDD-ADD F	GGTGACTTATGCTGATGATAATCTGATTTTCAG
GDD-ADD R	CTGAAATCAGATTATCATCAGCATAAGTCACC
GDD-GAD F	GGTGACTTATGGTGCTGATAATCTGATTTTCAG
GDD-GAD R	CTGAAATCAGATTATCAGCACCATAAGTCACC
GDD-GED F	GGTGACTTATGGTGAAGATAATCTGATTTTCAG
GDD-GED R	CTGAAATCAGATTATCTTCACCATAAGTCACC

For verification of the GDD mutants of RNA-1

GDD check F 2	GCCAATGGAATATAATTTGGTTCG
GDD check R 2	CGCTTCTTTCTCAAAGACAAAGG

For verification of inserts cloned in between the 5'UTR and 3' UTR of *HT*

C1	AACGTTGTCAGATCGTGCTTCGGCACC
C3	CTGAAGGGACGACCTGCTAAACAGGAG

For amplification of RNA-2 from AUG 512 to the end of the *vp60* gene

48K-AgeI-F	GTTGACCGGTTCGATGGAAAGCATTATGAG
48K-SbfI-F	TGTCCTGCAGGCGATGGAAAGCATTATGAG
VP60-StuI-R	AATAGGCCTACCTAAGCAGCAGTAGC
VP60-XmaI-R	ATACCCGGGACCTAAGCAGCAGTAGC

For amplification of RNA-2 from AUG 161 to the end of the *vp60* gene

58K-AgeI-F	GTTGACCGGTTCGATGTTTTCTTTCCTG
58K-SbfI-F	TGTCCTGCAGGCGATGTTTTCTTTCCTG
VP60-StuI-R	AATAGGCCTACCTAAGCAGCAGTAGC
VP60-XmaI-R	ATACCCGGGACCTAAGCAGCAGTAGC

For introduction of peptides at the N-terminus of CPMV-L for mineralization

FePt-blunt/start/XmaI-F	ATGCATAATAAACATTTGCCTTCTACTCAACCTTTGG CTC
FePt-blunt/start/XmaI-R	CCGGGAGCCAAAGGTTGAGTAGAAGGCAAATGTTTAT TATGCAT

For introduction of the RGD peptide at the C-terminus of S for targeting

RGD-XmaI/ blunt-F	CCGGGAATGCTGTTCTAATTTGAGAGGTGATTTGCA AGTTTTGGCTCAAAAAGTTGCTAGAAGTTAG
RGD-XmaI/ blunt-R	CTAAGTTCTAGCAACTTTTTGAGCCAAAAGTTGCAAA TCACCTCTCAAATTAGGAACAGCATTC

For SDM of P19 to generate pEAQspecialKm-based plasmids

P19-R43W-SDM-F	CGAGTTGGACTGAGTGGTGGCTACATAACGATGAG
P19-R43W-SDM-R	CTCATCGTTATGTAGCCACCACTCAGTCCAAGTTCG

For amplification of the gene encoding GFP

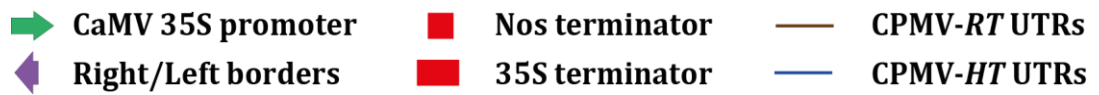
GFP-start-XhoI-F	GACTCGAGCTATGACTAGCAAAGGG
GFP-stop-XmaI-R	GATCCCGGGTATTATTGTATAGTTCATCC

For creation of the 3' UTR mutants of pEAQexpress-RT-GFP

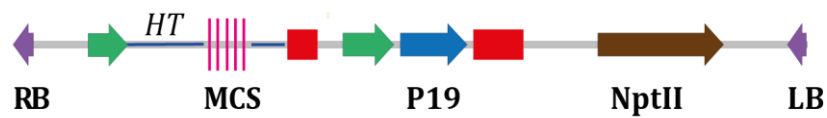
RT-del3'UTR-F	CGATCCCGGGTTGATCGTTCAAACATTTGG
RT-del3'UTR-R	GACTCTAGAGGATCCCTTAAATCGATATGG
RT-HT3'UTR-F	CGATCCCGGGCTTAACTCTGGTTTCATTAA

Appendix II: List of Vectors

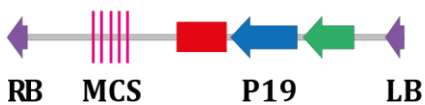
The T-DNA regions of all vectors used for the work described in this thesis are shown below. Key elements have been labelled in each figure. Other elements are represented as follows:



T-DNA of pEAQ-HT



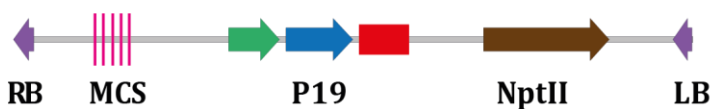
T-DNA of pEAQexpress



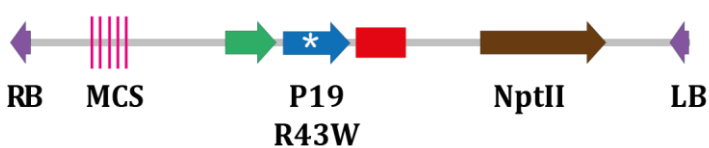
T-DNA of pEAQselectK

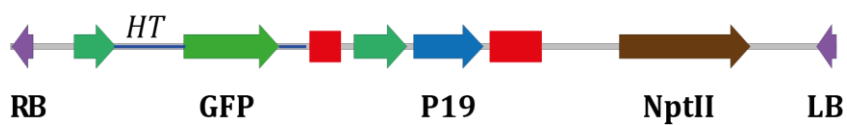
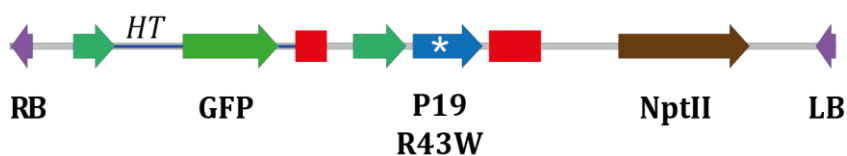
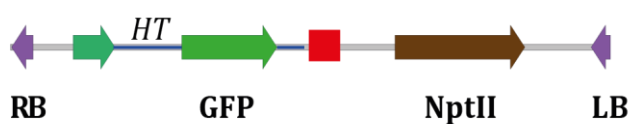
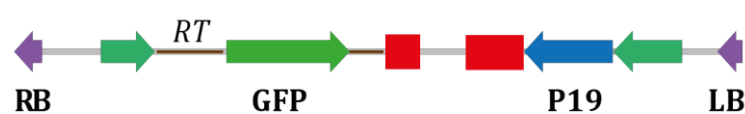
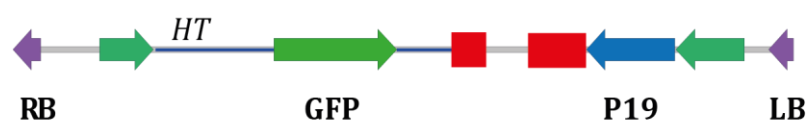
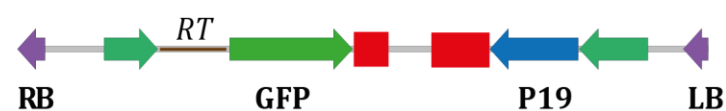
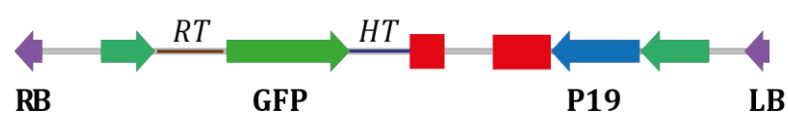


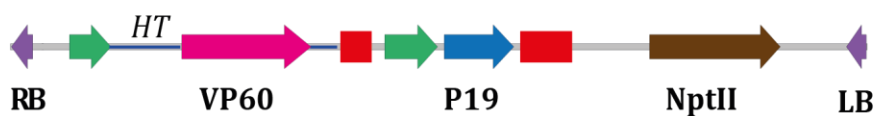
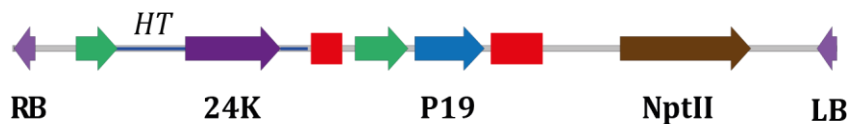
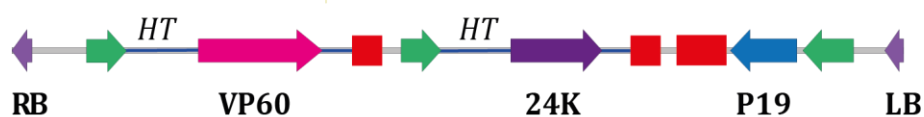
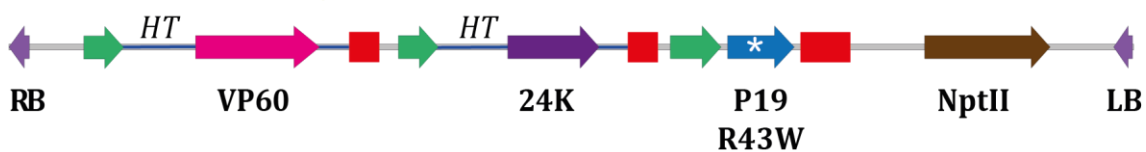
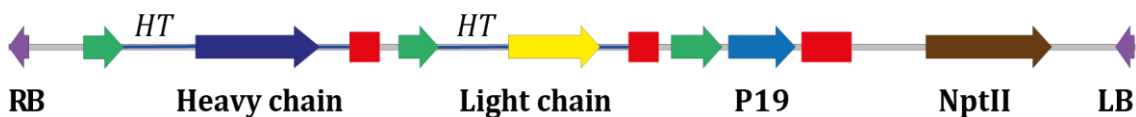
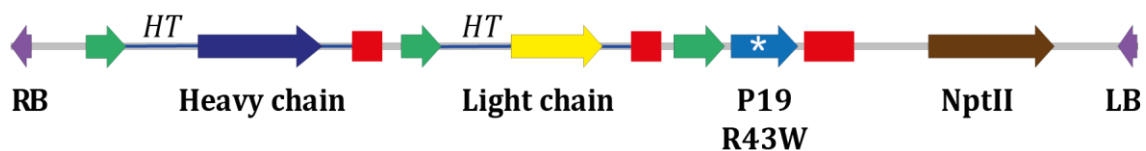
T-DNA of pEAQspecialK

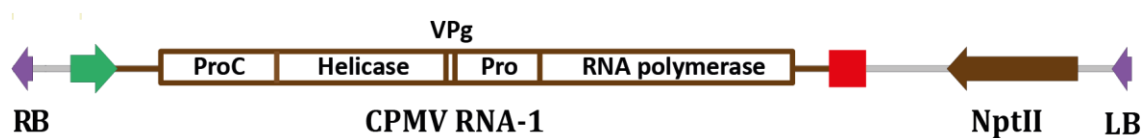
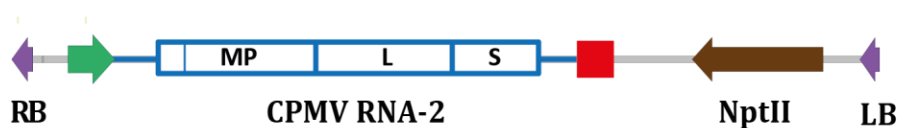
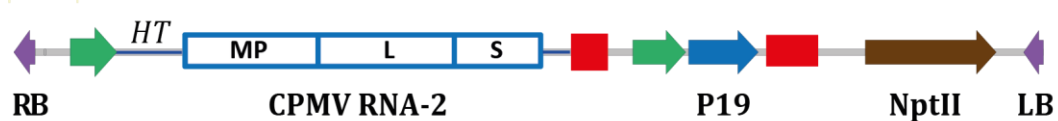
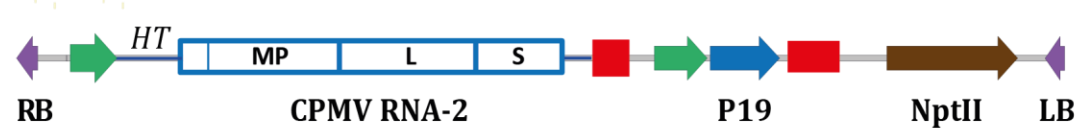


T-DNA of pEAQspecialKm



T-DNA of pEAQspecialK-GFP-HT**T-DNA of pEAQspecialKm-GFP-HT****T-DNA of pEAQselectK-GFP-HT****T-DNA of pEAQexpress-RT-GFP****T-DNA of pEAQexpress-HT-GFP****T-DNA of pEAQexpress-RT-GFP-del3'UTR****T-DNA of pEAQexpress-RT-GFP-HT3'UTR**

T-DNA of pEAQ-HT-VP60**T-DNA of pEAQ-HT-24K****T-DNA of pEAQexpress-eVLP****T-DNA of pEAQspecialKm-eVLP****T-DNA of pEAQspecialK-HEL****T-DNA of pEAQspecialKm-HEL**

T-DNA of pBinPS-1-NT**T-DNA of pBinPS-2-NT****T-DNA of pBinP-32E-NT****T-DNA of pEAQ-HT-RNA-2****T-DNA of pEAQ-HT-full length RNA-2**

Appendix III: Publications

Some of the work described in this thesis has been published in peer-reviewed journals. A copy of each publication is enclosed. The citations of the publications are as follows:

- (1) Saxena, P., Hsieh, Y.C., Alvarado, V.Y., Sainsbury, F., Saunders, K., Lomonossoff, G.P. and Scholthof, H.B. (2011). Improved foreign gene expression in plants using a virus-encoded suppressor of RNA silencing modified to be developmentally harmless. **Plant Biotechnology Journal** 9(6): 703-712.
- (2) Montague, N.P., Thuenemann, E.C., Saxena, P., Saunders, K., Lenzi, P. and Lomonossoff, G.P. (2011). Recent advances of cowpea mosaic virus-based particle technology. **Human Vaccine** 7(3): 383-390.
- (3) Wen, A.M., Shukla, S., Saxena, P., Aljabali, A. A. A., Yildiz, I., Dey, S., Mealy, J. E., Yang, A. C., Evans, D. J., Lomonossoff, G. P. and Steinmetz, N. F. (2012). Interior engineering of a viral nanoparticle and its tumor homing properties. **Biomacromolecules** 13: 3990–4001.
- (4) Sainsbury, F., Saxena, P., Geisler, K., Osbourn, A. and Lomonossoff, G.P. (2012). Using a virus-derived system to manipulate plant natural product biosynthetic pathways. **Methods in enzymology** 517: 185-202.

Improved foreign gene expression in plants using a virus-encoded suppressor of RNA silencing modified to be developmentally harmless

Pooja Saxena^{1,†}, Yi-Cheng Hsieh^{2,†}, Veria Y. Alvarado², Frank Sainsbury^{1,‡}, Keith Saunders¹, George P. Lomonosoff^{1,*} and Herman B. Scholthof^{2,*}

¹John Innes Centre, Norwich Research Park, Colney, Norwich, UK

²Department of Plant Pathology and Microbiology, Texas A&M University, College Station, TX, USA

Received 18 June 2010;

revised 13 September 2010;

accepted 22 September 2010.

*Correspondence (fax: +44 1603 450018;
+1 979 845 6383; e-mails:

george.lomonosoff@bbsrc.ac.uk;

herscho@tamu.edu)

[†]These authors contributed equally and
share first authorship.

[‡]Present address: Département de
Phytologie, Université Laval, Québec,
Canada.

Keywords: heterologous expression,
silencing suppression, P19 mutant,
CPMV-HT.

Summary

Endeavours to obtain elevated and prolonged levels of foreign gene expression in plants are often hampered by the onset of RNA silencing that negatively affects target gene expression. Plant virus-encoded suppressors of RNA silencing are useful tools for counteracting silencing but their wide applicability in transgenic plants is limited because their expression often causes harmful developmental effects. We hypothesized that a previously characterized tombusvirus P19 mutant (P19/R43W), typified by reduced symptomatic effects while maintaining the ability to sequester short-interfering RNAs, could be used to suppress virus-induced RNA silencing without the concomitant developmental effects. To investigate this, transient expression in *Nicotiana benthamiana* was used to evaluate the ability of P19/R43W to enhance heterologous gene expression. Although less potent than wt-P19, P19/R43W was an effective suppressor when used to enhance protein expression from either a traditional T-DNA expression cassette or using the CPMV-HT expression system. Stable transformation of *N. benthamiana* yielded plants that expressed detectable levels of P19/R43W that was functional as a suppressor. Transgenic co-expression of green fluorescent protein (GFP) and P19/R43W also showed elevated accumulation of GFP compared with the levels found in the absence of a suppressor. In all cases, transgenic expression of P19/R43W caused no or minimal morphological defects and plants produced normal-looking flowers and fertile seed. We conclude that the expression of P19/R43W is developmentally harmless to plants while providing a suitable platform for transient or transgenic overexpression of value-added genes in plants with reduced hindrance by RNA silencing.

Introduction

In applied biological plant sciences and biotechnology, there is an increasing demand for gene expression systems that allow for high levels of foreign protein production in plants, whether transgenically, transiently or by means of a virus vector (Scholthof *et al.*, 2002; Cañizares *et al.*, 2005). However, irrespective of the system, optimum expression is often not achieved or maintained because of the onset of RNA silencing (Scholthof, 2007). Therefore, it is highly desirable to establish a high-level expression platform in plants that is not subject to deleterious effects of RNA silencing.

Many plant viruses are known to encode one or more suppressors of RNA silencing (Voinnet, 2005), and these have been successfully used to enhance transient gene expression of co-expressed genes (Johansen and Carrington, 2001; Voinnet *et al.*, 2003; Sainsbury and Lomonosoff, 2008). An example of such a suppressor is the *Tomato bushy stunt virus* (TBSV)-encoded P19 that suppresses RNA silencing of foreign genes by sequestering short-interfering RNAs (siRNAs) in a manner that is neither sequence-specific nor organism-dependent (Scholthof, 2006). However, the toxic effect associated with expression

of P19 in plants (Scholthof *et al.*, 1995) results in the situation that the only transformants that survive accumulate poor levels of P19 (Silhavy *et al.*, 2002; Papp *et al.*, 2003; Dunoyer *et al.*, 2004; Alvarez *et al.*, 2008; Siddiqui *et al.*, 2008). Still, in these cases, severe negative consequences on plant performance and development occur, which may be associated with the binding of P19 to microRNAs (miRNAs) (Papp *et al.*, 2003; Chapman *et al.*, 2004). A similar problem has also been found with the transgenic expression of other silencing suppressors (Mallory *et al.*, 2002; Siddiqui *et al.*, 2008). In the current study, we aimed to develop and test a system in which desirable traits of P19 with respect to enhancing gene expression are uncoupled from unwanted side effects.

TBSV P19 is an intriguing multifunctional pathogenicity protein because it is a very critical host-range determinant, as well as an important contributor to viral symptoms, and it has host-dependent effects on virus invasion (Chu *et al.*, 2000). Many of these biological effects are related to the activity of P19 as a suppressor of virus-induced RNA silencing (Silhavy *et al.*, 2002; Lakatos *et al.*, 2004; Park *et al.*, 2004; Omarov *et al.*, 2006). To enable this suppression function, P19 self-interacts to form dimers that specifically sequester 21 nucleotide (nt) siRNAs in a

sequence-nonspecific manner (Vargason *et al.*, 2003; Ye *et al.*, 2003). This prevents the programming of a RNA interference-associated RNA-induced silencing complex, thereby blocking the antiviral RNA silencing and consequently protecting viral RNA from degradation during infection (Omarov *et al.*, 2007; Pantaleo *et al.*, 2007).

Our previous studies showed that the different host-dependent biological activities and sequestration of siRNAs are all structurally modulated by the same central region on P19 that is positioned at the inner core of the dimer (Chu *et al.*, 2000; Scholthof, 2006). One mutation at amino acid 43 of the P19 protein [P19/R43W; substitution of Arg43 (R43) with Trp (W)] that is located more at the periphery of each monomer in the dimer (Fig. 1a) strongly reduces the symptoms of TBSV infection (Chu *et al.*, 2000) while maintaining the ability to bind siRNAs (Omarov *et al.*, 2006). We have demonstrated that P19/R43W prevents virus-induced silencing (Qiu *et al.*, 2002) and thus protects TBSV RNA from silencing-mediated degradation during invasion of plants (Omarov *et al.*, 2006). This outcome, in combination with the absence of severe symptoms, suggests that P19/R43W is an active suppressor that, compared with wt-P19,

interferes far less with endogenous events, possibly including miRNA function.

Based on the aforementioned observations, we hypothesized that the nontoxic P19/R43W suppressor would represent a biotechnological tool to enhance foreign gene expression in plants while minimizing negative effects on plant development and performance. To examine this, we used three different methods to illustrate the biotechnological potential of the mutant suppressor: (i) transient expression of P19/R43W along with target constructs [green fluorescent protein (GFP) and the pharmaceutically valuable human anti-HIV-1 IgG antibody 2G12], (ii) transgenic expression of P19/R43W to test its effect on plant development and to allow transient introduction of test constructs and (iii) transgenic co-expression of P19/R43W with GFP using the versatile and highly expressing CPMV-HT system (Sainsbury and Lomonosoff, 2008; Sainsbury *et al.*, 2009).

Collectively, the results showed that even though P19/R43W was not quite as potent a suppressor as wild-type P19, its transient or transgenic expression yielded detectable levels of protein that did not negatively affect *Nicotiana benthamiana* plants, as evidenced by the absence of severe deformations and

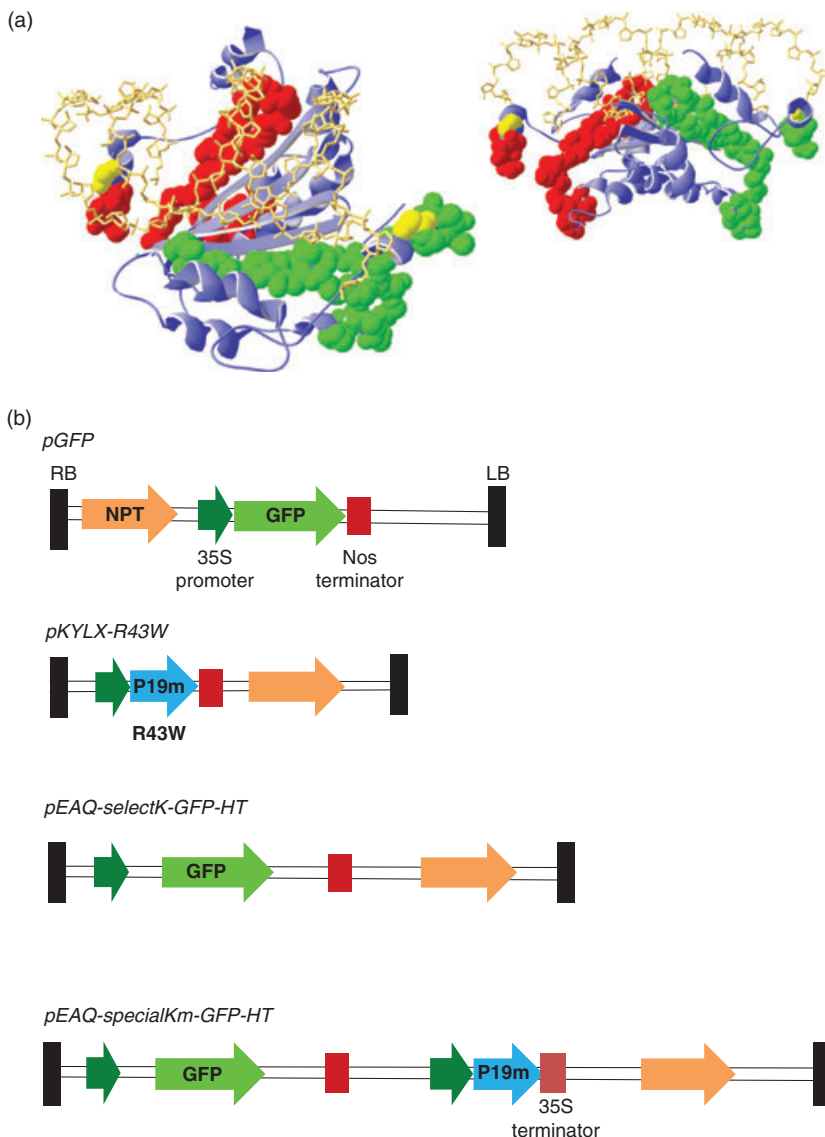


Figure 1 P19/R43W. (a) Three-dimensional views of the location of R43 in the P19/siRNA structure. The red and green regions indicate the amino acids in two P19 monomers important for siRNA sequestration. The yellow balls on the P19 dimer indicate the location of P19/R43 that is close to the Trp reading head of P19 that measures 21-nt siRNAs. The blue ribbon represents the backbone of the P19 dimer, and the siRNA duplex is shown as the gold chain. The protein structure profile was downloaded from the NCBI protein structure database and viewed/modified by DeepView/Swiss-PdbViewer v3.7. (b) Schematic representation of select T-DNA expression cassettes used in this study. LB and RB represent left and right border, respectively, and other expression elements are described within the diagram. Abbreviations are as follows: 35S promoter = *Cauliflower mosaic virus* 35S promoter; NPT = Neomycin phosphotransferase; Nos terminator = Nopaline synthase terminator; P19m = P19 carrying the R43W mutation. 35S terminator = *Cauliflower mosaic virus* 35S terminator.

the setting of viable seeds. Several bioassays showed that P19/R43W was functionally active as a suppressor, for instance in boosting transient expression of GFP. Transformation of plants with constructs using the CPMV-*HT* system (Sainsbury and Lomonosoff, 2008; Sainsbury *et al.*, 2009) to simultaneously express GFP and P19/R43W showed a clear increase in GFP expression compared to levels in absence of suppressor. We conclude that expression of P19/R43W provides an environment in *N. benthamiana* cells that is not harmful to the plants and consequently provides a suitable platform, particularly in a transgenic context, for overexpression of heterologous genes.

Results

Suppression of RNA silencing by transient expression of P19/R43W

Even though it had been demonstrated that P19/R43W (Fig. 1a) sequesters virus-derived siRNAs and suppresses TBSV-induced RNA silencing (Qiu *et al.*, 2002; Omarov *et al.*, 2007), no evidence was yet available that the protein would effectively suppress RNA silencing of heterologous genes outside the context of TBSV infection. To test this, *N. benthamiana* plants were infiltrated with *Agrobacterium tumefaciens* cultures expressing GFP and with cultures expressing either wt-P19 or P19/R43W (Fig. 1b) and the levels of GFP expression were assessed (Johansen and Carrington, 2001; Voinnet *et al.*, 2003). Several T-DNA constructs for the transient expression of P19/R43W in different *Agrobacterium* strains were tested in these experiments (Fig. S1). The co-infiltration tests revealed some quantitative differences in GFP expression that were dependent on the T-DNA construct and/or bacterial strain. However, it was evident that the expression of P19/R43W enhanced and prolonged the green fluorescence but to a lesser extent than wt-P19 (Fig. S1).

To investigate whether P19/R43W would be effective in conjunction with a high-level protein expression system, modification of the highly efficient CPMV-*HT* expression system (Sainsbury and Lomonosoff, 2008; Sainsbury *et al.*, 2009) was undertaken using the vector pEAQspecialK-GFP-*HT* (Sainsbury *et al.*, 2009). This is a vector that contains the GFP expression cassette, the P19 cassette and the kanamycin resistance gene all on the T-DNA region of a single binary vector (Fig. 1b). It is effective for the high-level transient expression of GFP in plants and, as all the components are located on a single T-DNA, could potentially also be used for stable transformation. Plasmid pEAQspecialKm-GFP-*HT* was constructed by a single nucleotide substitution on pEAQspecialK-GFP-*HT*, resulting in the R43W mutation in P19 (Fig. 1b). Levels of GFP expression obtained after agroinfiltration of *N. benthamiana* leaves with pEAQspecialKm-GFP-*HT* (P19/R43W) were compared with those obtained after infiltration with pEAQspecialK-GFP-*HT* (wt-P19) and pEAQselectK-GFP-*HT*, which does not express any suppressor of silencing (Fig. 2). In the absence of a suppressor (pEAQselectK-GFP-*HT*), GFP expression levels of 0.1 g/kg of fresh weight tissue (FWT) were obtained, while pEAQspecialK-GFP-*HT* gave GFP levels of 1.4 g/kg of FWT, a result similar to that reported previously (Sainsbury *et al.*, 2009). In the case of pEAQspecialKm-GFP-*HT*, GFP levels of 0.7 g/kg of FWT were achieved, approximately half that observed when the wt-P19 was used and about sevenfold greater than obtained in the absence of a suppressor.

The ability of P19/R43W to enhance transient expression of a biotechnologically important protein was explored by expressing

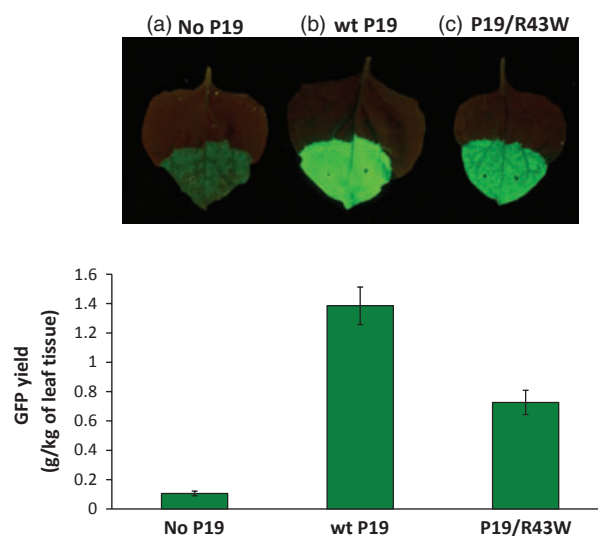


Figure 2 Effect of P19/R43W on transient GFP expression in *Nicotiana benthamiana*. Transient expression of GFP was assessed by visual inspection of leaves under UV light (upper panel) or by fluorimetry (lower panel) in the absence of any suppressor (a), presence of wt-P19 (b) and presence of P19/R43W (c). P19/R43W enhances expression by about 7-fold, which is half the level achieved with wt-P19. Error bars represent the standard deviation for the triplicate samples.

the heavy and light chains of the human anti-HIV antibody 2G12 (Buchacher *et al.*, 1994) in *N. benthamiana* (Fig. 3). Assembled and active molecules of 2G12 have previously been expressed in *N. benthamiana* leaves to levels of 400 mg/kg of FWT by infiltration of a pEAQ construct encoding the 2G12 heavy (H) and light (L) chains plus wt P19 (Sainsbury *et al.*, 2009). In this study, the two pEAQ constructs were created to express the H and L chains of 2G12 in presence of either wt-P19 (pEAQspecialK-HEL) or P19/R43W (pEAQspecialKm-HEL), all from a single T-DNA. Levels of 2G12 were estimated by SDS-PAGE of total protein extracts under reducing and nonreducing conditions and using known amounts of Chinese hamster ovary (CHO)-produced 2G12 as standards (Fig. 3). In presence of wt-P19, 2G12 expression levels approaching 400 mg/kg of FWT were attained, while in presence of P19/R43W, 2G12 expression levels appeared to be about half as much. This is consistent with the results obtained with GFP expression and reiterates the observation that P19/R43W retains significant, if reduced, activity to suppress gene silencing when deployed in conjunction with the CPMV-*HT* expression system.

Transgenic expression of P19/R43W does not lead to negative effects on plant growth and development

The first questions to be addressed if P19/R43W is to prove useful in a transgenic context were whether plants transformed solely for expression of P19/R43W would yield detectable levels of a functional suppressor protein and would such plants be developmentally normal. To assess this, the transformation construct pKYLX7-P19/R43W was created (Fig. 1b). Transient assays with two different *Agrobacterium* strains showed that pKYLX7-P19/R43W expressed readily measurable levels of P19/R43W protein that enhanced GFP expression though, as expected, at somewhat reduced levels compared to wt-P19 (Fig. 4). Also, the levels obtained with this construct, designed

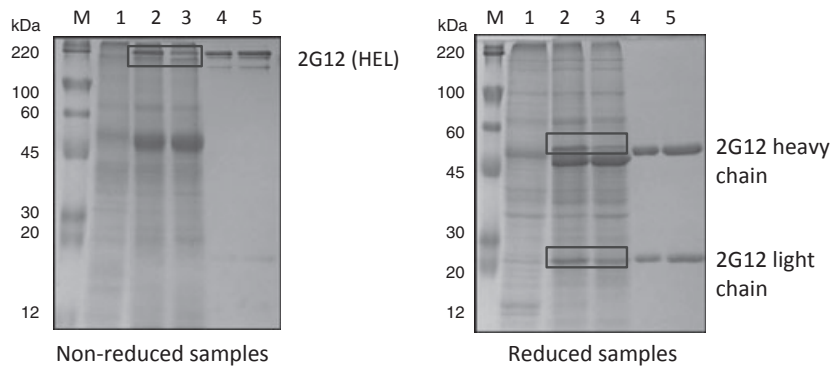


Figure 3 Comparison of 2G12 expression in the presence of wt-P19 or P19/R43W. Total protein extracts of infiltrated leaves were subjected to SDS-PAGE under nonreducing (left-hand panel) or reducing conditions (right-hand panel) and the gel stained with InstantBlue Coomassie stain. Lane M: protein markers; Lane 1: Negative control (Empty pEAQ-HT vector); Lane 2: pEAQspecialK-HEL (containing 2G12 H chain, L chain and wt-P19 in pEAQ-HT); Lane 3: pEAQspecialKm-HEL (containing 2G12 H chain, L chain and P19/R43W in pEAQ-HT); Lane 4: 1 μ g CHO-expressed 2G12; Lane 5: 2 μ g CHO-2G12. 2G12 expression levels can be estimated from the gel to be 400 mg/kg of FWT in presence of wt-P19 and 200 mg/kg of FWT in presence of P19/R43W.

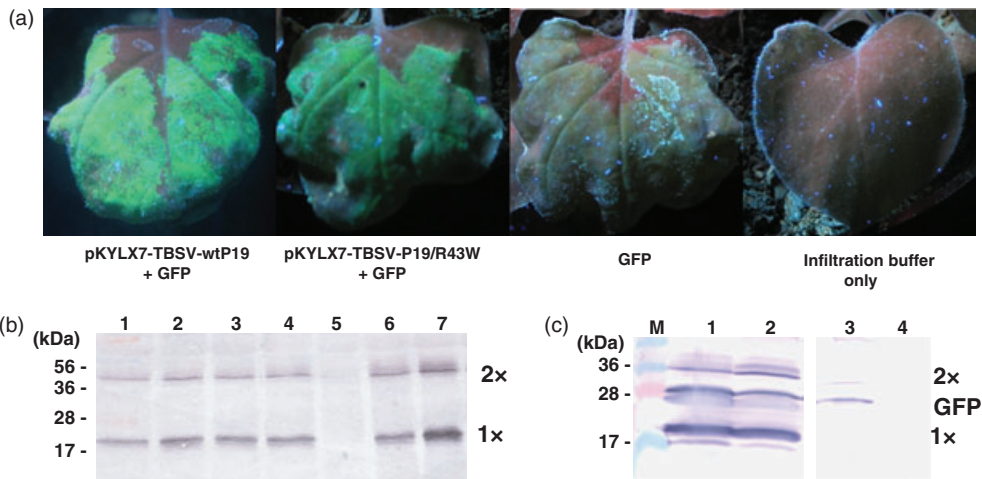


Figure 4 Transient suppression of GFP silencing by P19/R43W expressed from a plant transformation construct. (a) Fluorescence on *Nicotiana benthamiana* leaves co-infiltrated with pGFP, a GFP-expressing construct (GFP) (Voignet *et al.*, 1998; Qiu *et al.*, 2002) and either pKYLX7-P19 or pKYLX7-P19/R43W. All constructs were transformed into *Agrobacterium* strain C58 for this transient assay. (b) Western blot detection of TBSV P19 monomers (1x) and dimers (2x) in total protein extracts from 7 dpi *Agrobacterium*-infiltrated *N. benthamiana* leaves. Lane 1: pKYLX7-P19/R43W isolate 1 in C58; Lane 2: pKYLX7-P19/R43W isolate 2 in C58; Lane 3: pKYLX7-P19/R43W isolate 1 in EHA; Lane 4: pKYLX7-P19/R43W isolate 2 in EHA; Lane 5: Mock (infiltration buffer only); Lane 6: pKYLX7-wt-P19 in C58; Lane 7: pCass4N-wt-P19 in C58. (c) Codetection of GFP and P19 protein in co-infiltrated leaves at 7 dpi. Lane 1: pKYLX7-wt-P19; Lane 2: pKYLX7-P19/R43W; Lane 3: GFP only; Lane 4: Mock; the two panels are from the same blot with irrelevant lanes removed.

for the creation of transgenic plants, were comparable to those achieved with a vector normally used for transient assays only (Fig. 4b, lane 7).

The pKYLX-P19/R43W construct was used for plant transformation, and 14 *N. benthamiana* T0 plants (1–15; plant number 10 was inadvertently omitted) were selected and grown to maturity; these all flowered and set seed that was collected from each plant. Western blot analyses on the T0 plants using a routine (but with relatively inferior sensitivity) alkaline phosphatase-mediated detection showed that P19/R43W protein was accumulating in three individuals (43-3, 43-12 and 43-15). However, only the SDS-recalcitrant P19-dimer (Park *et al.*, 2004) and not the monomer was discernable (data not shown). The phenotype of these T0 plants accumulating detectable levels of

P19/R43W was quite similar to those not expressing the protein, although upon very close inspection some evidence of cup-shaped leaves and mild swelling or blistering was visible (Fig. 5a). The T0 plants developed normally, flowered and set seed that was collected and germinated on MS agar plates in presence of kanamycin to select for transgenic T1 individuals followed by Western blot screening on progeny plants from each original transgenic T0 line. Progeny from 43-3, 43-12 (but not 43-14 or -15) tested positive for P19 expression and, in addition, 43-2, -5, -6, -8, -11, -13 now yielded P19/R43W protein monomers and/or dimers (Fig. 5b). It is important to note in the context of these positive immune-detection results for the T1 plants that the germination rate of each batch of T0-produced seed was approximately 95% illustrating that the

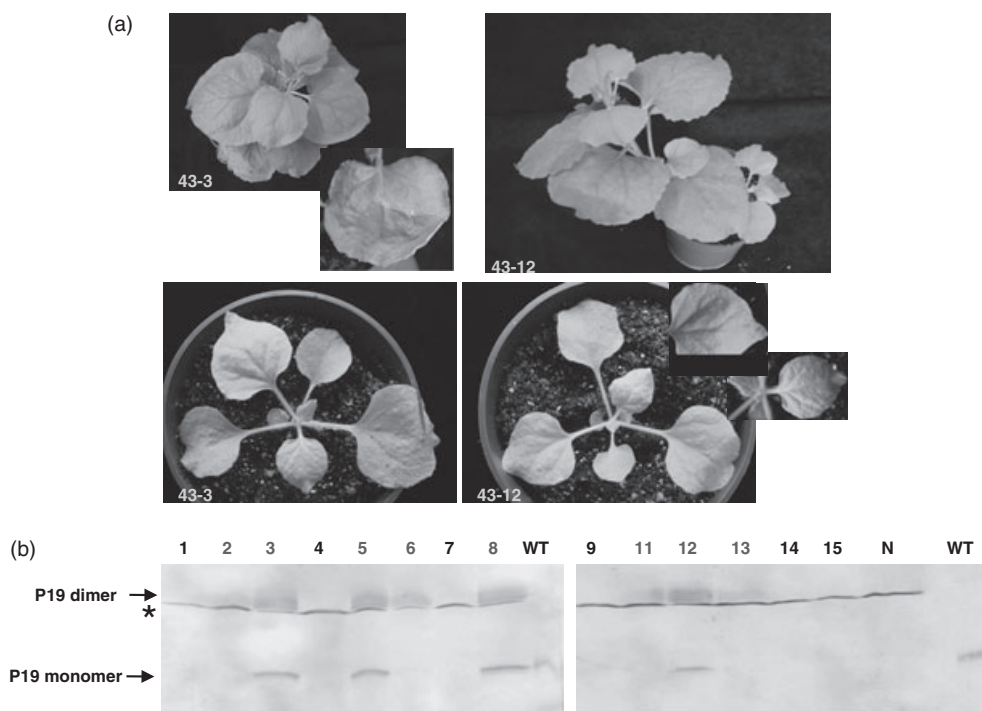


Figure 5 P19/R43W-transgenic plants. (a) Representative P19/R43W transgenic lines 43-3 (Left) and 43-12 (Right) displaying mild morphological features such as leaf cupping, wrinkling or blistering. (b) Detection of P19/R43W in total protein extracts from putative transgenic *Nicotiana benthamiana* T1 lines using Western blotting with alkaline phosphatase-mediated detection. Lanes denote lines with the same number, and those in grey show accumulation of monomers and dimers, or only dimers that appear as a fuzzy band above the sharper band representing a protein that for unknown reasons cross-reacts with the P19 antiserum (*); those in black colour failed to give a positive signal for P19/R43W. The WT sample is from nontransformed wt-TBSV infected *N. benthamiana* plants, and N denotes non-P19/R43W-transgenic *N. benthamiana* obtained after transformation. The origin of the nonspecific band in these plants is not known, nor why it is absent in WT nontransformed plants.

readily detectable levels of P19/R43W had no negative effect on seed fertility, germination and growth.

Collectively, these tests provided evidence that P19/R43W can accumulate at detectable levels in transgenic *N. benthamiana* with minimal effects on plant morphology, flowering and setting of fertile seed.

Functionality of transgenically expressed P19/R43W

Several approaches were used to address whether the transgenically expressed P19/R43W (Line 3 and Line 12) was functional. Briefly, the experiments showed that the transgenically expressed P19/R43W often complemented *p19*-defective TBSV constructs (Fig. S2), but for reasons not yet understood, this was not always evident. Most importantly, for this study that focuses on determining the effect of P19/R43W on expression of heterologous foreign genes, we showed that agroinfiltration of the transgenic plants with pGFP (Fig. 1b) yielded higher levels of GFP when compared to that in nontransgenic plants (Fig. 6). In fact, the effect mimicked that observed upon co-infiltration of pGFP with a wild-type P19-expressing construct in nontransgenic plants (Fig. 6).

In summary, the P19/R43W-transgenic plants were shown to (i) express the suppressor protein at detectable levels, (ii) suffer no harmful developmental effects and (iii) express a P19/R43W protein that is functional for the suppression of transiently- or virus-induced gene silencing. These observations provided confidence and impetus for pursuing the biotechnologically attractive prospect of cotransgenic expression of P19/R43W with target foreign genes, as described in sections below.

P19/R43W-mediated enhancement of a co-expressed heterologous transgene

To examine whether P19/R43W can be used to enhance expression of a heterologous transgene, the pEAQspecialKm-GFP-HT (P19/R43W), pEAQspecialK-GFP-HT (wt-P19) and pEAQselectK-GFP-HT (no suppressor) (Fig. 1b) were used to stably transform *N. benthamiana* using the leaf disc method of Horsch and Klee (Horsch and Klee, 1986). While a number of primary transformants (T0) could be isolated when pEAQspecialKm-GFP-HT or pEAQselectK-GFP-HT was used for transformation, no plants could be regenerated when pEAQspecialK-GFP-HT, expressing wt-P19, was used, a result consistent with previously reported toxic properties of wt-P19 (Scholthof, 2006). One line for each of the plants transformed with pEAQspecialKm-GFP-HT (Line 5, expressing P19/R43W) or pEAQselectK-GFP-HT (Line 3, no suppressor) was selected for more detailed analysis. The T0 plants representing Line 3 and Line 5 grew normally and fluoresced under UV light, showing successful stable integration of the GFP gene. The T0 plants were self-fertilized, and a T1 population of over 50 plants from each line was produced by germinating the resultant seeds. The T1 plants of both Lines 3 and 5 showed no developmental defects and grew and flowered normally. Initial characterization of GFP expression was performed by visually scoring each T1 plant for green fluorescence under UV light followed by verification with a quantitative GFP assay (data not shown). The progeny from both Lines 3 and 5 appeared to give three distinct levels of GFP fluorescence, with the ratio of plants with high, medium and no GFP

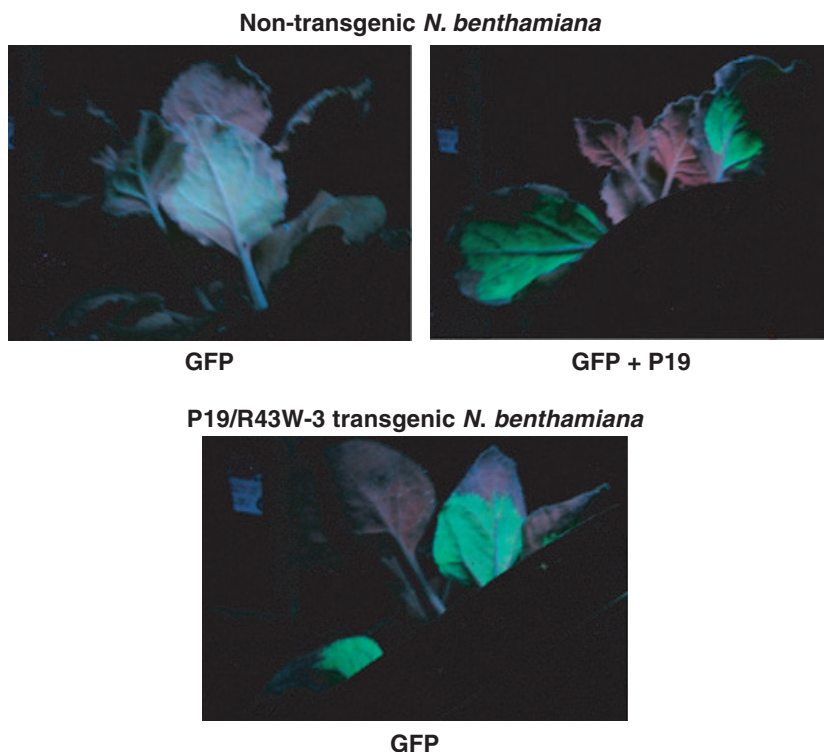


Figure 6 Suppression activity of transgenically expressed P19/R43W in *Nicotiana benthamiana*. Images are of abaxial sides of leaves photographed with same exposure times under ultraviolet light four days post-infiltration with *Agrobacterium* cultures. The top panels show transient GFP expression in nontransgenic *N. benthamiana* upon (co-)infiltration with constructs expressing either GFP only (left) pGFP or GFP plus wild-type P19 (right) using pGFP and pKYLX-P19 (Figs 1b and S1). The panel on the bottom shows a leaf of the P19/R43W transgenic Line 3 infiltrated with a construct expressing only GFP. The differences in the digital images accurately reflect what was observed upon visual examination of the leaves in three biological repeats.

fluorescence being approximately 1 : 2 : 1 for both Lines 3 and 5. Even though we cannot assume a strict correlation between zygosity and level of expression, this potentially fits with a single integration event occurring in both cases, with the ratio 1 : 2 : 1 corresponding to homozygotes:heterozygotes:null segregants.

From the T1 population, leaf tissue was harvested from the 15 highest expressing plants of each Line (3 and 5) and fluorescence was again measured by spectrofluorometry. Although there was considerable variation in the levels of GFP expression in the different T1 plants from the same line, overall, T1 plants from Line 5 (containing P19/R43W present as transgene) had higher GFP expression levels in comparison with those from Line 3 (not expressing any suppressor of silencing) (Fig. 7), indicating that transgenically expressed P19/R43W enhances expression of a heterologous transgene. Upon comparing the average yield of homozygous plants of both lines, the presence of P19/R43W appears to enhance the expression approximately 1.7-fold in a statistically significant manner (Fig. 7).

Plants homozygous for co-expression of GFP and P19/R43W are phenotypically normal

If transformation with P19/R43W is to be a practical method of enhancing transgene expression, it will be essential that plants homozygous for the mutant suppressor are phenotypically normal and fertile. To identify homozygotes among the T1 progeny, high-expressing individuals of Lines 3 and 5 were self-fertilized and the seeds from 10 of these plants were germinated on kanamycin-containing plates. T1 plants numbered 3.26, 5.5, 5.10 and 5.12 were identified as homozygotes because 100% of their progeny was resistant to kanamycin and expressed GFP (Fig. S3). Because kanamycin resistance is conferred by the *nptII* gene present in the integrated T-DNA region and the entire T2 generation of these plants was resistant, we conclude that the T1 plants listed earlier are homozygous for

the T-DNA region, including the genes encoding GFP and P19/R43W (Fig. 1b). Homozygous individuals of Line 3 (expressing only GFP) and Line 5 (expressing GFP and P19/R43W) exhibit a phenotype that is indistinguishable from that of nontransformed plants (Fig. 8).

Discussion

Transient and transgenic expression of P19/R43W

In previous studies, we demonstrated that the TBSV P19 mutant P19/R43W (Fig. 1a) was a suppressor of VIGS, that it sequestered siRNAs and that its symptom induction was substantially attenuated compared to wt-P19 (Chu *et al.*, 2000; Qiu *et al.*, 2002; Omarov *et al.*, 2006). Therefore, the initial objective was to examine the capacity of P19/R43W to suppress RNA silencing of heterologous genes and to compare this with the performance of wt-P19 tested under the same conditions using transient agroinfiltration experiments. These results provided evidence that P19/R43W was an effective suppressor of GFP silencing albeit with a capacity that was somewhat reduced (estimated 50%–70%) compared to wt-P19 (Figs S1 and 4). We also observed differential effects regarding the efficiency of suppression by wt-P19 or P19/R43W depending on the *Agrobacterium* strain (Fig. S1), in agreement with strain variations observed by others (Wroblewski *et al.*, 2005). The ability of P19/R43W to act as a transient suppressor was maintained when it was used in conjunction with the CPMV-*HT* expression system. Collectively, the transient expression-based results showed that P19/R43W is an effective suppressor of RNA silencing that can be used to significantly boost the transient expression of foreign proteins in plants.

Previous reports have shown that transgenic expression of wt-P19 in *Arabidopsis thaliana*, *N. tabacum* and *N. benthamiana* often failed to yield detectable levels of P19, although the

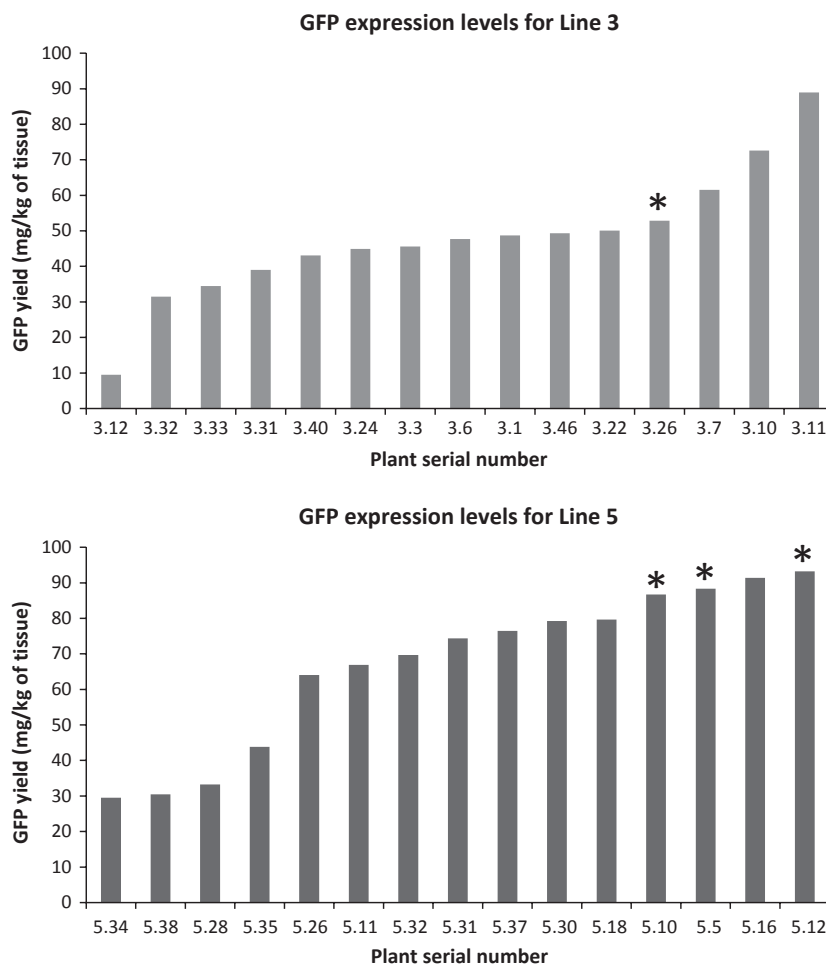


Figure 7 GFP expression levels in 15 highest expressing plants of Line 3 and Line 5 as assessed by fluorimetry of extracts. Overall, GFP expression was higher in Line 5, because of the suppression of silencing by P19/R43W. Homozygotes have been marked with an asterisk (*). The p-value in a one-sided t-test for Line 3 and Line 5 is 0.007832 at 95% confidence level.

plants exhibited deforming phenotypes (Silhavy *et al.*, 2002; Papp *et al.*, 2003; Dunoyer *et al.*, 2004; Scholthof, 2006; Alvarez *et al.*, 2008; Siddiqui *et al.*, 2008). These effects include variegated leaves, aberrant flower phenotype on *A. thaliana*, curled leaves on *N. benthamiana* and compromised fertility in those plants and in tomato. In comparison, transgenic *N. benthamiana* lines constitutively expressing P19/R43W had minor phenotypic differences with some oval, mildly puckered and blistered leaves (Fig. 5), which were not observed in nontransgenic plants. Several observations supported a conclusion that P19/R43W expressed in these normally developing transgenic *N. benthamiana* was functionally active; most relevant for this study was that the transient expression of an agroinfiltrated GFP construct was enhanced in the transgenic plants compared to that in nontransgenic plants (Fig. 6).

Transgenic co-expression of P19/R43W and GFP

Because transgenic expression of P19/R43W yielded fertile plants that accumulated measurable amounts of the functionally active suppressor, we explored an additional highly attractive possibility of co-expressing the suppressor with a target foreign gene in plants. The utility of P19/R43W for biotechnological uses was demonstrated by showing that P19/R43W retained its ability to enhance gene expression when used as a component of the pEAQ expression system. Transgenic *N. benthamiana* lines were obtained that showed elevated levels of GFP expression (Fig. 7). Even though the suppressor

activity of P19/R43W is weaker than that of wt-P19, these results confirmed the distinct advantage of the mutant that it is tolerated within stably transformed plants, even in the homozygous state (Figs 8 and S3). This could not be achieved using constructs expressing wt-P19.

Plants transgenic for P19/R43W produced higher levels of GFP than were found in the absence of the suppressor, and the lack of detrimental phenotypic effects allowed the identification of lines of plants homozygous for both transgenes. The ability to produce homozygous plants is a prerequisite for the creation of true-breeding transgenic lines, and thus this study paves the way for development of lines of transgenic plants expressing high levels of heterologous proteins. The enhancement of the GFP expression level over that seen in the absence of a suppressor (an average of 1.7-fold) was relatively modest. However, because the emphasis was on providing a proof-of-concept, no attempt has yet been made to optimize the level of P19/R43W expression in the transgenic lines. Furthermore, despite the absence of developmentally disturbing effects, it is possible that a substantial portion of the P19/R43W protein pool is sequestering siRNAs or miRNAs unrelated to GFP-mRNA, and therefore the effectively available levels of P19/R43W left over to suppress GFP silencing might be lower than originally expected.

The expression associated with the CPM-HT system was previously in itself already shown to be superior to other systems (Sainsbury and Lomonosoff, 2008; Sainsbury *et al.*, 2009), and this study shows that P19/R43W enhances this utility even

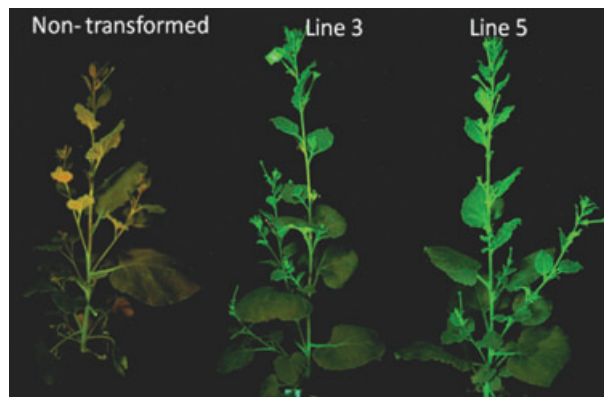


Figure 8 Phenotype of P19/R43W-expressing plants. Individuals of Lines 3 and 5 were brought to flower to illustrate their normal development independent of the presence of P19/R43W. Under UV light, GFP fluorescence is evident and even though this is not a quantitative assay, the enhanced fluorescence is notable for Line 5. Furthermore, based on weekly inspections with UV illumination, GFP is expressed throughout the lifetime of the plants and there is a visible difference in expression level with P19/R43W in plants up to 8 weeks old. After this, the difference becomes less distinct. In all cases, maximum fluorescence is observed in the youngest leaves, as is apparent in the figure.

further. A particular advantage of the pEAQ vector system that we have used for the co-expression of GFP and P19/R43W is that the same construct can be used for both transient and stable transgenic expression. Thus, it is possible to rapidly screen a number of candidate proteins and optimize their expression using the transient approach prior to undertaking the more time-consuming process of plant transformation and regeneration.

Conclusion

While TBSV P19 has already enjoyed considerable success in enhancing gene expression in transient assays, it has not been deployed in stably transgenic plants because of its deleterious effects on development. Our study on the nontoxic but suppression-active P19 mutant (P19/R43W) is the first to report the accumulation of readily detectable levels of constitutively expressed P19-protein in transgenic plants without severe morphological effects, allowing the transgenic plants to flower normally and set fertile seed. In turn, this permitted the generation of lines of developmentally normal, fertile transgenic *N. benthamiana* plants which co-expressed P19/R43W and GFP from the same T-DNA using the CPMV-*HT* high level expression system. This P19/R43W-based technology, especially in combination with the versatile CPMV-*HT* system, may find application in a variety of biotechnologically attractive plant species. The application of P19/R43W might reach even further because it is known that P19 functions as a suppressor in a variety of organisms because of its ability to bind siRNAs in a sequence-independent manner.

Experimental procedures

Constructs- and *Dpnl*- mediated site-directed mutagenesis PCR

Plasmids for transient expression that expressed TBSV P19 were pCB301-p19 (provided by S. Kamoun, Norwich research park,

Norwich, UK), pJL-p19 (provided by J. Lindbo, Ohio State Univ., Wooster, USA) and pCass4N-P19 (provided by S. Gowda and Bill Dawson, Univ. Florida, Lake Alfred, USA). The QuickChange kit (Stratagene, La Jolla, CA, USA) was used for site-directed mutagenesis, and standard molecular biology protocols were followed for the isolation and manipulation of plasmid DNA (Sambrook *et al.*, 1989). The construct pCass4N-P19/R43W was generated by site-directed mutagenesis PCR (P19/R43W-F primer- 5'-actgagtggtggctacataacgatgagacgaattcgaat-3'; P19/R43W-R primer- 5'-tatgtagccAccactcagtcctcaactcggacttcctcag-3').

For construction of pKYLX7-R43W, plasmid pKYLX7-p22 (expressing both P22 and P19) (provided by J. Schoelz, University of Missouri, Columbia, USA) was first mutated to inactivate the start codon of P22 (pKYLX-p22 stop-F primer- 5'-ctc-gagaGggatactgaatacga-3'; pKYLX-p22 stop-R primer- 5'-ttcgt-attcagatcccCtctcag-3') to solely express P19 and subsequently was verified by Western blot analysis. pKYLX7-R43W was obtained using the mutagenesis protocol and primer described for pCass4N-P19/R43W above. All mutations were verified by sequencing.

Creation of pEAQ constructs

pEAQspecialK-GFP-HT was made by sub-cloning the P19 cassette into the *AsiSI/MluI* site of pEAQselectK-GFP-HT (Sainsbury *et al.*, 2009). Site-directed mutagenesis of P19 in pGEM-T EASY (Promega, Madison, WI) was performed using QuickChange method (Stratagene) to create the R43W mutation with the following primers: pGEM-P19-R43W-F, 5'-CGAGTTGGACTGAG TGGTGGCTACATAACGATGAG -3'; pGEM-P19-R43W-R 5'-CTCATCGTTATGTAGCCACCCTCAGTCCAACTCG -3'. The expression cassette containing the mutant P19 gene was sub-cloned into the *AsiSI/MluI* site of pEAQselectK-GFP-HT to make pEAQspecialKm-GFP-HT.

To create pEAQ constructs that express the IgG 2G12 in presence of wt-P19 or P19/R43W, pEAQspecialK-HEL and pEAQspecialKm-HEL were constructed as follows: the expression cassettes containing the endoplasmic reticulum-retained heavy chain (HE) and light chain (L) genes of 2G12 were amplified from pEAQex-2G12HEL (Sainsbury *et al.*, 2009). Using designed primers, *PacI* sites were introduced on both ends of the HE gene cassette and *Ascl* sites were introduced on both ends of the L gene cassette. The GFP cassettes from pEAQspecialK-GFP-HT and pEAQspecialKm-GFP-HT was removed by *PacI/Ascl* digestion and replaced with a multiple cloning site (Sainsbury *et al.*, 2009). The HE and L cassettes were cloned into the *PacI* and *Ascl* sites of pEAQspecialK and pEAQspecialKm to create pEAQspecialK-HEL and pEAQspecialKm-HEL, respectively.

Agroinfiltration of *N. benthamiana*

Binary vectors were transformed into *A. tumefaciens* strains LBA4404, C58 or EHA101 by electroporation (GIBCO-BRL Cell-Porator system). Media for overnight induction contained 200 μ M MES, pH 5.85 [monohydrate 2-(*N*-morpholino) ethanesulfonic acid] and 19.5 μ M acetosyringone. The agrobacterium infiltration buffer included 10 mM MES (pH 5.85), 10 mM MgCl₂ and 2.25 mM acetosyringone. *Agrobacterium* suspensions were infiltrated into expanded leaves at the abaxial surface of approximately 4-week-old *N. benthamiana* plants using a simple syringe. The use of the 35S:GFP T-DNA construct in *Agrobacterium* C58C1 was described previously (Voinnet *et al.*, 1998; Qiu *et al.*, 2002).

Inoculation and analysis of plant tissues

Tomato bushy stunt virus virions purified from infected *N. benthamiana* plants infected with *in vitro*-generated transcripts of full-length TBSV cDNAs expressing wt-P19 and defective P19 (Δ P19) were used for inoculation. Plants were inoculated with virus plus 1% Celite, 50 mM KH_2PO_4 (pH 7.0), following standard procedures (Scholthof *et al.*, 1993). Transcripts from TBSV-GFP and the mutant derivative were prepared as described previously (Qiu and Scholthof, 2007).

Transgenic plants

Plasmid pKYLX7-P19/R43W was sequenced to confirm its identity and sent to the Ralph M. Parsons Foundation Plant Transformation Facility, U. C. Davis, for transformation of *N. benthamiana* using routine transformation and selection protocols (David M. Tricoli, personal communication), similar to those used for the transformation and regeneration of plants expressing another virus (symptom causing) protein (Goldberg *et al.*, 1991). Fourteen lines were regenerated by this facility, which were labelled as 072106-001 to 072106-009, 072106-011 to 072106-015 (072106-010 was missing). For our purposes, these lines were later abbreviated as 43-1, etc. Healthy nontransgenic *N. benthamiana* plants regenerated at same facility from the same callus were used as negative controls. These P19/R43W transgenic *N. benthamiana* plants were grown in the laboratory on light shelves at ambient temperature (approximately 25–28 °C) with a 14-h photoperiod. Seeds from parental transgenic plants were harvested separately from each plant. The F1 seed was germinated in MS (Murashige and Skoog) medium (Life Technologies, Rockville, MD, USA) with 30 $\mu\text{g}/\text{ml}$ kanamycin. For genome integration of the T-DNA region of pEAQ vectors, *N. benthamiana* leaf discs were transformed with *A. tumefaciens* with strain LBA4404 cultures harbouring the desired pEAQ construct using the 'leaf disc method' (Horsch and Klee, 1986).

Protein extractions and detection

Upon co-infiltration or when analysing P19/R43W transgenic lines, leaves were extracted with Tris-EDTA (TE) buffer, and protein samples were separated by standard SDS-PAGE in 15% polyacrylamide gels and transferred to nitrocellulose membranes (Osmonics, Westborough, MA, USA). The membranes were stained with Ponceau S (Sigma, St. Louis, MO, USA) to verify the efficiency of protein transfer. The P19 antiserum was applied at the dilution of 1 : 5000. Alkaline phosphatase-conjugated goat anti-mouse or rabbit antiserum (Sigma) was used as the secondary antibody and applied at a dilution of 1 : 1000. The immune complexes were visualized by hydrolysis of the substrate tetrazolium-5-bromo-4-chloro-3-indolyl phosphate (BCIP) in the presence of nitro-blue tetrazolium chloride. In some experiments, horseradish peroxidase-conjugated to goat anti-mouse antiserum (Bio-Rad, Hercules, CA, USA) was used as the secondary antibody at the dilution of 1 : 5000, and the immune complexes were visualized by using the enhanced chemiluminescence detection kit (Pierce, Rockford, IL, USA). Mouse monoclonal IgG_{2a} GFP antibody [GFP (B-2): sc-9996; Santa Cruz Biotechnology, CA, USA] was used to quantify GFP expression.

In case of plant material used in combination with the pEAQ system, GFP was extracted from infiltrated leaf tissue by

homogenizing 60 mg of leaf tissue in 240 μl of extraction buffer [50 mM Tris-HCl pH 7.25, 150 mM NaCl, 2 mM ethylenediaminetetraacetic acid (EDTA), 0.1% (v/v) Triton X-100]. To extract 2G12, 60 mg of infiltrated leaf tissue was homogenized in 240 μl of phosphate-buffered saline (PBS) with 5 mM EDTA, 3 mM β -mercaptoethanol and 0.05% (v/v) Triton X-100. Lysates were clarified by centrifugation, and protein concentrations determined by the Bradford assay. A 1 : 100 dilution of the GFP-containing extract was used for the GFP fluorescence assay. Approximately 12.5 μg of the 2G12-containing protein extract was separated by Tris-Glycine SDS-PAGE using 12% NuPAGE gels (Invitrogen, Paisley, UK) under reducing and nonreducing conditions and stained with InstantBlue Coomassie stain (Expedeon, Cambridge, UK).

GFP imaging and fluorescence assay

Green fluorescent protein (GFP) signals on the inoculated *N. benthamiana* leaves were monitored with a 100 W handheld long-wave ultraviolet (UV) lamp (Black Ray model B100AP; UV products, Upland, CA, USA). An Olympus DP70 camera was used for the image acquisition of DIC and wide field fluorescent images.

GFP fluorescence measurements were made using a slightly modified version of a previously described protocol (Richards *et al.*, 2003). Soluble protein extracts were diluted in 0.1 M Na_2CO_3 and loaded in triplicate onto a fluorescently neutral black 96-well plate. Recombinant GFP from Clontech, which is the same variant of GFP as the one used in this study, was used to generate standard curves in a control plant extract at the same dilution as the test samples. Excitation (395 nm) and emission (509 nm) maxima were matched to Clontech's GFP and read using a SPECTRAmax spectrofluorometer (Molecular Devices; <http://www.moleculardevices.com>). Measurements were carried out in triplicate on the pooled samples of 6 independently infiltrated leaves to account for experimental variation and averaged to give a final value for each sample.

Acknowledgements

We are grateful to Karen-Beth G. Scholthof for helpful discussions and editing the manuscript. We thank Dong Qi and Rustem Omarov for helpful comments; and Bill Dawson, Siddarama Gowda, Sophien Kamoun, John Lindbo and Jim Schoelz for sharing P19-expression constructs; D. Baulcombe for the 35S:GFP construct, and Emma Sherwood for assistance with construction of pEAQspecialKm. Components of this project that were performed at TAMU were mainly supported by Plant Bioscience Ltd. Norwich UK, with additional support by Texas Agrilife Research (TEX08387), NIH (1R03-AI067384-01) and USDA/CSREES-NRI-CGP (2006-35319-17211). F.S. acknowledges funding from a Marie Curie Early Stage Training Fellowship MEST-CT-2004-504273 and the Trustees of the John Innes Foundation. P.S. was supported by a Biotechnology and Biological Science Research Council (BBSRC) doctoral training grant to the John Innes Centre (JIC). Work at the JIC was supported, in part, by the EU FP7 "PLAPROVA" project (Grant Agreement No. KBBE-227056). JIC is grant-aided by the BBSRC. GPL dedicates this paper to the memory of his mother, Mrs. Peggy Browning, who died on 9th June 2010, aged 91, while the manuscript was being prepared.

References

- Alvarez, M.L., Pinyerd HL, E.T. and Cardineau, G.A. (2008) P19-dependent and P19-independent reversion of F1-V gene silencing in tomato. *Plant Mol. Biol.*, **68**, 61–79.
- Buchacher, A., Predl, R., Strutzenberger, K., Steinfellner, W., Trkola, A., Purtscher, M., Gruber, G., Tauer, C., Steindl, F., Jungbauer, A. and Katringer, H. (1994) Generation of human monoclonal antibodies against HIV-1 proteins; electrofusion and Epstein-Barr virus transformation for peripheral blood lymphocyte immortalization. *AIDS Res. Hum. Retroviruses*, **10**, 359–369.
- Cañizares, M.C., Nicholson, L. and Lomonosoff, G.P. (2005) Use of viral vectors for vaccine production in plants. *Immunol. Cell Biol.*, **83**, 263–270.
- Chapman, E., Prokhnevsky, A.I., Gopinath, K., Dolja, V.V. and Carrington, J.C. (2004) Viral RNA silencing suppressors inhibit the microRNA pathway at an intermediate step. *Genes Dev.*, **18**, 1179–1186.
- Chu, M., Desvoyes, B., Turina, M., Noad, R. and Scholthof, H.B. (2000) Genetic dissection of Tomato bushy stunt virus p19-protein-mediated host-dependent symptom induction and systemic invasion. *Virology*, **266**, 79–87.
- Dunoyer, P., Lecellier, C.H., Parizotto, E.A., Himber, C. and Voinnet, O. (2004) Probing the microRNA and small interfering RNA pathways with virus-encoded suppressors of RNA silencing. *Plant Cell*, **16**, 1235–1250.
- Goldberg, K.B., Kiernan, J. and Shepherd, R.J. (1991) A disease syndrome associated with expression of gene-VI of Caulimoviruses may be a nonhost reaction. *Mol. Plant-Microbe Interact.*, **4**, 182–189.
- Horsch, R.B. and Klee, H.J. (1986) Rapid assay of foreign gene expression in leaf discs transformed by *Agrobacterium tumefaciens*: role of T-DNA borders in the transfer process. *Proc. Natl. Acad. Sci. USA*, **83**, 4428–4432.
- Johansen, L.K. and Carrington, J.C. (2001) Silencing on the spot. Induction and suppression of RNA silencing in the *Agrobacterium*-mediated transient expression system. *Plant Physiol.*, **126**, 930–938.
- Lakatos, L., Szittyá, G., Silhavy, D. and Burgyan, J. (2004) Molecular mechanism of RNA silencing suppression mediated by the p19 protein of tombusviruses. *EMBO J.*, **23**, 876–884.
- Mallory, A.C., Parks, G., Endres, M.W., Baulcombe, D., Bowman, L.H., Pruss, G.J. and Vance, V.B. (2002) The amplicon-plus system for high-level expression of transgenes in plants. *Nat. Biotechnol.*, **20**, 622–625.
- Omarov, R., Sparks, K., Smith, L., Zindovic, J. and Scholthof, H.B. (2006) Biological relevance of a stable biochemical interaction between the tombusvirus-encoded P19 and short interfering RNAs. *J. Virol.*, **80**, 3000–3008.
- Omarov, R.T., Ciomperlik, J.J. and Scholthof, H.B. (2007) RNAi-associated ssRNA-specific ribonucleases in Tombusvirus P19 mutant-infected plants and evidence for a discrete siRNA-containing effector complex. *Proc. Natl. Acad. Sci. USA*, **104**, 1714–1719.
- Pantaleo, V., Szittyá, G. and Burgyan, J. (2007) Molecular basis of viral RNA targeting by viral small interfering RNA-programmed RISC. *J. Virol.*, **81**, 3797–3806.
- Papp, I., Mette, M.F., Aufsatz, W., Daxinger, L., Schauer, S.E., Ray, A., van der Winden, J., Matzke, M. and Matzke, A.J.M. (2003) Evidence for nuclear processing of plant microRNA and short-interfering RNA precursors. *Plant Physiol.*, **132**, 1382–1390.
- Park, J.-W., Faure-Rabasse, S., Robinson, M.A., Desvoyes, B. and Scholthof, H.B. (2004) The multifunctional plant viral suppressor of gene silencing P19 interacts with itself and an RNA binding host protein. *Virology*, **323**, 49–58.
- Qiu, W. and Scholthof, H.B. (2007) Tomato bushy stunt virus derived gene vectors. *Curr Prot Microbiol* **7**:16l.14.11–16l.14.16.
- Qiu, W.P., Park, J.-W. and Scholthof, H.B. (2002) *Tombusvirus* P19-mediated suppression of virus induced gene silencing is controlled by genetic and dosage features that influence pathogenicity. *Mol. Plant-Microbe Interact.*, **15**, 269–280.
- Richards, H.A., Halfhill, M.D., Millwood, R.J. and Stewart Jr, C.N. (2003) Quantitative GFP fluorescence as an indicator of recombinant protein synthesis in transgenic plants. *Plant Cell Rep.*, **22**, 117–121.
- Sainsbury, F. and Lomonosoff, G.P. (2008) Extremely high-level and rapid transient protein production in plants without the use of viral replication. *Plant Physiol.*, **148**, 1212–1218.
- Sainsbury, F., Thuenemann, E.C. and Lomonosoff, G.P. (2009) pEAQ: versatile expression vectors for easy and quick transient expression of heterologous proteins in plants. *Plant Biotechnol. J.*, **7**, 682–693.
- Sambrook, J., Fritsch, E.F. and Maniatis, T. (1989) *Molecular cloning: A laboratory manual*. Cold Spring Harbor, N.Y.:Cold Spring Harbor Laboratory.
- Scholthof, H.B. (2006) The Tombusvirus-encoded P19: from irrelevance to elegance. *Nat. Rev. Microbiol.*, **4**, 405–411.
- Scholthof, H.B. (2007) Heterologous expression of viral RNA interference suppressors: RISC management. *Plant Physiol.*, **145**, 1110–1117.
- Scholthof, H.B., Morris, T.J. and Jackson, A.O. (1993) The capsid protein gene of Tomato bushy stunt virus is dispensable for systemic movement and can be replaced for localized expression of foreign genes. *Mol. Plant-Microbe Interact.*, **6**, 309–322.
- Scholthof, H.B., Scholthof, K.-B.G. and Jackson, A.O. (1995) Identification of tomato bushy stunt virus host-specific symptom determinants by expression of individual genes from a potato virus X vector. *Plant Cell*, **7**, 1157–1172.
- Scholthof, K.-B.G., Mirkov, T.E. and Scholthof, H.B. (2002) Plant viral gene vectors: biotechnology applications in agriculture and medicine. *Genet. Eng. Principles Methods*, **24**, 67–86.
- Siddiqui, S.A., Sarmiento, C., Truve, E., Lehto, H. and Lehto, K. (2008) Phenotypes and functional effects caused by various viral RNA silencing suppressors in transgenic *Nicotiana benthamiana* and *N. tabacum*. *Mol. Plant-Microbe Interact.*, **21**, 178–187.
- Silhavy, D., Molnar, A., Luciola, A., Szittyá, G., Hornyik, C., Tavazza, M. and Burgyan, J. (2002) A viral protein suppresses RNA silencing and binds silencing-generated, 21- to 25-nucleotide double-stranded RNAs. *EMBO J.*, **21**, 3070–3080.
- Vargason, J.M., Szittyá, G., Burgyan, J. and Tanaka- Hall, T.M. (2003) Size selective recognition of siRNA by an RNA silencing suppressor. *Cell*, **115**, 799–811.
- Voinnet, O. (2005) Induction and suppression of RNA silencing: insights from viral infections. *Nat. Rev. Genetics*, **6**, 206–220.
- Voinnet, O., Vain, P., Angell, S. and Baulcombe, D.C. (1998) Systemic spread of sequence-specific transgene RNA degradation in plants is initiated by localized introduction of ectopic promoterless DNA. *Cell*, **95**, 177–187.
- Voinnet, O., Rivas, S., Mestre, P. and Baulcombe, D. (2003) An enhanced transient expression system in plants based on suppression of gene silencing by the p19 protein of tomato bushy stunt virus. *Plant J.*, **33**, 949–956.
- Wroblewski, T., Tomczak, A. and Michelmore, R. (2005) Optimization of *Agrobacterium*-mediated transient assays of gene expression in lettuce, tomato and *Arabidopsis*. *Plant Biotechnol. J.*, **3**, 259–273.
- Ye, K., Malinina, L. and Patel, D. (2003) Recognition of small interfering RNA by a viral suppressor of RNA silencing. *Nature*, **426**, 874–878.

Supporting information

Additional Supporting information may be found in the online version of this article:

Figure S1 Comparison of transient GFP expression upon co-infiltration of pGFP with different P19-expressing constructs.

Figure S2 Examples of complementation by P19/R43W observed in transgenic plants.

Figure S3 Example of germination of transgenic seed on agar plates and visualization of seedlings under UV light.

Please note: Wiley-Blackwell are not responsible for the content or functionality of any supporting materials supplied by the authors. Any queries (other than missing material) should be directed to the corresponding author for the article.

Recent advances of cowpea mosaic virus-based particle technology

Nicholas P. Montague, Eva C. Thuenemann, Pooja Saxena, Keith Saunders, Paolo Lenzi and George P. Lomonosoff*

Department of Biological Chemistry; John Innes Centre; Norwich UK

Key words: Cowpea mosaic virus, chimaera, virus-like particles, Real-time PCR controls, pI adjustment

Abbreviations: CPMV, cowpea mosaic virus; eVLP, empty virus-like particle; GFP, green fluorescent protein

Particles of cowpea mosaic virus (CPMV) have enjoyed considerable success as a means of presenting peptides for vaccine purposes. However, the existing technology has limitations in regard to the size and nature of the peptides which can be presented and has problems regarding bio-containment. Recent developments suggest ways by which these problems can be overcome, increasing the range of potential applications of CPMV-based particle technology.

Introduction

Viruses and virus-like particles (VLPs) are attracting much attention in the field of biomedicine as they have a number of potential applications. These include the display of antigens to create novel vaccines, their use as imaging agents and their potential as drug delivery vehicles. Systems based on bacteriophage, yeast Ty particles and animal viruses have been investigated for one or more of these applications. Cowpea mosaic virus (CPMV) was the first plant virus to be developed as a system for the display of foreign peptides¹⁻³ and the particles have been used extensively for chemical modification.⁴ CPMV is a bipartite RNA virus, whose particles of approximately 28 nm diameter consist of 60 copies each of a Large (L) and a Small (S) coat protein arranged with icosahedral symmetry (Fig. 1). The L protein contains two β -barrel domains (marked the B and C domains in Fig. 1B) while the S protein consists of a single β -barrel (marked A domain in Fig. 1B). Both coat proteins are produced by proteolytic cleavage of a precursor (VP60) by the virus-encoded 24K proteinase.^{5,6} The virus coat proteins encapsidate a single copy of either RNA-1 (6 kb) or RNA-2 (3.5 kb) and both RNAs are required for infection. Infectious clones of both RNA molecules have been available for over 20 years and the most efficient method of initiating an infection is by the “agro-infiltration” of cloned viral DNAs.⁷ This approach makes use of the ability of the soil-living bacterium, *Agrobacterium tumefaciens*, to efficiently deliver part of its DNA (the T-DNA) to the nucleus of plant cells where

it is integrated into the plant's genomic DNA. This allows the transferred DNA to be transcribed by the plant cell as if were part of the normal complement of plant genes. To make use of this ability of *A. tumefaciens* to transfer DNA, full-length double-stranded DNA copies of the CPMV RNAs were positioned between a plant-specific promoter (the cauliflower mosaic virus 35S promoter) and a transcription terminator and the cassettes were introduced into the T-DNA region of an *A. tumefaciens* plasmid. Infection is initiated by simply infiltrating bacterial suspensions into leaf tissue, where the liquid displaces the air in the intercellular spaces. After T-DNA transfer and transcription, the transcribed RNA is able to initiate a virus infection. In fact, the transfer and transcription of inserted genes is so efficient using this technique, that constructs which can no longer replicate can also be expressed to high level. All the research described in this paper utilizes this approach.

CPMV particles are attractive candidates for both genetic and chemical modification for a number of reasons: they can be purified in large quantities from infected tissue, they are very robust, surviving at 60°C for at least one hour, across the range of pH 4–9, and in some organic solvent-water mixtures. Furthermore, the three-dimensional (3D) structure of the particles is known to atomic resolution⁸ and they can be readily purified by a simple procedure involving precipitation with polyethylene glycol (PEG) and differential centrifugation—a process that can be carried out within a single day. The availability of infectious cDNA clones of both RNAs has enabled precise genetic changes to be introduced into the capsid proteins. Knowledge of the detailed 3D structure of the virus particles has also enabled a rational choice to be made regarding potential sites for the insertion of heterologous peptides into the viral coat proteins such that they would be surface-exposed and would not adversely affect particle assembly.^{9,10} A number of sites were identified as suitable for the insertion of foreign peptides. In most cases, the foreign peptide has been inserted into the most exposed loop of the virus surface, the β B- β C loop of the S protein (indicated by the arrow Fig. 1A and B). However, other sites, such as the β E- α B loop of the L protein and the β C'- β C" loop of the S protein, have also been used successfully.¹¹⁻¹⁴ Generally, provided the inserted peptide was less than 40 amino acids and had a pI below 9.0,¹⁴ the yields of modified particles were similar to those obtained with wild-type CPMV (up to 1 mg of particles per gram of infected leaf tissue). In each case, the chimaeric virus particles present 60

*Correspondence to: George P. Lomonosoff;
Email: george.lomonosoff@bbsrc.ac.uk
Submitted: 12/21/10; Revised: 01/24/11; Accepted: 01/28/11
DOI: 10.4161/hv.7.3.14989

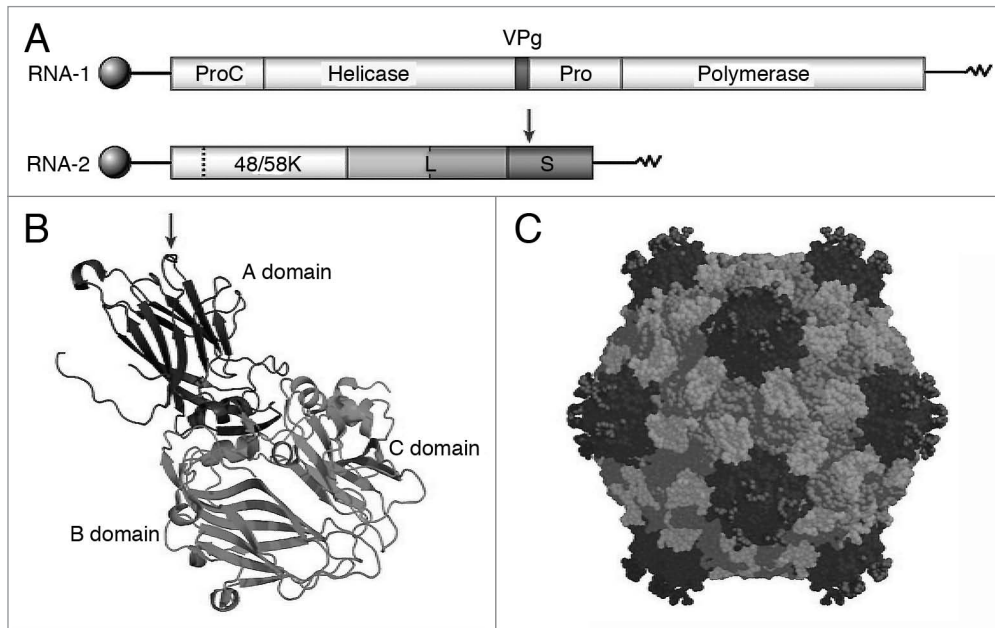


Figure 1. Cowpea mosaic virus (CPMV) as a peptide-presentation system. The βB - βC loop of the small (S) coat protein (indicated by the arrows in A and B) is the most commonly used site for the insertion of foreign peptides. (A) Genome organization of CPMV RNAs. (B) Ribbon diagram of the icosahedral asymmetric unit, consisting of the two domains of the large (L) coat protein (light grey) and the S coat protein (dark grey). (C) Space-filling drawing of the CPMV capsid displaying an epitope from HRV-14 inserted into the βB - βC loop of the S protein. ProC, proteinase cofactor; VPg, genome-linked protein; Pro, 24K proteinase; 48/58K, movement protein; L, large coat protein; S, small coat protein. (C) was kindly provided by Dr. T. Lin and Prof. J.E. Johnson, The Scripps Research Institute, La Jolla, CA. Modified from reference 24.

copies of the inserted peptide on the virus surface. Work on the production of chimaeras for vaccine purposes culminated in the demonstration of protective immunity in target animals,^{15,16} the dissection of a major antigenic site of HIV^{17,18} and the ability to correlate the structure that a peptide adopts with its immunological properties.^{12,19} For further information on the immunological properties of CPMV chimaeras, see references 20–24.

Despite the considerable success in the development of CPMV-based chimaeras, it is noticeable that none have been developed for commercial use. There are probably two main reasons for this: the limitations on the range of peptides that can be stably expressed¹⁴ and the fact that preparations of chimaeras isolated from infected plants contain the viral RNAs and hence are infectious. The first issue limits the application of the CPMV technology and it is significant that chimaeras containing antigenic sequences from a number of important pathogens, such as foot-and-mouth disease virus (FMDV), proved impossible to propagate or purify.^{2,14} The second causes problems with biocontainment and causes regulatory issues. This article describes recent advances in CPMV-based particle technology based on research carried at the John Innes Centre, Norwich, UK which have shown how these problems can be relieved.

Systems Based on Infectious Virus Particles

Propagating recalcitrant chimaeras. Though CPMV particles have been used to present a wide variety of peptides, there have been several instances where the propagation and purification of specific chimaeras has proved problematic. These have

manifested themselves in terms of reduced infectivity on plants, reduced or no yield on purification and loss of all or part of the inserted sequence on virus passage. One problem concerns the size of the insert which is tolerated; generally the maximum size of insert that can be stably incorporated is approximately 30 amino acids. Once this size is exceeded, deletions readily occur within the insert and it is difficult, if not impossible to isolate particles expressing the full-sized epitope.¹⁴ The reason for this instability has not been investigated in detail but is unlikely to be directly due to the increase in size of RNA-2 affecting its replication since constructs containing heterologous sequences up to 1 kb have been shown to be relatively stable.²⁴ It is more likely that the expression of large peptides on the surface of particles interferes either with the ability of the particles to assemble or with their ability to interact productively with the plasmodesmata to allow virus spread. Thus any deletions which alleviate these problems are likely to be selected and come to dominate an infection.

The size of a peptide is not the only factor limiting the ability to propagate CPMV chimaeras. One of the first chimaeras to be created presented a 19 amino acid epitope consisting of residues 141–159 from VP1 of FMDV serotype O1 inserted into the βB - βC loop of the CPMV S protein to give chimaera FMDV-V.² However, this chimaera was unable to produce a systemic infection, was difficult to passage and purification of the virus from the infected leaves yielded little or no viral particles. Further investigation showed that the particles with the FMDV-V sequence remained in the pellet formed from the initial low speed spin of the purification protocol.² It was subsequently noticed that many of the chimaeras which proved problematic contained inserts

Table 1. Properties of CPMV chimaeras with pI-adjusted inserts in the β B- β C loop of the S protein

Name of Chimaera	Sequence of insert ^a	Size of insert	pI of insert	Symptoms		Virus yield
				Inoc ^c	upper ^c	
CPMV FMDV-V	VPN LRG DLQ VLA QKV ART L	19	11.47	None	none	N/A
CPMV FMDV-V D-D	DVP NLR GDL QVL AQK VAR TLD	21	6.50	WT	MSS ^b	Reduced
CPMV FMDV-V-DD	VPN LRG DLQ VLA QKV ART LDD	21	6.50	WT	MSS ^b	Reduced
CPMV FMDV B	RYS RNA VPNV RYS RNA VPN V	20	12.10	None	none	N/A
CPMV FMDV B EDED	EDE DRY SRN AVP NVR YSR NAV PNV	24	6.93	Mild ^b	MSS ^b	Very low
CPMV FMDV B ED-ED	EDR YSR NAV PNV RYS RNA VPN VED	24	6.93	Mild ^b	MSS ^b	Very low
CPMV BPV	TRN SSK PAK RKK IKA	15	12.57	None	none	N/A
CPMV BPV DEDE-DDE	DED ETR NSS KPA KRK KIK ADD E	22	7.06	None	none	N/A

^aIntroduced acidic residues (D or E) are shown in bold typeface. ^bDelayed appearance of symptoms compared to wild-type CPMV. ^cSymptoms on inoculated and upper leaves after serial passaging; WT, wild-type symptoms; MSS, mild systemic symptoms.

with a high pI.¹⁴ Multiple virus passage with such chimaeras in some cases eventually led to the production of particles which could be purified in reasonable amounts. However, these invariably contained mutations which reduced the pI of the insert.¹⁴ This suggested that it may be possible to propagate recalcitrant chimaeras by deliberately incorporating acidic amino acids to reduce the overall pI of the particles.

To examine whether adjustment of the pI of an insert by the incorporation of flanking acidic residues could render problematic CPMV chimaeras more amenable to effective virus passage and particle purification, three chimaeras which had previously proved difficult or impossible to propagate were modified. These were FMDV-V (insert pI 11.47) which was discussed above, a chimaera (FMDV-B) expressing a tandem repeat sequence from VP1 of FMDV²⁵ which has an even higher pI (12.10) and a chimaera (BPV-L1) expressing an epitope from the L1 protein of Bovine papilloma virus (BPV) with an extremely high pI of 12.57.¹⁴ These were chosen as the size of the insert should not be a factor in their propagation. Though FMDV-V had previously been shown to give a phenotype of reduced severity on cowpea plants (see above), the other two, FMDV-B and BPV-L1, appeared to be completely non-infectious.¹⁴ The pI of these inserts was adjusted to be close to 7 by addition of an appropriate number of acidic residues (D or E) at either or both sides of the insert. Details of the constructs are given in **Table 1**. In each case, the construct was introduced into cowpea plants by agro-infiltration in the presence of RNA-1 and compared to the performance of the original, non-pI-adjusted construct introduced in the same way. In all cases, no symptoms were observed on the infiltrated primary leaves. This is usual when constructs are introduced by agro-infiltration, as the leaf is flooded with inoculum so no specific infection foci are produced. To determine if infection was occurring, sap from the infiltrated leaves was serially passaged to healthy cowpea plants.

In the case of FMDV-V, no infection could be passaged to further plants, consistent with previous observations.^{2,14} For FMDV-V-DD (with two aspartic acid residues at the C-terminus of the FMDV-specific insert) and FMDV-V D-D (with one aspartic acid at either end of the insert), the first two passages (P1 and P2) resulted in symptoms that appeared more slowly when compared

to a wild type infection and gave a very low virus yield (in the order of 0.1 μ g/g of primary leaf tissue). However, after four passages the yield of virus had increased to ~0.2 mg/g of primary leaf tissue and the virus was able to move systemically. Sequence analysis of the RNA isolated from purified virus particles indicated that no reversions or mutations had taken place following serial virus passaging. The functionality of the inserted FMDV-specific sequence was confirmed by showing that they were able to bind to anti-FMDV specific antibodies and the integrin, α v β 6 (Montague N, Burman A, Clark S, Lomonosoff GP and Jackson T, unpublished). These results indicate that the charge neutralisation strategy had been successful in the case of FMDV-V.

For the inserts with higher pIs, the strategy of adding acidic residues to the ends of the inserted sequence proved less successful. In the case of FMDV-B DE-DD (with two acidic residues at both ends of the insert) and FMDV-B EDED (with four acidic residues at the C-terminus), only mild symptoms were observed on serial virus passaging and a systemic infection rarely developed; attempts to purify virus particles gave only very low yields. In the case of BPV-L1 DEDE-DDE (with a total of seven acidic residues positioned either side of the insert), attempts at virus passaging failed to produce any visible infection and no virus-specific RNA could be detected by RT-PCR. Thus it appears that BPV-L1 is truly non-infectious even after the charge of the insert has been neutralized.

Adjustment of the pI by addition of charged residues at the end of an inserted peptide, as well as only being partially successful, has additional disadvantages. The incorporation of acidic residues could cause problems with the structure that the insert adopts, and hence affect its immunological properties. It also inevitably increases the size of the insert, which could adversely affect virus yield. An alternative approach is to compensate for high positive charge within an epitope by the addition of acidic residues into an adjacent loop on the virus surface. This should help the foreign inserted peptide to produce as natural a conformation as possible and obviate the need to increase the length of the peptide within a given loop. To this end, acidic residues have been expressed on the adjacent β C'- β C'' loop, a surface exposed loop near to the β B- β C loop on CPMV, which has previously been successfully used to express foreign sequences.¹²

Table 2. Effect of presence of acidic residues in $\beta C'-\beta C''$ loop of the S protein on yield of virus particles with high pI inserts in $\beta B-\beta C$ loop

Name of chimaera	$\beta B-\beta C$ charge at pH 7 ^a	$\beta C'-\beta C''$ charge at pH 7 ^b	Yield
BPV-L1C''+2	+7	-2	No yield
BPV-L1C''+5	+7	-5	No yield
FMDV-B-C''+2	+4	-2	Reduced ^c
FMDV-B-C''+7	+4	-7	Reduced
C''+2	/	-2	Reduced
C''+5	/	-5	Very low
C''+7	/	-7	No yield

^aCalculated on number of basic residues within insert. ^bCalculated on number of acidic residues within insert. ^cCompared with wild-type virus.

Either two, five or seven acidic residues were inserted into the $\beta C'-\beta C''$ loop to give a broad range of compensatory charges so that epitopes with a range of high pIs could be simultaneously expressed on the CPMV surface using the $\beta B-\beta C$ loop. Initially, the viability of chimaeras with just the acidic residues within the $\beta C'-\beta C''$ was determined. Only those chimaeras with two and five, but not seven, acidic residue inserts in the $\beta C'-\beta C''$ loop were viable (Table 2). The apparent non-infectivity of the chimaera with seven acidic amino acids was ascribed to the excessive negative charge introduced into S protein when no compensating high pI insert was present in the $\beta B-\beta C$ loop. The simultaneous expression of the FMDV-B epitope in the $\beta B-\beta C$ loop and either two or seven acidic residues in the $\beta C'-\beta C''$ gave rise to a detectable infection and it proved possible to purify virus particles, albeit at reduced yield compared with wild-type CPMV. This represents the first time it has proved possible to purify a chimaera expressing the FMDV-B sequence and confirmed that the infectivity of chimaera with seven acidic amino acids could be restored by the simultaneous presence of a high pI insert. However, none of the BPV-L1 chimaeras with the acidic residues in the $\beta C'-\beta C''$ loop proved viable. Nonetheless, as a result of these studies, a new series of CPMV-based vectors is now available with two, five and seven acidic residues in the $\beta C'-\beta C''$ loop and these can be used to display epitopes with a range of high pIs.

Bio-contained encapsidated mimics. As a result of studies aimed at developing CPMV as a vector for the expression of polypeptides in plant cells,²⁴ it was demonstrated that RNA-2 molecules harboring additional lengths of heterologous sequence can be efficiently packaged in virions. Such encapsidated RNA is highly resistant to degradation. These observations have been exploited to design modified versions of RNA-2 harboring pathogen-specific sequences that can act as positive controls (encapsidated mimics) in highly sensitive real-time PCR-based diagnostic reactions.²⁶ However, one problem with the technology is that it involves the use of infectious virus particles with concomitant problems of bio-containment. These can be reduced by isolating only those particles which contain RNA-2 which is not infectious in the absence of RNA-1.²⁶ However, this approach, which involves multiple rounds of density gradient centrifugation, is time consuming and often only partially successful.

In an alternative approach, 456 nucleotides encoding the central region of the 48K movement protein (Fig. 1) were deleted from an infectious clone of RNA-2. Deletions within this region of the genome still permit RNA-2 to be replicated by RNA-1 and particles to be formed within infected cells but prevent virus movement to neighboring cells.²⁷ Such spread is not required to obtain adequate quantities of virus particles when agro-infiltration is used to initiate an infection as the process is so efficient, with more than 90% of cells in an infiltrated region of a leaf being infected. However, the purified particles are unable to cause anything other than a symptomless subliminal infection when mechanically inoculated on to plants. Thus this approach provides a high degree of bio-containment. Insertion of heterologous sequences into the deleted RNA-2 construct is facilitated by the positioning of a pair of unique restriction enzyme sites downstream of the region encoding the S protein and it is now possible to rapidly produce a wide range of mimics to order. Encapsidated mimics produced in this way are currently marketed by the Veterinary Laboratories Agency (UK).

Production of CPMV Virus-Like Particles without the Need for Virus Infection

All the studies described above have been conducted using particles, either wild-type or genetically modified, produced by the infection of plants. Approximately 90% of the particles produced in this way contain either RNA-1 or RNA-2 and the preparations retain their ability to infect plants, if only subliminally. In addition, while CPMV RNAs have not been shown to be able to replicate in mammalian cells, uptake of particles does occur both in vitro and in vivo,⁴ raising biosafety concerns. The presence of RNA within CPMV particles has also prevented them being used to encapsidate other, foreign material, limiting their potential use as nanoscale vessels.

Initial attempts to address these issues involved inactivation or elimination of the viral RNAs within CPMV preparations either by irradiation with ultraviolet (UV) light^{16,28} or chemically.^{29,30} However, these post-production processes have to be carefully monitored as they risk altering the structural properties of the particles and require that the original virus retains its ability to infect and spread in plants. Furthermore, UV irradiation, though eliminating infectivity, does not remove the RNA from the particles.

Recent developments in plant-based expressed technologies²⁴ have provided an alternative route for producing RNA-free particles of CPMV. In particular, it has been observed that co-expression in plants of separate Agrobacterium plasmids containing the sequences of the precursor to the L and S coat proteins (VP60) and the viral proteinase (24K) (Fig. 2A), introduced by the agroinfiltration technique, resulted in the production of empty (RNA-free) CPMV capsids (eVLPs).⁶ Particles produced in this way are devoid of RNA yet stable and amenable to modification. Thus many future studies involving the modification of the outer surface may well be conducted using particles produced in this manner rather than by infection.

Increasing the efficiency of eVLP production. The production of eVLPs requires the co-expression of VP60 and 24K in

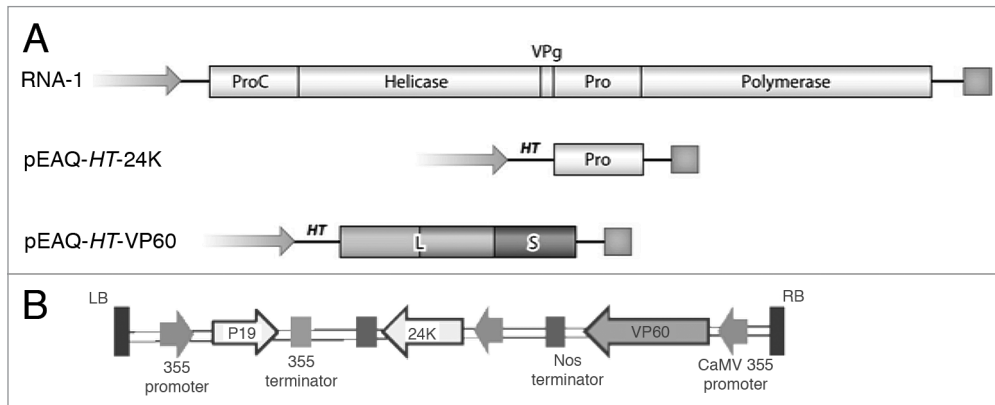


Figure 2. Production of CPMV empty virus-like particles (eVLPs). (A) Schematic representation of the two constructs, pEAQ-HT-VP60 and pEAQ-HT-24K, originally used to create empty virus-like particles (eVLPs). (B) Structure of the T-DNA region of pEAQexpress-VP60-24K which contains the coding regions of both VP60 and the 24K proteinase.

same plant cell. Originally,⁶ this was achieved by co-infiltration of leaves with a mixture of two *Agrobacterium* strains, each harboring a plasmid, pEAQ-HT-VP60 or pEAQ-HT-24K encoding one of the two genes (Fig. 2A). To ensure efficient co-expression, each strain had to be present at a high concentration, making the inoculum dense and difficult to infiltrate. Even then, it could not be guaranteed that every cell would receive both genes, and consequently the yields of eVLPs were considerably lower than those found for RNA-containing particles produced as a result of the natural infection process.

A potential solution to the inefficient delivery of separate T-DNA constructs is to co-deliver the two genes of interest from the same T-DNA. Cloning two genes into the same T-DNA has been made possible by the development of the pEAQ vector series, a versatile and user-friendly CPMV-based expression vector system.³¹ The vector pEAQexpress contains a suppressor of gene silencing (P19) cassette and cloning sites for two further expression cassettes within the same T-DNA region. To demonstrate the benefits of co-expression of two proteins from one T-DNA on pEAQexpress as compared to expression from two separate T-DNAs, expression cassettes for two reporter genes, *eyfp* and *ecfp*, were cloned either into two separate pEAQ vectors, to give pEAQ-HT-EYFP and pEAQ-HT-ECFP or into a single pEAQexpress vector, to give pEAQexpress-ECFP-EYFP (Fig. 3A). These three constructs were agro-infiltrated separately at an optical density (OD₆₀₀) of 0.2, and a mixture of constructs pEAQ-HT-EYFP and pEAQ-HT-ECFP was co-infiltrated at an overall OD₆₀₀ of 0.4. Confocal microscopy was used to detect expression of both fluorescent proteins in the infiltrated leaf tissue with EYFP appearing green and ECFP appearing red, while co-expression results in a yellow color (Fig. 3B).

When infiltrated individually, pEAQ-HT-EYFP and pEAQ-HT-ECFP constructs express only EYFP or ECFP, respectively and an OD₆₀₀ of 0.2 was sufficient to achieve expression in every cell. Co-infiltration of these two constructs resulted in fluorescent protein expression in all cells, as expected, but the co-expression was not uniform, with most cells showing more accumulation of one protein in relation to the other, thus appearing either

green or red rather than yellow (Fig. 3B). On serial two-fold dilution, this situation became more noticeable, eventually leading to cells expressing only one or the other protein (data not shown). In contrast, tissue infiltrated with pEAQexpress-ECFP-EYFP showed efficient co-expression of both proteins in every cell which had received the construct, as witnessed by their yellow fluorescence, though the total number of fluorescent cells decreased with increasing inoculum dilution (data not shown). These results confirm the benefit of expressing two proteins from the same T-DNA.

To exploit the above findings for eVLP production, sequences encoding VP60 and 24K were cloned into the T-DNA region of pEAQexpress to generate pEAQexpress-VP60-24K (Fig. 2B). Infiltration of pEAQexpress-VP60-24K into *N. benthamiana* and purification of particles using a protocol adapted from that used for the purification of wild-type CPMV particles³² resulted in yields of eVLPs up to 0.5 mg/g leaf tissue which is considerably in excess of those achieved when VP60 and 24K were expressed from separate plasmids (Fig. 4). The use of pEAQexpress-VP60-24K, in conjunction with vacuum- rather than syringe-infiltration, has enabled the production of significant quantities of eVLPs for further studies.

Genetic modification of eVLPs. To investigate the potential ability of eVLPs to tolerate radical modifications, the carboxyl terminus of VP60 was modified by replacing the terminal 24 amino acids of the S protein with 6 histidine residues in the vector pEAQ-HT-VP60 (Fig. 2A). Previous attempts to introduce modifications at this position using the infection route resulted in the recovery of only very low levels of particles.³³ Plants were co-infiltrated with the modified VP60 construct, pEAQ-HT-VP60-His and pEAQ-HT-24K and a leaf extract subsequently applied to a nickel-affinity chromatography column. Proteins possessing a histidine sequence were eluted from the column with imidazole and analyzed by polyacrylamide gel electrophoresis and sucrose gradient centrifugation. Protein products corresponding to both CPMV capsid proteins, L and S, were present in the affinity-purified extracts indicating that the viral proteinase was able to cleave the modified VP60. Furthermore, sedimentation of the extract in

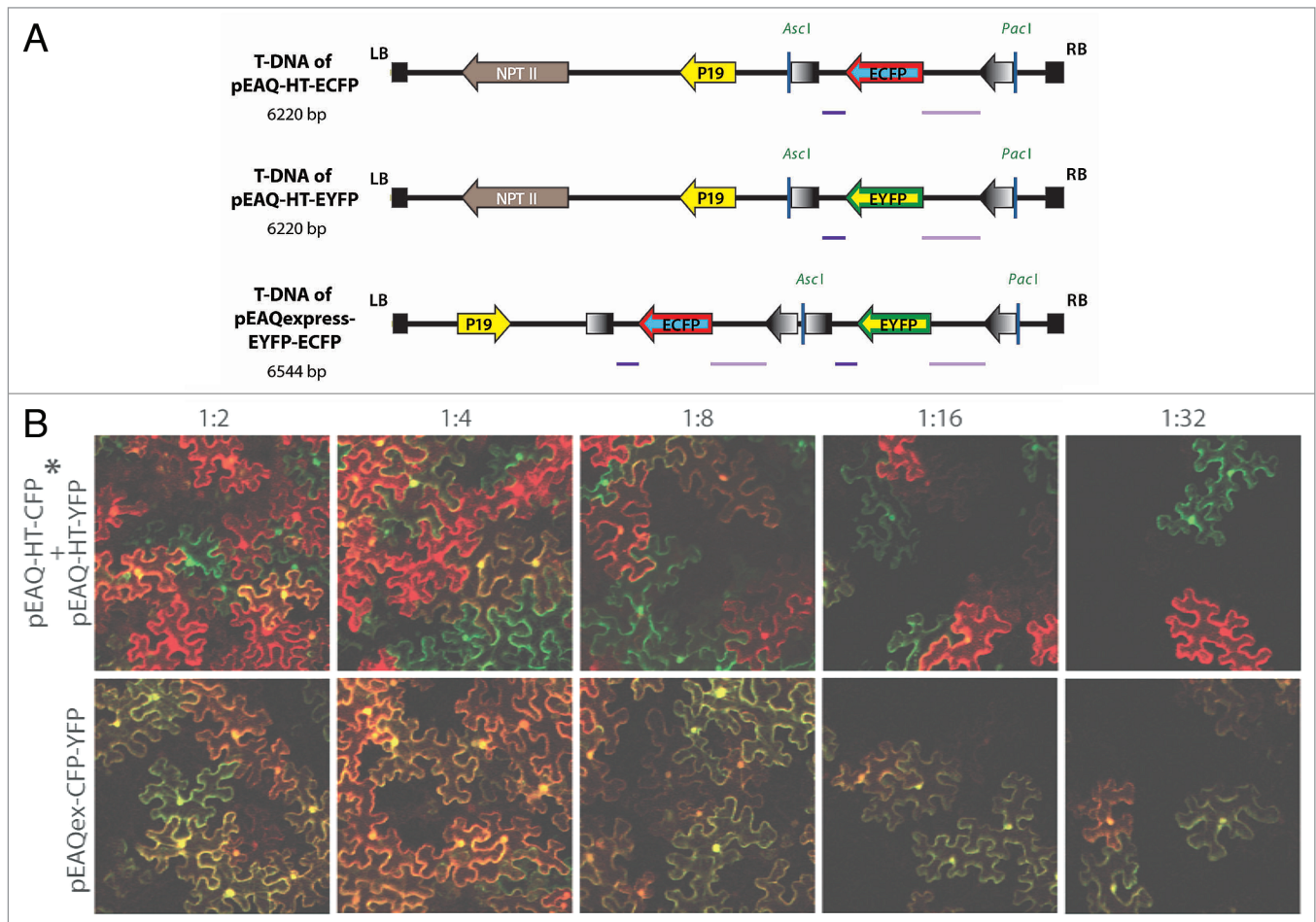


Figure 3. Co-expression of EYFP and ECFP in *N. benthamiana* cells. (A) Schematic representation of the T-DNA regions of pEAQ-HT-ECFP, pEAQ-HT-EYFP and pEAQexpress-EYFP-ECFP. (B) Leaf tissue was agro-infiltrated with inocula of above constructs at $OD_{600} = 0.2$ (* for co-infiltration an overall OD_{600} of 0.4 was used). Six days post infiltration, leaf tissue was imaged for EYFP (green) and ECFP (red) and channels digitally merged, showing co-localization in yellow.

sucrose gradients indicated that the coat proteins co-sedimented at a position characteristic of eVLPs. Transmission electron microscopy confirmed the presence of eVLPs in the preparation (Fig. 5A), indicating that capsid assembly was not affected by the replacement of the naturally occurring C-terminal 24 amino acids of the S protein with the six histidine residues. These results demonstrate that it is possible to replace the C-terminal region of the S protein with a heterologous sequence when eVLP technology is used. Furthermore, the incorporation of a His-tag opens further possibilities for particle purification.

To determine whether it is possible to present a whole protein on the surface of eVLPs, green fluorescent protein (GFP) was fused to the C-terminus of the wild type S coat protein of the VP60 precursor in the vector pEAQ-HT-VP60 (Fig. 2A), resulting in the production of pEAQ-HT-VP60-GFP. Plants co-infiltrated with this vector and pEAQ-HT-24K, exhibited GFP fluorescence three days post infiltration, suggesting correct folding of the GFP expressed from the construct. To check whether the GFP remained attached to the S protein after the processing of VP60, virus particles were purified from the infiltrated tissue and subjected to western blot analysis using an anti-GFP

antibody. This detected bands the size of free GFP, GFP attached to the S protein and GFP attached to uncleaved VP60 (Fig. 5B). These results show that while a portion of GFP is still attached to virus particles, some is cleaved off during purification, probably as a result of cleavage which occurs at the last 24 amino acids of the S protein.⁸ The presence of VP60-GFP also suggests that the presence of GFP may interfere with the correct processing of VP60. Nonetheless, these studies suggest that the display of whole proteins on the surface of eVLPs should be possible.

Conclusions

One of the initial attractions of using plant virus particles for bio-medical purposes was the fact that the infection process is highly productive, potentially enabling gram quantities of wild-type or modified particles to be produced with ease. In terms of epitope presentation, this opened up the prospect of producing novel vaccines at low cost. However, although some CPMV chimaeras have been shown to be capable of acting as experimental vaccines, the limitations on the size and sequence of the epitopes that

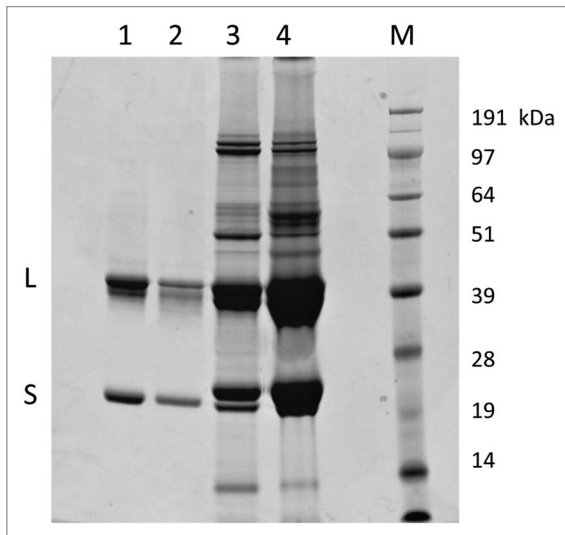


Figure 4. Purified eVLPs analysed on a 12% SDS-PAGE gel. Lane 1: 4 µg wild-type CPMV as a standard. Lane 2: 2 µg wild-type CPMV as a standard. Lane 3: 2 µl of purified particles extracted from 100 g of plant tissue co-infiltrated with pEAQ-HT-VP60 and pEAQ-HT-24K. Lane 4: 2 µl of purified particles extracted from 100 g of plant tissue infiltrated with pEAQexpress-VP60-24K. Lane M: Protein standards. The gel was stained with Coomassie blue and positions of the L and S coat proteins and size of the marker proteins are shown on the left and right-hand sides of the gel, respectively.

are tolerated on particles produced from infected plants severely curtailed the development of this technology. The presence of infectious RNA within the particles also raised major regulatory issues, though, as described above, the encapsidated RNA can be used to develop real-time PCR-based diagnostic reagents.

The recent developments reported in this article, using both infection-based and eVLP technologies have given a new impetus to the development of CPMV particles for a number of potential applications including their use as novel vaccines and drug delivery vehicles. The development of an efficient method for the production of particles devoid of RNA, as well as increasing the range of modifications that can be introduced, also enables the particle to be loaded with a range of foreign materials.³⁴ Though there is still clearly quite a way to go before their full potential is realized, the authors are confident that CPMV-based particle technologies have a bright future in several fields, including the production of new vaccines for use in humans.

Acknowledgements

This work was supported, in part, by the EU FP7 “PLAPROVA” project (Grant Agreement No. KBBE-227056). N.P.M. and P.S. were supported by Biotechnology and Biological Science

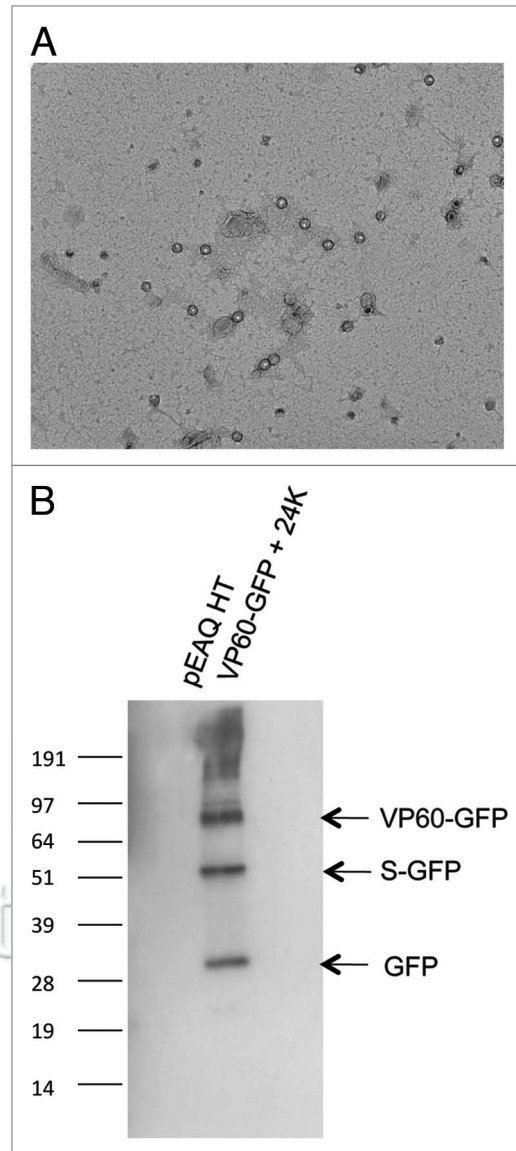


Figure 5. Modified eVLPs. (A) Electron micrograph of particles bearing a His-tag at the C-terminus of the S protein purified by nickel affinity chromatography. (B) Western blot analysis of particles produced after infiltration of *N. benthamiana* with pEAQ-HT-VP60-GFP and pEAQ-HT-24K. The blot was probed with anti-GFP antibodies. The positions of the marker proteins are indicated on the left-hand side of the blot and the identity of the protein products is shown on the right.

Research Council (BBSRC) doctoral training grants to the John Innes Centre (JIC). E.C.T. acknowledges funding from a Marie Curie Early Stage Training Fellowship MEST-CT-2005-019727 and the Trustees of the John Innes Foundation. JIC is grant-aided by the BBSRC.

References

- Usha R, Rohll JB, Spall VE, Shanks M, Maule AJ, Johnson JE, et al. Expression of an animal virus antigenic site on the surface of a plant virus particle. *Virology* 1993; 197:366-74.
- Porta C, Spall VE, Loveland J, Johnson JE, Barker PJ, Lomonossoff GP. Development of Cowpea mosaic virus as a high-yielding system for the presentation of foreign peptides. *Virology* 1994; 202:949-55.
- Porta C, Spall VE, Lin T, Johnson JE, Lomonossoff GP. The development of cowpea mosaic virus as a potential source of novel vaccines. *Intervirology* 1996; 39:79-84.
- Steinmetz NF, Lin T, Lomonossoff GP, Johnson JE. Structure-based engineering of an icosahedral virus for nanomedicine and nanotechnology. *Current Topics Microbiol Immunol* 2009; 327:23-58.
- Franssen H, Goldbach R, Broekhuijsen M, Moerman M, van Kammen A. Expression of middle-component RNA of cowpea mosaic virus: in vitro generation of a precursor to both capsid proteins by a bottom-component RNA-encoded protease from infected cells. *J Virol* 1982; 41:8-17.
- Saunders K, Sainsbury F, Lomonossoff GP. Efficient generation of cowpea mosaic virus empty virus-like particles by the proteolytic processing of precursors in insect cells and plants. *Virology* 2009; 393:329-37.
- Liu L, Lomonossoff GP. Agroinfection as a rapid method for propagating cowpea mosaic virus-based constructs. *J Virol Meth* 2002; 105:343-48.
- Lin T, Johnson JE. Structures of Picorna-like plant viruses: Implications and Applications. *Adv Virus Res* 2003; 62:167-239.
- Lomonossoff GP, Johnson JE. Eukaryotic viral expression systems for polypeptides. *Semin Virol* 1995; 6:257-67.
- Johnson JE, Lin T, Lomonossoff GP. Presentation of heterologous peptides on plant viruses: genetics, structures and function. *Annu Rev Phytopathol* 1997; 35:67-86.
- Brennan FR, Jones TD, Gilleland LB, Bellaby T, Xu F, North PC, et al. *Pseudomonas aeruginosa* outer-membrane protein F epitopes are highly immunogenic in mice when expressed on a plant virus. *Microbiology* 1999; 145:211-20.
- Taylor KM, Lin T, Porta C, Mosser AG, Giesing HA, Lomonossoff GP, et al. Influence of three-dimensional structure on the immunogenicity of a peptide expressed on the surface of a plant virus. *J Molec Recognit* 2000; 13:71-82.
- Chatterji A, Burns LL, Taylor SS, Lomonossoff GP, Johnson JE, Lin T, et al. Cowpea mosaic virus: from the presentation of antigenic peptides to the display of active biomaterials. *Intervirology* 2002; 45:362-70.
- Porta C, Spall VE, Findlay KC, Gergerich RC, Farrance CE, Lomonossoff GP. Cowpea mosaic virus-based chimaeras. Effects of inserted peptides on the phenotype, host-range and transmissibility of the modified viruses. *Virology* 2003; 310:50-63.
- Dalsgaard K, Uttenthal Å, Jones TD, Xu F, Merryweather A, Hamilton WDO, et al. Inactivated vaccine protects target animals against a plant disease. *Nature Biotechnol* 1997; 15:248-52.
- Langeveld JP, Brennan FR, Martinez-Torrecuadrada JL, Jones TD, Boshuizen RS, Vela C, et al. Inactivated recombinant plant virus protects dogs from a lethal challenge with canine parvovirus. *Vaccine* 2001; 19:3661-70.
- Burrati E, McLain L, Tisminetzky S, Cleveland SM, Dimmock NJ, Baralle FE. The neutralizing antibody response against a conserved region of human immunodeficiency virus type 1 gp41 (amino acid residues 731-752) is uniquely directed against a conformational epitope. *J Gen Virol* 1998; 79:2709-16.
- Cleveland SM, Burrati E, Jones TD, North P, Baralle F, McLain L, et al. Immunogenic and antigenic dominance of a nonneutralizing epitope over a highly conserved neutralizing epitope in the gp41 envelope glycoprotein of human immunodeficiency virus type 1: its deletion leads to a strong neutralizing response. *Virology* 2000; 266:66-78.
- Lin T, Porta C, Lomonossoff G, Johnson JE. Structure-based design of peptide presentation on a viral surface: The crystal structure of a plant/animal virus chimaera at 2.8 Å resolution. *Folding and Design* 1996; 1:179-87.
- Lomonossoff GP, Hamilton WDO. Cowpea mosaic virus-based vaccines. *Current Topics Microbiol Immunol* 1999; 240:177-89.
- Cañizares MC, Lomonossoff GP, Nicholson L. Development of Cowpea mosaic virus-based vectors for the production of vaccines in plants. *Expert Rev Vaccines* 2005; 4:687-97.
- Lomonossoff GP. Antigen Delivery Systems: Use of recombinant plant viruses. In: Mestecky J, Bienenstock J, Lamm ME, Mayer L, McGhee JR, Strober W, (Eds.). *Mucosal Immunology*, 3rd Edition, Amsterdam, Elsevier 2005; 1061-72.
- Lomonossoff GP. Virus particles and the uses of such particles in bio- and nanotechnology. In: Caranta C, Aranda M, Tepfer M, Lopez-Moya JJ. (Eds). *Recent Advances in Plant Virology*, Caister, Caister Academic Press 2010; 363-85.
- Sainsbury F, Cañizares MC, Lomonossoff GP. Cowpea mosaic virus: the plant virus-based biotechnology workhorse. *Annu Rev Phytopathol* 2010; 48:437-55.
- Zamorano PI, Wigdorovitz A, Perez Filgueira DM, Escibano JM, Sadir AM, Borca MV. Induction of anti foot and mouth disease virus T and B cell responses in cattle immunized with a peptide representing ten amino acids of VP1. *Vaccine* 1998; 16:558-63.
- King DP, Montague N, Ebert K, Reid SM, Jukes JP, Schädlich L, et al. Development of a novel recombinant encapsidated RNA particle: Evaluation as an internal control for diagnostic RT-PCR. *J Virol Meth* 2007; 146:218-25.
- Bertens P, Wellink J, Goldbach R, van Kammen A. Mutational analysis of the cowpea mosaic virus movement protein. *Virology* 2000; 267:199-208.
- Rae C, Koudelka KJ, Destito G, Estrada MN, Gonzales MJ, Manchester M. Chemical addressability of ultraviolet-inactivated RNA particle: Evaluation as an internal control for diagnostic RT-PCR. *J Virol Meth* 2007; 146:218-25.
- Ochoa W, Chatterji A, Lin T, Johnson JE. Generation and structural analysis of the cowpea mosaic virus movement protein. *Virology* 2000; 267:199-208.
- Rae C, Koudelka KJ, Destito G, Estrada MN, Gonzales MJ, Manchester M. Chemical addressability of ultraviolet-inactivated RNA particle: Evaluation as an internal control for diagnostic RT-PCR. *J Virol Meth* 2007; 146:218-25.
- Ochoa W, Chatterji A, Lin T, Johnson JE. Generation and structural analysis of the cowpea mosaic virus movement protein. *Virology* 2000; 267:199-208.
- Phelps JP, Dang N, Rasochova L. Inactivation and purification of cowpea mosaic virus-like particles displaying peptide antigens from *Bacillus anthracis*. *J Virol Meth* 2007; 141:146-53.
- Sainsbury F, Thuenemann EC, Lomonossoff GP. pEAQ: versatile expression vectors for easy and quick transient expression of heterologous proteins in plants. *Plant Biotechnol J* 2009; 7:682-93.
- van Kammen A. Purification and properties of the components of cowpea mosaic virus. *Virology* 1967; 31:633-42.
- Cañizares MC, Taylor KM, Lomonossoff GP. Surface-exposed C-terminal amino acids of the small coat protein of *Cowpea mosaic virus* are required for suppression of silencing. *J Gen Virol* 2004; 85:3431-5.
- Aljabali AAA, Sainsbury F, Lomonossoff GP, Evans DJ. Cowpea mosaic virus unmodified virus-like particles can be loaded with metal and metal Oxide. *Small* 2010; 6:818-21.

Interior Engineering of a Viral Nanoparticle and Its Tumor Homing Properties

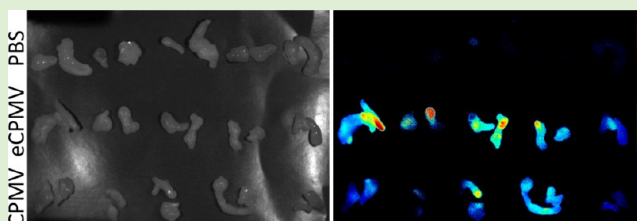
Amy M. Wen,[†] Sourabh Shukla,[†] Pooja Saxena,^{||} Alaa A. A. Aljabali,^{||,⊥} Ibrahim Yildiz,[†] Sourav Dey,[†] Joshua E. Mealy,^{†,‡,¶} Alice C. Yang,[†] David J. Evans,^{||,▽} George P. Lomonosoff,^{||} and Nicole F. Steinmetz^{†,‡,§,*}

[†]Department of Biomedical Engineering, [‡]Radiology, [§]Materials Science and Engineering, Case Western Reserve University, 10900 Euclid Avenue, Cleveland, Ohio 44106, United States

^{||}Department of Biological Chemistry, John Innes Centre, Norwich Research Park, Norwich, NR4 7UH, U.K.

Supporting Information

ABSTRACT: The development of multifunctional nanoparticles for medical applications is of growing technological interest. A single formulation containing imaging and/or drug moieties that is also capable of preferential uptake in specific cells would greatly enhance diagnostics and treatments. There is growing interest in plant-derived viral nanoparticles (VNPs) and establishing new platform technologies based on these nanoparticles inspired by nature. *Cowpea mosaic virus* (CPMV) serves as the standard model for VNPs. Although exterior surface modification is well-known and has been comprehensively studied, little is known of interior modification. Additional functionality conferred by the capability for interior engineering would be of great benefit toward the ultimate goal of targeted drug delivery. Here, we examined the capacity of empty CPMV (eCPMV) particles devoid of RNA to encapsulate a wide variety of molecules. We systematically investigated the conjugation of fluorophores, biotin affinity tags, large molecular weight polymers such as poly(ethylene glycol) (PEG), and various peptides through targeting reactive cysteines displayed selectively on the interior surface. Several methods are described that mutually confirm specific functionalization of the interior. Finally, CPMV and eCPMV were labeled with near-infrared fluorophores and studied side-by-side in vitro and in vivo. Passive tumor targeting via the enhanced permeability and retention effect and optical imaging were confirmed using a preclinical mouse model of colon cancer. The results of our studies lay the foundation for the development of the eCPMV platform in a range of biomedical applications.



INTRODUCTION

Nanomaterials are currently under investigation for platform development for applications in nanomedicine. They have favorable properties for the detection, imaging, and treatment of diseases such as cancer and cardiovascular disease as they can carry large payloads of imaging reagents and/or drugs and can be engineered to direct the payload specifically to target cells. The fact that *multifunctional* units can be designed and developed makes nanoparticles attractive candidates for the development of novel therapeutics and diagnostics.

Many different platforms have been developed, including synthetic man-made nanomaterials and naturally occurring bionanomaterials, such as protein cages and viral nanoparticles (VNPs).¹ Although viral nanotechnology is considered a novel and emerging field, recombinant virus-based materials have been used as vaccines and gene delivery vectors since the 1970s. Several recombinant virus-like particle-based vaccines are now used in the clinic, e.g., the *Human papillomavirus* (HPV) vaccine Gardasil (Merck & Co Inc.). Several gene therapies based on *Adenovirus*, *Adeno-associated virus*, and *Lentivirus* are undergoing clinical trials.^{2–4} For the past 20 years chemists, materials scientists, and engineers have developed a range of

methodologies that can be applied to fine-tune and engineer VNPs for desired applications. VNPs are genetically encoded biomaterials and can therefore be genetically modified. In addition, chemical engineering procedures including chemical bioconjugation, mineralization, infusion, and encapsulation techniques have been widely developed and applied.^{5,6} VNPs offer several sites for modification: the exterior surface, the interior surface, the coat protein interface, and the interior cavity, all of which have been utilized for modification. The application of a combination of techniques facilitates the development of highly sophisticated multifunctional nanoprobes.⁷

In this work we turned toward the development of the plant virus *Cowpea mosaic virus* (CPMV). CPMV is a 30 nm-sized icosahedron; it has been used as a model system for various applications ranging from electronic materials^{8–10} and sensors^{11,12} to imaging probes.^{13,14} CPMV has been studied extensively because of its biocompatibility, high stress tolerance,

Received: August 13, 2012

Revised: November 1, 2012

Published: November 2, 2012

low toxicity, and diverse possibilities for surface modification by conjugation and genetic engineering. CPMV nanoparticles consist of 60 copies each of a large (L) and small (S) coat protein. Wild-type CPMV can be produced with ease and in high yields in black-eyed pea plants. Recently a RNA-free version of the capsid, referred to as empty CPMV (eCPMV), has been developed. These are produced by agroinfiltrating *Nicotiana benthamiana* leaves with a construct expressing the precursor of the L and S coat proteins (VP60) and the virus-derived proteinase (24K) required for its processing.¹⁵ The particles produced in this way are completely devoid of RNA of either viral or host origin although structurally identical to wild-type particles in terms of their proteins.

Several bioconjugation chemistries have been successfully applied to modify the exterior surface of CPMV. These include exterior lysine modification using *N*-hydroxysuccinimide (NHS) esters,^{16,17} carbodiimide-mediated amine coupling to solvent-exposed carboxylates,¹⁸ and maleimide coupling to genetically or chemically introduced thiols.^{19,20} Further, advanced bio-orthogonal reactions such as Cu(I)-catalyzed azide-alkyne cycloaddition²¹ and hydrazone ligation procedures²² have been applied with great success. Exterior surface modification of CPMV has been extensively studied and is well understood. In stark contrast, only few studies have been reported that address the chemical engineering of the interior CPMV surface.^{23,24}

With growing interest to develop CPMV-based nanomaterials for applications in materials and medicine, the generation of multifunctional materials is a requirement and thus interior engineering in addition to exterior labeling is becoming more and more important. For example, CPMV nanoparticles have a natural affinity to cancer cells such as HeLa (cervical cancer), HT-29 (colon cancer), and PC-3 (prostate cancer); surface domains of CPMV specifically interact with cell surface-expressed vimentin and promote cell internalization.^{25–27} This property can be utilized to image cancer neovasculature or to target CPMV to cancer cells *in vitro* and *in vivo*.^{14,25,28} To utilize CPMV probes for the study or targeting of surface vimentin-expressing cells, it is desired to develop chemistries on the interior particle surface, e.g., to install imaging moieties; this will ensure conservation of the particle surface and CPMV-vimentin interaction. CPMV can also be redirected to other receptors, such as folic acid receptors,²⁹ vascular endothelial growth factor receptor-1,²⁹ and gastrin-releasing peptide receptors,¹³ by decorating the CPMV particle surface with the appropriate targeting ligands. With the long-term application of targeted drug delivery or optical imaging in mind, it is of interest to establish chemistries that allow interior cargo loading in addition to exterior surface modifications.

The recent development of the eCPMV formulation now opens a new avenue to further advance the CPMV platform technology. In this study, we systematically investigated the interior labeling capacity of RNA-free eCPMV and RNA-containing wild-type CPMV nanoparticles using negatively and positively charged fluorophores, small molecule biotin tags, large polymers such as poly(ethylene glycol) (PEG), and negatively and positively charged peptide sequences: penta-(arginine), hexa(histidine), and FLAG tag peptide. The *in vitro* and *in vivo* properties of fluorescently labeled CPMV and eCPMV were investigated in tissue culture and a preclinical mouse model of colon cancer.

■ MATERIALS AND METHODS

Materials. Oregon Green 488 (OG488) maleimide, OG488 succinimidyl ester, and Rhodamine Red C₂ (RR) maleimide were purchased from Invitrogen. DyLight 488 (DL488) maleimide, sulfo-NHS-LC-biotin, and maleimide-PEG₂-biotin were purchased from Pierce. Poly(ethylene glycol) maleimide (MW 2000 Da) and poly(ethylene glycol) succinimidyl ester (MW 2000 and 5000 Da) were purchased from Nanocs. Maleimido trioxa-6-formyl benzamide (MTFB), succinimidyl-4-formyl benzoate (S-4FB), His6 Tag-HyNic, and FLAG Tag-HyNic were purchased from Solulink. A biotinylated 6-hydrazinopyridyl-polyarginine peptide (bio-R5-HyNic) was synthesized as described elsewhere.³⁰ Aniline and dimethyl sulfoxide (DMSO) were purchased from Fisher.

Propagation and Isolation of Wild-Type and eCPMV Particles. *CPMV Production.* Black-eyed peas (*Vigna unguiculata*) were inoculated with 100 ng/ μ L CPMV in 0.1 M potassium phosphate buffer (pH 7.0) and propagated for 18–20 days using established procedures.³¹ Virus concentration in plant extracts was determined by UV/vis spectroscopy ($\epsilon_{260\text{ nm}} = 8.1\text{ mg}^{-1}\text{ mL cm}^{-1}$), and virus integrity was determined by size exclusion chromatography (SEC; see below).

eCPMV Production. Agrobacterium LBA4404 cultures harboring the binary plasmid pEAQexpress-VP60-24K, which encodes the coat protein precursor VP60 and viral proteinase 24K,³² were introduced into *N. benthamiana* leaves using syringe-infiltration. Infiltrated tissue was harvested 6 days post infiltration and homogenized in 0.1 M sodium phosphate buffer (pH 7.0). eCPMV was purified further using a protocol adapted from established procedures for wild-type CPMV³¹ and the particle concentration was determined by UV/vis spectroscopy ($\epsilon_{280\text{ nm}} = 1.28\text{ mg}^{-1}\text{ mL cm}^{-1}$). eCPMV integrity was examined using transmission electron microscopy (TEM) on an FEI Technai20.

Bioconjugation Using CPMV and eCPMV. For all reactions using maleimide and NHS chemistries, CPMV and eCPMV particles were used at a final concentration of 2 mg/mL in 0.1 M potassium phosphate buffer (pH 7.0) and incubated with the chemical label (e.g., dye, biotin) at room temperature overnight, with agitation. For all hydrazone ligation reactions, CPMV and eCPMV particles modified with MTFB (final concentration 0.5 mg/mL) were incubated with the peptide (e.g., FLAG-HyNic) in 0.1 M potassium phosphate buffer (pH 7.0) containing 10 mM aniline catalyst overnight at room temperature, with agitation. The final DMSO concentration was adjusted to 10% of the reaction volume. Particles were purified with 10 kDa molecular weight cutoff centrifugal filter units (Millipore) and analyzed with UV/vis spectroscopy, native and denaturing gel electrophoresis, and SEC. For initial studies, labeling with dyes, S4FB, and MTFB was performed using 6000 molar excess of the chemical per particle, with biotin and PEG using 2000 molar excess, and with peptides using 360 molar excess. For comparisons between externally and internally dye-labeled CPMV and eCPMV, the molar excess was adjusted to match the number of dyes, as confirmed by UV/vis spectroscopy. For *in vivo* studies, 4500 molar excess of mPEG5000-NHS was used. Western blotting was performed for biotinylated particles. The 4FB labeling efficiency of CPMV-S4FB_e and CPMV-MTFB₁ was determined using the Solulink 4FB molar substitution ratio protocol (MSR), in which 10 μ g of 4FB-modified CPMV particles were mixed with a 0.5 mM solution of 2-hydrazinopyridine-2-HCl (2-HP) prepared in 0.1 M 2-(*N*-morpholino)ethanesulfonic acid (MES) buffer (pH 5.5). The reaction was incubated at 37 °C for 30 min and analyzed by UV/vis spectroscopy. The number of 4FB labels per particle was calculated using the bond-specific extinction coefficient at 350 nm ($\epsilon = 18,000\text{ M}^{-1}\text{ cm}^{-1}$). Similarly, peptide attachment was quantified using the bond-specific extinction coefficient at 354 nm ($\epsilon = 29,000\text{ M}^{-1}\text{ cm}^{-1}$) for the hydrazone bond.

Size Exclusion Chromatography. All labeled particles were analyzed by SEC using a Superose6 column on the ÄKTA Explorer chromatography system (GE Healthcare). Samples (100 μ g/100 μ L) were analyzed at a flow rate of 0.4 mL/min using 0.1 M potassium phosphate buffer (pH 7.0).

Transmission Electron Microscopy. Drops of labeled particles were placed on carbon-coated copper TEM grids (5 μ L, 0.1 mg/mL),

allowed to adsorb for 5 min, washed with deionized (DI) water, then negatively stained with 2% (w/v) uranyl acetate for 1 min. Samples were examined using a Zeiss Libra 200FE transmission electron microscope operated at 200 kV.

Gel Electrophoresis. Native gel electrophoresis was performed using 1.2% agarose gels in 1x Tris/Borate/EDTA (TBE) buffer (45 mM Tris, 45 mM boric acid, 1.25 mM EDTA in Milli-Q water) with 1x TBE running buffer and 10 μ g of sample. Protein subunits were analyzed on denaturing 4–12% NuPAGE gels (Invitrogen) using 1x 3-(*N*-morpholino)propanesulfonic acid (MOPS) running buffer (Invitrogen) and 10 μ g of sample. After separation, the gel was photographed using an AlphaImager (Biosciences) imaging system before and after staining with Coomassie Blue, or further processed for Western blotting.

Western Blotting. To detect biotinylated particles, CPMV, CPMV-bio_E, eCPMV-bio_E, and eCPMV-R5-bio_I were analyzed by Western blotting. One microgram samples were separated on a 4–12% NuPAGE Bis-Tris gel using MOPS buffer (see above). After separation, the proteins were transferred onto a nitrocellulose membrane (Thermo Scientific) using NuPAGE Transfer Buffer (Invitrogen). The membrane was blocked at room temperature for 1 h using 0.1 M TBS (pH 7.6) containing 5% w/v skimmed milk powder and 0.05% w/v Tween 20. Detection was carried out using alkaline phosphatase-conjugated streptavidin (Sigma Aldrich) (1:1000) in blocking buffer solution. Alkaline phosphatase activity was detected using the BCIP/NBT liquid substrate system (Sigma Aldrich).

Avidin Agarose Affinity Binding Assay. CPMV, CPMV-bio_E, and eCPMV-bio_I were tested for binding to avidin agarose resin (Pierce) to confirm interior eCPMV modification with biotin maleimide. The batch method provided by the supplier was used, with some modifications: 50 μ g of the samples in 50 μ L of 0.1 M potassium phosphate buffer (pH 7.0) were added to 50 μ L of the resin (100 μ L of slurry) and mixed for 1 h at room temperature, with agitation. The supernatant was then recovered, and the resin was washed twice using 50 μ L of 0.1 M potassium phosphate buffer (pH 7.0). Any bound sample was eluted with 50 μ L of 0.5 M glycine-HCl buffer (pH 2.8), and the pH was immediately adjusted with 5 μ L of 1 M Tris buffer (pH 7.5). The samples were analyzed by running 30 μ L of the first recovered and eluted fractions on a denaturing gel.

Ni-NTA Affinity Binding Assay. CPMV, eCPMV, CPMV-His6_E, and eCPMV-His6_I were tested for binding to HisPur Ni-NTA resin (Pierce) to confirm interior eCPMV modification with His6. The batch method provided by the supplier was used, with some modifications: 50 μ g of the samples in 100 μ L of equilibration buffer (20 mM sodium phosphate, 300 mM sodium chloride, 10 mM imidazole, pH 7.4) were added to 50 μ L of the resin (150 μ L of slurry) and mixed for 30 min at room temperature, with agitation. The supernatant was then recovered, and the resin was washed twice using 100 μ L of wash buffer (20 mM sodium phosphate, 300 mM sodium chloride, 25 mM imidazole, pH 7.4). Any bound sample was eluted with 50 μ L of elution buffer (20 mM sodium phosphate, 300 mM sodium chloride, 250 mM imidazole, pH 7.4). The samples were analyzed by running 30 μ L of the first recovered and eluted fractions on a denaturing gel.

Cell Cultures. HeLa cells (ATCC) were grown and maintained in minimal essential medium (MEM), while HT-29 cells (ATCC) were cultured in RPMI medium at 37 °C in a 5% CO₂ humidified atmosphere. The media were supplemented with 10% (v/v) heat inactivated fetal bovine serum (FBS), 1% (v/v) L-glutamine, and 1% (v/v) penicillin–streptomycin. All reagents were obtained from Gibco.

Confocal Microscopy Imaging. HeLa cells (20 000 cells/750 μ L MEM/well) were grown for 24 h on glass coverslips placed in an untreated 24-well plate. The media was then replaced with 250 μ L of fresh MEM containing 10 μ g of CPMV-OG488_E or eCPMV-OG488_I ($\sim 5 \times 10^7$ VNPs/cell) and incubated at 37 °C, 5% CO₂ for 2 h. Post incubation, cells were washed thoroughly with sterile saline and incubated for a further 24 h in fresh medium. The cells were then fixed using 4% v/v paraformaldehyde and 0.3% v/v glutaraldehyde in Dulbecco's phosphate-buffered saline (DPBS) (pH 7.2) for 5 min. Cell

membranes were stained using wheat germ agglutinin (WGA) conjugated with Alexa Fluor 555 (WGA-A555) (Invitrogen) at 1 μ g/mL in 5% goat serum (GS) (Invitrogen) for 45 min. Cell nuclei were stained using 4',6-diamidino-2-phenylindole (DAPI) (MP Biomedicals) at 0.13 μ g/mL in DPBS for 5 min. All steps were carried out in the dark at room temperature; in between each step the coverslips were washed 3x with DPBS. The coverslips were then mounted using Permount (Fisher) on glass slides and sealed using nail polish. Confocal images were obtained using Olympus FluoView FV1000 LSCM and data processed using Image J 1.44o (<http://imagej.nih.gov/ij>).

Fluorescence Measurements. Fifty microliters of dye-labeled CPMV and eCPMV were added to a black 384-well plate at a concentration of 50 μ M. Potassium phosphate buffer (0.1 M) was used for pH 7.0 measurements, and 0.1 M MES buffer was used for pH 5.0 measurements. Particles were incubated in their respective buffers for 3 h. Fluorescence intensity was measured using a Tecan Infinite 200 plate reader (Ex/Em wavelengths 600/665 for A647 and 435/495 for OG488).

Flow Cytometry. HeLa cells (750 000 cells/200 μ L MEM/well) were added to an untreated 96-well v-bottom plate. CPMV, CPMV-A647_E, eCPMV, and eCPMV-A647_I particles were added at a concentration of 100 000 particles/cell in triplicates and incubated for 3 h at 37 °C and 5% CO₂. Following incubation, cells were spun down at 500g for 4 min. The supernatant was removed, and the cells were resuspended in FACS buffer (0.1 mL 0.5 M EDTA, 0.5 mL FBS, and 1.25 mL 1 M HEPES, pH 7.0 in 50 mL Ca²⁺ and Mg²⁺ free PBS). This washing step was repeated twice. The cells were then fixed in 2% (v/v) paraformaldehyde in FACS buffer for 10 min at room temperature and washed another three times. Analysis was carried out using the BD LSR II flow cytometer, and a total of 10 000 events per sample were collected.

Tumor Homing with HT-29 Xenografts. All animal procedures were performed in accordance with approved protocols from the Institutional Animal Care and Use Committee at Case Western Reserve University. Tumor xenografts were established by injecting 5×10^6 HT-29 cells/100 μ L of a 1:1 preparation of RPMI medium and Matrigel (Fisher) subcutaneously in the flanks of six week old NCr-nu/nu mice. The mice were maintained on an alfalfa free diet (Teklad) to reduce tissue autofluorescence. Animals were observed closely, and tumor size was measured using calipers. After the tumors reached an average volume of 20 mm³ (10–12 days), the mice were randomly divided into three groups: PBS, CPMV, and eCPMV ($n = 5$). PEG5000_E-eCPMV-A647_I was administered intravenously at a dose of 200 μ g/100 μ L sterile PBS and PEG5000_E-CPMV-A647_E at a dose of 284.3 μ g/100 μ L sterile PBS to match the number of particles. Both formulations had 50 dyes/particle. Animals were sacrificed 24 h post administration, and the tumors on the flanks were excised and imaged using a Maestro fluorescence imaging instrument (yellow excitation and emission filters with an exposure time of 800 ms). After background subtraction in Maestro, the average fluorescence intensity over the tumor area was analyzed using ImageJ.

RESULTS AND DISCUSSION

Production of CPMV and eCPMV. CPMV particles were purified from infected black-eyed pea plants yielding 0.5–1 mg of CPMV per 1 g of infected leaves. The purity of the virus was confirmed based on the A260:A280 ratio (a ratio of 1.7–1.8 indicates pure and intact particles) and SEC. eCPMV particles were produced by coexpression of the precursor to the L and S coat proteins (VP60) and the viral proteinase (24K) in *N. benthamiana* leaves, and the particles were purified using a modified CPMV extraction procedure. Yields of up to 0.5 mg/g leaf tissue were achieved, somewhat lower than the yields achieved for wild-type CPMV via infection.

Structural Properties of (e)CPMV. One of the advantages of working with bionanoparticles such as VNPs is that their structures are known to atomic resolution. The structure of

CPMV has been solved to 2.8 Å resolution, and its coordinates are available at the Virus Particle Explorer database (<http://viperdb.scripps.edu>). The 30 nm-sized CPMV capsids have icosahedral symmetry and are formed by 60 copies of two different types of coat proteins, the S and L subunits. The S subunit (213 amino acids) folds into one jelly roll β -sandwich, the A domain, and the L subunit (374 amino acids) folds into two jelly roll β -sandwich domains: the B domain that covers the carboxy-terminus and the C domain that covers the amino-terminus. The three domains form the asymmetric unit and are arranged in a similar surface lattice to $T = 3$ viruses, except they have different polypeptide sequences; therefore the particle structure is described as pseudo $T = 3$, or $P = 3$, symmetry. While the B and C domains are clustered around the icosahedral 3-fold axis and form hexamers, the A domain is clustered around the 5-fold axis, forming pentamers³³ (Figure 1A,B). The interior surface is accessible through 12 pores at the 5-fold axis; at its narrowest point, the opening of the pore is 0.75 nm (as measured using PyMol 1.4.1 software) (Figure 1C).

The chemical addressability of the exterior surface has been extensively studied, and it is known that CPMV displays up to 300 reactive solvent-exposed surface lysine side chains (Figure 1D), all of which can be chemically labeled.^{16,17} CPMV particles do not display any reactive cysteine side chains on their exterior particle surface. However, reactive cysteine residues are located on the solvent-exposed *interior* particle surface (Figure 1E,F). In earlier studies, Wang et al. showed that small chemical modifiers such as ethylmercury phosphate (EMP), 5-maleimidofluorescein,²³ and thiol-selective stilbene derivatives²⁴ could be introduced to CPMV and covalently attached to interior cysteine residues.

Studying the structure of CPMV using PyMol software, we located eight cysteines per asymmetric unit on the solvent-exposed interior surface (Figure 1E,F): Cys 4 on the S protein, and Cys 108, 119, 132, 177, 187, 295, and 355 on the L protein. Thiols from two cysteine side chains, Cys 295 on L and Cys 4 on S, were found to be solvent-exposed (the thiol of Cys 4 appears to be exposed in a small pocket, which can be seen when looking at the asymmetric unit; see inset in Figure 1F). The thiols of Cys 187 and Cys 355 appear to be engaged in a disulfide bond (Figure 1E,F). Previous data from Wang et al. indicated that EMP reacted with Cys 295 on L but also indicated that 5-maleimidofluorescein attached to cysteines on both the S and L subunit; the exact positions could not be identified.²³ On the basis of the structural data, we propose that CPMV nanoparticles display at least 120 reactive cysteine residues, one each on L (Cys 295) and S (Cys 4) subunits. It is important to note that VNPs, although often depicted as rigid closed shells, are highly dynamic structures that can undergo various reversible structural transitions. The structural data generated from crystallography is just a snapshot.

Interior Labeling with Fluorophores. We studied the chemical reactivity of both eCPMV and CPMV toward several fluorophores. Prior to chemical labeling, eCPMV and CPMV were treated with 10 mM tris(2-carboxyethyl)phosphine (TCEP) in 0.1 M phosphate buffer pH 7.0. TCEP is a reducing reagent; treatment was performed to ensure that thiols were reduced and reactive toward maleimide-containing compounds. The reducing agent was removed using centrifugal spin filters with a cutoff of 10K prior to introduction of maleimide-containing fluorophores: Oregon Green 488 (OG488), DyLight 488 (DL488), Rhodamine Red (RR), and

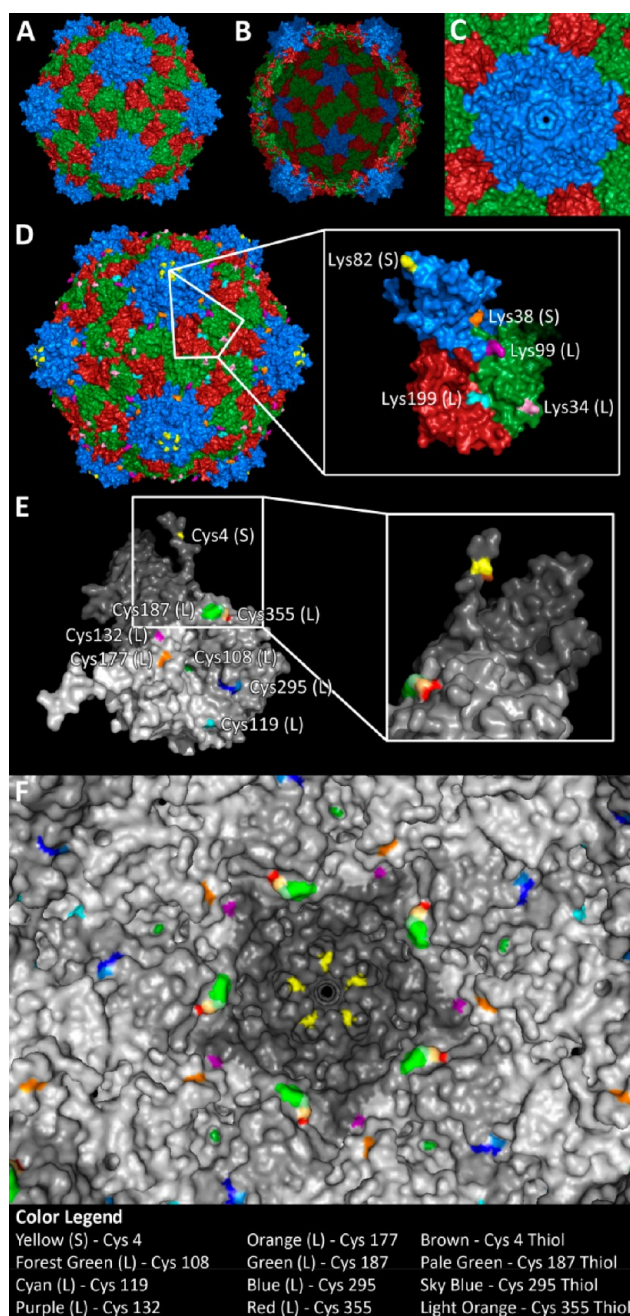


Figure 1. The structure of CPMV. CPMV consists of 60 copies of a small subunit (S, blue) and a large two-domain subunit (L, green and red). (A) Exterior view and (B) interior view. (C) Pore structure at the 5-fold axis; the pore diameter was measured to be 0.75 nm. (D) CPMV displays 300 reactive lysines on the surface, five per asymmetric unit. (E) CPMV also displays cysteines selectively on the *interior* surface, 8 per asymmetric unit (Cys 4 – yellow, 108 – forest green, 119 – cyan, 132 – purple, 177 – orange, 187 – green, 295 – blue, and 355 – red). Inset shows 90 degree rotation, revealing hidden reactive thiol of Cys 4. (F) View of interior with surface-exposed thiols highlighted (Cys 4 – brown, 187 – pale green, 295 – sky blue, and 355 – light orange).

Alexa Fluor 647 (A647) (Figure 2A). Different conditions were tested, i.e., varying incubation times and excess of reagent used (see Materials and Methods), and we found that the reaction efficiency reached a plateau using a 2000-fold excess of reagents. To ensure maximum labeling, the reactions were carried out under forcing conditions using a molar excess of

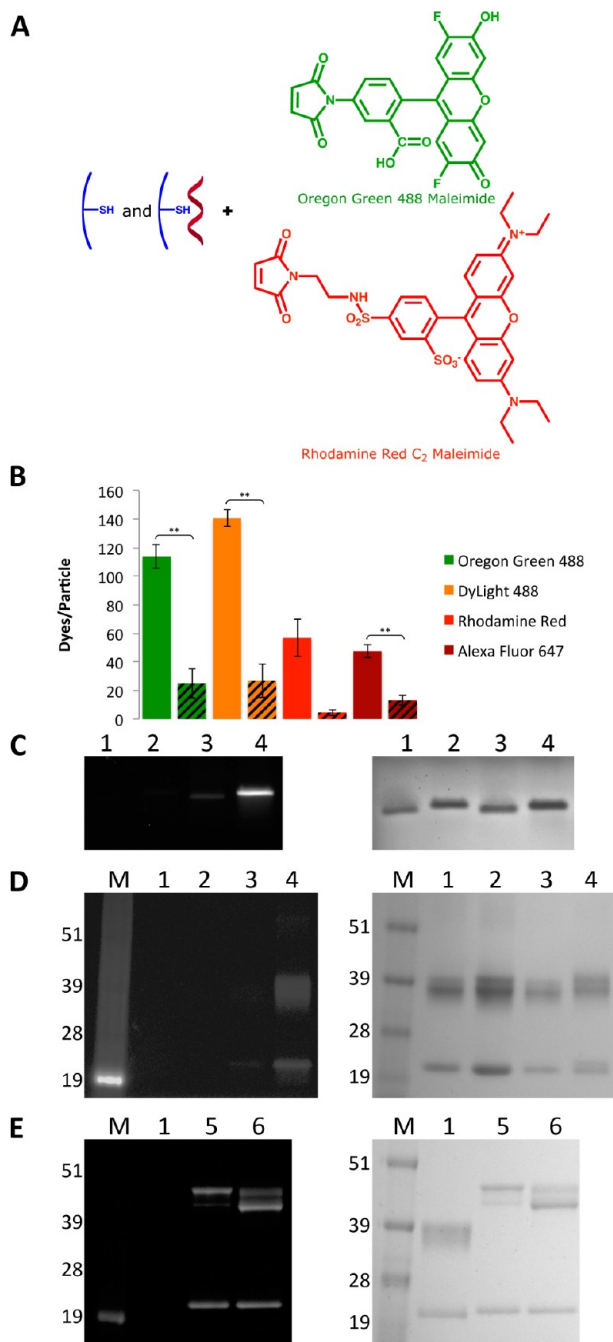


Figure 2. Characterization of CPMV-dye conjugates. (A) Schematic of internal functionalization of eCPMV and CPMV with OG488 and RR (DL488 and A647 structures are proprietary). (B) Representative data of the labeling efficiency of the various dyes for eCPMV vs CPMV. eCPMV data are shown as solid bars on the left, while CPMV data are shown as striped bars on the right. Asterisks denote statistical significance between eCPMV and CPMV formulations (** $p < 0.01$). (C) eCPMV- and CPMV-OG488 conjugates on a 1.2% agarose gel. The gel was visualized under UV light (left) and after Coomassie staining (right). 1 = CPMV; 2 = eCPMV; 3 = CPMV-OG488; 4 = eCPMV-OG488. (D) Same particles on a denaturing 4–12% sodium dodecyl sulfate polyacrylamide gel electrophoresis (SDS-PAGE) gel visualized under UV light (left) and after Coomassie staining (right). M = SeeBlue Plus2 molecular weight marker. (E) eCPMV-RR and CPMV-RR conjugates on a SDS-PAGE gel visualized under UV light (left) and after Coomassie staining (right). 1 = CPMV; 5 = CPMV-RR; 6 = eCPMV-RR.

6000 fluorophores per eCPMV and CPMV particle; the protein concentration was kept at 2 mg/mL (350 nM for CPMV, 500 nM for eCPMV). The reaction was allowed to proceed overnight, eCPMV-dye and CPMV-dye conjugates were purified using centrifugal filters with a size cutoff of 10K, and samples were resuspended in buffer and analyzed by UV/vis spectroscopy, SEC, TEM, and native and denaturing gel electrophoresis (Figures 2, S1, and S2).

In all cases, SEC and TEM confirmed that the particles remained structurally sound (Figures S1 and S2). The degree of conjugation was quantified, with the number of dye moieties per particle calculated based on the UV/vis spectrum using the Beer–Lambert law and the respective extinction coefficients: OG488 $\epsilon_{491 \text{ nm}} = 81\,000 \text{ M}^{-1} \text{ cm}^{-1}$, DL488 $\epsilon_{493 \text{ nm}} = 70\,000 \text{ M}^{-1} \text{ cm}^{-1}$, RR $\epsilon_{573 \text{ nm}} = 119\,000 \text{ M}^{-1} \text{ cm}^{-1}$, A647 $\epsilon_{651 \text{ nm}} = 265\,000 \text{ M}^{-1} \text{ cm}^{-1}$, CPMV $\epsilon_{260 \text{ nm}} = 8.1 \text{ mg}^{-1} \text{ mL cm}^{-1}$, MW of CPMV = $5.6 \times 10^6 \text{ g mol}^{-1}$, eCPMV $\epsilon_{280 \text{ nm}} = 1.28 \text{ mg}^{-1} \text{ mL cm}^{-1}$, and MW of eCPMV = $3.94 \times 10^6 \text{ g mol}^{-1}$. The data are summarized in Figure 2B. Overall, the labeling efficiency was significantly higher for each dye tested using eCPMV compared to CPMV. For eCPMV, it was found that approximately 110 OG488, 140 DL488, 60 RR, and 50 A647 were attached, while for CPMV, there were only 30 OG488, 30 DL488, less than 10 RR, and 10 A647 attached. The reproducibility and error lies within 10 dyes per particle. CPMV and eCPMV are structurally identical, but CPMV contains nucleic acids and eCPMV is nucleic acid-free. Labeling studies thus indicate that the presence of nucleic acids reduces labeling efficiency. It is possible the nucleic acids block the pores and thus reduce diffusion of the dyes into the capsid cavity. Electrostatic repulsion may also play a role. It is interesting to note that labeling with the negatively charged OG488 dye was most effective for eCPMV (see Figure 2A). The negative dye mimics the charge of the natural nucleic acid cargo; diffusion into the interior cavity and conjugation might thus be favored.

eCPMV- and CPMV-dye conjugates were analyzed by native and denaturing gel electrophoresis, and the gels were visualized under UV light before and white light after Coomassie staining (Figure 2C–E). In native gels, intact VNP are analyzed. The appearance of fluorescent bands under UV light confirms that the labels were indeed covalently attached to the particles, with brighter bands corresponding with more dyes attached. We had previously shown that exterior dye conjugation alters the mobility of CPMV in native agarose gels.¹³ The conjugation of chemical modifiers neutralizes the positive charge from the exterior lysine side chains, leading to increased mobility toward the anode. CPMV and eCPMV particles labeled with negatively or positively charged dyes on interior cysteines do not show an altered mobility in the gel, indicating that the labels are indeed attached to the interior.

Denaturing gels were analyzed to determine whether the dyes were attached to the S or L protein. A greater shift was observed in RR labeling of the L protein compared to OG488 labeling, most likely due to the almost 50% greater molar mass of RR (Figure 2D,E). It was found that in any case, dyes were attached to both the S and L proteins. Selective attachment to S or L was not observed for any formulation tested, indicating that a reactive cysteine is present on both subunits. This was found to be true even for the CPMV-RR formulation in which we quantified less than 10 dyes per CPMV. The fact that the dye distribution follows a random pattern might indicate that

the thiols on S and L are both highly reactive. This is consistent with previous data from Wang et al. that indicated 5-maleimidofluorescein was attached to cysteines on both the S and L subunits of CPMV at higher dye-to-subunit ratios.²³

CPMV- and eCPMV-Biotin Conjugates: Labeling (e)CPMV Inside and Out. Next, we sought to determine whether labels were indeed attached to the interior surface. The employed maleimide chemistry is selective toward thiols; however, cross-reactivity with lysines has been reported.³⁴ Since CPMV and eCPMV display 300 reactive lysine side chains on the exterior, we sought to rule out that nonspecific conjugation to exterior lysines instead of interior cysteine conjugation occurred. To do this, we chose biotin as a label. Biotin is a small molecule, a vitamin that specifically binds with high affinity to streptavidin and avidin. It is a popular label employed in biochemistry. Two particle conjugates were made: (1) CPMV was labeled at exterior lysines using 2000 molar excess of an NHS reactive biotin probe (referred to as CPMV-bio_E) and (2) eCPMV was labeled at interior cysteines using 2000 molar excess of a maleimide-activated biotin derivative (referred to as eCPMV-bio_I) (Figure 3A).

Purified CPMV-bio_E and eCPMV-bio_I conjugates were analyzed on native and denaturing gels and by Western blotting (Figure 3B–D). Native gel electrophoresis gave a first indication that biotin labels were indeed attached to interior cysteine side chains. Altered mobility is observed comparing CPMV and eCPMV. The absence of negatively charged RNA in eCPMV results in a retardation of movement through the gel toward the anode (Figure 3B), as previously described.¹⁹ Exterior labeling of CPMV with biotin results in an increased mobility of CPMV-bio_E versus CPMV toward the anode. The increased mobility can be explained by altered exterior surface modification. Biotin is a noncharged chemical modifier; conjugation to the exterior lysines of CPMV results in neutralization of the positive charge derived from lysine side chains, resulting in an overall more negatively charged particle. Labeling the interior of eCPMV does not affect the size or charge of the particle. Despite having a degree of biotin labeling similar to that of CPMV-bio_E (Figure 3D), eCPMV-bio_I appears to have comparable electrophoretic mobility to eCPMV, thus indicating that labels were indeed attached to the interior cysteines (as opposed to nonspecific external lysine conjugation) (Figure 3B).

To analyze the S and L proteins and to determine whether labels introduced were selective to just one or both coat proteins, denaturing gel electrophoresis and Western blotting were conducted. Membranes were probed with an alkaline phosphatase-labeled streptavidin. Data confirm successful biotinylation. Further, data indicate that biotin was attached to both the S and L proteins for both formulations, CPMV-bio_E and eCPMV-bio_I. This is in agreement with fluorescent dye attachment and indicates that reactive thiols are present on each coat protein unit (Figure 3D).

We developed an assay using avidin agarose beads to determine whether labels were indeed attached on the interior capsid surface using eCPMV (Figure 3E). CPMV, CPMV-bio_E, and eCPMV-bio_I particles were mixed with avidin agarose beads. CPMV and eCPMV-bio_I were not expected to bind to the beads, as neither of these formulations display surface-exposed biotin groups. By contrast, CPMV-bio_E displaying multiple biotin labels on its exterior surface was expected to strongly bind to the beads via the biotin-avidin interaction. Each formulation was incubated with the beads, beads were

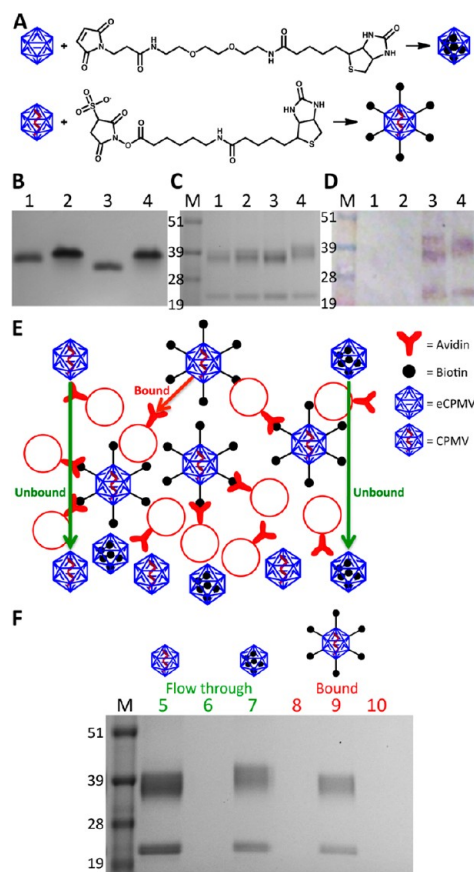


Figure 3. (A) Schematic of biotin functionalization of eCPMV-bio_I and CPMV-bio_E, respectively. (B) Biotinylated particles on a 1.2% agarose gel visualized after Coomassie staining. 1 = CPMV; 2 = eCPMV; 3 = CPMV-bio_E; 4 = eCPMV-bio_I. (C) Same particles on a 4–12% denaturing SDS-PAGE gel stained with Coomassie. M = SeeBlue Plus2 molecular weight marker. (D) Western blot probed with streptavidin-alkaline phosphatase confirms biotinylation. (E) Schematic of the avidin bead binding assay. (F) Flow through and eluted particles from binding assay on a SDS-PAGE gel after staining with Coomassie. 5 = CPMV flow through; 6 = CPMV-bio_E flow through; 7 = eCPMV-bio_I flow through; 8 = bound CPMV; 9 = bound CPMV-bio_E; 10 = bound eCPMV-bio_I.

washed, and the flow through was collected. Then, the beads were treated with 0.5 M glycine-HCl buffer, pH 2.8, to disrupt the biotin-avidin interaction and elute any bound particles from the beads. Both the flow through from the washing steps and the eluent after treatment were collected and analyzed on a denaturing gel (Figure 3F). As expected, CPMV and eCPMV-bio_I were detected in the washing steps, indicating these formulations did not interact with the avidin agarose beads. CPMV-bio_E was not detected in the flow through but was detected in the final eluent, as these particles did bind to the beads (Figure 3F). These observations support that maleimide chemistry is indeed selective and that biotin labels in eCPMV-bio_I were attached to the interior cysteine residues.

Labeling the eCPMV and CPMV Interior with High Molecular Weight Polymers. Next, we sought to test whether labeling with high molecular weight polymers could also be achieved. Polymers present an important building block in medical research; they can be used for covalent or noncovalent drug loading and controlled drug release. For example, the chemotherapeutic doxorubicin was loaded onto the polymer polystyrene sulfonic acid and subsequently

encapsulated into VNPs from *Hibiscus chlorotic ringspot virus* (HCRSV).³⁵ In a different study, PEG-based polymers were grown on the surface of the phage Q β ; the chemotherapeutic doxorubicin was then covalently introduced into multivalent binding pockets provided by the polymers.³⁶

Our goal was to test whether high molecular weight polymers could diffuse inside the interior cavity and covalently attach to the interior cysteine side chains; we chose PEG-maleimide with a MW of 2000 Da as a test molecule. We compared the labeling efficiency of eCPMV with CPMV when treated with mPEG2000-maleimide. To rule out cross-reactivity and confirm functionalization of the interior, we carried out the same reactions using eCPMV and CPMV particles with surface lysines labeled with succinimidyl-4-formyl benzoate (S-4FB). Reaction of S-4FB-covered eCPMV and CPMV with an NHS ester-activated PEG with a MW of 2000 Da (mPEG2000-NHS) was used as a control to verify that the lysines are unavailable for modification with PEG (Figure 4A).

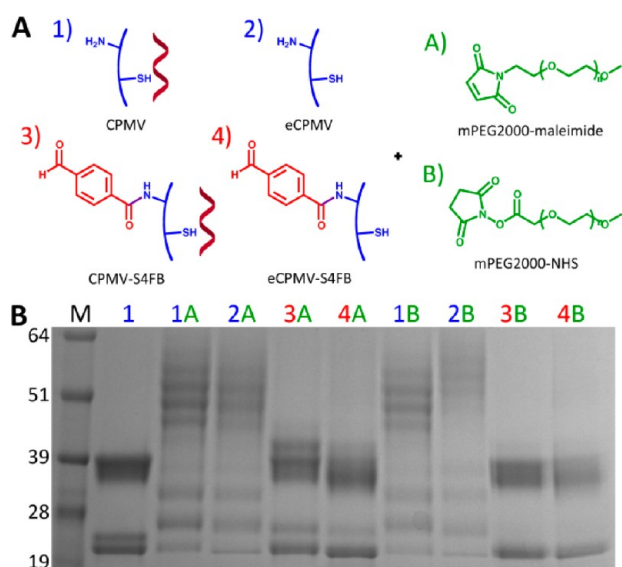


Figure 4. (A) Reactions to determine functionalizability of eCPMV and CPMV with maleimide- and NHS-mPEG2000 when surface lysines are either available or unavailable for modification. (B) Results of the reactions on a 4–12% denaturing SDS-PAGE gel stained with Coomassie Blue. M = SeeBlue Plus2 molecular weight marker; 1 = CPMV; 2 = eCPMV; 3 = CPMV-S4FB; 4 = eCPMV-S4FB; A = mPEG2000-maleimide; B = mPEG2000-NHS.

An electrophoretic mobility shift assay using denaturing gel electrophoresis was carried out to ascertain covalent attachment of PEG. Successful PEG conjugation was verified by the appearance of a laddering effect on the gel (Figure 4B). The additional, lower mobility bands correspond to coat proteins that have been labeled with PEG. With the surface lysines free, PEG labeling was achieved using both maleimide (lanes 1A and 2A) and NHS (lanes 1B and 2B) chemistries. However, while PEG could be attached to eCPMV and CPMV covered with S-4FB using mPEG2000-maleimide (lanes 3A and 4A), as expected, no PEG conjugation was observed with mPEG2000-NHS (lanes 3B and 4B). In addition, densitometry analysis of the S protein bands was performed to determine an estimate of the degree of labeling. The L protein bands were not used because they were less distinct, but the degree of covalent modification appears to be comparable if not greater

than the S protein. The density ratio of labeled to unlabeled S coat proteins indicate approximately 80% PEG labeling for eCPMV and 75% for CPMV, regardless of S-4FB coverage. These findings indicate that mPEG2000-maleimide is indeed attached to the interior cysteine residues. This is further supported by SEC data, where CPMV particles labeled at the exterior surface with mPEG2000-NHS elute earlier from the column, consistent with an increase in size. By contrast, the elution profile of eCPMV particles labeled with mPEG2000-maleimide at the interior surface resembles that of unlabeled particles, suggesting that PEG chains are presented on the interior surface (Figure S2).

It is interesting that the high molecular weight polymer PEG was able to diffuse into the eCPMV and CPMV formulations and react with interior cysteines. The pore at the 5-fold axis (Figure 1C) was measured to be 0.75 nm at its narrowest point. Consistent with these structural measurements, previous experiments showed that rigid gold nanoparticles with a diameter of 1.4 nm could not diffuse inside CPMV particles.²³ Now, the size of PEG in solution can be calculated based on the Flory dimension with $R_F = aN^{3/5}$, where a is the persistence length of the PEG monomer ($a = 0.35$ nm)³⁷ and N is the number of PEG monomers ($N = 45$ for PEG2000).³⁸ This gives a Flory dimension for PEG with a MW of 2000 Da of R_F PEG2000 = 3.45 nm. On the basis of the Flory dimension, it would appear that their size would prevent the polymers from being able to diffuse inside the cavity and react with interior cysteines. However, the Flory radius is only an estimate of the size when PEG is in a mushroom conformation. PEG is a highly flexible polymer, and its conformation in solution is dynamic. The steric hindrance from the small pore size would promote the brush conformation. When the PEG is stretched out in this conformation, it is small enough to diffuse through the pores. In addition, the pore size of CPMV was determined by the crystal structure and based on a snapshot. The combination of the flexible polymer and dynamic CPMV structure provides access for large polymer systems to enter the interior of the nanoparticles. At this point, it is unknown whether the whole molecule is within the particle. It is possible that only the maleimide portion of the molecule entered the cavity and reacted with the Cys 4 residue that is in close proximity to the pore. Nevertheless, these findings of polymer loading may open the door for polymer-mediated drug loading studies.

Interior Peptide Loading of CPMV and eCPMV Using Hydrazone Ligations. Recently, it has been shown that it is possible to chemically link peptides to the outer surface of CPMV particles in order to catalyze the deposition of specific minerals around the particles.³⁹ Here we have investigated whether peptides could be introduced to the interior of eCPMV and CPMV in order to promote specific mineralization within particles since mineralized particles could have applications in nanomedicine. Three candidate peptides were chosen: the positively charged penta(arginine) and hexa-(histidine) peptides as well as the negatively charged FLAG tag peptide (Figure 5A). To facilitate efficient loading with charged peptides, we turned toward bio-orthogonal chemistries. Standard coupling procedures using maleimide-activated reagents have slow reaction kinetics, and large excesses of reagents have to be used to facilitate efficient labeling. Cu(I)-catalyzed azide–alkyne cycloaddition and hydrazone ligation chemistry overcome these limitations;⁵ these chemistries are highly efficient bioconjugation methods that require low concentrations and excesses of the reagent or ligand of interest.

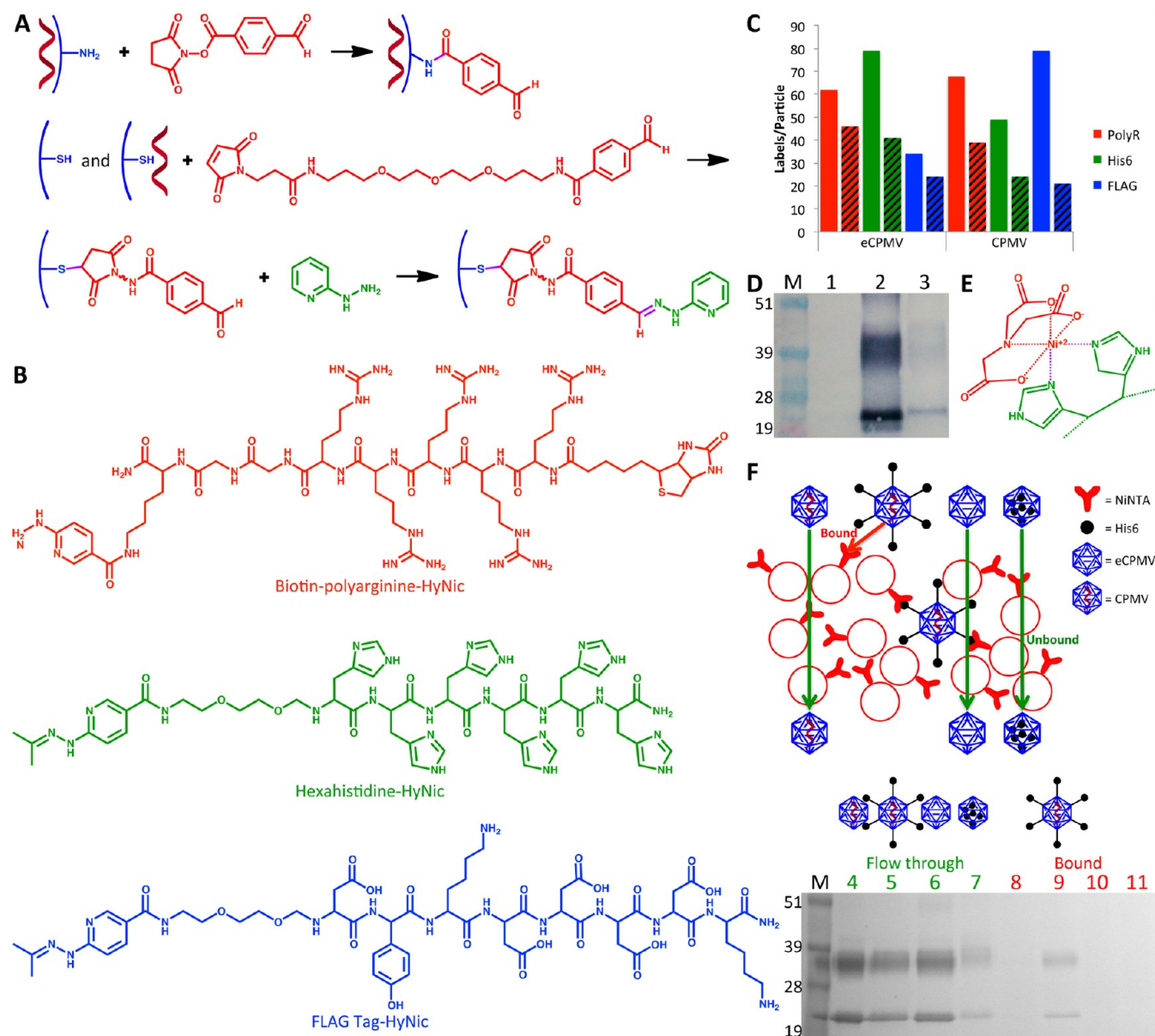


Figure 5. Hydrazone ligation. (A) Functionalization of the exterior of CPMV with S-4FB (top) and the interior of eCPMV and CPMV with MTFB (middle) to provide aldehyde ligation handles. Example of hydrazone ligation using 2-hydrazinopyridine to quantify the MSR (bottom). (B) Polyarginine, hexahistidine, and FLAG peptides attached using hydrazone ligation. (C) Representative data of the labeling efficiency of MTFB (solid bars) and the various peptides (striped bars) to the interior of eCPMV vs CPMV. (D) Western blot probed with streptavidin-alkaline phosphatase confirms successful incorporation of biotinylated R5 peptide into the interior of eCPMV. M = SeeBlue Plus2 molecular weight marker; 1 = eCPMV; 2 = eCPMV-bio; 3 = eCPMV-R5. (E) Affinity of Ni-NTA to histidines was exploited for testing the binding of CPMV, CPMV-His6_E, eCPMV, and eCPMV-His6_I, to Ni-NTA beads using a similar test as performed for biotinylated particles. (F) Schematic of the bead binding assay (top) illustrates the expected results. SDS-PAGE gel stained with Coomassie (bottom) confirms only CPMV-His6_E binds to the beads, indicating internal attachment of His6 to eCPMV. M = SeeBlue Plus2 molecular weight marker; 4 = washed CPMV; 5 = washed CPMV-His6; 6 = washed eCPMV; 7 = washed eCPMV-His6; 8 = eluted CPMV; 9 = eluted CPMV-His6; 10 = eluted eCPMV; 11 = eluted eCPMV-His6.

Peptide conjugation was carried out using a two-step hydrazone ligation procedure: first, interior cysteines on eCPMV and CPMV were labeled with benzaldehydes using the maleimide-reactive linker MTFB; second, peptide coupling was performed using hydrazinopyridine-modified peptide conjugates (Figure 5A,B). MTFB was introduced using a 6000-fold excess to ensure maximum labeling. Quantification of MTFB modification was determined using the Solulink MSR assay and 2-hydrazinopyridine. The resulting hydrazone bond is UV traceable (A at 350 nm, $\epsilon = 18,000 \text{ M}^{-1} \text{ cm}^{-1}$). We found that reaction with MTFB showed poor reproducibility; between

40 and 80 MTFB linkers were attached (Figure 5C, solid bars). No statistically significant differences between eCPMV and CPMV were observed. This is consistent with observations made using PEG2000 and may be explained by the hydrophilic nature of the ligand; MTFB contains a PEG₃ spacer (Figure 5A).

The aldehyde moiety of eCPMV-MTFB_I and CPMV-MTFB_I was then coupled with the hydrazine functionality of the penta(arginine), hexa(histidine), and FLAG tag peptides. Hydrazone chemistry has recently been applied to the CPMV platform and was shown to be a versatile strategy allowing the

decoration of CPMV with targeting ligands specific for vascular endothelial growth factor receptor-1.²² We optimized the ligation reaction further using the catalyst aniline, which accelerates the rate of hydrazone bond formation by 2 orders of magnitude, allowing the reaction to proceed rapidly even at neutral and basic pH (the optimum of pH for hydrazone chemistry is 4.5).⁴⁰

eCPMV and CPMV peptide conjugates were purified from excess reagents and characterized using SEC, UV/vis spectroscopy, denaturing gel electrophoresis, and Western blotting. The R5 peptide used in this study displays a biotin tag (Figure 5B), allowing detection using enzyme-tagged streptavidin probes and Western blotting. Western blotting was performed using alkaline phosphatase-conjugated streptavidin. Alkaline phosphatase activity was detected using the BCIP/NBT liquid substrate system. Data confirmed the covalent decoration of eCPMV and CPMV with R5 peptides. In agreement with dye-, biotin-, and PEG-labeling, labels were found to be introduced to both the S and L proteins (Figure 5D).

Quantification of peptide labeling was based on the UV-traceable hydrazone bond formed (A at 354 nm, $\epsilon = 29,000 \text{ M}^{-1} \text{ cm}^{-1}$). Overall, eCPMV appeared to show better reactivity. From the data, it was not clear whether the charges of the various peptides impact the success of labeling. It appears that peptide labeling using hydrazone ligation results in high variability. Statistical analysis showed no significant differences between the conjugates. The previous dye-labeling studies indicated that negatively charged molecules may be preferred for entrance through the pores. However, the negatively charged FLAG tag is also larger than the positively charged penta(arginine) and hexa(histidine) peptides, a fact that could explain why this trend was not observed for the peptides. Between 20 and 40 peptides could be introduced using a molar excess of 360 peptides per CPMV/eCPMV. We attempted to increase the labeling efficiency by increasing the molar excess of peptides used or by extending the incubation time. However, in both cases, aggregation was observed, and the recovered yield was less than 10%, indicating that the charged peptides induce electrostatically driven aggregation upon a threshold. We have observed similar trends in exterior peptide conjugation experiments using charged peptides. It has been shown that metals ions can be diffused into the internal cavity and converted to metal or metal oxide.⁴¹ On the basis of previous observations showing that 60 genetically introduced hexa(histidine) peptides were sufficient to serve as nucleation centers to promote external mineralization of eCPMV with cobalt,⁴² we propose that chemical labeling with up to 40 peptides will achieve similar results.

To verify that peptide labels were indeed conjugated to the interior particle surface, we adapted the agarose bead assay aforementioned for use in determining the spatial location of introduced biotin labels (see above). Agarose beads labeled with nickel-nitrilotriacetic acid (Ni-NTA) were used. Hexa(histidine) sequences have a high affinity to Ni-NTA (Figure 5E). We tested four particle formulations: eCPMV, CPMV, eCPMV-His_{6I} and CPMV-His_{6E}. The latter formulation was generated by decorating the exterior CPMV surface with benzaldehydes using the NHS derivative S-4FB, followed by hydrazone ligation using the HyNic-hexa(histidine) peptide. eCPMV, CPMV, eCPMV-His_{6I}, and CPMV-His_{6E} were all found in the flow through. However, only CPMV-His_{6E} displaying exterior hexa(histidine) tags was detected in the eluent after treatment with imidazole, a chemical known to

disrupt the Ni-NTA–hexa(histidine) interaction. Thus, out of all the formulations, only CPMV-His_{6E} had any affinity to the Ni-NTA beads. This is as expected and indicates that the peptide sequences in eCPMV-His_{6I} were indeed attached to the interior surface; there was no indication of eCPMV-His_{6I} being bound to the beads. Since CPMV-His_{6E} was also found in the initial flow through, binding to the beads was incomplete (Figure 5F). The difference in binding between this assay and the previous assay for biotinylated particles could be due to the 9 orders of magnitude lower affinity of the interaction between His₆ and Ni-NTA ($K_d = 10^{-6} \text{ M}$)⁴³ compared to the interaction between biotin and avidin ($K_d = 10^{-15} \text{ M}$).⁴⁴ Overall, these data support that peptide labels were selectively attached to the interior surface. This opens a new avenue for peptide-mediated internal mineralization of CPMV.

Toward Medical Applications: Cellular Imaging and Tumor Homing of Internally and Externally Labeled (e)CPMV. Fluorescent dyes are widely employed in optical imaging, and the versatility of fluorescently labeled CPMV nanoparticles has been demonstrated for several applications: CPMV-dye conjugates have been used (i) to target and image cancer cells in vitro and in vivo,^{13,25,29} (ii) for intravital vascular imaging, including tumor neovasculature mapping,^{14,45} and (iii) to study its biodistribution in vivo.⁴⁶ In each case, the fluorophores were attached to the exterior CPMV surface. The conjugation of the imaging labels to the interior surface would offer a clear advantage. For example, it would allow modification of exterior residues with other biomedically relevant moieties such as targeting ligands to redirect and target specific cells and tissues and PEG, a hydrophilic polymer used to shield nanomaterials and increase their pharmacokinetics while reducing undesired side effects such as immunogenicity. Here, we evaluated the use of internally labeled eCPMV versus externally labeled CPMV for optical imaging applications in tissue culture and preclinical tumor mouse models.

First, we evaluated the optical stability and molecular quenching of dye-labeled CPMV and eCPMV (Figure 6). We

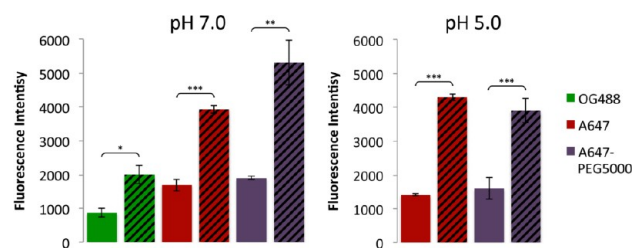


Figure 6. Fluorescence intensity data of interior labeled eCPMV compared to exterior labeled CPMV in pH 7.0 potassium phosphate buffer (left) and of A647-labeled particles in pH 5.0 MES buffer (right). eCPMV data are shown as solid bars on the left, while CPMV data are shown as striped bars on the right. Asterisks denote statistical significance between fluorescence intensities of eCPMV and CPMV formulations (* $p < 0.05$, ** $p < 0.01$, *** $p < 0.001$).

examined CPMV-OG488_E particles labeled with 80 OG488 at exterior surface lysine side chains and eCPMV-OG488_I labeled with 70 OG488 at interior cysteines for potential use in confocal microscopy studies. In addition, we looked at non-PEGylated and PEGylated formulations of CPMV-A647_E and eCPMV-A647_I labeled with 50 dyes each for use in flow cytometry and tumor homing studies, respectively. Fluorescence was measured for 50 μM solutions of the particles,

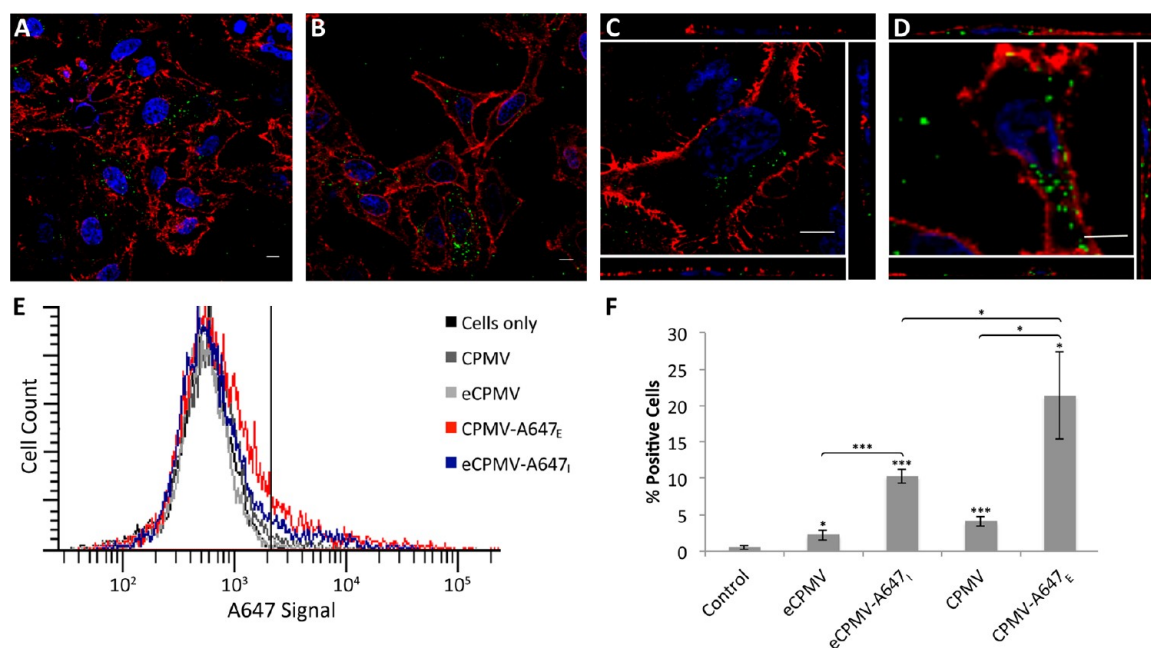


Figure 7. In vitro evaluations of CPMV-OG488_E and eCPMV-OG488_I. Representative confocal images depict uptake of CPMV-OG488_E (A,C) and eCPMV-OG488_I (B,D) by HeLa cells. Side panels in C and D are orthogonal sections from the respective images confirming internalization of VNPs. Both CPMV and eCPMV were tagged with OG488 (green), the cell membrane was stained with WGA-Alexa Fluor 555 (red), and the nucleus was stained with DAPI (blue). Flow cytometry was performed to measure cell uptake (E). Cells to the right of the vertical line were considered positive for A647, and the percent of positive cells for each sample was quantified (F). Unpaired asterisks denote statistical significance as compared to cells only control (* $p < 0.05$, *** $p < 0.001$). Difference in fluorescence intensity between eCPMV and CPMV formulations was also statistically significant ($p < 0.05$).

maintaining equal amounts of dyes and particles for comparison. Measurements indicated that some quenching occurred when labels were conjugated to the interior eCPMV surface, and the fluorescence intensity reached only about half of the fluorescence intensity measured for CPMV decorated with dyes on its exterior surface. This phenomenon was independent of the dye used, i.e., OG488 or A647, and was also pH-independent, i.e., pH 7.0 versus 5.0 (Figure 6). Despite the weakened fluorescence signal of the eCPMV formulation compared to CPMV, the fluorescence is still suitable for optical imaging applications, and the potential for additional functionalities on the exterior of eCPMV remains promising. As the interior labeled eCPMV particles appeared strongly fluorescent in gels even though they are less fluorescent when measured in bulk in aqueous buffers, environmental factors clearly play a role in observed fluorescence. A difference may also be observed when imaging the particles within cells. Consequently, we went on to evaluate the in vitro and in vivo properties of eCPMV.

Cell imaging was studied using HeLa cells, a cervical cancer cell line. HeLa cells are an ideal model for this analysis because previous studies have shown that CPMV binds to vimentin displayed on the surface of HeLa cells and is then taken up by endocytosis.²⁶ OG488- and A647-labeled constructs from the fluorescence measurements were used for confocal microscopy imaging and flow cytometry analysis, respectively. For confocal microscopy studies, live cells were incubated with CPMV-OG488_E and eCPMV-OG488_I, washed, and subsequently fixed. Cell membranes were stained with WGA, and nuclei were stained with DAPI (Figure 7A-D). There were no apparent differences between the CPMV-OG488_E and eCPMV-OG488_I formulations, and fluorescent signals were comparable. From z-stacks analyzed using ImageJ software, CPMV and eCPMV

nanoparticles were found to be internalized. Flow cytometry measurements were performed to gain quantitative data (Figure 7E,F). Signals obtained from eCPMV-A647_I were reduced compared to signals derived from cells that were treated with CPMV-A647_E. Nevertheless, both formulations were detectable in HeLa cells at similar levels as reported previously.^{25,26}

Finally, the *in vivo* tumor homing properties of internally labeled eCPMV versus externally labeled CPMV were studied using a nude mouse xenograft model of colon cancer. In a one-pot synthesis reaction, CPMV and eCPMV were conjugated with A647 on their exterior and interior surfaces, respectively, together with mPEG5000-NHS on their exterior. These reactions yielded formulations with 50 fluorophores and approximately 30% PEGylation, as indicated by UV/vis spectroscopy, denaturing gels, and band analysis (not shown). Integrity of the particles was verified by TEM and SEC (Figures S1 and S2).

NCr-nu/nu mice were used and tumors were induced through subcutaneous injection of HT-29 colon cancer cells. The mice were kept on an alfalfa-free diet to reduce tissue autofluorescence. Equal amounts of the particles (and thus equal amounts of dye) were injected intravenously (200 μg of eCPMV and 284.3 μg of CPMV) and allowed to circulate for 24 h for delivery to the tumors. The animals were then sacrificed, and their tissues were collected and imaged *ex vivo* using a Maestro imaging system (Figure 8). No fluorescence was observed for the PBS control, while there was prominent fluorescence in the liver and some in the spleen for the eCPMV and CPMV particles due to clearing by the reticuloendothelial system (not shown). There was clear tumor homing via the enhanced permeability and retention effect, with fluorescent signal observed for both eCPMV and CPMV. The average signal over the tumor area for each mouse was analyzed using

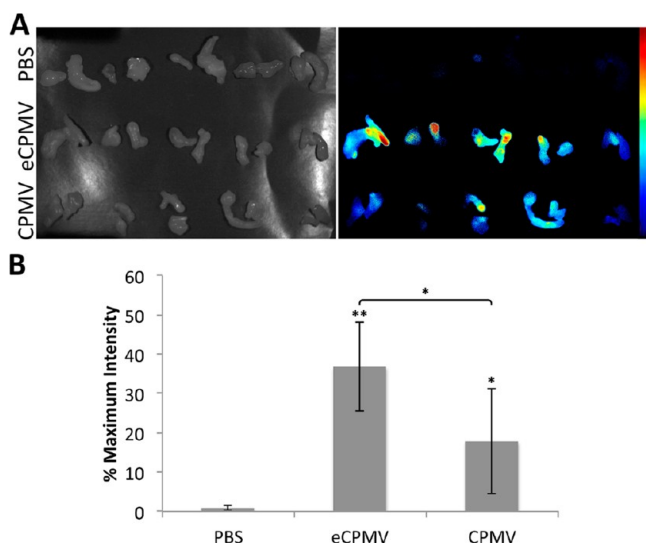


Figure 8. Tumor homing of PEG5000_E-eCPMV-A647_I and PEG5000_E-CPMV-A647_E. (A) Images from the Maestro imaging system of tumor tissues under white light (left) and their fluorescent signal (right). (B) Quantitative data of average fluorescence signal from the tumor tissues. Asterisks denote statistical significance as compared to PBS control (* $p < 0.05$, ** $p < 0.01$). Difference in fluorescence intensity between eCPMV and CPMV formulations was also statistically significant ($p < 0.05$).

ImageJ. There is some variability between the animals, but the fluorescence intensities from mice injected with the eCPMV formulation appear to be consistently higher, with the difference between the two formulations being statistically significant ($p < 0.05$). This is an interesting result given the previous fluorescence measurements and flow cytometry studies. Some possible explanations for this difference could be that the display of A647 on the outside of the CPMV somewhat hinders its delivery to the tumor or the exterior dyes may be more easily degraded in vivo.

HT-29 tumor cells express surface vimentin, and targeting of CPMV to these tumor cells has been previously confirmed in vitro and in vivo.²⁵ PEG was used in our design, as this allows shielding of the particles during circulation and increased tumor homing. Over short time periods (a few hours), PEGylation shields CPMV from cell interactions. However, over longer time periods, vimentin-specific cell uptake has been observed.²⁵ On the basis of these previous observations, we propose the eCPMV formulation provides an advantage for in vivo tumor homing applications. The imaging labels can be installed on the interior surface, thus preserving cellular interactions with the native particle surface. Furthermore, eCPMV provides the possibility for additional modifications on the exterior for synthesis of multifunctional nanoparticles for targeted delivery applications.

CONCLUSION

In this study, we successfully established the use of bioconjugation methods for interior cargo loading of CPMV. We illustrated that this method can be used to encapsulate dyes, large PEG polymers, and a variety of negatively and positively charged peptides. From our findings, we hypothesize that the factors that may govern the entrance of molecules through the pore and into the cavity of eCPMV include size, charge, and hydrophobicity. The pore size was measured to be

0.75 nm, which excludes larger molecules other than flexible polymers that can adapt their conformation such as PEG. In terms of charge, the greatest extent of labeling was observed using negatively charged dyes. Their diffusion into the cavity may be favored because they mimic the charge of the natural nucleic acid cargo. This trend was not observed for peptide labeling, but the negatively charged FLAG tag also had greater steric hindrance. Finally, hydrophilic molecules such as PEG2000 and MTFB appear to be able to diffuse into the cavity more freely than other molecules, as no difference in labeling between eCPMV and wild-type CPMV was observed.

Our results lead the way for imaging, polymer-mediated drug loading, and peptide-mediated mineralization applications. We have shown that RNA-free eCPMV is necessary to achieve significant dye loading compared to wild-type CPMV and that these interior dye-labeled eCPMV are suitable for fluorescence imaging in vitro and in vivo. eCPMV is able to passively accumulate in tumors through the EPR effect and has a higher signal intensity in vivo than exterior labeled CPMV. In addition to these individual applications, interior modification leaves reactive lysines on the exterior surface free for functionalization with other moieties such as PEG for masking nonspecific interactions and prolonging circulation time, targeting ligands to confer tissue-specificity, and contrast agents for magnetic resonance and PET imaging. Interior conjugation is thus the first step in the advancement of the eCPMV platform for further development of multifunctional nanoparticles for *in vivo* applications. The feasibility to encapsulate biomedically relevant molecules within CPMV has great potential for future therapeutics incorporating tissue-specific targeting, drug delivery, and/or imaging in a single formulation.

ASSOCIATED CONTENT

Supporting Information

Experimental details of the characterization of eCPMV and CPMV conjugates by TEM and SEC are provided. This information is available free of charge via the Internet at <http://pubs.acs.org/>.

AUTHOR INFORMATION

Corresponding Author

*Mailing address: Department of Biomedical Engineering, Radiology, Materials Science and Engineering, Case Western Reserve University School of Medicine, 10900 Euclid Avenue, Cleveland, OH 44106, USA. Phone: 216-368-5590; e-mail: nicole.steinmetz@case.edu.

Present Addresses

[†]Department of Cardiovascular Medicine, University of Oxford, Level 6 West Wing, John Radcliffe Hospital, Headley Way, Headington, Oxford, OX3 9DU, UK.

[#]Department of Bioengineering, University of Pittsburgh, 300 Technology Dr., Pittsburgh, PA 15219, USA.

[∇]Department of Chemistry, University of Hull, Cottingham Road, Hull, HU6 7RX, UK.

Notes

The authors declare no competing financial interest.

ACKNOWLEDGMENTS

This work was supported by NIH/NIBIB Grants R00 EB009105 (to N.F.S.) and P30 EB011317 (to N.F.S.), the Mt. Sinai Foundation (to N.S.F.), an NIH/NIBIB training grant T32 EB007509 (to A.M.W.), an NSF REU training grant

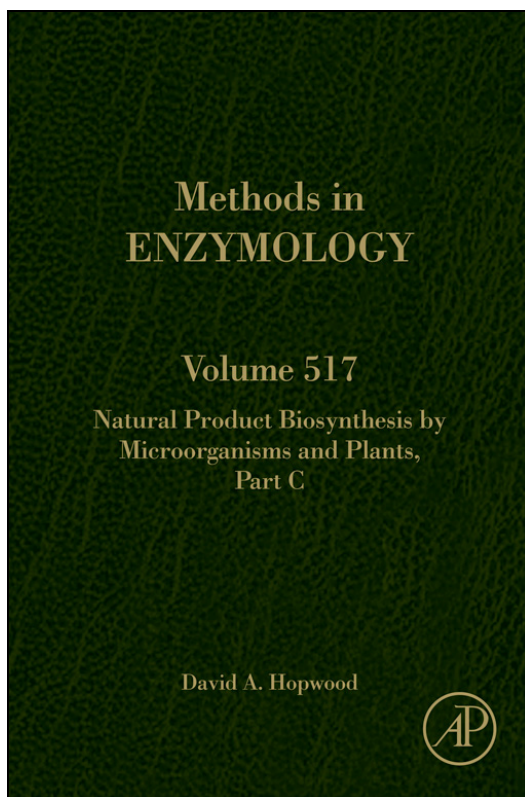
EEC-0552804 (to J.E.M.), and Alcoa undergraduate student funding (to A.C.Y.). At the John Innes Centre (JIC), the work was supported by BB/J004561/1 from the UK Biotechnology and Biological Sciences Research Council (BBSRC) and the John Innes Foundation (to D.J.E. and G.P.L.), and a BBSRC DTG (to A.A.A. and P.S.). Dr. Anouk Dirksen and Prof. Phil Dawson (The Scripps Research Institute) are thanked for providing the R5 peptide.

REFERENCES

- (1) Young, M.; Willits, D.; Uchida, M.; Douglas, T. *Annu. Rev. Phytopathol.* **2008**, *46*, 361–384.
- (2) Barzon, L.; Stefani, A. L.; Pacenti, M.; Palu, G. *Expert Opin. Biol. Ther.* **2005**, *5*, 639–662.
- (3) Choi, V. W.; McCarty, D. M.; Samulski, R. J. *Curr. Gene Ther.* **2005**, *5*, 299–310.
- (4) Cockrell, A. S.; Kafri, T. *Mol. Biotechnol.* **2007**, *36*, 184–204.
- (5) Pokorski, J. K.; Steinmetz, N. F. *Mol. Pharmaceutics* **2011**, *8*, 29–43.
- (6) Douglas, T.; Young, M. *Science* **2006**, *312*, 873–875.
- (7) Yildiz, I.; Shukla, S.; Steinmetz, N. F. *Curr. Opin. Biotechnol.* **2011**, *22*, 901–908.
- (8) Aljabali, A. A.; Barclay, J. E.; Butt, J. N.; Lomonosoff, G. P.; Evans, D. J. *Dalton Trans.* **2010**, *39*, 7569–7574.
- (9) Aljabali, A. A.; Barclay, J. E.; Lomonosoff, G. P.; Evans, D. J. *Nanoscale* **2010**, *2*, 2596–2600.
- (10) Steinmetz, N. F.; Lomonosoff, G. P.; Evans, D. J. *Small* **2006**, *2*, 530–533.
- (11) Sapsford, K. E.; Soto, C. M.; Blum, A. S.; Chatterji, A.; Lin, T.; Johnson, J. E.; Ligler, F. S.; Ratna, B. R. *Biosens. Bioelectron.* **2006**, *21*, 1668–1673.
- (12) Blum, A. S.; Soto, C. M.; Wilson, C. D.; Cole, J. D.; Kim, M.; Gnade, B.; Chatterji, A.; Ochoa, W. F.; Lin, T.; Johnson, J. E.; Ratna, B. R. *Nano Lett.* **2004**, *4*, 867–870.
- (13) Steinmetz, N. F.; Ablack, A. L.; Hickey, J. L.; Ablack, J.; Manocha, B.; Mymryk, J. S.; Luyt, L. G.; Lewis, J. D. *Small* **2011**, *7*, 1664–1672.
- (14) Lewis, J. D.; Destito, G.; Zijlstra, A.; Gonzalez, M. J.; Quigley, J. P.; Manchester, M.; Stuhlmann, H. *Nat. Med.* **2006**, *12*, 354–360.
- (15) Saunders, K.; Sainsbury, F.; Lomonosoff, G. P. *Virology* **2009**, *393*, 329–337.
- (16) Chatterji, A.; Ochoa, W.; Paine, M.; Ratna, B. R.; Johnson, J. E.; Lin, T. *Chem. Biol.* **2004**, *11*, 855–863.
- (17) Wang, Q.; Kaltgrad, E.; Lin, T.; Johnson, J. E.; Finn, M. G. *Chem. Biol.* **2002**, *9*, 805–811.
- (18) Steinmetz, N. F.; Lomonosoff, G. P.; Evans, D. J. *Langmuir* **2006**, *22*, 3488–3490.
- (19) Steinmetz, N. F.; Evans, D. J.; Lomonosoff, G. P. *ChemBioChem* **2007**, *8*, 1131–1136.
- (20) Wang, Q.; Lin, T.; Johnson, J. E.; Finn, M. G. *Chem. Biol.* **2002**, *9*, 813–819.
- (21) Hong, V.; Presolski, S. I.; Ma, C.; Finn, M. G. *Angew. Chem., Int. Ed.* **2009**, *48*, 9879–9883.
- (22) Brunel, F. M.; Lewis, J. D.; Destito, G.; Steinmetz, N. F.; Manchester, M.; Stuhlmann, H.; Dawson, P. E. *Nano Lett.* **2010**, *10*, 1093–1097.
- (23) Wang, Q.; Lin, T.; Tang, L.; Johnson, J. E.; Finn, M. G. *Angew. Chem., Int. Ed.* **2002**, *41*, 459–462.
- (24) Wang, Q.; Raja, K. S.; Janda, K. D.; Lin, T.; Finn, M. G. *Bioconjugate Chem.* **2003**, *14*, 38–43.
- (25) Steinmetz, N. F.; Cho, C. F.; Ablack, A.; Lewis, J. D.; Manchester, M. *Nanomedicine* **2011**, *6*, 351–364.
- (26) Koudelka, K. J.; Destito, G.; Plummer, E. M.; Trauger, S. A.; Siuzdak, G.; Manchester, M. *PLoS Pathog.* **2009**, *5*, e1000417.
- (27) Steinmetz, N. F.; Maurer, J.; Sheng, H.; Bensussan, A.; Maricic, I.; Kumar, V.; Braciak, T. A. *Cancers* **2011**, *3*, 2870–2885.
- (28) Aljabali, A. A.; Shukla, S.; Lomonosoff, G. P.; Steinmetz, N. F.; Evans, D. J. *Mol. Pharmaceutics* **2012**, DOI: 10.1021/mp3002057.
- (29) Destito, G.; Yeh, R.; Rae, C. S.; Finn, M. G.; Manchester, M. *Chem. Biol.* **2007**, *14*, 1152–1162.
- (30) Wu, Z.; Chen, K.; Yildiz, I.; Dirksen, A.; Fischer, R.; Dawson, P. E.; Steinmetz, N. F. *Nanoscale* **2012**, *4*, 3567–3576.
- (31) Wellink, J. *Methods Mol. Biol.* **1998**, *81*, 205–209.
- (32) Montague, N. P.; Thuenemann, E. C.; Saxena, P.; Saunders, K.; Lenzi, P.; Lomonosoff, G. P. *Hum. Vaccines* **2011**, *7*, 383–390.
- (33) Lin, T.; Chen, Z.; Usha, R.; Stauffacher, C. V.; Dai, J. B.; Schmidt, T.; Johnson, J. E. *Virology* **1999**, *265*, 20–34.
- (34) Brewer, C. F.; Riehm, J. P. *Anal. Biochem.* **1967**, *18*, 248–255.
- (35) Ren, Y.; Wong, S. M.; Lim, L. Y. *Bioconjugate Chem.* **2007**, *18*, 836–843.
- (36) Pokorski, J. K.; Breitenkamp, K.; Liepold, L. O.; Qazi, S.; Finn, M. G. *J. Am. Chem. Soc.* **2011**, *133*, 9242–9245.
- (37) Svergun, D. I.; Ekstrom, F.; Vandegriff, K. D.; Malavalli, A.; Baker, D. A.; Nilsson, C.; Winslow, R. M. *Biophys. J.* **2008**, *94*, 173–181.
- (38) de Gennes, P. G. *Adv. Colloid Interface Sci.* **1987**, *27*, 189–209.
- (39) Aljabali, A. A.; Shah, S. N.; Evans-Gowing, R.; Lomonosoff, G. P.; Evans, D. J. *Integr. Biol.* **2011**, *3*, 119–125.
- (40) Dirksen, A.; Dawson, P. E. *Bioconjugate Chem.* **2008**, *19*, 2543–2548.
- (41) Aljabali, A. A.; Sainsbury, F.; Lomonosoff, G. P.; Evans, D. J. *Small* **2010**, *6*, 818–821.
- (42) Sainsbury, F.; Saunders, K.; Aljabali, A. A.; Evans, D. J.; Lomonosoff, G. P. *ChemBioChem* **2011**, *12*, 2435–2440.
- (43) Nieba, L.; Nieba-Axmann, S. E.; Persson, A.; Hämäläinen, M.; Edebratt, F.; Hansson, A.; Lidholm, J.; Magnusson, K.; Karlsson, A. F.; Plückthun, A. *Anal. Biochem.* **1997**, *252*, 217–228.
- (44) Green, N. M. *Biochem. J.* **1963**, *89*, 585–591.
- (45) Leong, H. S.; Steinmetz, N. F.; Ablack, A.; Destito, G.; Zijlstra, A.; Stuhlmann, H.; Manchester, M.; Lewis, J. D. *Nat. Protoc.* **2010**, *5*, 1406–1417.
- (46) Rae, C. S.; Khor, I. W.; Wang, Q.; Destito, G.; Gonzalez, M. J.; Singh, P.; Thomas, D. M.; Estrada, M. N.; Powell, E.; Finn, M. G.; Manchester, M. *Virology* **2005**, *343*, 224–235.

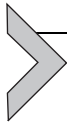
**Provided for non-commercial research and educational use only.
Not for reproduction, distribution or commercial use.**

This chapter was originally published in the book *Methods in Enzymology*, Vol. 517 published by Elsevier, and the attached copy is provided by Elsevier for the author's benefit and for the benefit of the author's institution, for non-commercial research and educational use including without limitation use in instruction at your institution, sending it to specific colleagues who know you, and providing a copy to your institution's administrator.



All other uses, reproduction and distribution, including without limitation commercial reprints, selling or licensing copies or access, or posting on open internet sites, your personal or institution's website or repository, are prohibited. For exceptions, permission may be sought for such use through Elsevier's permissions site at: <http://www.elsevier.com/locate/permissionusematerial>

From: Frank Sainsbury, Pooja Saxena, Katrin Geisler, Anne Osbourn and George P. Lomonosoff, Using a Virus-Derived System to Manipulate Plant Natural Product Biosynthetic Pathways. In David A. Hopwood, editor: *Methods in Enzymology*, Vol. 517, Burlington: Academic Press, 2012, pp. 185-202.
ISBN: 978-0-12-404634-4
© Copyright 2012 Elsevier Inc.
Academic Press



Using a Virus-Derived System to Manipulate Plant Natural Product Biosynthetic Pathways

Frank Sainsbury^{*}, Pooja Saxena[†], Katrin Geisler[‡], Anne Osbourn[‡],
George P. Lomonosoff^{†,1}

^{*}Département de Phytologie, Pavillon des Services, Université Laval, Québec, QC, Canada

[†]Department of Biological Chemistry, John Innes Centre, Norwich, United Kingdom

[‡]Department of Metabolic Biology, John Innes Centre, Norwich, United Kingdom

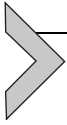
¹Corresponding author: e-mail address: george.lomonosoff@jic.ac.uk

Contents

1. Introduction	186
2. Deleted Vectors Based on Cowpea Mosaic Virus	186
2.1 Replication-competent deleted vectors	187
2.2 The CPMV- <i>HT</i> expression system	190
2.3 The pEAQ series of vectors	191
3. Expression of Enzymes in Plants Using pEAQ Vectors	196
3.1 Materials	196
3.2 Creating expression plasmids	198
3.3 Agroinfiltration of <i>N. benthamiana</i>	199
3.4 Monitoring expression levels in <i>N. benthamiana</i> leaves	200
4. Conclusions and Perspectives	200
Acknowledgments	201
References	201

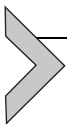
Abstract

A series of vectors (the pEAQ series) based on cowpea mosaic virus has been developed which allows the rapid transient expression of high levels of foreign protein in plants without the need for viral replication. The plasmids are small binary vectors, which are introduced into plant leaves by agroinfiltration. They are modular in design and allow the insertion of multiple coding sequences on the same segment of T-DNA. These properties make the pEAQ vectors particularly suitable for use in situations, such as the investigation and manipulation of metabolic pathways, where the coexpression of multiple proteins within a cell is required.



1. INTRODUCTION

The past 20 years have seen the development of many RNA viruses as vectors for the transient expression of foreign peptides and polypeptides in plants (Porta & Lomonosoff, 2002; Scholthof, Scholthof, & Jackson, 1996). The advantages of using viruses, as opposed to stable genetic transformation, for such expression include the facts that (i) viral genomes are small and therefore easy to manipulate, (ii) infection of plants with modified viruses is much simpler and quicker than the regeneration of stably transformed lines, and (iii) a sequence inserted into a virus vector will be highly amplified during viral replication. Initially, plant virus-based vectors were based on replication-competent full-size virus genomes, with the gene to be expressed being added to the full complement of viral genes. Inevitably, there were a number of disadvantages to this approach: there are size constraints on the sequences which can be inserted while retaining virus viability, the inserted sequence is susceptible to “genetic drift” during virus replication, and there are bio-containment concerns over the use of vectors based on fully competent viruses as these retain their ability to spread in the environment. As a result, in the past decade, attention has turned toward the development of plant virus-based expression systems based on defective versions of viral RNAs, which alleviate some or all of these disadvantages (Cañizares, Liu, Perrin, Tsakiris, & Lomonosoff, 2006; Gleba, Marillonnet, & Klimyuk, 2004). These studies have resulted in the creation of systems in which the ability of the virus to spread both within the plant and in the environment is curtailed and has culminated in the development of a system in which the need for replication to achieve high-level expression has been eliminated.



2. DELETED VECTORS BASED ON COWPEA MOSAIC VIRUS

Among the plant viruses which have been developed into an expression system is cowpea mosaic virus (CPMV; Sainsbury, Cañizares, & Lomonosoff, 2010). This virus infects a number of legume species and grows to particularly high titers in its natural host, cowpea (*Vigna unguiculata*); it also infects the commonly used experimental host, *Nicotiana benthamiana*. The genome of CPMV consists of two separately encapsidated positive-strand RNA molecules of 5889 (RNA-1) and 3481 (RNA-2) nucleotides. The RNAs each contain a single open reading frame (ORF) and

are expressed through the synthesis and subsequent processing of precursor polyproteins. RNA-1 encodes proteins involved in the replication of viral RNAs and polyprotein processing while RNA-2, which is entirely dependent on the proteins encoded by RNA-1 for its replication, encodes the movement protein and the two coat proteins, large (L) and small (S) that are essential for cell-to-cell movement and systemic spread. The development of CPMV-based expression systems has focused entirely on modifying the sequence of RNA-2; replication functions, when required, are provided by coinoculating the RNA-2 constructs with RNA-1 (Fig. 9.1A).

A particular attraction of CPMV as a virus-based vector is the fact that it is naturally bipartite. This means that two RNA molecules have to be replicated within the same cell, implying that virus exclusion will not occur. Virus exclusion is the phenomenon whereby the presence of a replicating RNA within a cell effectively excludes the replication of a second construct based on the same virus. Thus, systems based on monopartite, replication-competent viruses, such as tobacco mosaic virus, are essentially limited to the production of a single protein within a given cell unless a second, different noncompeting virus is used for the expression of the second protein (Giritch et al., 2006). The utility of CPMV for the coexpression of multiple proteins was first demonstrated using full-length versions of RNA-2 harboring either the yellow or cyan fluorescent protein (YFP or CFP) or the heavy and light chains of an IgG. In each case, the two RNA-2-based constructs were inoculated in conjunction with RNA-1 to provide the replication functions (Sainsbury, Lavoie, D'Aoust, Vezina, & Lomonosoff, 2008). However, although successful coexpression was demonstrated in the inoculated tissue, segregation of the different RNA-2-based constructs occurred on systemic movement, leading to cells expressing either YFP or CFP but rarely both. Since, for practical purposes, this limits the expression of multiple genes to the inoculated tissue, it was rationalized that there was little to be lost in terms of levels of expression if those features necessary for the spread of the virus were removed from RNA-2. This would have the advantage of creating vectors which are unable to spread in the environment and are therefore biocontained.

2.1. Replication-competent deleted vectors

An expression system based on a defective form of CPMV RNA-2 (Fig. 9.1B) was created using the observation that the sequences necessary for replication of RNA-2 by the RNA-1-encoded replication complex lie exclusively at the 5' and 3' ends of the RNA (Rohll, Holness,

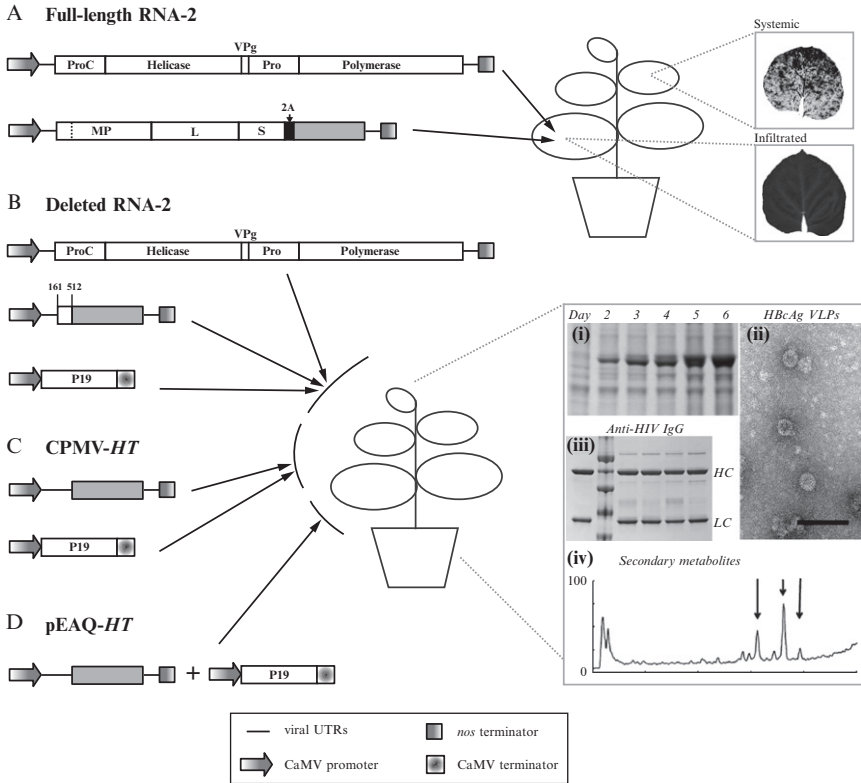


Figure 9.1 Development of CPMV-based expression vectors. (A) Full-length vectors based on the entire genome of CPMV where RNA-1 provides replication functions for RNA-2 molecules modified to contain the gene of interest (gray) following the FMDV 2A catalytic peptide. Also shown is an example of an expression pattern following infiltration and systemic movement (black tissue). (B) Deleted RNA-2 vectors where the entire coding sequence of RNA-2 is replaced by the gene of interest. RNA-1 provides replication functions and P19 supplies silencing suppressor functions in lieu of the small coat protein. (C) CPMV-HT vectors based on the modified UTRs of RNA-2 where P19 provides a silencing suppressor function. (D) Schematic representation of pEAQ-HT where all elements for CPMV-HT are present on a single T-DNA. (i) Time-course of GFP expression from CPMV-HT, (ii) TEM image of crude extracts showing assembled HBCAg particles following expression from CPMV-HT, (iii) purified anti-HIV antibody following expression from deleted RNA-2 and CPMV-HT, (iv) example high performance liquid chromatography (HPLC) trace representing metabolic engineering enabled by CPMV-based vectors.

Lomonosoff, & Maule, 1993). This allows most of the RNA-2 ORF to be deleted without affecting the ability of RNA-2 to be replicated. However, while the essential 3'-terminal sequences lie exclusively within the 3'-UTR, the essential 5' sequence extends beyond the first in-frame AUG (position 161)

as far as the second in-frame AUG at position 512; deletion or frameshift mutations introduced between the two AUG codons abolish replication, as does elimination of the AUG at 161 (Holness, Lomonosoff, Evans, & Maule, 1989; Rohll et al., 1993). This means that initiation of translation of the foreign gene must be driven by the second in-frame AUG at position 512 if the ability of the construct to be replicated by RNA-1 is to be retained (Cañizares et al., 2006). To create a vector in which the heterologous coding sequence can be precisely fused to AUG 512, site-directed mutagenesis of a full-length copy of RNA-2 in an *Escherichia coli* plasmid was used to introduce a *Bsp*HI site (TCATGA) around AUG 512 and a *Stu*I site (AGGCCT) after UAA 3299, the termination codon for the RNA-2-encoded polyprotein; in addition, two *Bsp*HI sites from the vector backbone were removed (Liu & Lomonosoff, 2002). The resulting vector, termed pM81B-S2NT-1, allows the whole of the RNA-2 ORF downstream of AUG 512 to be excised by digestion with *Bsp*HI and *Stu*I and replaced with any sequence with *Bsp*HI and *Stu*I (blunt)-compatible ends. The use of the *Bsp*HI site is important as it preserves the AUG at 512 and this initiator is used to drive translation of the inserted gene. To express the foreign gene in plants, the pM81B-S2NT-1-derived plasmids are digested with *As*I and *Pac*I and the fragment containing the foreign sequence flanked by the CaMV 35S promoter and *nos* terminator, as well as the CPMV RNA-2-derived UTRs, is transferred to similarly digested pBINPLUS and the resulting plasmids are finally introduced by transformation into *Agrobacterium tumefaciens*. For expression, *A. tumefaciens* suspensions harboring the desired RNA-2-based constructs are coinfiltrated into *N. benthamiana* leaves with plasmids encoding a full-length copy of RNA-1 and a suppressor of gene silencing, usually P19 from Tomato bushy stunt virus (TBSV; Fig. 9.1B). This approach has been used successfully to express assembled particles of Hepatitis B core antigen (HBcAg; Mechtcheriakova, Eldarov, Beales, Skryabin, & Lomonosoff, 2008) and to express a fully assembled, functional IgG (Sainsbury, Sack, et al., 2010). Initially, it was believed that replication of the deleted RNA-2 by RNA-1 was essential for high levels of protein expression. However, the presence of a strong suppressor of silencing, such as P19, increases the stability of mRNA to such a degree that amplification of RNA levels by replication results in little further increase in expression levels (Sainsbury, Sack, et al., 2010). As a result, the deleted RNA-2-based vectors (delRNA-2 vectors) described above, though replication competent, can be deployed for expression of

proteins in plants in the absence of RNA-1. Details of the construction and method of use of these replication-competent vectors are described in detail in [Sainsbury, Liu, and Lomonossoff \(2009\)](#).

The vectors described above were originally created to express proteins, such as vaccine candidates and antibodies, which would be subsequently purified and characterized. However, [Mugford et al. \(2009\)](#) showed that the vectors could also be used to express active enzymes within *N. benthamiana* leaves with the aim of manipulating plant metabolism and analyzing enzyme function rather than obtaining the protein itself. In these experiments, the expression of a serine carboxypeptidase-like acyltransferase from oat leaves (*Sad 7*, an enzyme from the avenacin biosynthetic pathway; see [Chapter 6](#)) was shown to be able to catalyze the transfer of both *N*-methyl anthraniloyl- and benzoyl-groups to des-acyl avenacins when expressed in *N. benthamiana*. These studies paved the way for the use of virus-based vectors for the manipulation of metabolic pathways in plants. The use of replication-competent CPMV RNA-2 based vectors for the expression of active enzymes in plants is described in detail in [Chapter 14](#).

2.2. The CPMV-*HT* expression system

A major drawback with the replication-competent RNA-2 system is the need to precisely fuse the sequence to be expressed to AUG 512. This makes the cloning strategy a somewhat cumbersome, two-step procedure (see [Sainsbury, Liu, & Lomonossoff, 2009](#)). Further, coinfiltration with a separate construct containing a suppressor of silencing is necessary to obtain high levels of expression. The observation that replication is not essential for high-level protein expression led [Sainsbury and Lomonossoff \(2008\)](#) to examine whether it is possible to simplify the structure of the expression plasmids, particularly around the 5'-UTR, to facilitate the insertion of foreign sequences. These studies showed that elimination of both AUG 161 and an upstream out-of-frame AUG at position 115, though abolishing replication, actually substantially increased expression levels of a variety of proteins. This effect was caused by the modified 5'-UTR rendering the mRNAs "hyper-translatable" and expression systems using them have been termed CPMV-*HT*. The levels of foreign protein produced using the *HT* leaders far exceeded those achieved from replicating full-length or delRNA-2 vectors in transient expression studies. Achieving high-level expression without replication has a number of substantial advantages: the problems associated with genetic drift and virus exclusion are eliminated and there is no obvious

limitation on the size or complexity of the sequences that can be expressed. Thus, CPMV-*HT* is ideally suited to the simultaneous expression of multiple proteins within the same cell. A number of pharmaceutically relevant proteins have been expressed to high level using the CPMV-*HT* system (Fig. 9.1C and D). They include approximately 1 g/kg of agroinfiltrated tissue of assembled HBcAg particles (Sainsbury & Lomonossoff, 2008), and up to 0.4 g/kg of the human antihuman immunodeficiency virus IgG, 2G12 (Sainsbury, Sack, et al., 2010). However, in its initial form the CPMV-*HT* expression system still required a two-step cloning procedure and coinfiltration with a suppressor of silencing (Fig. 9.1C).

2.3. The pEAQ series of vectors

To refine the CPMV-*HT* expression system, its various components (the CPMV-*HT* expression cassette and the P19 sequence) were placed on the T-DNA region of a binary vector for *Agrobacterium*-mediated delivery to plant cells (Fig. 9.1D). This was achieved by constructing a new series of binary vectors, the pEAQ series (Table 9.1; Fig. 9.2A). These vectors are less than half the size of the original pBINPLUS plasmid while retaining all the essential components for efficient transient expression and stable transformation (Sainsbury, Thuenemann, & Lomonossoff, 2009). In addition to a variety of T-DNA configurations, each pEAQ vector contains a polylinker of unique restriction sites that, while designed for use with the modular cloning of the CPMV-*HT* cassette as discussed below, may also be used to insert any expression cassette or sequence (Fig. 9.2A). The removal of reading frame dependence, essential for replication but evidently adversely affecting translation, permits the use of a one-step cloning procedure either through the use of a multiple cloning site for restriction enzyme-based cloning or via the GATEWAY[®] system of recombination-based cloning. Further expanding their usefulness, these expression vectors also contain the appropriate sequences for N- or C-terminal His-tagging of proteins of interest, allowing for straightforward purification from plant tissue (Tables 9.2 and 9.3). The use of such pEAQ-based CPMV-*HT* vectors has so far enabled high-level expression and purification via a His-tag of a number of heterologous proteins, including human gastric lipase (Vardakou, Sainsbury, Rigby, Mulholland, & Lomonossoff, 2012) and a rice chitinase (Miyamoto et al., 2012).

Though expression of a single protein during transient expression is useful in several cases, there are many instances where coexpression of more

Table 9.1 The pEAQ vector series

Plasmid name	GenBank accession	Features
pEAQ- <i>HT</i>	GQ497234	<p>Designed for easy and quick cloning of a gene of interest into the CPMV-<i>HT</i> system. Its T-DNA comprises:</p> <ul style="list-style-type: none"> • the CPMV-<i>HT</i> expression cassette with a polylinker (Table 9.2) to insert the gene of interest; • the suppressor of gene silencing P19; • neomycin phosphotransferase II (<i>nptII</i>) to confer resistance to kanamycin.
pEAQexpress	GQ497230	<p>Designed for cloning multiple CPMV-<i>HT</i> expression cassettes in the same vector for transient expression only. Its T-DNA comprises:</p> <ul style="list-style-type: none"> • a multiple cloning site for insertion of multiple expression cassettes digested using enzymes <i>PacI</i> and <i>AsdI</i>; • the suppressor of gene silencing P19.
pEAQselectK	GQ497231	<p>Designed for expression from a CPMV-<i>HT</i> expression cassette in the absence of a suppressor of silencing. Its T-DNA comprises:</p> <ul style="list-style-type: none"> • a multiple cloning site for insertion of the expression cassettes; • neomycin phosphotransferase II (<i>nptII</i>) to confer resistance to kanamycin.
pEAQspecialK	GQ497232	<p>Designed for expression from a CPMV-<i>HT</i> expression cassette in the presence of a suppressor of silencing. Its T-DNA comprises:</p> <ul style="list-style-type: none"> • a multiple cloning site for insertion of the expression cassette; • the suppressor of gene silencing P19; • neomycin phosphotransferase II (<i>nptII</i>) to confer resistance to kanamycin.
pEAQspecialKm	GQ497233	<p>Best suited for stable expression of proteins in whole plants. Its T-DNA comprises:</p> <ul style="list-style-type: none"> • a multiple cloning site for insertion of the expression cassette;

Table 9.1 The pEAQ vector series—cont'd

Plasmid name	GenBank accession	Features
		<ul style="list-style-type: none"> • the modified suppressor of gene silencing P19/R43W (Saxena et al., 2011); • neomycin phosphotransferase II (<i>nptII</i>) to confer resistance to kanamycin.
pEAQ- <i>HT</i> -DEST1	GQ497235	<p>Designed for easy and quick cloning using the gateway[®] system to express wild-type protein in plants. Its T-DNA comprises:</p> <ul style="list-style-type: none"> • the CPMV-<i>HT</i> expression cassette with attR sites to introduce the gene of interest from the entry clone via recombination; • the suppressor of gene silencing P19; • neomycin phosphotransferase II (<i>nptII</i>) that confers resistance to kanamycin.
pEAQ- <i>HT</i> -DEST2	GQ497236	<p>Designed for easy and quick cloning using the gateway[®] system to express N-terminally His-tagged protein in plants. Its T-DNA comprises:</p> <ul style="list-style-type: none"> • the CPMV-<i>HT</i> expression cassette with attR sites to introduce the gene of interest from the entry clone via recombination; • the suppressor of gene silencing P19; • neomycin phosphotransferase II (<i>nptII</i>) that confers resistance to kanamycin.
pEAQ- <i>HT</i> -DEST3	GQ497237	<p>Designed for easy and quick cloning using the gateway[®] system to express C-terminally His-tagged protein in plants. Its T-DNA comprises:</p> <ul style="list-style-type: none"> • the CPMV-<i>HT</i> expression cassette with attR sites to introduce the gene of interest from the entry clone via recombination; • the suppressor of gene silencing P19; • Neomycin phosphotransferase II (<i>nptII</i>) that confers resistance to kanamycin.

than one protein is required. The simplest way of achieving this is to coinfiltrate *Agrobacterium* suspensions each containing a plasmid designed to express a single protein. Although this is a highly flexible approach, to ensure efficient coexpression of constructs within the same cell, each

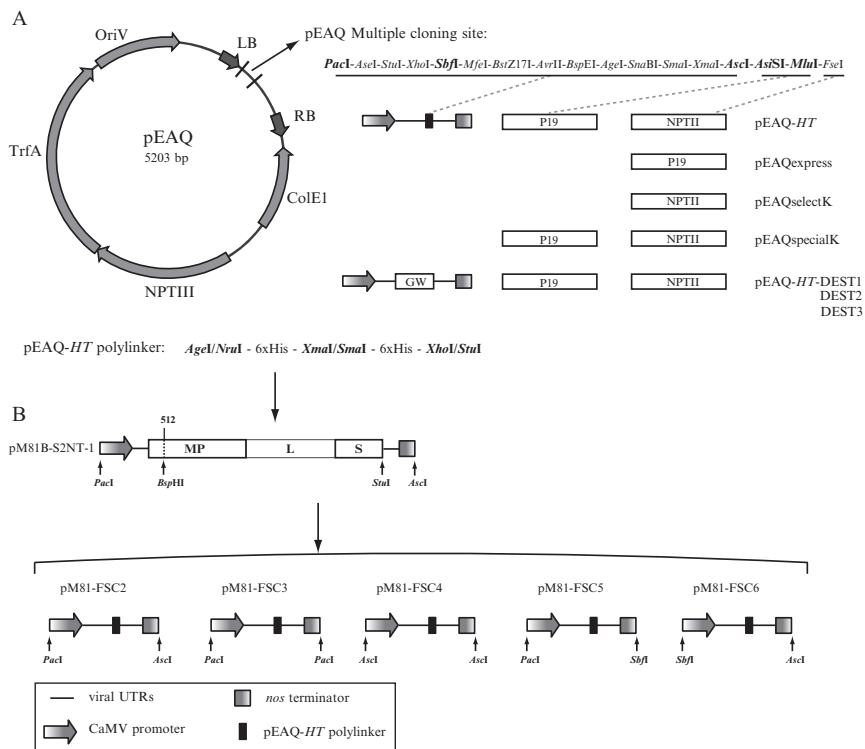


Figure 9.2 Schematic representation of the pEAQ vector system. The series of vectors enables direct cloning into expression vectors of the assembly of multiple expression cassettes via a modular series of cloning vectors. (A) Representation of the minimal plasmid backbone of the pEAQ series and various configurations of the T-DNA designed for different applications. GW, GATEWAY. (B) Representation of the modular series of cloning vectors each containing the pEAQ-*HT* polylinker and designed for CPMV-*HT* cassette insertion into the pEAQ multiple cloning site.

Table 9.2 Restriction enzyme pairs to use for restriction enzyme-based cloning into pEAQ-*HT* depending on whether or not a His-tag is required

For expression of wild-type protein *NruI* or *AgeI* *XhoI* or *StuI* at the 3' end at the 5' end

For expression of protein with a His-tag at the N-terminus *XmaI* or *SmaI* *XhoI* or *StuI* at the 3' end at the 5' end

For expression of protein with a His-tag at the C-terminus *NruI* or *AgeI* *XmaI* or *SmaI* at the 3' end at the 5' end

Each position contains the option of using a restriction enzyme that leaves an overhang or a blunt end.

Table 9.3 Appropriate pEAQ-HT-DEST vector to use depending on whether or not a His-tag is required

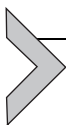
For expression of wild-type protein	Do the LR reaction of your entry clone with pEAQ- <i>HT</i> -DEST1
For expression of protein with a His-tag at the N-terminus	Do the LR reaction of your entry clone with pEAQ- <i>HT</i> -DEST2
For expression of protein with a His-tag at the C-terminus	Do the LR reaction of your entry clone with pEAQ- <i>HT</i> -DEST3

bacterial suspension has to be present at a high concentration, making the inoculum dense and difficult to infiltrate. Even then, it cannot be guaranteed that every cell will receive all the infiltrated constructs (Montague et al., 2011). This problem can be addressed by expressing multiple CPMV-*HT* expression cassettes from the same T-DNA, which is facilitated by the fact that an essential part of the design of the pEAQ vector series is its modular nature (Fig. 9.2).

The CPMV-*HT* cassette, consisting of the gene of interest flanked by the 35S promoter and the modified RNA-2 5'-UTR on one side and the 3'-UTR and *nos* terminator on the other, is also present on a series of cloning vectors based on pM81B-S2NT-1, named pM81-FSC2 through to pM81-FSC6 (Fig. 9.2B). Each cassette contains the same polylinker found in pEAQ-*HT* (Table 9.2; Fig. 9.2B) replacing the entire coding region of RNA-2 and enabling N- or C-terminal His-tagging of proteins to be expressed. They are flanked by restriction sites that allow for the insertion of multiple cassettes into the pEAQ polylinker (Fig. 9.2). For example, up to five cassettes may be inserted sequentially into the basic transient expression vector, pEAQexpress. Alternatively, two CPMV-*HT* cassettes can be simultaneously inserted through multipart ligations into *PacI/AscI*-digested pEAQ vectors. This approach has been used to assemble an antibody-expression construct in pEAQspecialK using pM81-FSC3 and pM81-FSC4 containing the heavy and light chain of an IgG molecule, respectively (Frank Sainsbury, Pooja Saxena & George Lomonosoff, unpublished data).

The benefit of expressing genes from the same T-DNA rather than coinfiltrating separate constructs has been illustrated for the production of assembled antibodies, where coexpression of the heavy and light chains in the same cell is required (Sainsbury, Thuenemann, & Lomonosoff, 2009) and for the production of empty (RNA-free) particles of CPMV, which requires the coexpression of the coat protein precursor and the enzyme necessary for its processing (Montague et al., 2011).

The properties of the CPMV-*HT* system make it ideal for use in situations where the simultaneous expression of multiple proteins within the same cell is required. Thus, the pEAQ series of vectors have proved extremely useful not only in situations where large amounts of a protein are required (e.g., Matic, Rinaldi, Masenga, & Noris, 2012; Saunders, Sainsbury, & Lomonosoff, 2009; Vardakou et al., 2012) but also in situations where manipulation of metabolism, through the coexpression of several enzymes, is required. This has been illustrated in experiments in which an oxidosqualene cyclase and a CYP450 from oat were expressed in *N. benthamiana* leaves, either separately or in combination. Expression of the oxidosqualene cyclase alone resulted in the *N. benthamiana* leaves producing β -amyrin (Fig. 9.3), a metabolite not normally produced by this species. Infiltration with a pEAQexpress-based construct containing the sequence of both the oxidosqualene cyclase and the CYP450 resulted in reduction of the signal for β -amyrin and the appearance of a new peak representing a novel compound, the structure of which is currently being examined. Thus, the pEAQ vectors can be used to express metabolic enzymes with the aim of understanding their function, the analysis of intermediates produced by their action or, ultimately, to produce novel compounds in plants.



3. EXPRESSION OF ENZYMES IN PLANTS USING pEAQ VECTORS

This section constitutes a practical guide for using the pEAQ vector series to express foreign proteins, including active enzymes in plants.

3.1. Materials

3.1.1 Media, buffers, and solutions

- Luria-Bertani (LB) medium: 10 g/L bacto-tryptone, 10/L NaCl, and 5 g/L yeast extract, pH 7.0.
- LB agar: as LB with 10 g/L agar added.
- SOC: 20 g/L bacto-tryptone, 5 g/L yeast extract, 0.58 g/L NaCl, 0.19 g/L KCl, 2.03 g/L MgCl₂, 2.46 g/L magnesium sulfate 7-hydrate, 3.6 g glucose.
- MMA: 10 mM MES (2-[*N*-morpholino]ethanesulfonic acid; Sigma-Aldrich), pH 5.6, 10 mM MgCl₂, 100 μ M acetosyringone (Sigma-Aldrich).
- 1 \times TBE: 10.8 g/L Tris-HCl, 5.5 g/L boric acid, 2 mM EDTA.

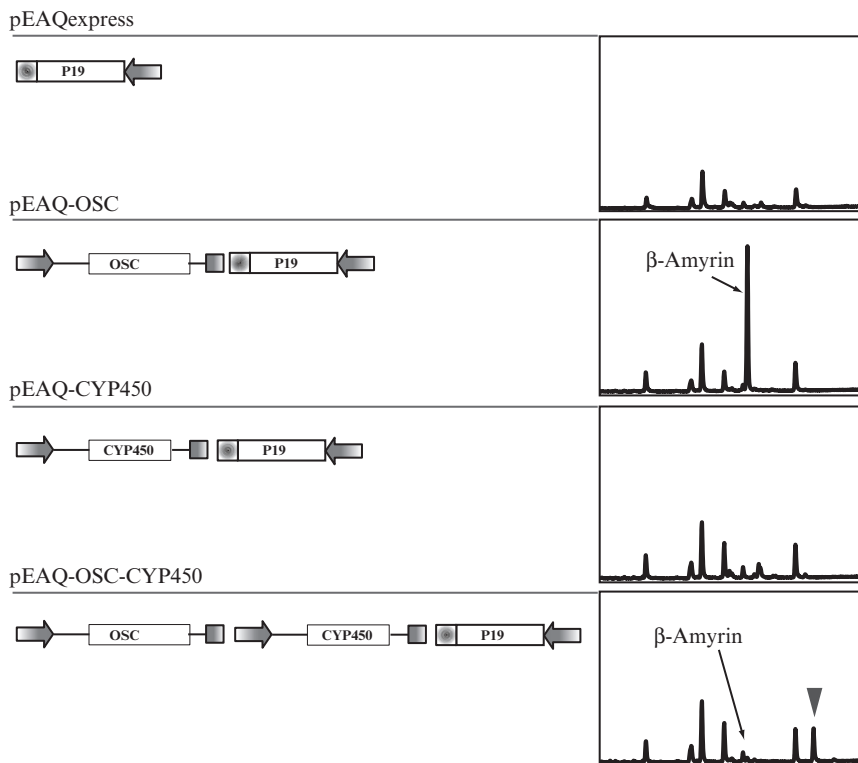


Figure 9.3 Use of CPMV-*HT*-based vectors for metabolic engineering. *N. benthamiana* leaves were infiltrated with either: the empty vector pEAQexpress, which contains just the P19 silencing suppressor expression cassette, Fig. 9.2; pEAQ-OSC, which contains the sequence of an oat oxidosqualene cyclase (OSC) in a CPMV-*HT* cassette; pEAQ-CYP450, which contains a cytochrome P450 (CYP450) in a CPMV-*HT* cassette; pEAQ-OSC-CYP450, which contains the sequences of both OSC and CYP450 on the same T-DNA. The position of β -amyrin is indicated in the HPLC traces on the right. The arrowhead indicates the presence of a novel compound resulting from the expression of both OSC and CYP450 from a single construct.

3.1.2 Bacterial strains

- One Shot[®] TOP10 chemically competent *E. coli* (Invitrogen) is used for propagation of recombinant plasmids.
- One Shot[®] ccdB survival 2T1R chemically competent *E. coli* (Invitrogen) is used for propagation of pEAQ-DEST plasmids before recombination with entry clones.
- *A. tumefaciens* strain LBA4404 (Hoekema, Hirsch, Hooykaas, & Schilperoort, 1983) is used for plant transformations.

3.1.3 Plants

N. benthamiana plants are grown in glasshouses maintained at 25 °C with supplemental lighting to provide 16 h of daylight throughout the year. Plants are watered daily.

3.2. Creating expression plasmids

3.2.1 Choice of expression vector

Using the features described in Table 9.1, choose the most appropriate pEAQ vector for the expression of your gene of interest.

3.2.2 Restriction enzyme-based cloning

1. Generate the insert with appropriate restriction sites at both ends using PCR.
2. Digest both the insert and plasmid pEAQ-*HT* with appropriate restriction enzymes (Table 9.2) by mixing components including the appropriate buffer according to the enzyme manufacturer's recommendation. For expression using pEAQ vectors other than pEAQ-*HT*, the insert should first be cloned in the polylinker of pEAQ-*HT* or one of the FSC cloning vectors (Fig. 9.2B). Then, the entire expression cassette can be moved to other pEAQ vectors using the appropriate restriction enzymes.
3. Dephosphorylate linearized vector with alkaline phosphatase following the manufacturer's instructions. This should be done after heat inactivation of the restriction enzymes.
4. Resolve digests on a 1% agarose gel and purify the vector and inserts using QIAQuick gel extraction kit.
5. Combine the vector and insert (in molar ratio 1:3) in ligase buffer with T4 DNA ligase and incubate according to manufacturer's recommendations.
6. Transform competent *E. coli* and plate onto LB agar plates with kanamycin (50 µg/mL) selection.
7. Colonies may be screened by PCR or restriction analysis. Positive clones are grown overnight and plasmids are extracted for sequencing (to confirm insertion) and *Agrobacterium* transformation.

3.2.3 Cloning by GATEWAY recombination

1. Generate the insert with bacteriophage lambda attachment B (*attB*) sites at both ends using PCR.
2. Using BP clonase II, transfer the PCR fragment to a GATEWAY donor vector via directional recombination. The resultant plasmid is the entry clone.

3. Using LR clonase II, transfer the gene of interest from the entry vector to the appropriate pEAQ-*HT*-DEST vector (see Table 9.3).
4. Transform competent *E. coli* and plate onto LB agar plates with kanamycin (50 µg/mL) selection.
5. Colonies may be screened by PCR or restriction analysis. Positive clones are grown overnight, and plasmids are extracted for sequencing (to confirm insertion) and *Agrobacterium* transformation.

3.2.4 Transformation of *Agrobacterium*

Once the expression construct is generated, it is introduced into *A. tumefaciens* strain LBA4404 or AGL1 using electroporation. After electroporation at 2.5 kV, cells are recovered at 28 °C for 1 h and plated on LB agar containing rifampicin 50 µg/mL (for LBA4404) and kanamycin 50 µg/mL (for carried plasmid). Transformed colonies are visible on plates in 2–3 days.

3.3. Agroinfiltration of *N. benthamiana*

3.3.1 Preparation of *Agrobacterium* suspensions

1. Prepare 10–100 mL LB with appropriate antibiotics for the *Agrobacterium* strain (rifampicin 50 µg/mL for LBA4404) and carried plasmid (kanamycin 50 µg/mL for pEAQ vectors). The volume of the culture depends on the scale of your experiment. Generally, a 10-mL culture is enough to infiltrate 4–5 leaves (ca. 5 g fresh-weight tissue).
2. Inoculate the liquid culture by picking a single colony from a plate. Grow the culture at 28 °C in a shaking incubator until the optical density (OD) at 600 nm is ≥ 2 . Typically, inoculate the culture in the afternoon and grow overnight.
3. Spin cells at $4000 \times g$ for 10 min at room temperature to pellet them and discard the supernatant.
4. Resuspend cells gently in the required volume of MMA to make a solution of final $OD_{600} = 0.4$. For coexpression of two constructs, prepare solutions of individual $OD_{600} = 0.8$ which when mixed 1:1 will result in a final $OD_{600} = 0.4$ for each construct.
5. Leave the solutions at room temperature for 0.5–3 h.

3.3.2 Infiltration of leaves with *Agrobacterium* suspensions

There are two different methods for introducing *Agrobacterium* suspensions into leaves. The method of choice largely depends on the scale of the experiment.

- Syringe-infiltration (small-scale expression; 1–10 plants)

To infiltrate leaves, nick the leaf surface with a sterile needle or a sterile pipette tip. Aspirate infiltration solution into a sterile 1-mL plastic syringe (take care to avoid bubbles) and, place the syringe over the leaf wound while keeping a finger behind the leaf for support. Gently press the solution into the intercellular space. For best results, 3–4-week-old *N. benthamiana* plants are used and the youngest fully expanded leaves are chosen for infiltration.

- Vacuum-infiltration (large-scale expression; 10–100 plants)

Cover the base of a 3–4-week-old plant such that the soil is retained in the pot during the infiltration procedure. Invert the plant into a beaker containing the *Agrobacterium* suspension and place the beaker in the center of the vacuum desiccator unit. Ensure that all the leaves are submerged in the *Agrobacterium* suspension. Close and seal the desiccator and apply vacuum for 60 s at negative pressure of 25 in. Hg (170 mbar). Release the vacuum gently and return the infiltrated plant to the growth room. More than one plant can be infiltrated at the same time depending on the size of the desiccator unit.

3.4. Monitoring expression levels in *N. benthamiana* leaves

The precise method for monitoring expression will depend on the nature of the experiment. Harvesting of *N. benthamiana* leaves is typically done at 3–10 days postinfiltration (dpi). Tissue can be processed fresh or snap-frozen and stored at -80°C . A time-course should be done to assess optimum expression as expression levels might vary depending on the nature of your protein. In the case of green fluorescent protein (GFP), expression is visible *in vivo* under UV illumination. Therefore, it is sensible to include inoculation with a GFP-expressing construct (such as pEAQ-*HT*-GFP) as a control in each experiment. Using the *HT* system, expression of GFP in *N. benthamiana* becomes visible after 2 days, reaches its peak at 5 dpi, and remains at this level until day 7, after which the leaves start showing necrotic symptoms.



4. CONCLUSIONS AND PERSPECTIVES

The use of the pEAQ vector series to manipulate plant natural product biosynthetic pathways is currently in its infancy. However, the data obtained to date suggest that this approach is likely to be widely applicable. The ease of use of the vectors, coupled with the speed of expression, means that many possible combinations of enzymes can be rapidly screened. The modular nature of the vectors means that a mix-and-match approach, in which enzymes from different origins are combined, is feasible, raising the possibility of the synthesis of new-to-nature compounds.

Aside from allowing extremely high-level transient protein expression, the pEAQ series has also been adapted for stable genetic transformation. Although the vectors can be used directly to produce transgenic cell cultures (Sun et al., 2011), expression of the wild-type P19 suppressor of silencing is highly detrimental to the regeneration of fertile plants. This can be overcome by deploying versions of the pEAQ series harboring a mutant version of P19 with reduced suppression activity (Saxena et al., 2011). Using this approach, it is possible to produce homozygous plants expressing high levels of the protein(s) of interest. Thus, transient expression can initially be used to rapidly investigate and/or manipulate a biosynthetic pathway followed by stable transformation to produce lines of plants with the appropriate characteristics.

ACKNOWLEDGMENTS

This work was supported by a Danish FOBI International PhD studentship (K.G.), and the UK Biotechnological and Biological Sciences Research Council (BBSRC) Institute Strategic Programme Grant “Understanding and Exploiting Plant and Microbial Secondary Metabolism” (BB/J004596/1) and the John Innes Foundation (F.S., P.S. G.P.L., A.O.).

REFERENCES

- Cañizares, M. C., Liu, L., Perrin, Y., Tsakiris, E., & Lomonossoff, G. P. (2006). A bipartite system for the constitutive and inducible expression of high levels of foreign proteins in plants. *Plant Biotechnology Journal*, *4*, 183–193.
- Giritch, A., Marillonnet, S., Engler, C., van Eldik, G., Botterman, J., Klimyuk, V., et al. (2006). Rapid high-yield expression of full-size IgG antibodies in plants coinfecting with noncompeting viral vectors. *Proceedings of the National Academy of Sciences of the United States of America*, *103*, 14701–14706.
- Gleba, Y., Marillonnet, S., & Klimyuk, V. (2004). Engineering viral expression vectors for plants: The ‘full virus’ and the ‘deconstructed virus’ strategies. *Current Opinion in Plant Biology*, *7*, 182–188.
- Hoekema, A., Hirsch, P. R., Hooykaas, P. J. J., & Schilperoort, R. A. (1983). A binary plant vector strategy based on separation of vir- and T-region of the *Agrobacterium tumefaciens* Ti-plasmid. *Nature*, *303*, 179–180.
- Holness, C. L., Lomonossoff, G. P., Evans, D., & Maule, A. J. (1989). Identification of the initiation codons for translation of cowpea mosaic virus middle component RNA using site directed mutagenesis of an infectious cDNA clone. *Virology*, *172*, 311–320.
- Liu, L., & Lomonossoff, G. P. (2002). Agroinfection as a rapid method for propagating cowpea mosaic virus-based constructs. *Journal of Virological Methods*, *105*, 343–348.
- Matic, S., Rinaldi, R., Masenga, V., & Noris, E. (2012). Efficient production of chimeric human papillomavirus 16 L1 protein bearing the M2e influenza epitope in *Nicotiana benthamiana* plants. *BMC Biotechnology*, *11*, 106.
- Mechcheriakova, I. A., Eldarov, M. A., Beales, L., Skryabin, K. G., & Lomonossoff, G. P. (2008). Production of hepatitis B virus core particles in plants using a CPMV-based vector. *Voprosy Virusologii*, *53*, 15–20.
- Miyamoto, K., Shimizu, T., Lin, F., Sainsbury, F., Thuenemann, E., Lomonossoff, G., et al. (2012). Identification of an E-box motif responsible for the expression of jasmonic acid-induced chitinase gene OsChia4a in rice. *Journal of Plant Physiology*, *169*, 621–627.

- Montague, N. P., Thuenemann, E. C., Saxena, P., Saunders, K., Lenzi, P., & Lomonossoff, G. P. (2011). Recent advances of cowpea mosaic virus-based particle technology. *Human Vaccines*, *7*, 383–390.
- Mugford, S. T., Qi, X., Bakht, S., Hill, L., Wegel, E., Hughes, R. K., et al. (2009). A serine carboxypeptidase-like acyltransferase is required for synthesis of antimicrobial compounds and disease resistance in oats. *The Plant Cell*, *21*, 2473–2484.
- Porta, C., & Lomonossoff, G. P. (2002). Viruses as vectors for the expression of foreign sequences in plants. *Biotechnology and Genetic Engineering Reviews*, *19*, 245–291.
- Rohll, J. B., Holness, C. L., Lomonossoff, G. P., & Maule, A. J. (1993). 3' Terminal nucleotide sequences important for the accumulation of cowpea mosaic virus M-RNA. *Virology*, *193*, 672–679.
- Sainsbury, F., Cañizares, M. C., & Lomonossoff, G. P. (2010). Cowpea mosaic virus: The plant virus-based biotechnology workhorse. *Annual Review of Phytopathology*, *48*, 437–455.
- Sainsbury, F., Lavoie, P.-O., D'Aoust, M.-A., Vezina, L.-P., & Lomonossoff, G. P. (2008). Expression of multiple proteins using full-length and deleted versions of *Cowpea Mosaic Virus RNA-2*. *Plant Biotechnology Journal*, *6*, 82–92.
- Sainsbury, F., Liu, L., & Lomonossoff, G. P. (2009). Cowpea mosaic virus-based systems for the expression of antigens and antibodies in plants. In L. Faye (Ed.), *Methods in molecular biology*, Vol. 483, (pp. 25–39). Humana Press Inc. New York, USA.
- Sainsbury, F., & Lomonossoff, G. P. (2008). Extremely high-level and rapid transient protein production in plants without the use of viral replication. *Plant Physiology*, *148*, 1212–1218.
- Sainsbury, F., Sack, M., Stadlman, J., Quendler, H., Fischer, R., & Lomonossoff, G. P. (2010). Rapid transient production in plants by replicating and non-replicating vectors yields high quality functional anti-HIV antibody. *PLoS One*, *5*, e13976. <http://dx.plos.org/10.1371/journal.pone.0013976>.
- Sainsbury, F., Thuenemann, E. C., & Lomonossoff, G. P. (2009). pEAQ: Versatile expression vectors for easy and quick transient expression of heterologous proteins in plants. *Plant Biotechnology Journal*, *7*, 682–693.
- Saunders, K., Sainsbury, F., & Lomonossoff, G. P. (2009). Efficient generation of *Cowpea Mosaic Virus* empty virus-like particles by the proteolytic processing of precursors in insect cells and plants. *Virology*, *393*, 329–337.
- Saxena, P., Hsieh, Y. C., Alvarado, V. Y., Sainsbury, F., Saunders, K., Lomonossoff, G. P., et al. (2011). Improved foreign gene expression in plants using a virus-encoded suppressor of RNA silencing modified to be developmentally harmless. *Plant Biotechnology Journal*, *9*, 703–712.
- Scholthof, H. B., Scholthof, K. B., & Jackson, A. O. (1996). Plant virus gene vectors for transient expression of foreign proteins in plants. *Annual Review of Phytopathology*, *34*, 299–323.
- Sun, Q. Y., Ding, L. W., Lomonossoff, G. P., Sun, Y. B., Luo, M., Li, C. Q., et al. (2011). Improved expression and purification of recombinant human serum albumin from transgenic tobacco suspension culture. *Journal of Biotechnology*, *155*, 164–172.
- Vardakou, M., Sainsbury, F., Rigby, N., Mulholland, F., & Lomonossoff, G. P. (2012). Expression of active recombinant human gastric lipase in *Nicotiana benthamiana* using the CPMV-HT transient expression system. *Protein Expression and Purification*, *81*, 69–74.